Molecular basis for the therapeutic uses of botulinum neurotoxin for arthritic pain

Thesis submitted for the degree

of

Doctor of Philosophy

by

Sanjaykumar Boddul, M.Sc.

Supervised by

Prof. J. Oliver Dolly and Dr. Jianghui Meng

International Centre for Neurotherapeutics,
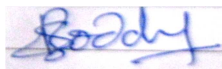
School of Biotechnology,

Dublin City University,

Ireland.

January 2014

Declaration

I hereby certify that this material, which I now submit for assessment on the programme of study leading to the award of Ph.D. is entirely my own work, that I have exercised reasonable care to ensure that the work is original, and does not to the best of my knowledge breach any law of copyright, and has not been taken from the work of others save and to the extent that such work has been cited and acknowledged within the text of my work.

Signed: Sanjaykumar Boddul   **ID No**.:58125132   **Date:**   Jan. 2014

Acknowledgements

First of all, I would like to thank god for all He has done to show me this day.

I wish to express my deep sense of appreciation and gratitude to Prof. J. Oliver Dolly, Director of the International Centre for Neurotherapeutics for recruiting me and offering expert guidance during the course of this study. I am thankful to him for providing highly sophisticated instruments for my work.

I have pleasure in expressing my deep sense of indebtedness and heart felt gratitude to Dr. Jianghui Meng and Dr. Jiafu Wang for expert and valuable guidance and continuous encouragement given to me during the Ph.D. course. I am very grateful for Dr. Jianghui Meng step-by-step guidance throughout this research. Her wide knowledge and experience in this field has been tremendously helpful in guiding the course of this work.

I am thankful to my friends Dhairyasheel Desai, Marie O'Connell, Tushar Borase, Sudharshan Patil, Rashmi, Sachin Bacahte, Sanjay Bansode, Dhananjay, Bhimrao, Sanjay Jadhav, Sachin Thorat, Seshukumar Kaza, Nilesh, Alisa, Alan. I feel privileged to acknowledge the co-operation rendered to me by all my colleagues. I would like thank to Ms. Sharon Whyte for her help and support. My special thanks to Ms. Gillian O'Meara and Ms. Carolyn Wilson for helping and supporting me in the Bio-Resources unit. I also thank IRCSET, Allergan Inc. and DCU for providing a research project and funding. I dedicate my thesis to my mom and brother for their support, understanding and patience.

I will end up with this infinite gratitude, which cannot possibly cover all the names.

Publications and Poster Presentations

Papers

1) Jiafu Wang, Tomas H. Zurawski, MacDara O. Bodeker, Jianghui Meng, **Sanjay Boddul,** K. Roger Aoki and J. Oliver Dolly. Longer-Acting and Highly-Potent Chimeric Therapeutics for Excessive Exocytosis Created by Combining Domains of Botulinum Neurotoxin A and B. Biochem J. 2012 May 15;444(1):59-67.

2) **Sanjay Boddul,** Jianghui Meng, J. Oliver Dolly, Jiafu Wang. SNAP-23 and VAMP-3 contribute to the release of IL-6 and TNF-α from a human synovial sarcoma cell line. FEBS J. 2013 (DOI: 10.1111/febs.12620).

Posters

1) Marie O'Connell, **Sanjay Boddul,** Jiafu Wang, Jianghui Meng and J. Oliver Dolly. A pain laboratory to screen therapeutics *in vivo* to treat pain: presentation to the (Bio)pharmaceuticals and Pharmacological Sciences meeting at Dublin City University, Dublin-9, (2011).

2) **Sanjay Boddul**, Jiafu Wang, Jianghui Meng and J. Oliver Dolly. Pain-relieving and anti-inflammatory effects of SNARE-cleaving toxins in arthritis; presentation to Science Foundation Ireland meeting at Dublin City University (DCU), Dublin-9, (2010).

Abbreviations

ACh Acetylcholine

ACLT Anterior cruciate ligament transection

ACR American College of Rheumatism

ANOVA Analysis of variance

BoNT Botulinum neurotoxin

BCA Bicinchoninic acid assay

BSA Bovine serum albumin

C-terminal Carboxyl-terminal

CGNs Cerebellar granule neurons

CFA Complete Freunds' adjuvant

CGRP Calcitonin gene-related peptide

CNS Central nervous system

CRP C-reactive protein

DAS Disease activity score

DAPI 4', 6'-diamino-2-phenylindole

Rat dorsal root ganglion neurons rDRGs

DMARD Disease-modifying antirheumatic drugs

DMEM Dulbecco's modified Eagle's medium

D-PBS Dulbecco's phosphate buffered saline

ECL Enhanced chemiluminesence

ELISA Enzyme-linked immunosorbent assay

EGTA Ethylene glycol-bis (b-aminoethylether)-N, N, N', N'-tetraacetic acid

ESR Erythrocyte sedimentation rate

FLS Fibroblast-like synoviocytes

h hour

H Heavy chain

HBSS Hank's balanced salt solution

HEPES N-2-hydroxyethylpiperazine-N'-2-ethanesulfonic acid

HLA Human Leukocyte antigen

SW982 Human synovial sarcoma cell line

g Gram

IFN Interferon

IHC Immunohistochemistry

IL Interleukin

KD Knock down

kDa Kilo Dalton

LC/D Light chain of BoNT/D

LC/E400(K224D) LC/E mutant

LVs Lentiviral particles

LPS Lipopolysaccharide

ml Millilitre

MCP-1 Monocyte chemoattractant protein-1

MIA Monosodium iodoacetate

MMP Matrix metalloproteinase

MOI Multiplicity of infection

MOPS 4-morpholinepropanesulfonic acid

MTT methylthiazolyldiphenyl-tetrazolium bromide

μl Microlitre

N Sample size

NS Not significant

NGF Nerve growth factor

NK-1R Neurokinin-1 receptor

NPY Neuropeptide Y

NSAIDs Non-steroidal anti-inflammatory drugs

NT Neurotrophin

OA Osteoarthritis

OD Optical density

p Probability

PAM Pressure application measurement

PAGE Polyacrylamide gel electrophoresis

PBS Phosphate buffer saline

RAW264.7 Mouse macrophage cell line

rSCs Rat synoviocytes

RA Rheumatoid arthritis

RF Rheumatoid factor

SNARE Soluble N-ethylmaleimide-sensitive factor attachment protein receptor

SNAP-23 Synaptosomal-associated protein, 23kDa

SEM Standard error of the mean

SDS Sodium dodecyl sulphate

SP Substance P

SV2 Synaptic vesicle protein 2

SW982 Human synovial cell line

TL Targeted ligand

TBS Tris-buffered saline

TBST TBS with Tween-20

TNF-α Tumour necrosis factor-alpha

Tris Tris(hydroymethyl) aminomethane

Trk Tyrosine receptor kinase

VAMP Vesicle-associated membrane protein

VIP Vasoactive intestinal peptide

VAS Visual analogue scale

VEGF Vascular endothelial growth factor

U Unit

WT Wild type

WB Western blot

Table of Contents

List of Figures

xiii

List of Tables

Abstract

Arthritis, including osteoarthritis (OA) and rheumatoid arthritis (RA), is an important public health problem. This study used a human synovial cell line (SW982), macrophages, and sensory neurons related to those innervating the knee joint that secretes cytokines or neuropeptides upon onset of the disease. These are amongst most the important cell types in the progression of OA and RA. Recent publications report that injecting botulinum neurotoxin (BoNT) into knee joints of arthritic patients and mouse models of arthritis alleviates pain.

Fibroblast-like synoviocytes are important mediators of inflammatory joint damage in arthritis through the release of cytokines, but it is unknown if exocytosis from these particular cells is SNARE-dependent. Wild type SW982 expressed SNAP-23, VAMP-3, syntaxin 2-4 and synaptic vesicle protein 2C (SV2C). Specific KD of SNAP-23 or VAMP-3 decreased the exocytosis of IL-6 and TNF-α. Also, such reduction of the expression of SNAP-23 caused accumulation of SV2 in the peri-nuclear area. A monoclonal antibody specific for VAMP-3 precipitated SNAP-23 and syntaxin-2 (and -3 to a lesser extent). The formation of SDS-resistant complex(es) by SNAP-23 and VAMP-3 was lowered upon knocking down SNAP-23. Though syntaxin isoform -2, -3 and -4 are expressed in SW982, KD of each did not affect the release of cytokines. These collective findings establish that SNAP-23 and VAMP-3 participate in IL-1β induced Ca^{2+}-dependent release of IL-6 and TNF-α from SW982 cells. In contrast, chimera BA and DA cleaved VAMP-3 in rat synoviocytes but failed to blockade of the release of cytokines; however, KD of VAMP-8 resulted in a decrease in inhibition of TNF-α and IL-6 release.

Targeted BoNTs were evaluated in mouse macrophage cell line (RAW264.7), SW982 and sensory neurons for truncation of VAMP-2/3 and inhibition of the release of cytokines and neuropeptides. ARA-7, a recombinantly expressed cell surface receptor-specific ligand conjugated to BoNT, dose-dependently and potently cleaved VAMP-2/3 and inhibited release of two cytokines and substance-P whereas the control protein (LC.H$_N$/D) failed to truncate VAMP-2/3. Moreover, lentiviral particles expressing LC/D successfully truncated VAMP-3 in synoviocytes or macrophages and blocked the release of cytokines (TNF-α and IL-6), confirming the finding from KD of VAMP-3 in SW982 cells.

CHAPTER 1 GENERAL INTRODUCTION

1.1 PAIN

Pain is an unpleasant sensory and emotional experience associated with actual or potential damage (or described in terms of such damage). It is a complex perceptual experience that, in addition to conveying sensory information such as location, type, and intensity of stimulus, has profound affective and cognitive features (Merskey, 1978; Smith et al., 2001). The sensation of pain is the final product of a complex information-processing network. Whether or not a particular stimulus will be perceived as painful depends not only on the nature of the stimulus but, also, on the context within which it is experienced; memories-emotions and so on (Roth-Isigkeit et al., 2005; Breivik et al., 2006).

A number of theories have been postulated to describe mechanisms underlying pain perception. In the 16th century, the French philosopher and mathematician Rene Descartes set the basis for one of the original theories of pain. The specificity (or labeled line) theory, developed in the 19th century, considers pain as an independent sensation with specialized peripheral sensory receptors (nociceptors), which respond to damage and send signals through pathways (along nerve fibers) in the nervous system to target centers in the brain. These brain centers process the signals to produce the experience of pain.

In 1955, Sinclair and Weddell developed the peripheral pattern theory. They proposed that all skin fiber endings (with the exception of those innervating hair cells) are identical, and that pain is produced by intense stimulation of these fibers. Therefore, touch, warmth and other non-damaging as well as to damaging stimuli, give rise to non-painful or painful experiences as a result of differences in the patterns (in time) of the signals sent through the nervous system.

In the 20th-century, a new pain theory was introduced by Wall and Melzack: the gate control theory. The authors proposed that both thin (pain) and large diameter (touch, pressure, vibration) nerve fibers carry information from the site of injury to two destinations in the dorsal horn of the spinal cord, and that the more large-fiber activity relative to thin-fiber activity at the inhibitory cell, the less pain is felt. Both peripheral pattern theory and gate control theory have been superseded by more modern theories of pain.
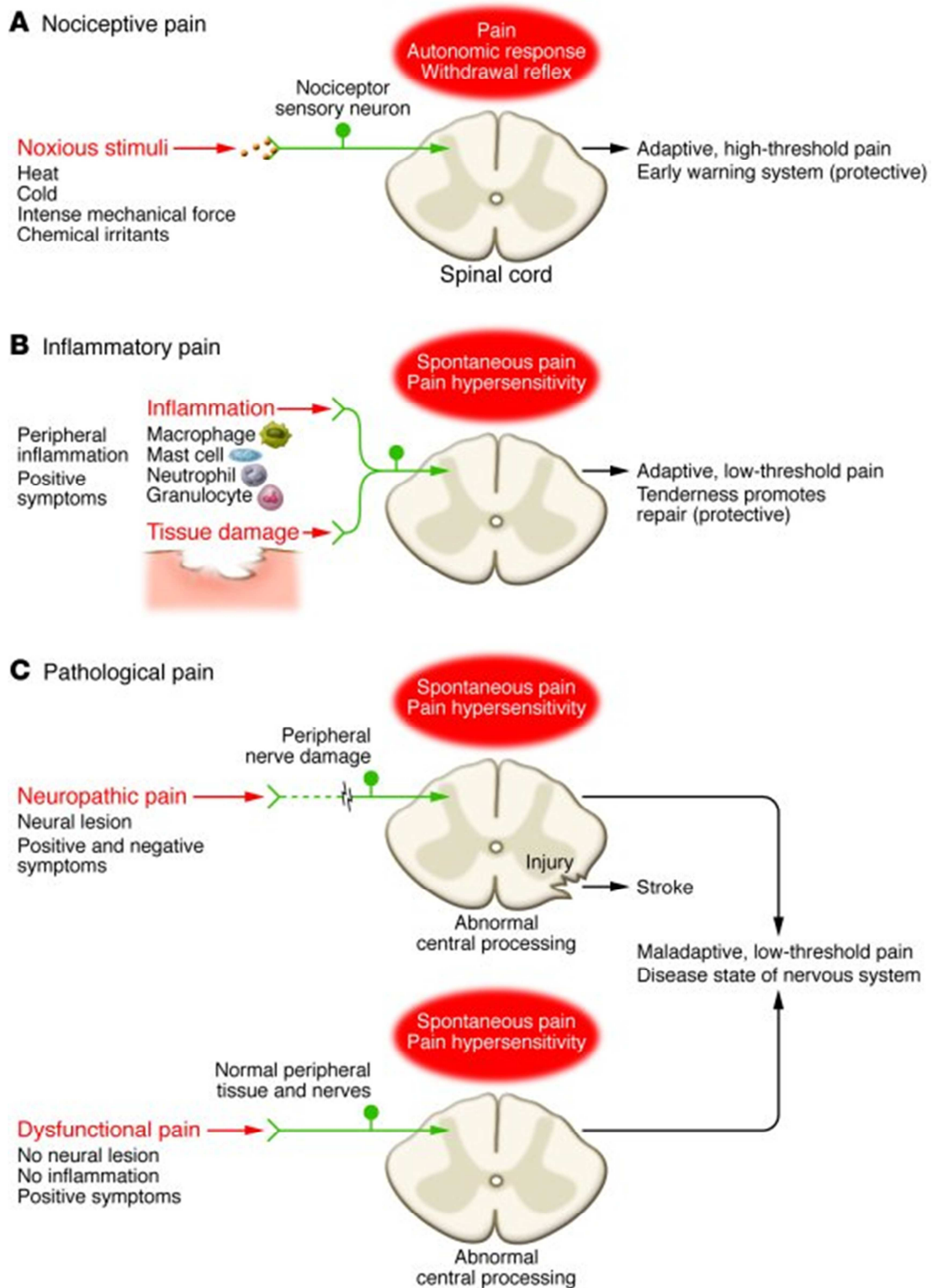
Fig.1-1 Classification of pain.

Pain can be classified as nociceptive, inflammatory and pathological. The body's early protective response to noxious stimuli of different modalities (heat, cold, mechanical or chemical) is referred as nociceptive pain. It involves the activation of

nociceptive sensory neurons only by intense (i.e. high-threshold) noxious stimulation, and elicits a withdrawal reflex which keeps the affected body area away from the potentially harmful stimuli. On the other hand, inflammatory pain is caused by an immune reaction driven by immune cells such as macrophages, mast cells and neutrophils, in response to tissue damage. Under these conditions, hypersensitivity to both noxious and non-noxious stimuli develops in the injured area and surrounding tissue. This helps to reduce the risk of further damage and promotes recovery and repair, as in the case of a surgical wound or in an inflamed joint. Therefore, this type of pain is adaptive. Typically, inflammatory pain disappears after resolution of the initial tissue injury. However, in chronic disorders, such as rheumatoid arthritis, the pain persists for as long as inflammation is active.

Finally, pathological pain is caused by an abnormal function of the nervous system. It may occur in absence of peripheral activation of nociceptors by different types of stimuli, and in contrast, arises spontaneously. The correlation between the intensity of peripheral noxious stimuli (if any) and the intensity of pain sensation is lost, therefore, in these clinical syndromes, pain is maladaptive and non-protective. Neuropathic pain falls into this category, and it develops due to damage of the nervous system. In contrast, a second kind of pathological pain, dysfunctional pain, emerges in absence of identifiable neural injury or inflammation. This pain is characteristic of syndromes such as fibromyalgia and irritable bowel syndrome (Fig. 1-1) (Woolf, 2010, 2011).

Based on its duration, pain can also be classified as acute or chronic. Acute pain is of a sudden onset and occurs after bone, muscle, organ or other tissue damage. It resolves with the healing of the underlying cause. Chronic pain persists for over 6 months, and, when associated to an injury, outlasts the normal time of healing.

1.2 PAIN TRANSMISSION

Pain sensations are transmitted from the periphery by the primary afferent neurons, whose cell bodies are located in the trigeminal and the dorsal root ganglia. However, central mechanisms also play a role in the maintenance of chronic pain conditions as indicated by the contribution of descending input from the rostral ventral medulla to the maintenance of both inflammatory and neuropathic pain (Fig. 1-2) (Bingham et al., 2009).
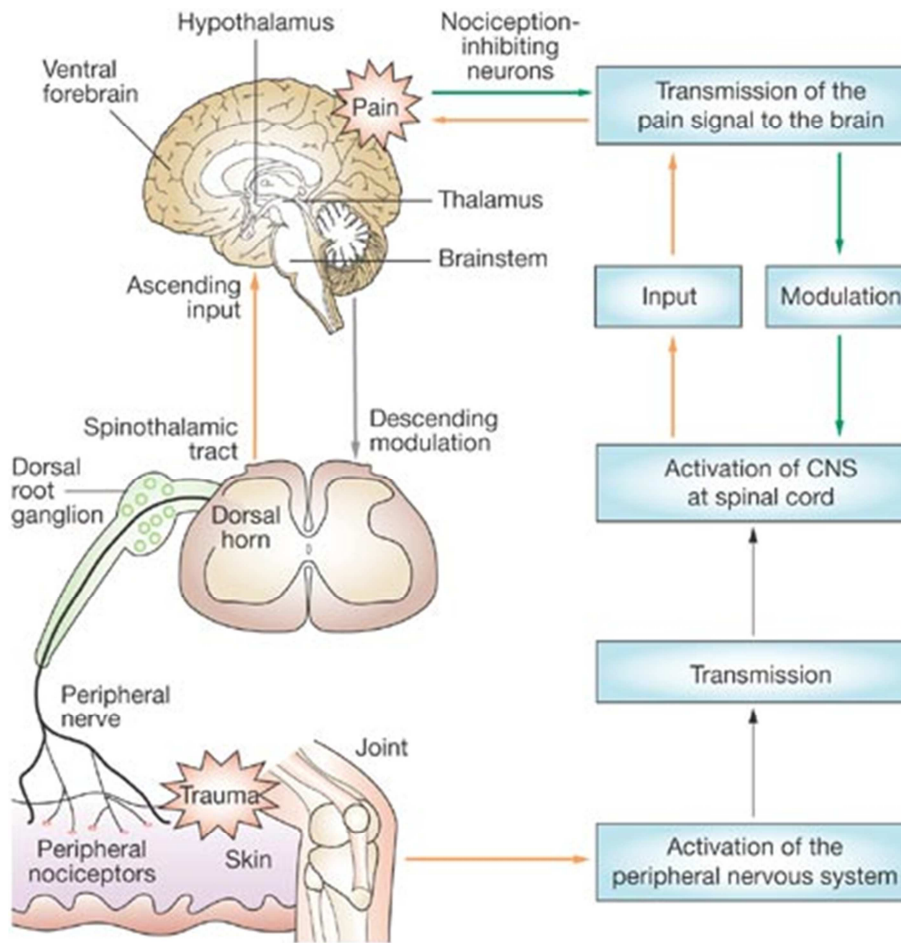
Fig. 1-2 The nociceptive pain pathway. CNS, central nervous system.

It was thought that a sensory input, such as a pinprick, would simply cause a pain "signal" to be sent directly to the brain via a single nerve. Although still not completely understood today, the science of pain reveals a much more complex process, and theories still continue to evolve today. Pain is a conscious experience that emerges from brain activity. The activation of peripheral pain receptors (also called nociceptors) by noxious stimuli, such as tissue injury or chemical mediators, generates signals that travel to the dorsal horn of the spinal cord via the dorsal root ganglion neurons mainly by faster A-delta and slower C-fibers as these detect mechanical, thermal and chemical stimuli. Peripheral pain receptors terminate in the dorsal horn of the spinal cord, where they have connections with many spinal neurons. The signals from dorsal horn are carried along by ascending pain pathway or the spinothalamic tract to the thalamus and the cortex. Then descending signals originating in supraspinal centers can modulate activity in the dorsal horn by controlling spinal pain transmission.
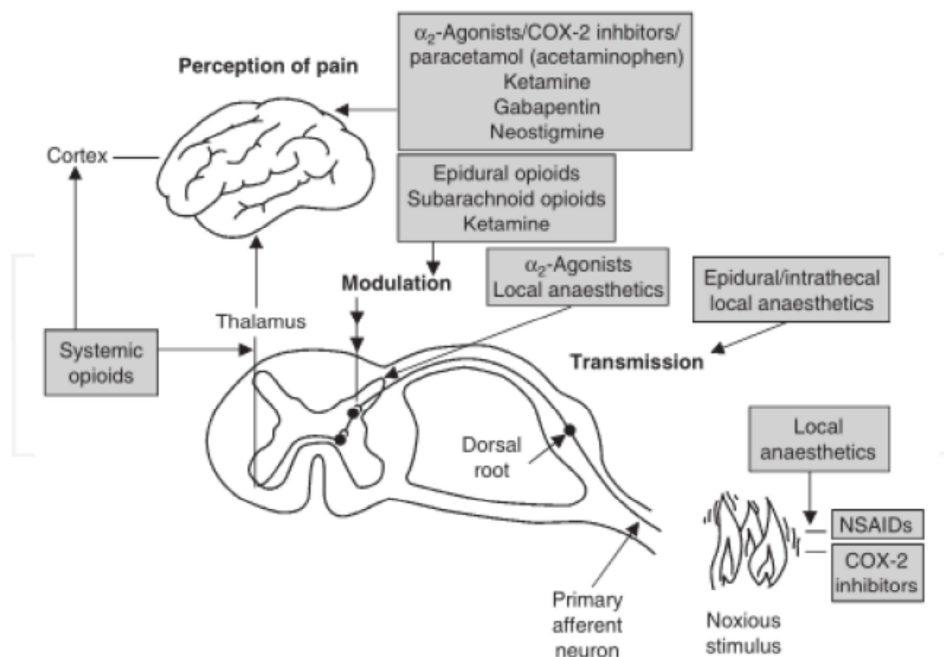
Fig. 1-3 Pain pathway and various sites of action of analgesics.

The effectiveness of treatments can be increased by combining effects of various mechanisms to achieve synergistic effects. Paracetamol (acetaminophen) when combined with NSAIDS (non-steroidal anti-inflammatory drugs) provide additive analgesic effect in mild to moderate acute pain. The synergistic effects of α-adrenergic and opioid systems have been shown with the effects of clonidine potentiating the effects of morphine. Epidural analgesia with a combination of local anaesthetics and opioids is an excellent multimodal method for better analgesia and enhanced recovery. Pain relief can be attained by the conventional pharmacological option of administering opioids like morphine or fentanyl (Gottschalk and Smith, 2001; Bingham et al., 2009). Morphine and fentanyl have been the analgesic drugs of choice for anaesthesia for decades. Cyclooxygenase, the key enzyme for the production of prostaglandins in inflammatory exudates and inhibitors of the COX-2 have similar efficacy to other NSAIDs but have reduced gastrointestinal side effects (Fig. 1-3). (See pharmacology of these drugs in later section).
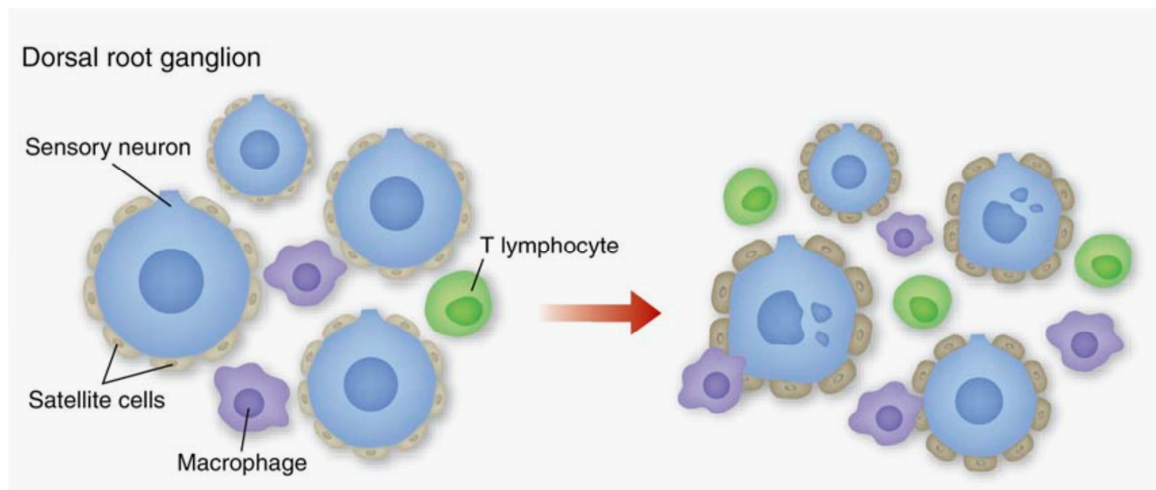
Fig. 1-4 Peripheral inflammatory reactions.

The link between the nervous and immune systems is an important one. Cytokines, a type of proteins found in the nervous system, are also part of the body's immune system. Cytokines can trigger pain by promoting inflammation, even in the absence of injury or damage. After trauma, cytokine levels rise in the brain and spinal cord and at the site in the peripheral nervous system (sensory neurons) where the injury occurred (Fig. 1-4). Immune response in the dorsal root ganglia (DRGs) driven by macrophages, lymphocytes and satellite cells results in peripheral nerve injury.

Pain-peptides such as substance P and calcitonin-gene related peptide (CGRP) are released from sensory neurons due to injury stimulates immune cells like macrophages and synoviocytes which results in secretion of pro-inflammatory cytokines such as TNF-α and IL-6. On the other hand, neurodegeneration causes release of pain-peptides such as substance P and CGRP from sensory neurons which stimulate immune cells to release cytokines. Understanding of the role of cytokines in producing pain, especially pain resulting from injury (Scholz and Woolf, 2007; Chiu et al., 2012), may lead to generation of new classes of drugs that can block the action of these substances.

1.3 ARTHRITIS

Arthritis means joint inflammation, one of the body's natural reactions to disease or injury, and includes swelling, pain, and stiffness. Inflammation that lasts for a very long time or recurs, as in arthritis, can lead to tissue damage. Over time, stiffness, pain, inflammation and loss of movement develop in affected joints. People with arthritis may have difficulty with very basic movements and every day activities, such

as walking, climbing stairs, typing, or brushing their teeth. Arthritis affects 43 million U.S. adults and is the leading cause of disability in the United States. These patients are affected by musculoskeletal signs or symptoms, including limitation of motion and pain of the joint.

1.3.1 Articular joints

Human articular joints are composed of several different tissues (cartilage, calcified cartilage, bone, synovium, ligament, meniscus, and patella) (Fig. 1-5) that function inter-dependently to allow the joint to function for many years under normal conditions. These tissues are all important to the health of the whole joint so if one tissue is compromised, it inevitably has an impact on the others. When this delicate balance between the tissues gets upset, a cascade of abnormal physiological reactions is often triggered, ultimately leading to the total failure of the joint. The primary bearing surface in a synovial joint is the articular cartilage (Fig. 1-5).
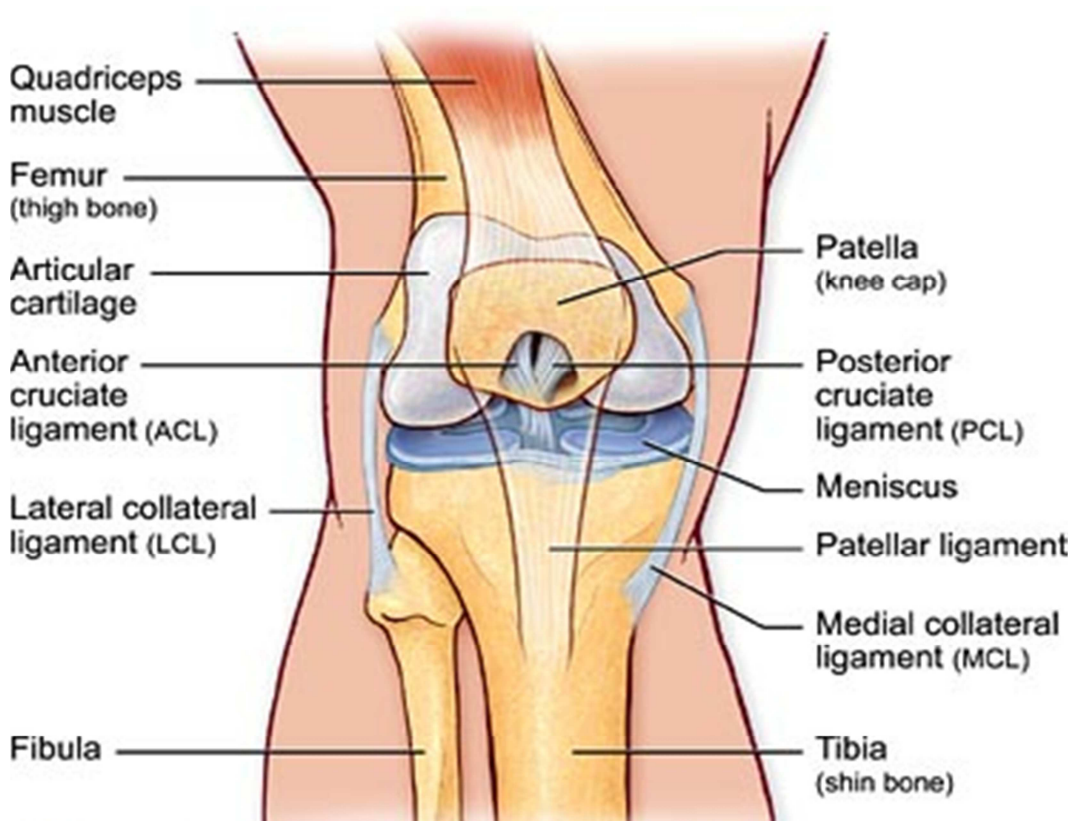
Fig. 1-5. Anatomy of the human knee joint.

A normal knee joint consists of cartilage, meniscus, patella and ligaments (Moskowitz et al., 2004).

The collagen and proteoglycans in the articular cartilage are arranged to withstand primarily tensile and shear stresses at the surface, and compressive stresses in the deeper cartilage layers (O'Connell, 2000). The knee is a "hinge type" joint which is formed by two bones held together by flexible ligaments. The bones are the femur (thigh bone) and the tibia and fibula (shin bone). The knee cap (patella) also forms part of the knee joint. It glides over the end of the femur as the knee bends. The moving parts of a normal knee are covered with a layer of articular cartilage which is a white smooth substance about 1/4 of an inch thick on the patella and 1/8 of an inch thick on the femur and tibia. Synovial membrane is a tissue lining the joint and sealing it into a joint capsule. The synovial membrane secretes synovial fluid (a clear, sticky fluid) around the joint to lubricate it (Moskowitz et al., 2004). Synoviocytes are cells derived from synovial membrane, which contains synovial fibroblasts and macrophages. These cells are involved in the progression of arthritis by producing cytokines.

1.3.2 Rheumatoid arthritis (RA)

This is an inflammatory autoimmune joint disease that occurs in approximately 1% of the human population. RA mainly affects the synovium, the cartilage and subchondral bone but the disease can have systemic effects with increased comorbidity and mortality, particularly due to cardiovascular disease (Wallberg-Jonsson et al., 1997). There are well-developed criteria for the characterization of RA in clinical practice, *i.e.*, the so-called American College of Rheumatology (ACR) criteria (Arnett et al., 1988). Briefly, these are as follows: (1) morning stiffness, (Flynn and Clark) arthritis of 3 or more joint areas, (3) arthritis of the hand joints, (4) symmetrical arthritis, (5) presence of rheumatoid nodules, (6) detectable serum rheumatoid factor (RF), and (7) radiographic changes. An assay using anti-cyclic citrullinated peptide/protein antibody, with higher specificity than for RF but equal sensitivity has been developed, increasing diagnostic capability for RA (Rantapaa-Dahlqvist, 2005).

The exact mechanisms of disease initiation and propagation are still essentially unknown. However, research on the etiology of RA has been, and still is, extensive and it is now well-established that genetic factors, both human leukocyte antigen (HLA) and non-HLA genes are important for disease onset (Gregersen, 1999; Bowes and Barton, 2008). The disease is characterized by joint inflammation, *i.e.* synovitis (inflammation in the synovium) together with hyperplasia (thickening of the synovial

membrane) leading to pannus formation. Cartilage and bone destruction gradually appear, in the end leading to deformity of the inflamed joints which in the case of the knee joints, eventually may lead to prosthesis operations. Nevertheless, RA is a multifactorial disease in which environmental and life-style factors, *e.g.*, obesity and smoking, are potentially relevant (Symmons, 2003). No curative treatment is available but disease modifying anti-rheumatic drugs (DMARDs) (*e.g.*, methotrexate, sulphazalasine, leflunomide, *etc.*) can reduce the symptoms when used efficiently. Treatment has recently been improved by the use of drugs targeting tumor necrosis factor alpha (TNF-α) (Emery, 2006). For evaluation of disease status, several clinical parameters are employed. Laboratory analyses of both C-reactive protein (CRP) and erythrocyte sedimentation rates (ESR) are valuable, and easily performed, procedures for estimating the degree of inflammation. To evaluate response of the disease to therapy over time, disease activity scores (DAS) are calculated. These are based on the number of tender and swollen joints, patients global assessment (visual analogue scale, VAS) and ESR. DAS has been validated in different studies and currently used with a DAS score of 28 (Prevoo et al., 1995).

1.3.3 Osteoarthritis (OA)

OA of the joints is a common disease affecting humans but its prevalence increases with age. OA can be primary or secondary to trauma, surgery, infection or other disease processes. OA of the joint is diagnosed using Altman's diagnostic criteria (Altman et al., 1986). The disease is caused by an imbalance in cartilage metabolism, *i.e.*, levels of synthesis *vs.* destruction, which leads to degradation of cartilage. There is also inflammation in the synovium and damage to the subchondral bone. The processes of OA are very complex and its etiology is not well defined. Many different mediators in various cell types are involved including cytokines, growth factors, matrix metalloproteinases (MMPs) and chondrodegradative enzymes (Moskowitz et al., 2004). When the disease is very pronounced, a knee joint prosthesis operation may have to be performed. The extent of involvement in the knee joint OA is determined radiographically and graded according to Ahlback's criteria (Ahlback, 1968).

1.4 NON-NEURONAL AND NEURONAL INVOLVEMENT IN THE PROGRESSION OF ARTHRITIS

1.4.1 Synovial tissue and its cells

The synovial membrane in normal joints is thin, consisting of only a few layers of cells. In the deep parts, it is composed of loose connective, fibrous and adipose tissues (Fig. 1-5). Collagen, particularly type I and III, fibronection and proteoglycans are present in the matrix of the synovium. Main functions of the synovium are production of synovial fluid and removal of debris from the joint space. The cells in normal synovial tissue are predominantly phagocytic cells, generated from monocytes (tissue specific macrophages) and fibroblasts. The synovium in patients with RA is hypertrophic and contains numerous mononuclear cells (Fig. 1-6). Pannus tissue, the destructive tissue in RA, is a hypertrophic and inflammatory synovial tissue localized at the junction of the synovial lining and cartilage and bone. Macrophages and fibroblast-like synoviocytes (FLS) are the predominant cell types in the inflamed synovium (Tak and Bresnihan, 2000). The macrophages are particularly important for inflammation in RA due to a high density around the inflamed synovial membrane and at the cartilage-pannus junction (Mulherin et al., 1996; Kinne et al., 2007); they are pro-inflammatory and major contributors to the joint destruction via secretion of cytokines and MMPs.

Normal   **Rheumatoid Arthritis**

inflamed synovial membrane

synovial membrane

cartilage

major cell types:
T lymphocytes
macrophages

capsule

pannus

minor cell types:
fibroblasts
plasma cells
endothelium
dendritic cells

synovial fluid

major cell type:
neutrophil

NORMAL   **OSTEOARTHRITIS**

Subchondral bone cyst

Thickened joint

Capsule joint

Inflammation of the synovitis membrane

Synovium membrane

Early degeneration of articular cartilage

Articular cartilage

Cartilage cap of ostephyte

Joint cavity

Bone of ostephyte

Bone

'Fibrillated' cartilage

Altered bone turnover, "sclerosis" on radiograph

Fig. 1-6. A schematic overview of an arthritic joint.

In RA, synovium becomes hyperplastic and synovial fluid level increases, whereas OA causes degradation of cartilage and osteophyte formation. In both conditions, immune cells starts producing cytokines which results in cartilage and synovium degradation (Ahlback, 1968).

13

The FLS are, together with osteoclasts, involved in the processes of bone erosion and destruction of cartilage plus bone (Goldring and Gravallese, 2000; Abeles and Pillinger, 2006). They function in a direct manner by secreting MMPs and indirectly by secreting cytokines leading to recruitment of many other cells such as monocytes, lymphocytes, neutrophils and mast cells (Abeles and Pillinger, 2006). Lymphocytes, neutrophils and mast cells also participate in the process(es) of joint destruction in RA (Tak and Bresnihan, 2000). It is well-established that both T- and B-lymphocytes in the synovium play central roles in the pathogenesis of RA (Bugatti et al., 2007; Lundy et al., 2007), being important, not least for autoantibody production, whilst T-lymphocytes contribute to inflammation and tissue destruction (Bugatti et al., 2007; Lundy et al., 2007). Fine venules and capillaries occur beneath the lining cells of the synovium. These superficial vessels have a fenestrated endothelium via which fluid transudates in order to contribute to the joint fluid; larger vessels are present in the deep parts of the synovium. Angiogenesis is crucial for the formation of the pannus in RA; hence, the ingrowth of arterioles and venules occurs in the deep parts of the synovium. In this context, it is known that vascular endothelial growth factor (VEGF) plays an important role for the angiogenesis in RA synovium (Malemud, 2007). There are also several other factors which are of potential interest in the neo-angiogenesis in RA, *e.g.*, growth hormone and insulin like growth factor-1 (IGF-1) (Malemud, 2007).

1.4.2 Mechanoreceptors and chemical receptors

The knee joint mechanoreceptors consist of pacinian and Ruffini corpuscles that respond to mechanical pressure and distortion. These are mainly present in joint capsule, ligaments and menisci. Pacinian corpuscles are free nerve endings sensitive to small changes in deformation caused by mechanically applied pressure and initiate vigorous discharge of electrical potentials during acceleration or deceleration of the moving joint. Therefore, pacinian corpuscles are fast-adapting receptors initiating signal when there is dynamic change in the joint motion and joint deformation, while being insensitive to constant or steady movement. Ruffini mechanoreceptors are thinly encapsulated and sensitive to low level mechanical deformation. The Ruffini endings are slow-adapting, which implies that they may register changes in tissue stress and strain as well as continue to signal the new steady state for prolonged periods of time. These receptors have static and dynamic factors present in joint

angle, velocity and intra-articular pressure and strain and are mainly found in the ligaments, joint capsule and menisci.

Chemoreceptors respond to water-soluble and lipid-soluble compounds that contact their cell membranes. Chemoreceptive neurons in the CNS respond to changes in the pH and carbon dioxide concentrations of the cerebrospinal fluid; those along arterial trunks monitor the oxygen content of the blood. Chemical signal transmission is a key process for intracellular communication; in neurons, neurotransmitters are accumulated in the synaptic vesicles and are released upon stimulation and these released neurotransmitters stimulate target cells by binding to the specific receptors. The cytokine like IL-1 binds to specific receptor (IL-1 receptor) on immune cells (e.g. macrophages, synoviocytes) to transduce signal to signaling molecules (IKK and IkB) by phosphorylation, then NF-κB binds to promoter, and transcription and translation of genes occur which result in release of other pro-inflammatory cytokines, such as IL-6 and TNF-α. Many drugs based on disruption of cytokines binding to their receptors are currently under development. Toll-like receptors (TLRs) are responsible for the recognition of pathogen-associated molecular patterns expressed by a wide spectrum of infectious agents. TLRs activate the NF-κB pathway, which regulates cytokine expression through several adaptor molecules. Activation of the NF-κB pathway links innate and adaptive immune response by production of inflammatory cytokines such as IL-1, IL-6, IL-8, TNF and IL-12. Activation of TLRs by the cytokines and other components in knee joint then results in release of other pro-inflammatory cytokines. TLR4 is a receptor and signaling molecule, responding to bacterial lipoproteins like LPS, which has been implicated in inflammation.
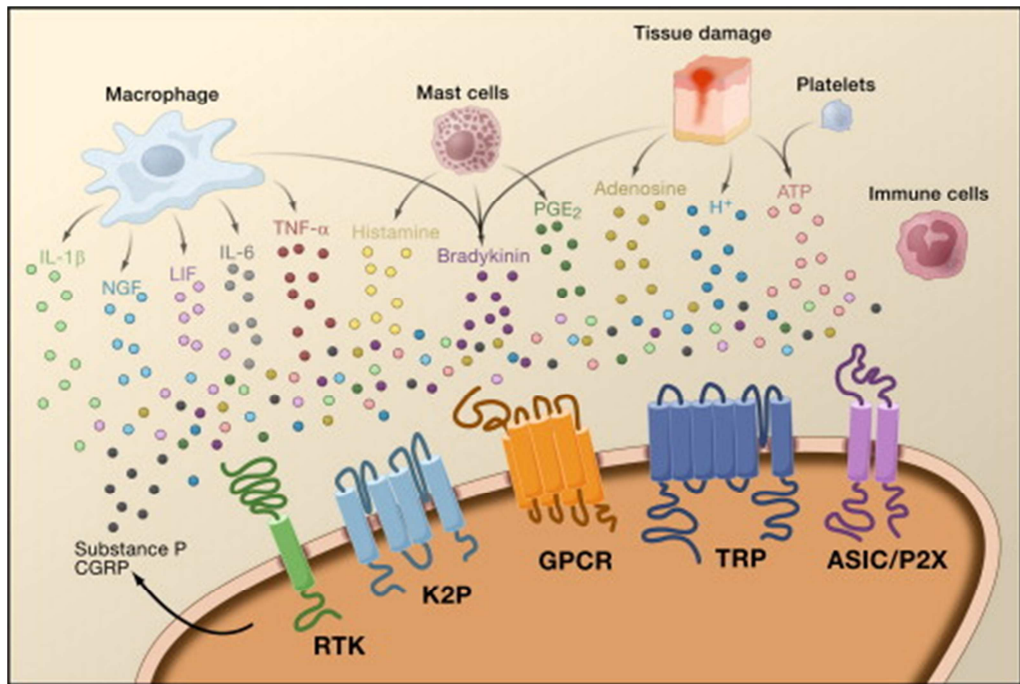
Fig.1-7 Peripheral Mediators of Inflammation.

The tissue damage due to injury leads to the release of inflammatory mediators by activated sensory nerves or non-neural cells like macrophages, fibroblasts, neutrophils, and mast cells that infiltrate into the injured area. This mixture of inflammatory mediators of signalling molecules include serotonin, histamine, glutamate, ATP, adenosine, substance P, CGRP, bradykinin, eicosanoids (prostaglandins, thromboxanes, leukotrienes), endocannabinoids, nerve growth factor (NGF), TNF-α, IL-1β, extracellular proteases, and protons. These mediators act directly on the nociceptor by binding to one or more cell surface receptors, including G protein-coupled receptors (GPCR), Transient Receptor Potential channels (TRP), acid-sensitive ion channels (ASIC), two-pore potassium channels (K2P), and receptor tyrosine kinases (RTK) (Fig. 1-7). These interactions enhance excitability of the nerve fibre, thereby increasing its sensitivity to temperature or touch. TRPV1, a member of the transient potential family of receptors allows transient influx of cations, can be activated by a diverse variety of stimuli, including heat, acid and capsaicin. Abnormal activation at peripheral neurons contributes to neuropathic pain and the inflammatory response at damaged tissue. TRPV1 also found on non-neuronal cells like synoviocytes where it initiates signaling that culminates in pain perception in inflammatory diseases (Julius, 2013).

Receptors that are classified according to the source of the stimulus are placed in one of the following three categories: exteroceptors, proprioceptors, or interoceptors. Proprioception is conscious and/or unconscious perception of position and movement of an extremity or a joint in space. Knee proprioception derives from the integration of afferent signals from proprioceptive receptors in different structures of the knee and is influenced by signals from the outside of the knee. Proprioceptive information is used to protect the knee against possible injurious movements by reflex response. Impairment in proprioception was reported in OA. Exteroceptive receptors respond to stimuli from external environment including visual, auditory and tactile stimuli, while interceptive receptors detect internal events such as change in blood pressure. Exteroceptive receptors are located on the surface of the bodies of animals and humans (including the mucous membranes of the nose, mouth, and tongue). Depending on the nature of the stimulus perceived, a distinction is made between mechanoreceptors of the skin (tactile), chemoreceptors (gustatory and olfactory organs) and thermoreceptors of the skin. Primary interoceptive representation in the dorsal posterior insula engenders distinct highly resolved feelings from the body that include pain, temperature, itch, sensual touch, muscular and visceral sensations (Knoop et al., 2011).

1.4.3 Joint innervations

It has been observed that knee joints are supplied with sensory, sympathetic nerve endings and mechanoreceptors (Samuel, 1952; Skoglund, 1956; Heppelmann, 1997), and these have studied in both normal and inflamed joint tissue (Heppelmann, 1997). The innervation pattern consists of group I – IV sensory afferents and sympathetic fibres (Table 1-1) (Heppelmann, 1997).

Peptide containing sensory (Saito and Koshino, 2000) as well as sympathetic (Miller et al., 2000) nerve fibres have been found in the human knee joint synovium. The presence of substance-P (SP) in the sensory innervation in animal joints has been frequently documented (Miller et al., 2000).

Table 1-1 List of articular nerve endings in knee joints
(Heppelmann, 1997).

Type	Morphology	Location	Parent nerve fibres	Behavioural characteristics
I	Thinly encapsulated globular corpuscles (100 x 40µm)	Fibrous capsule of joint (mainly superficial layers)	Small myelinated (6-9µm)	Static and dynamic mechanoreceptors; low-threshold, slow adopting
II	Thickly encapsulated conical corpuscles (280 x 120 µm), in a cluster of 2-4 corpuscles	Fibrous capsule of joint (mainly deeper layers). Articular fat pads	Medium size myelinated (9-12 µm)	Dynamic mechanoreceptors low threshold, rapidly adapting
III	Thinly encapsulated fusiform corpuscles (600 x 100 µm)	Joint ligaments (intrinsic and extrinsic)	Large myelinated (13-17 µm)	Dynamic mechanoreceptors; high threshold, very slow adapting
IV	Plexuses and free nerve endings	Fibrous capsule, articular fat pads, ligaments and walls of blood vessels	Very small myelinated (2-5 µm) Unmyelinated (<2 µm)	Pain receptors; high threshold, non-adapting

It has been suggested that an imbalance between sympathetic and sensory innervation in the arthritic joint may be of importance for the inflammation therein (Weidler et al., 2005). Interestingly, findings from studies on rat knee joints indicates that monoarthritis leads to increase in neuropeptide levels in the synovial fluid (Bileviciute et al., 1993); likewise, SP and calcitonin gene-related peptide (CGRP) in the spinal cord (Mapp et al., 1993).

The main function of sensory nerves in joints is to detect and transmit mechanical information to the central nervous system. The process of pain in arthritis is, to a large extent, unknown although much effort has been made in understanding this process (McDougall, 2006). Nevertheless, early studies showed that sensory denervation with capsaicin attenuated inflammation and nociception in arthritic rats (Cruwys et al., 1995). Joint innervation is of interest as the nervous system generally is assumed to be involved in the development of arthritis. For example, it is known that the paralytic limb of hemiplegic patients with RA is spared from the inflammatory process (Thompson and Bywaters, 1962; Glick, 1967). The involvement of the richly-innervated peripheral joints in RA also suggest that this may be of importance in the pathogenesis of RA (Konttinen et al., 2006). Neuro-immune pathways are, on the whole, suggested to be important for the modulation of arthritic processes (Kane et al., 2005).

The joint nerves contain sensory, Aβ-, Aδ- and C-fibers. Under normal physiological conditions, nociceptive signals are produced by intense stimulation of primary afferent sensory A and C nerve fiber terminals by chemicals, thermal and mechanical stimuli in the joints. The first relay in pain pathways activated by Aδ- and C-nociceptors is the spinal dorsal horn and, as such, this represents an important site for the modulation of pain signals. Corpuscular endings of Aβ-fibers have been identified in the ligaments and the fibrous capsule. Sensory nerve endings were found in all structures of the joint except the normal cartilage (Wong, 1993; Riedel and Neeck, 2001; Grubb, 2004). Pain is elicited when noxious mechanical, thermal and chemical stimuli are applied to the fibrous structures such as ligaments and fibrous capsule. While most fibers in the Aβ-fiber range show responses to innocuous movements of the joints, a large number of Aδ- and C-fibers show thresholds for noxious stimuli. One group of so-called "silent nociceptors" of mainly C-fibers consisting does not respond even to noxious mechanical stimuli of the normal joint (Schaible et al., 2006; Schaible, 2007); they begin to respond to mechanical stimulation during inflammation of the joint.

1.4.4 Synovial joint fluid

This consists of hyaluronic acid produced by the lining cells and fluid from superficial capillaries and venules, together with low molecular weight proteins. Normal synovial fluid has a high viscosity and is difficult to aspirate. However, a synovial fluid sample

from a patient with inflammatory arthritis, *e.g.*, RA, has a lower viscosity and contains numerous polymorphonuclear cells (Choy and Panayi, 2001; Dieppe and Lohmander, 2005). Inflammatory markers and nerve signaling substances can also be detected in the synovial fluid from patients with RA or OA.

1.4.5 Articular cartilage

The ends of all the bones at the joint are covered by articular cartilage. This is a glistening white substance that has the consistency of firm rubber. However, it is actually a mixture of collagen and special large, sponge-like molecules that are maintained by living cells (chondrocytes). Hyaline cartilage is found on the joint surfaces of the bones forming the knee joint. It functions as the self-lubricating, low-friction gliding and load-distributing joint surface. This articular cartilage, as well as other types of cartilage, contain two types of cells – chondrocytes and chondroblasts (A chondroblast is a cell which originates from a mesenchymal stem cell and forms chondrocytes, commonly known as cartilage cells). Furthermore, articular cartilage is made up of a fibrillar meshwork of collagen II fibres and proteoglycans (Dieppe and Lohmander, 2005). The chondrocytes have secretary capacities, not least including production of collagen and chondromucoprotein. The articular cartilage obtains nutrients from the synovial fluid. The level of proliferation of chondrocytes in healthy individuals is limited, as is the level of penetration of other cell types from the joint cavity into the articular cartilage (Otero and Goldring, 2007). The destruction of cartilage in arthritis occurs at the junction between the pannus and cartilage (Kobayashi and Ziff, 1975; Woolley et al., 1977). Both FLS and macrophages can attach to the cartilage and initiate the destruction by secreting proteinases (Edwards, 2000). The chondrocytes respond to different mediators by alteration in their metabolism and can start to produce and secrete pro-inflammatory factors such as nitric oxide and prostaglandin E2 (PGE2) (Otero and Goldring, 2007). Osteoclasts (bone-resorbing cells) also contribute to the destruction of cartilage (Bromley and Woolley, 1984; Gravallese et al., 1998).

1.4.6 Cytokines in arthritis disease progression

The immunology of RA synovial inflammation actually involves numerous pro-inflammatory cytokines and extensive research in this area has been made during the past two decades. Cytokines are mainly produced by monocytes and macrophages,

but also by other cells such as lymphocytes and fibroblasts (Chu et al., 1991). Pro-inflammatory cytokines such as TNF-α, interleukin-1 (IL-1β), IL-6, IL-15 among others are of great importance in the pathogenesis (Fig.1-8) and inflammatory processes in RA (Koch et al., 1995). TNF, IL-1, IL-6 and IL-17 upregulate the expression of RANKL (receptor activator of NF-κB ligand) in osteoblasts and synovial fibroblasts. RANKL mediates differentiation, survival and activation of osteoclasts. It also has a function in the immune system, where it is expressed by T helper cells and is thought to be involved in dendritic cell maturation. Osteoprotegerin (OPG), a member of the tumour necrosis factor receptor superfamily, is a soluble decoy receptor for the osteoclast differentiation factor RANKL that inhibits interaction between RANKL and its membrane-bound receptor RANK. RANKL exhibits several properties with relevance to atherogenesis, such as promotion of inflammatory responses in T cells and dendritic cells, induction of chemotactic properties in monocytes, induction of matrix metalloproteinase (MMP) activity, which also play role in inflammation.

TNF-α, produced by fibroblasts and macrophages, promotes differentiation and survival of osteoclasts. IL-6 is largely produced by fibroblasts and macrophages; it enhances the expression of RANKL and contributes to the induction of Th17 cells. Th17 cells secrete IL-17, but mast cells are probably a main source of synovial IL-17 (Fig. 1-8). TNF-α is a potent inducer of other important cytokines such as IL-1β, IL-6 and also MMPs. TNF-α is found in elevated levels in synovial fluid and highly expressed in the pannus from patients with RA (Saxne et al., 1988; Chu et al., 1991; Brennan et al., 1992). It is also involved in peripheral mediation of neuropathic pain. There are two cellular receptors for TNF-α, TNFR1 and TNFR2, which are present in circulating blood and synovial fluid following cleavage of the extracellular portions by proteases (Cope et al., 1992). Both receptors' distinct and overlapping signal transduction pathways lead to a range of cellular responses, which include cell death, survival, differentiation, proliferation and migration. The biological function of TNF-α is a host defense to bacterial, viral and other infections but its excessive production can lead to the inflammation. For example, over-production of TNF-α in knee joint causes inflammation in RA and OA.

IL-6, produced by T-cells, monocytes, macrophages and FLS, is also of importance for synovial inflammation in RA (Van Snick, 1990). IL-6 acts as both a pro-inflammatory and anti-inflammatory cytokine. IL-6's anti-inflammatory role is

mediated through its inhibitory effects on TNF-α and IL-1, and activation of IL-1ra (IL-1 receptor antagonist) and IL-10. Other main functions of IL-6 are promoting the development of B-cells into plasma cells, induction of C-reactive protein (CRP), formation of osteoclasts and proliferation of FLS (Van Snick, 1990). IL-6 also plays a role in establishing the FLS phenotype, including the induction of FLS proliferation. Release of IL-6 by FLS may induce further FLS activation and proliferation. This could explain elevated levels of IL-6 in synovial fluid and sera of patients with RA (Houssiau et al., 1988). It has been shown that IL-6 contributes to the production of autoantibodies such as RF (rheumatoid factor) and anti-citrullinated peptide antibody and leads to RA. Increased angiogenesis and vascular permeability of synovial tissue, a pathological feature of RA is also induced by IL-6. Therefore, IL-6 plays important role in immunological abnormalities which lead to joint inflammation in RA and OA.
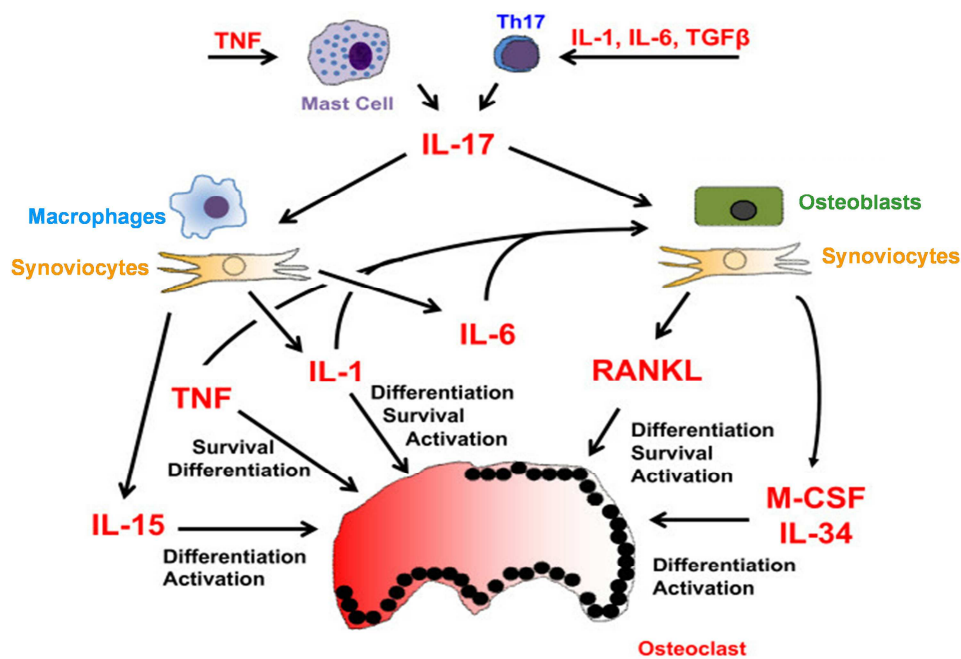
Fig. 1-8. *The role of cytokines in arthritis. (Braun and Zwerina, 2011).*

IL-1β is mainly produced by monocytes and macrophages, but also by B- and T-cells (Koch et al., 1995). It is an important pro-inflammatory cytokine which can induce secretion of TNF-α and chemokines from chondrocytes and fibroblasts (Arend and Dayer, 1990). IL-1β can also stimulate release of MMPs from fibroblasts and chondrocytes (von Banchet et al., 2007).

1.5 CURRENT AVAILABLE TREATMENTS FOR ARTHRITIS

Analgesic therapies for acute and chronic pain conditions currently rely on three major classes of drugs: nonsteroidal anti-inflammatory drugs (NSAIDs), opioids, and a group of drugs with diverse pharmacological actions collectively known as adjuvants (antidepressants, anticonvulsants, local anaesthetics, 2-adrenoceptor agonists) (Brown, 2000; Colmegna et al., 2012). The systemic administration of both NSAIDs and opioids exhibit a variety of adverse actions (nausea, vomiting, gastric ulcer, kidney failure, liver failure, respiratory depression, cough suppression, etc.), and many chronic pain states are not adequately controlled by these agents, particularly those involving nerve injury (Brown, 2000; Mugnier and Bouvenot, 2000; Saag et al., 2008; Tugwell et al., 2011). With adjuvants, it is often necessary to titrate the dosage until adequate pain relief or intolerable side effects develop. Unfortunately, the latter outcome often occurs, and the degree of pain relief that results is only partial. An alternative important approach to pain control is to apply drugs locally to the peripheral site of origin of the pain. This can be attained by the topical application of a cream, lotion, gel, aerosol, or patch to skin or by injections directly into the joints. These application methods allow a higher local concentration of the drug at the site of initiation of the pain and lower or negligible systemic drug levels, producing fewer or no adverse drug effects. Other potential advantages of localized applications are the absence of drug interactions, this lack of need to titrate doses to tolerability and, importantly, the ease of use. Both acute and chronic pain conditions are likely to be amenable to this approach but, to date; there are only a limited number of topical therapies available for the relief of somatic pain (Mugnier and Bouvenot, 2000; Senolt et al., 2009; Tugwell et al., 2011).

1.5.1 Non-steroidal anti-inflammatory drugs (NSAIDs)

The major effect of NSAIDs is anti-inflammatory antinociceptive by inhibiting cyclooxygenase enzymes and later decrease the level of prostaglandins such as PGE2 (Kidd et al., 2007). The COX enzyme converts arachidonic acid liberated from the phospholipid membrane by phospholipases to prostanoids such as prostaglandins. Two forms of COX are well characterized, a constitutive form (COX1) that is normally expressed in tissues such as stomach and kidney and plays a physiological role in maintaining tissue integrity, and a form that is induced by inflammatory mediators (COX2) which serves a significant role in pain and inflammation (Edwards

et al., 2005). The potential clinical benefit of COX-2 inhibitors is significant due to the number of patients chronically treated with NSAIDs and the higher risk of gastrointestinal injury and death associated with traditional NSAIDs. Systemic administration of NSAIDs is also associated with several side effects, including nausea, vomiting, diarrhea, constipation, decreased appetite, rash, dizziness, headache, and drowsiness.

1.5.2 Opioids

The central effects of opioids on pain transmission by acting within the dorsal horn of the spinal cord, at brainstem and other supraspinal sites have been recognized for some time. Patients who are not responsive to NSAIDs are treated with opioids. The main active agent in opioids is morphine, which is used to treat many forms of chronic pain in humans. Opioid receptor subtypes were identified by their different anatomical location and pharmacological profiles of compounds that eventually used to name them, i.e. morphine (μ), ketocyclazocine (κ) and vas deferens (δ). These 3 different types of opioid receptors- the μ, δ and κ- which are widely expressed in both central and peripheral nervous systems (Bidlack, 2000). The pharmacodynamic response to an opioid depends upon the receptor to which it binds, its affinity for that receptor, and whether the opioid is an agonist or an antagonist. for eg, a μ acts as spinal and supraspinal analgesia, δ as spinal analgesia and κ receptor as spinal analgesia and supraspinal analgesia. Activation of these receptors inhibits the formation of cAMP, close voltage-gated Ca^{2+} channels and opens inwardly rectifying K^+ channels. The net effect of these cellular actions is to reduce neuronal excitability and neurotransmitter release (Dieppe and Lohmander, 2005; Kidd et al., 2007). The opioid drugs produce analgesia by acting at several levels of the nervous system, causing inhibition of neurotransmitter release from the primary afferent terminals in the spinal cord and activation of descending inhibitory controls in the midbrain. The main side effect of opioids is constipation, nausea and vomiting.

1.5.3 Corticosteroids

This therapy for RA acts mainly through the reducing circulating monocytes plus macrophages and cytokine secretion which, in turn, inhibits collagenase and prostaglandins (Kidd et al., 2007). The most commonly used corticosteroids are glucocorticoids which exert anti-inflammatory effect by binding of glucocorticoid or

glucocorticoid receptor complex to glucocorticoid responsive element in the promoter region of genes or transcription factor such as nuclear factor-κB which causes inhibition of translation and transcription of cytokines. Intra-articular injection of corticosteroid cause a significant reduction in pain and tenderness in OA. Patients are treated with corticosteroids if they not respond to other drugs. However, steroids possess numerous side effects which include bone loss, increased susceptibility to infection, osteoporosis and peptic ulcers.

1.5.4 Disease-modifying anti-rheumatic drugs (DMARDs)

These are often given to patients as combination therapy with NSAIDs. This category of drugs includes hydroxychloroquine, methotrexate, auranofin, sulfasalazine, d-penicillamine, cyclosporine, azathioprine and cyclophosphamide (Breedveld and Combe, 2011; Curtis and Singh, 2011, 2011).

DMARDs alleviates arthritis pain by decreasing inflammation eg. Sulaphasalamine lowering the translocation of NF-kB into the nucleus by inhibiting IkB-alpha kinase which results in inhibition of cytokines and chemokines (De Silva et al., 2010). Methotrexate inhibits T-cell activation and proliferation, down regulates the expression of some activation and adhesion molecules, for example, intercellular adhesion molecule-1, decreases immunoglobulin production, inhibits cyclooxygenases and lipooxygenases, and modulates monocyte and macrophage secretion of various cytokines. Methotrexate is effectively used to treat RA but this therapy has some limitations. Azathioprine is an immunosuppressant, which inhibits the enzyme required for DNA synthesis in dividing cells like T-cells, macrophages and B-cells, thereby blocking immune response. Cyclophosphamide is another immunosuppressant, it adds alkyl group to guanine bases of DNA and inhibits DNA synthesis in proliferating cells like T-cells which produce cytokines.

1.5.5 Anti-cytokine therapy

Cytokines released from immune cells, chondrocytes and synoviocytes have ability to stimulate the release of other pro-inflammatory cytokines. There are many different cytokines involved; however, TNF-α plays a major role by initiating and maintaining the inflammatory cascades. TNF-α stimulates production of many different cytokines and tissue degradative enzymes such as MMPs (Fernandes et al., 2002). TNF-α is produced mainly by macrophages, monocytes, T cells, B cells and synoviocytes, and

its levels increase upon disease onset. An anti- antibody against TNF-α has been shown to significantly decrease joint pain and inflammation (Barrera et al., 2001; Burmester et al., 2013). Five anti-TNF-α agents are available for RA treatment including infliximab, etanercept, golimumab, adalimumab and certolizumab pegol (Colmegna et al., 2012) (Table 1-2). Tocilizumab, another example of an anti-cytokine therapy, is an anti-IL-6 drug. This is a humanized mAb combining the complementarity-determining region of a murine anti-human-IL-6R (IL-6 receptor) with human IgG1 antibody. Tocilizumab inhibits IL-6 receptor signaling (Emery et al., 2008; Fujimoto et al., 2008) (Table 1-2).

Interleukin 1 (IL-1) is a general name for two distinct proteins, IL-1α and IL-1β, that are considered the first of a small (but possibly growing) family of regulatory and inflammatory cytokines (Bazan et al., 1996). IL-1α and IL-1β are synthesized as 31-33 kDa, variably glycosylated pro-cytokines that share 25% amino acid (aa) identity across their entire precursor structure, and 22% aa identity over their mature segments (March et al., 1985). IL-1α and IL-1β share same type of biological activities following binding to the IL-1R (IL-1 receptor). Thus, IL-1α and IL-1β differ in the subcellular compartments in which they are active as well as distinct intracellular metabolism/processing; IL-1α is mainly active as a cytosolic precursor (31 kD), while IL-1β is active only in its secreted form. Blockade of IL-1 release has recently been developed to treat RA. IL-1α and IL-1β are produced by macrophages, monocytes, lymphocytes and fibroblasts. Binding of IL-1 to IL-1R leads to production of other cytokines like IL-6 and TNF-α. Anakinra is an interleukin-1 (IL-1) receptor antagonist (Table 1-2), it blocks the biologic activity of naturally occurring IL-1, inflammation and cartilage degradation associated with RA, by competitively inhibiting the binding of IL-1 to the IL-1 type receptor, which is expressed in many tissues and organs (Fleischmann et al., 2006).

Table 1-2. Current biological agents to treat arthritis

(Fleischmann et al., 2006; Emery et al., 2008; Fujimoto et al., 2008; Caporali et al., 2009; Colmegna et al., 2012)

Agent	Structure	Pharmacology
Abatacept	Recombinant CTLA4 molecule dimerized to IgG	Blocks T-cell co-stimulation by preventing antigen-presenting cells (APCs) from delivering the co-stimulatory signal to T cells to fully activate
Adalimumab	Monoclonal antibody (Mab) against TNF-α	Reduces inflammatory reaction by binding to TNF-α preventing it from activating TNF receptors
Anakinra	Recombinant IL-1 receptor antagonist	Competitively inhibits the binding of naturally occurring IL-1 to the ILR1
Certolizumab pegol	Pegylated Mab Fab fragment from humanized TNF-α	A monoclonal antibody directed against TNF-α
Etanercept	Recombinant TNF-α receptor dimerized on IgG1	Functions as a decoy receptor that binds to TNF and reduces the effect of naturally present TNF
Golimumab	Human Mab against TNF-α	TNF-α inhibitor used as immunosuppressive drug
Infliximab	Chimeric Mab against TNF-α	Binds to the TNF-α and inhibits or prevents the effective binding of TNF-α with its receptors
Rituximab	Chimeric Mab against CD20	Destroys overactive or dysfunctional B-cell by binding to CD20 expressed on these cells
Tocilizumab	Humanized Mab against IL-6R	Binds soluble as well as membrane bound interleukin-6 receptors, hindering IL-6 from exerting its pro-inflammatory effects

CTLA4, cytotoxic T-lymphocytes antigen 4; IL, interleukin; TNF-α, tumour necrosis factor alpha.

1.6 SNARES CYTOKINES, NEUROPEPTIDES AND BOTULINUM NEUROTOXINS

Exocytosis is a multistage process involving a fusion between the vesicle and the plasma membranes, leading to the formation of a channel, through which secretions are released from the vesicle to the cell exterior (Jahn et al., 2003; Jahn, 2004). In neurons and non-neuronal cells, signalling molecules are stored in membrane-bound secretory vesicles inside the cells and are released into the extracellular space after fusion of the secretary vesicle membrane with the plasma membrane. SNARE [soluble-NSF (N-ethylmaleimide-sensitive factor) attachment receptor] proteins drive membrane fusion and contribute to membrane/protein targeting and delivery in all eukaryotic cells. This SNARE complex is formed from syntaxin 1, SNAP-25 (Synaptosomal-associated protein 25) and VAMP (Vesicle associated membrane proteins) (Jahn et al., 2003). The vesicular membrane carries a v-SNARE and the target membrane, a t-SNARE. In neuronal exocytosis, syntaxin and synaptobrevin are anchored in respective membranes by their C-terminal domains, whereas SNAP-25 is tethered to the plasma membrane via several cysteine-linked palmitoyl chains. The core SNARE complex is a four-α-helix bundle, where one α-helix is contributed by syntaxin-1, one α-helix by synaptobrevin and two α-helices are contributed by SNAP-25. Thus, progression of SNARE-mediated fusion can be divided into a step-wise process involving – a) assembly of free SNAREs into an acceptor complex, a process probably mediated by the SM (Sec-Munc proteins) proteins, b) association with VAMP from synaptic vesicles to form a loose trans-SNARE complex and c) creation of tight SNARE complexes which is catalysed by complexins and syntaxin and formation of a stable cis-SNARE complex. For vesicle fusion influx of Ca^{2+} into the cell is required. Synaptotagmin and SV2 (synaptic vesicle protein) are present on synaptic vesicles and act as calcium sensors which regulate Ca^{2+} at the synapse. The two SNAREs can form a fusion particle with energy input from the hydrolysis of ATP and cause membrane fusion (Scales et al., 2000) and release of neurotransmitter into synaptic cleft. SNARE proteins function in fusion by a cycle of assembly into complexes that fuel membrane fusion, and disassembly of the complexes by NSF and SNAPs that makes SNARE proteins available again for another round of fusion (Fig. 1-9, Fig. 1-11).
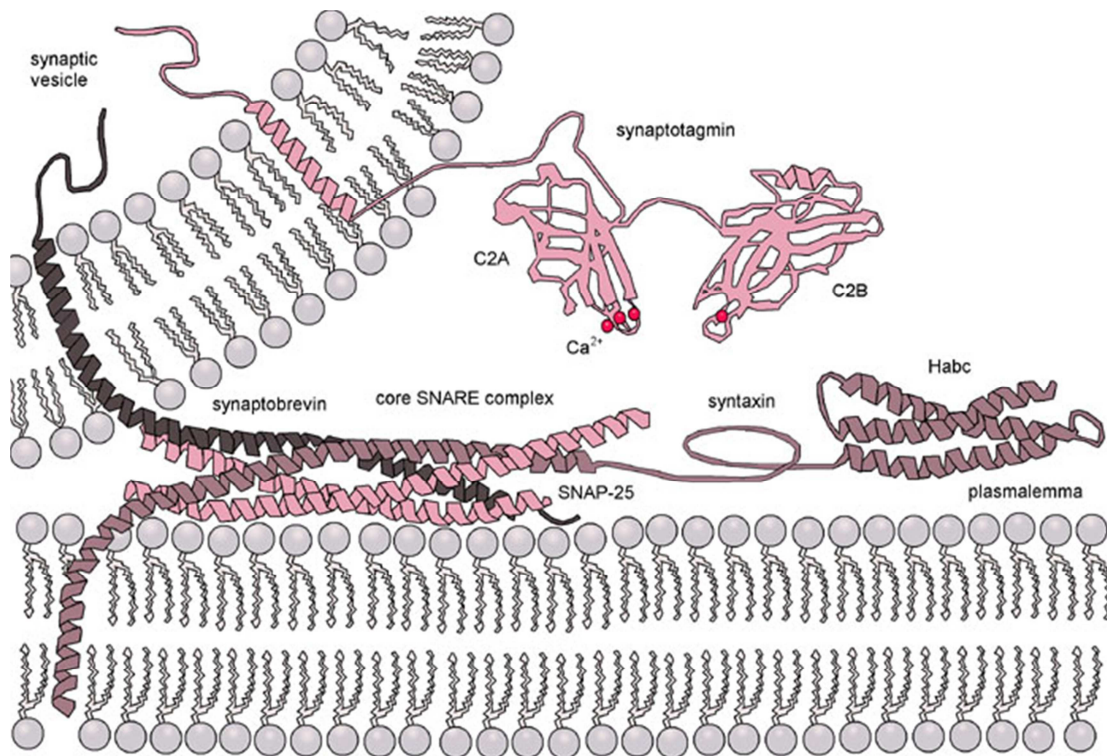
Fig. 1-9 Formation of SNARE complex.

The core SNARE complex is formed by four α-helices contributed by synaptobrevin (VAMP), syntaxin and SNAP-25, synaptotagmin serves as a calcium sensor and regulates intimately the SNARE zipping and membrane fusion.

The involvement of SNARE molecules in cytokine and granules release from immune cells has been shown recently (Table 1-3). The secretion of immune mediators, phagocytosis and endocytosis and the release of stored inflammatory mediators from secretary granules, all require SNARE-mediated membrane fusion (Stow et al., 2009). In macrophages, neutrophils, platelets, eosinophils, secretion of cytokines or granules requires SNAREs (Stow et al., 2006) (Table 1-3).

Table 1-3. List of SNAREs and their function in immune cells
(Logan et al., 2003; Stow et al., 2006; Lacy and Stow, 2011)

SNARE	Cell type	SNARE partners	Immune function
R-SNAREs			
VAMP-1	Neutrophils	STX4–SNAP23	Secretion from all granules
VAMP2	Neutrophils	STX4–SNAP23	Secretion from specific and gelatinase granules
	Eosinophils	ND	Secretion from small secretory vesicles, CCL5
VAMP3	Macrophages	STX6–STX7–Vti1b, STX4–SNAP23	Phagocytosis and TNF secretion
	Platelets	STX4	Secretion from both dense and ∝-granules
	NK cells	STX4	IFNγ, TNF
VAMP7	Macrophages	ND	Phagocytosis
	Neutrophils	STX4	Secretion from all granules
	Eosinophils	ND	Secretion from crystalloid granules
VAMP8	Platelets	STX4	Secretion from dense granules
	Macrophages	STX4, STX6	TNF
Qa-SNAREs			
STX2	Platelets	SNAP23	Secretion from ∝-granules, dense granules and lysosomes
STX4	Macrophages	SNAP23–VAMP3	Phagocytosis and TNF secretion
	Platelets	ND	Secretion from ∝-

			granules and lysosomes
	Mast cells	SNAP23–VAMP2, SNAP23–VAMP3, SNAP23–VAMP8	Degranulation
	Neutrophils	SNAP23–VAMP1, SNAP23–VAMP2, VAMP7	Secretion from specific, gelatinase and azurophilic granules
	Eosinophils	SNAP23	Secretion from crystalloid granules
STX7	Macrophages	STX6–Vti1b–VAMP3	TNF secretion and phagosome maturation
STX13	Macrophages	ND	Phagosome maturation
STX18	Macrophages	ND	Phagocytosis
Qb-SNAREs			
Vti1b	Macrophages	STX6–STX7–VAMP3	TNF secretion
Qc-SNAREs			
STX6	Macrophages	STX7–Vti1b–VAMP3	TNF secretion
	Neutrophils	ND	Secretion from specific and azurophilic granules
Qb,c-SNAREs			
SNAP23	Macrophages	STX4–VAMP3	TNF secretion and phagocytosis
	Platelets	STX2	Secretion from dense granules and lysosomes
	Mast cells	STX4–VAMP2, STX4– VAMP3,	Degranulation, TNF, CCL3

		STX4– VAMP8, STX3– VAMP8, STX2, STX3	
	Neutrophils	STX4–VAMP1, STX4–VAMP2	Secretion from specific and gelatinase granules
	Plasma cells	ND	Antibody secretion
	Eosinophiles	STX4	CCL5

*ND, not determined; **SNAP**, soluble-N-ethylmaleimide-sensitive-factor accessory protein; **SNARE**, SNAP receptor; **STX**, syntaxin; **TNF**, tumour-necrosis factor; **VAMP**, vesicle-associated membrane protein; **Vti1b**, vesicle transport through interaction with t-SNAREs homologue 1b*

Botulism is a neuroparalytic disease, most commonly caused by foodborne ingestion of neurotoxin types A, B or E. The German scientist Justinus Kerner (1786-1862) described botulism as "sausage poison" or "fatty poison". After few years, Emile Pierre van Ermengem discovered causative agent as *Clostridium botulinum*. Much later, the botulinum neurotoxin (BoNT) (Fig. 1-10) was applied successfully to treat diseases, pioneered by Alan B. Scott and Edward J. Schantz (Erbguth, 2004).

BoNTs are produced by *Clostridium botulinum* as a complex of proteins containing the neurotoxic moiety associated with nontoxic components. Seven immunologically- distinct serotypes of BoNT target peripheral cholinergic neurons where they selectively proteolyse SNAP-25 (BoNT/A, /C1, and /E), syntaxin1 (/C1), and synaptobrevin (BoNT/B, /D, /F, and /G) at specific site of SNAREs (Fig. 1-11; Table 1-4).
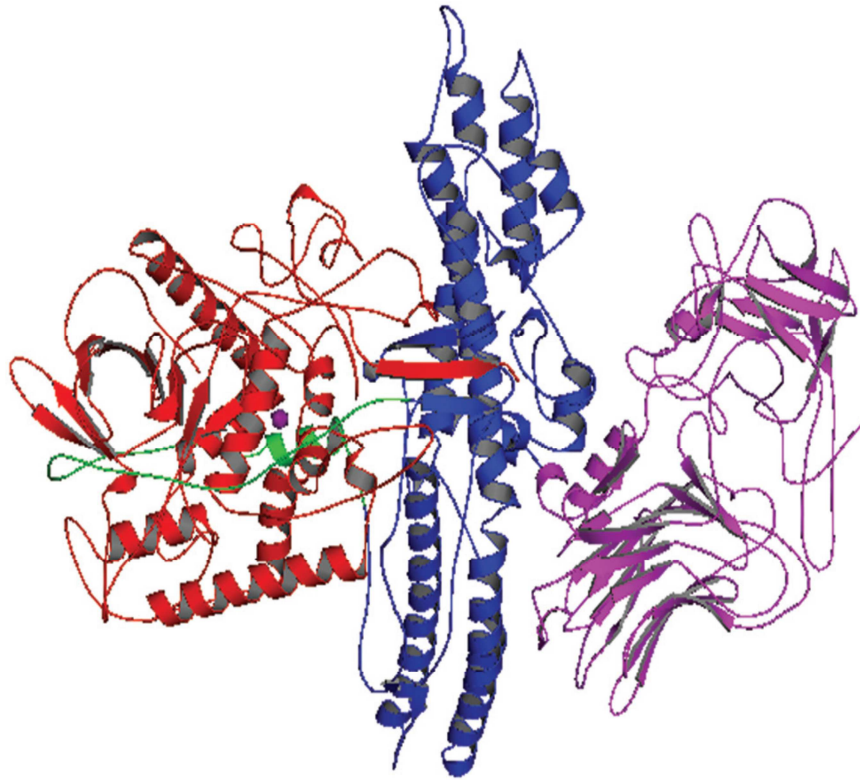
Fig. 1-10. Crystal structure of BoNT/A.

This protein is composed of a ~50 kDa light chain (LC-red) and a ~100 kDa heavy chain (HC) linked by a single disulphide and non-covalent bonds. The HC contains two functional ~50kDa domains; a C-terminal ganglioside binding moiety (H_C-purple) and N-terminal translocation domain (H_N-blue) (Lacy et al., 1998).

These serologically-distinct BoNT serotypes all act by inhibiting release of signal chemicals packaged in neuronal vesicles (Dolly and Aoki, 2006).
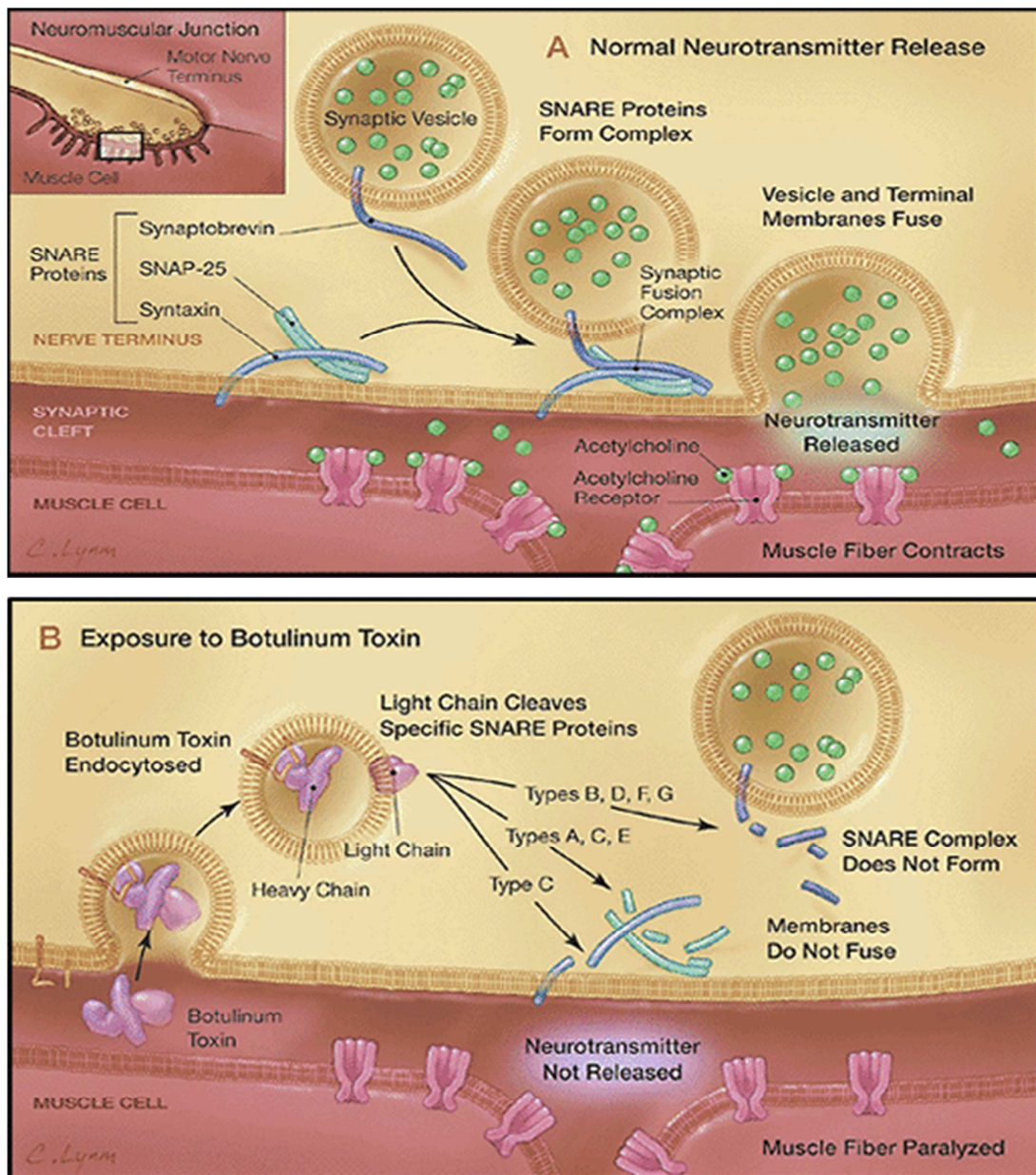
Fig. 1-11. Mechanism of action of BoNTs (Arnon et al., 2001)

BoNTs bind to the pre-synaptic nerve endings of cholinergic neurons and enter by receptor-mediated endocytosis [synaptic vesicle protein (SV2) is an acceptor for BoNT/A, /D, /E and F and synaptotagmin I/II for /B and /G]. Acidity in the endosome is believed to induce pore formation, which allows translocation of the catalytic domain into the cytosol. The catalytic domain of the seven BoNT serotypes specifically cleaves one of three different SNARE proteins essential for synaptic vesicle fusion with the plasmalemma (SNAP-25 is cleaved by /A, /C1 and /E; syntaxin by /C1 and VAMP by /B, /D, /F and /G). It is noteworthy that in non-neuronal cells SNAP-25 cleaving serotypes are not effective as levels of SNAP-25 in

these cells are very low and present SNAP-23 doesn't get efficiently cleaved by BoNTs. Thus VAMP cleaving BoNTs provide therapeutical advantage by cleaving SNAREs present in both neuronal and non-neuronal cells.

BoNTs affect striated muscle by creating a chemical denervation that is temporary through highly potent inhibition of acetylcholine release at the neuromuscular junction (Montecucco et al., 2009). BoNTs have been found to affect the release of multiple SNARE-dependent neuropeptides, including SP, glutamate, cytokines and CGRP, all important mediators of articular pain transmission (Aoki and Francis, 2011).

Table 1-4. BoNTs and their substrates

(Binz et al., 2010)

Serotype	Intracellular target protein	Cleavage sites in rat
/A	SNAP-25	EANQ^{197}RATK
/B	VAMP-1, 2	GASQ^{76}FETS
/C1	SNAP-25 Syntaxin-1A/B	ANQR^{198}ATKM DTKK^{254}AVKY/DTKK^{253}AVKY
/D	VAMP-1, 2	RDQK^{61}KSELD for I and II
/E	SNAP-25	QIDR^{180}IMEK
/F	VAMP-1, 2	ERDQ^{60}KLSE for I ERDQ^{58}KLSE for II
/G	VAMP1, 2	ETSA^{83}AKLK for I ETSA^{81}AKLK for II

BoNTs are the most potent neurotoxins known. However, small doses are successfully used as cosmetic and musculoskeletal therapies. Currently, BoNT/A is the best characterized and widely used clinically because of its long duration of action. BoNT/A injections are analgesic for painful muscle contractions associated with cervical dystonia, migraine/tension headaches, and myofascial pain syndromes (Smith et al., 2002; Ranoux et al., 2008; Dolly et al., 2011).

In BoNT/A treatment of painful soft tissue syndromes, pain relief preceded the resolution of muscle contractions, suggesting that BoNTs may have antinociceptive effects independent of known effects on neuromuscular junctions (Aoki, 2003). Efficacy of intra-articular BoNT/A for refractory arthritis pain in humans, and in murine models of arthritis joint pain, has been reported. Intra-articular BoNT/A reduced lower extremity arthritis pain by an average of 55%, and shoulder pain by an average of 71% in a study of 11 patients with chronic arthritis pain refractory to intra-articular corticosteroids, with no noted adverse effects (Mahowald et al., 2006). In a pre-clinical study, intra-articular injection of BoNT/A resulted in reduced joint tenderness and increased nocturnal wheel running in a mouse model of carrageenan-induced inflammatory arthritis (Krug et al., 2009).

In clinical studies, intra-articular injection of BoNT/A produced a significant decrease in pain score at 3 months (Mahowald et al., 2006; Mahowald et al., 2009) and also decreased pain and joint stiffness (Boon et al., 2010). Similar results were found in a randomized placebo-controlled trial of BoNT/A in chronic severe shoulder pain. BoNT is used in the treatment of strabismus, blepharospasm, hemifacial spasm, adductor spasmodic dysphonia, bruxism, mandibular dystonia, cervix dystonia, local or segmental dystonia, hypercontractility of the internal anal sphincter, detrusor dyssynergy, spasticity, and stuttering. These observations support the hypothesis that chronic arthritis pain may be amplified by neuropeptide release in the periphery (Naumann et al., 2008; Dolly et al., 2009). This selective chemodenervation of articular pain fibres with intra-articular injection of neurotoxins is a novel local approach to treatment of arthritis joint pain.

The novel BoNT-based bio-therapeutics for certain neuronal disorders including pain are being developed in ICNT. For example, BoNT/A, unlike BoNT/E, was found to be unable to abolish the CGRP1 receptor-mediated effect of capsaicin, a nociceptive TRPV1 stimulant, or its elevation of CGRP release from trigeminal ganglionic neurons (TGNs) in culture. It was established that TGNs lack SV2A/B acceptor for BoNT/A but expresses SV2C an acceptor for BoNT/E. To allow LC/E entry to the TGNs, recombinant chimera (EA) of BoNT/A and /E was engineered. This chimera effectively bound to SV2C via binding domain of BoNT/A and cleaved SNAP-25 by LC/E capable of inhibition of CGRP release (Meng et al, 2009).

Using this strategy, the chimera BA and DA were engineered by substituting $H_{(C)}/A$ (C-terminal half of BoNT/A heavy chain) into BoNT/B or /D which

successfully delivered the BoNT/B or /D protease via the BoNT/A acceptor into neurons, or non-neuronal cells like synoviocytes that lack SNAP-25, cleaving VAMP isoform. BA or DA were shown potential to block exocytosis from non-neuronal cells expressing BoNT/A acceptor but lacking SNAP-25 by cleaving VAMP isoforms (Wang J. et. al., 2012).

Thus, recombinant BoNT-based therapeutics developed in ICNT could be used to treat chronic pain and new molecules to treat arthritic pain were engineered.

1.7 PRINCIPLE GOALS OF THIS STUDY

Encouraged by recent reports on the ability of BoNT/A to treat tension headaches/migraines, rheumatologists found that injecting this bio-therapeutic into joints reduced the pain and inflammation in RA and OA patients, who were refractory to other anti-arthritic drugs. The proof of principle has been established in our laboratory that recombinant BoNTs can be used to treat pain by blocking release of cytokines or pain-peptides. Therefore it is warranted to develop new recombinant BoNT-based therapeutics to inhibit cytokine release from immune cells like synoviocytes and macrophages, as well as pain-peptide from sensory neurons, and test these in animal models of arthritic pain.

To achieve this, 3 different experimental approaches to inhibition of release of cytokines and pain-peptides were adopted and evaluated in synoviocytes, macrophages and sensory neurons.

- the lentiviral shRNA was used to knockdown selected SNAREs
- the lentiviral expression of LC/D was used to truncate selected SNAREs
- novel targeted BoNTs were created to preferentially enter non-neuronal cells

Objectives:

1) As recently reported, release of cytokines and pain-peptides in immune cells and sensory neurons requires SNAREs. *In-vitro* studies in non-neuronal cells (human and rat synoviocytes) were therefore carried out to demonstrate expression levels of different SNAREs. To truncate key SNARE, VAMP-3, recombinant BoNTs (chimera/BA and /DA) were engineered to deliver LC/B or /D to synoviocytes lacking receptor for BoNT/B or /D but expressing BoNT/A receptor.

In another approach, commercially available lentiviral shRNA to knockdown SNAP-23, VAMP-3, syntaxin isoforms or VAMP-8 was achieved in human synoviocytes and its effect on inhibition of cytokines was studied. The formation of SDS-resistant SNARE complex was evaluated in human synoviocytes (Chapter 3 and 4).

2) To increase therapeutic efficacy of BoNT by targeting to the requisite cells (e.g. synoviocytes, macrophages or rat dorsal root ganglion neurons) via an attached moiety capable of efficient endocytosis of toxin into cells lacking BoNT/A or /D acceptor was developed. We have previously shown that VAMP is required for release of cytokines in cells lacking SNAP-25. In this study synoviocytes, macrophages and sensory neurons were adopted to truncate VAMP which is present in both and investigate inhibition of release of cytokine/pain-peptide (Chapter 5). This targeted bio-therapeutic was specifically developed to attenuate inflammatory and neuropathic pain by targeting immune cells and sensory neurons and will be further evaluated in relevant animal models.

3) To further extend cleavage of VAMP in inflammatory cells and sensory neurons, lentiviral particles expressing LC/D were developed. The truncation of VAMP was carried out in synoviocytes and macrophages to inhibit release of cytokines and pain-peptides (Chapter 6).

CHAPTER 2 MATERIALS AND METHODS

2.1 *IN VITRO* STUDIES

2.1.1 Ethics statement

All procedures involving live animals were approved by the Research Ethics Committee of Dublin City University and licenses granted by the Minister for Health and Children under the Cruelty to Animals Act, 1876 as amended by European Communities Regulations 2002 and 2005. Experimental procedures had been approved by the Research Ethics Committee of Dublin City University and licensed by the Irish Authorities.

2.1.2 Reagents and antibodies

Rabbit affinity-purified polyclonal antibodies specific for IL-6 and IL-1 receptor were bought from Abcam (Cambridge, UK); cell culture reagents, rabbit polyclonal antibodies against SNAP-25, a syntaxin-1 mouse monoclonal, Penicillin and Streptomycin (Pen-Strep) and targeted and non-targeted lentiviral particles were from Sigma-Aldrich (Arklow, Ireland). Synaptic Systems GmbH (Goettingen, Germany) supplied rabbit polyclonal antibody against SNAP-23, VAMP-2, -3, -7 or -8, syntaxin -2, -3, -4, -5 or -6 and SV2A, 2B or 2C and synaptotagmin I/II. PAN (SV2) was purchased from Developmental Studies Hybridoma Bank). Goat anti-rabbit Alexa 568 (red fluorescence), donkey anti-mouse 488 (green fluorescence), 4',6-diamidino-2-phenylindole (DAPI) and precast NuPAGE gels were purchased from Bio-Sciences (Dun Laoghaire, Ireland). Donkey anti-rabbit and mouse horse radish peroxidase (HRP) secondary antibody from Jackson ImmunoResearch (Suffolk, UK); Enhanced chemiluminescence (ECL) reagent and Polyvinylidenfluoride mesh material (PVDF) membrane was bought from Merck Millipore (Cork, Ireland). The ELISA kit was purchased from Mabtech (Sweden), SPI-BIO (UK) and TrueBlot HRP secondary antibody from eBioscience (Hatfield, UK).

2.1.3 Cell culture

A human synovial cell line (SW982) and mouse macrophage cell line (RAW264.7) were obtained from the American Tissue Culture Collection (Manassas, VA) while Lenti-X 293T was from Clontech (Germany). The SW982 cells were routinely maintained in T-75 flasks (Corning, Ireland) in RPMI1640 medium containing 2 mM L-glutamine, 10% fetal bovine serum (FBS) and 1% Pen-Strep at 37 °C, 5% CO_2

(Yamazaki et al., 2003). Rat cerebellar granule neurons (rCGNs) were isolated and cultured as described previously (Meng et al., 2009). Dorsal root ganglion neurons from rat were isolated. Ganglions were isolated and digested with collagenase (1 mg/ml) for 30 min, centrifuged and cells suspendered in complete medium containing nerve growth factor before plating (Welch et al., 2000; Burkey et al., 2004). Rat trigeminal neurons (rTGNs) were isolated from trigeminal ganglions. The tissue was placed in ice-cold L15 medium, washed twice in ice-cold sterile HBSS before centrifugation at 170 g for 1 minute. After chopping into small pieces and passing through 10-ml Falcon pipettes pre-coated with L15 medium, the tissue was incubated while shaking at 37°C for 30 minutes in a 1:1 mixture of HBSS (containing 2.4 U/ml dispase II) and collagenase I (1 mg/ml). Cells were seeded onto 24-well plates precoated with poly-L-lysine (0.1 mg/ml) and laminin (20 μg/ml) in F12 medium supplemented with NGF (50 ng/ml) and maintained in a CO2 incubator at 37°C (Meng et al., 2007).

2.1.4 Isolation and culture of rat synoviocytes

Synovium, obtained from rat knee joint, was chopped into small pieces, washed in PBS and digested for 30 min. with collagenase (2 mg/ml) in sterile DMEM supplemented with 1% Pen-Strep in an incubator at 37°C. The cells were counted, seeded into 6-well tissue culture plates and left overnight to adhere.

2.1.5 Botulinum neurotoxins (BoNTs)

In our laboratory, novel BoNT chimeras DA, BA and mutated LC/E400(K224D) were designed, constructed, expressed and purified by Dr. Jiafu Wang. Chimera/DA (a recombinant BoNT which contains the protease and translocation domain of BoNT/D and the binding C-terminal moiety of BoNT/A) and chimera/BA (a BoNT variant which contains protease and translocation domain of BoNT/B and binding C-terminal moiety of BoNT/A). LC/E400(K224D), due to the mutation, is capable of cleaving human SNAP-23 (Chen and Barbieri, 2009).

2.1.6 shRNA reagents for knockdown of human SNAP-23, VAMP-3 and syntaxin-2, -3 or -4 gene expression in SW982

As synoviocytes are heavily involved in arthritis disease progression commercially available human synovial cell line was used for this study.

Targeted and non-targeted (control) shRNA lentiviral particles, at 20 multiplicity of infection (MOI) for each clone, were used to knockdown (KD) the expression level of individual SNAREs in SW982. After adding the requisite shRNA to the cells and culturing for 7-8 days, SNAP-23 KD stable cells were established by incubating with puromycin (5 µM) for 4-5 days before use in experiments. These cells were sub-cultured in the presence of puromycin to maintain KD of SNAP-23. Transient KD of VAMP-3 or -8, syntaxin-2, -3 or -4 was achieved by incubating SW982 with shRNA for 7-8 days, followed by culturing in medium containing puromycin for 3-4 days, before evaluating protein expression by Western blotting. In case of transient KD cells were not sub-cultured like SNAP-23 KD. KD of each protein, relative to an internal control (i.e. β-tubulin) was measured by densitometric scanning of the blots and analysis by Image J (NIH, USA). The ratio of the protein of interest (relative to internal control, β-tubulin) for shRNA-treated cells was subtracted from the value for control cells and the resultant number expressed over that of the control to give the % KD.

Table 2-1. shRNA target set for KD of human SNAP-23

Clone no.	shRNA TRC* no.	Sequence and targeting region
1	TRCN0000144 931	CCGGGCTCTTCTAATTGGGAGATAACTCGAGTTA TCTCCCAATTAGAAGAGCTTTTTTG Region: 3'UTR*
2	TRCN0000142 094	CCGGGCCAGAGCAAAGAAACTCATTCTCGAGAAT GAGTTTCTTTGCTCTGGCTTTTTTG Region: CDS*
3	TRCN0000144 789	CCGGGCAATGAGATTGATGCTCAAACTCGAGTTT GAGCATCAATCTCATTGCTTTTTTG Region: CDS*
4	TRCN0000145 326	CCGGGAACAACTAAACCGCATAGAACTCGAGTTC TATGCGGTTTAGTTGTTCTTTTTTG Region: CDS*
5	TRCN0000139 864	CCGGGCCATGAAGAAGGAAGCTGTACTCGAGTAC AGCTTCCTTCTTCATGGCTTTTTTG Region: CDS*

3'UTR, 3' untranslated region; CDS, coding sequence; TRC, the RNAi consortium

Table 2-2. shRNA target set for KD of human VAMP-3

Clone no.	shRNA TRC* no.	Sequence
1	TRCN0000029815	CCGGGCAGCCAAGTTGAAGAGGAAACTCGAGTTT CCTCTTCAACTTGGCTGCTTTTT Region: 3'UTR*
2	TRCN0000029816	CCGGTGGTGGACATAATGCGAGTTACTCGAGTAA CTCGCATTATGTCCACCATTTTT Region: CDS*
3	TRCN0000029817	CCGGCAGGCGCTTCTCAATTTGAAACTCGAGTTTC AAATTGAGAAGCGCCTGTTTTT Region: CDS*
4	TRCN0000330913	CCGGCAGGCGCTTCTCAATTTGAAACTCGAGTTTC AAATTGAGAAGCGCCTGTTTTTG Region: CDS*
5	TRCN0000330914	CCGGGCAGCCAAGTTGAAGAGGAAACTCGAGTTT CCTCTTCAACTTGGCTGCTTTTTG Region: CDS*

Table 2-3. shRNA target set for KD of human syntaxin-2

Clone no.	shRNA TRC* no.	Sequence
1	TRCN0000065283	CCGGCGAGCCAAGTTAAAGGCTATTCTCGAGAATAGCCTTTAACTTGGCTCGTTTTTG Region: CDS*
2	TRCN0000065284	CCGGCCTAGCAACAACATTGTCCTACTCGAGTAGGACAATGTTGTTGCTAGGTTTTTG Region: CDS*
3	TRCN0000065285	CCGGGCGTGTAGGAAGAATGATGATCTCGAGATCATCATTCTTCCTACACGCTTTTTG Region: CDS*
4	TRCN0000065286	CCGGCCATCTTCACTTCCGACATTACTCGAGTAATGTCGGAAGTGAAGATGGTTTTTG Region: CDS*
5	TRCN0000065287	CCGGGCATGAGATGTTCATGGACATCTCGAGATGTCCATGAACATCTCATGCTTTTTG Region: CDS*

Table 2-4. shRNA target set for KD of human syntaxin-3

Clone no.	shRNA TRC* no.	Sequence
1	TRCN0000065014	CCGGGCAGCTCACGACTGAGATTAACTCGAGTTAATCTCAGTCGTGAGCTGCTTTTTG Region: CDS*
2	TRCN0000303419	CCGGAGAGCATGGAGAAGCATATTGCTCGAGCAATATGCTTCTCCATGCTCTTTTTG Region: CDS*
3	TRCN0000379420	GTACCGGCAGACCTTCGGATTCGGAAATCTCGAGATTTCCGAATCCGAAGGTCTGTTTTTG Region: CDS*
4	TRCN0000382342	GTACCGGTTTCCGTTGGGCTGAATTAAGCTCGAGCTTAATTCAGCCCAACGGAAATTTTTTG Region: CDS*
5	TRCN0000065013	CCGGGCCCGGAAGAAATTGATAATTCTCGAGAATTATCAATTTCTTCCGGGCTTTTTG Region: CDS*

Table 2-5. shRNA target set for KD of human syntaxin-4

Clone no.	shRNA TRC* no.	Sequence
1	TRCN0000065 023	CCGGCCGTCAACACAAGAATGAGAACTCGAGTTC TCATTCTTGTGTTGACGGTTTTTG Region: CDS*
2	TRCN0000065 025	CCGGGCAATTCAATGCAGTCCGAATCTCGAGATT CGGACTGCATTGAATTGCTTTTTG Region: CDS*
3	TRCN0000065 027	CCGGGCTGCACGACATATTCACTTTCTCGAGAAA GTGAATATGTCGTGCAGCTTTTTG Region: CDS*
4	TRCN0000299 048	CCGGCCGTCAACACAAGAATGAGAACTCGAGTTC TCATTCTTGTGTTGACGGTTTTTG Region: CDS*
5	TRCN0000380 073	GTACCGGGTGACTCGACAGGCCTTAAATCTCGAG ATTTAAGGCCTGTCGAGTCACTTTTTTG Region: CDS*

Table 2-6. shRNA target set for KD of rat VAMP-8

Clone no.	shRNA TRC* no.	Sequence
1	TRCN0000110535	CCGGCCTCCCTAATATGTGCCAAGACTCGAGTCTTGGCACATATTAGGGAGGTTTTTG Region: CDS*
2	TRCN0000110536	CCGGCGTCTGAACACTTCAAGACAACTCGAGTTGTCTTGAAGTGTTCAGACGTTTTTG Region: CDS*
3	TRCN0000110537	CCGGCCACGTCTGAACACTTCAAGACTCGAGTCTTGAAGTGTTCAGACGTGGTTTTTG Region: CDS*
4	TRCN0000110538	CCGGCCGGAAGTTCTGGTGGAAGAACTCGAGTTCTTCCACCAGAACTTCCGGTTTTTG Region: CDS*
5	TRCN0000110539	CCGGCTGTGTGATTGTCCTTATCATCTCGAGATGATAAGGACAATCACACAGTTTTTG Region: CDS*

2.1.7 SDS-PAGE and Western blotting

Proteins were loaded onto 12% or 4-12% precast Bis-Tris gel and electrophoresis run at 180 volts, using MOPs running buffer (Appendix 2), until proteins were separated according to their molecular weights, as indicated by pre-stained protein markers. Proteins were then electrophoretically transferred to a Immobilon™ PVDF membrane for immunoassay. A piece of PVDF membrane with a rated pore size of 0.45 µm was placed for about 30 second in methanol followed by rinsing with ddH$_2$O twice, before soaking in transfer buffer (Appendix 2) for 15 mins; then a "sandwich" was assembled for transblotting in a transfer tank filled with transfer for 2-3 h at 45 volts at 4°C. The membrane was then immersed in blocking buffer for 1 h at room temperature (RT). Thereafter, the samples are incubated with primary antibody for 1 hour at RT, rinsed thrice with washing buffer before adding secondary antibody. After incubation, the blot was rinsed 3 times in washing buffer and proteins were detected

by ECL reagent. Images were recorded with a G-Box and analysed using Image J software (Wang et al., 2008).

2.1.8 2-Dimensional (2-D) gel electrophoresis

An established protocol in the laboratory was used to investigate whether SNAP-23, VAMP-3 and other SNAREs form SDS-resistant SNAREs complexes in KD and control cells. The cells were solubilised in LDS-sample buffer without boiling and the proteins separated on 12% PAGE gels. Each sample lane was cut into strips reflecting different distances of migration through the gel, chopped into small pieces and boiled for 10 mins in LDS buffer. After being left overnight at RT to extract proteins from gel sections, the samples were boiled again for 5 min. to solubilise proteins before loading onto a second 4-12% gel. The SNAREs released form complex after boiling were detected by Western blotting with specific antibodies (Lawrence and Dolly, 2002).

2.1.9 Co-immunoprecipitation

SW982 cells were incubated for 20 h with IL-1β (100 ng/ml) in complete medium, before centrifugation for 5 min at 170 g; cell pellets were lysed in lysis buffer (Appendix 2) supplemented with a cocktail of protease inhibitors for 30 min followed by brief sonication. After centrifugation at 15,000 g for 10 min, protein concentration of the supernatant was determined by Bradford's assay to be 1mg/ml. Protein extracts (300 µg in 300 µl) were incubated with VAMP-3-specific mouse antibodies (30 µg in 50 µl), pre-complexed with protein-A agarose for 1 h, before washing 5 times with lysis buffer. Negative controls were performed using mouse non-immune IgG, pre-labelled protein A agarose. Before binding, 50µg of protein in 20 µl of input were kept for analysing the efficiency of co-immunoprecipitation. The sealed agarose-bound samples were boiled for 10 min in 50 µl reducing LDS-sample buffer before 50% of the eluate was subjected to SDS-PAGE and Western blotting, using rabbit polyclonal antibodies specific for SNAP-23, syntaxin-2, -3 or -4, and mouse TrueBlot HRP secondary antibody.

2.1.10 Biotinylation of cell-surface proteins

Two T75 flasks of WT or SNAP-23 KD cells were grown to 90–95% confluence before being treated with or without IL-Iβ (100 ng/ml) for 20 h. Cells were washed

twice in the flasks with ice-cold PBS, pH 8.0 before being incubated with 0.5 mg/ml EZ-Link NHS-SS-Biotin in ice-cold PBS for 1 h at 4°C. The biotinylation of cell surface proteins was terminated by adding quenching solution and rinsing with Tris-buffered saline (Appendix 2). The cells were then harvested and lysed in the lysis buffer containing protease inhibitors; to improve solubilization, the cells were sonicated on ice and centrifuged at 10,000 $\times$ g for 2 min at 4°C. The biotinylated membrane proteins were adsorbed from the supernatant by immobilized NeutrAvidin gel slurry which was washed twice in washing buffer; proteins were eluted from the gel by heating at 95°C for 5 min in SDS-PAGE sample buffer in the presence of 50 mM DTT and subjected to Western blotting using an anti-IL-1 receptor antibody. IL-1 receptor expression in whole cell extracts (total) prior to incubation with agarose-NeutrAvidin was also subjected for Western blotting.

2.1.11 Assay of protein concentration by BCA kit

Protein concentrations were quantified using a commercially available BCA assay kit, as per instructions, with bovine serum albumin (BSA) as a standard.

2.1.12 Enzyme-linked immunosorbent assays (ELISAs)

ELISA for IL-6 or TNF-α was performed according to protocols provided with the kits supplied. A specific mAb for capturing the cytokine of interest is coated on a ELISA plate. A second mAb, used for detection, binds a different epitope on the cytokine; it is labelled with biotin which allows subsequent binding of a streptavidin-conjugated enzyme. Any unbound reagents are washed away. When substrate is added, a colour reaction develops that is proportional to the amount of cytokine bound. The concentration of cytokine is determined by comparison with a standard curve, of known concentrations of cytokine. Substance-P and CGRP were assayed likewise with their requisite commercial kits.

SW982 cells were stimulated overnight with IL-1β (100 ng/ml) in HEPES-buffered solution containing 60 mM K^+ with adjustment 3mM NaCl concentration or with/without EGTA for 4 h. Cell culture supernatant was harvested for ELISA assay.

RAW264.7 cells were stimulated with LPS (100 ng/ml) + IFN-γ (500 pg/ml) for 6h (Yeh et al., 2011).

2.1.13 Cytochemical staining and microscopic recording of images

Cells cultured on collagen-coated coverslips were washed three times with Dulbecco's phosphate buffered saline (lacking Mg^{2+} and Ca^{2+}, D-PBS) and then fixed for 20 min. with 3.7% paraformaldehyde at RT in the later buffer. The cells were washed three times with D-PBS, followed by permeabilisation for 5 min. in D-PBS containing 0.2% Trition X-100 before blocking with 1% BSA in D-PBS for 1 h. Primary antibodies were applied in the same solution and left overnight at 4^oC; after extensive washing, fluorescently-conjugated secondary antibodies were added and incubated for 1 h at RT. After adequate washing, the coverslips were mounted on slides using mounting medium containing DAPI for nuclei staining. Negative controls were performed with same procedure without primary antibody but incubated with secondary antibody. Immuno-fluorescent pictures were taken with an inverted confocal (Leica) or Olympus IX71 microscope equipped with a CCD camera (Meng et al., 2009).

2.1.14 Cell viability assay

This was performed using 1-(4,5-dimethylthiazol-2-yl)-3,5-diphenylformazan (MTT). Cells were incubated with MTT (5 mg/ml in 10% FBS) for 4-5 h at $37\ ^OC$, the plate was observed for formation of formazan crystals (artificial chromogenic products of the reduction of tetrazolium salts by oxidoreductase enzymes). The MTT dye was removed carefully without disturbing the cells at the bottom of each well and 90 µl of 20% SDS + 50% DMF solution added as a solvent for these crystals. The plate was incubated at $50\ ^OC$ for a period of 45 - 60 min before reading absorbance at 630 nm in an ELISA plate reader.

2.1.15 Production of LC/D expressing lentiviral particles

Lenti-X 293T cells were used for lentiviral production. A total of 6×15 cm poly L-lysine coated dishes of confluent Lenti-X 293T cells were grown in DMEM + 10% FBS. All 3 vectors (psPAX2, pMD2.G and pWPI-LC/D) with concentration of 20, 10 and 20 µg of plasmids for each plate were transfected into 293T cells by using $CaPO_4$ and 2X HBS (HEPES Buffered Saline, Appendix 2) precipitation method and incubated for 6 h at $37\ ^OC$ and 5% CO_2. After 6 h incubation, the culture medium was removed and cells were washed with PBS (Appendix 2) and replaced with complete medium and incubated for a further 4 days. Culture supernatant was harvested daily

for 4 days and stored at 5 °C. Supernatant containing lentiviral particles were concentrated by centrifuging at 70,000g for 2 h at 4 °C. in a Beckman SW28 rotor. The pellet was re-suspended in 500 µl of Hank's balanced salt solution (HBSS), aliquoted and stored at -80 °C until further use.

2.1.16 Protease activities of new BoNT variants

For analysis of VAMP-2 cleavage by BoNT/B and chimera/BA, DNA-encoding GFP (green fluorescent protein) was fused to nucleotides encoding rat VAMP-2 (residues 2–94) and a His$_6$ tag. The GFP–VAMP2 (2–94)–His$_6$ fusion protein, expressed in *E. coli* and purified by IMAC, acted as substrate in the fluorescence assay following an established protocol (Wang et al., 2008).

2.1.17 Cell-based SNARE cleavage assay

Preparation and maintenance of rat CGNs and trigeminal ganglion neurons (TGNs) followed standard methods (Wang et al., 2008; Meng et al., 2009). Neurons were cultured in presence of cytosine arabinoside (Ara-C) until complete removal of glial cells before use for experiments.

2.1.18 Mouse LD$_{50}$ assay

Toxins' lethalities were determined using a LD$_{50}$ assay after intraperitoneal injection into mice as described previously (Maisey et al., 1988). Groups of four mice were used for each concentration; the amount of each that killed half the animals within 4 days was taken as one LD$_{50}$ unit and specific neurotoxicities are expressed as the number of LD$_{50}$ units/mg of toxin.

2.1.19 Expression and purification of BoNT-based therapeutics

Expression of therapeutics was carried out in E. coli strain BL21.DE3 (Merck Bioscience), using an established autoinduction system. BoNT-based therapeutics were purified by immobilised metal affinity chromatography (IMAC) using 4 ml of superflow cobalt-based resin (TALON® Superflow™). The resin was added to a 20 ml column and washed twice with equilibration buffer (20 mM HEPES, 150 mM NaCl, pH 8.0). The clarified supernatant was mixed with equilibration buffer at a 1:1 ratio and incubated with the resin for 1 hr at 4°C on a roller. Following binding, the mixture was placed back into the column and the flow through collected. The protein bound to resin was washed three times with wash buffer (equilibration buffer plus 5

mM imidazole). Protein was eluted in 6 fractions with one bed volume 2 ml of elution buffer per fraction (20 mM HEPES, 150 mM NaCl, 500 mM imidazole). The eluted fractions were buffer exchanged into PBS using a PD10 column and concentrations of the eluates were estimated by Bio-Rad protein assay.

2.1.20 Digitonin permeabilisation of cells

The SW982 cells were washed twice with PBS and incubated with digitonin (40 μM) in complete medium for 30 min at 37°C and 5% CO_2 in presence of LC/E400(K224D). Cells were observed for any cell death or detachment. After 30 min of incubation, cells washed 3 times with PBS and harvested for SDS-PGAE and western blot analysis.

2.1.21 Statistical analysis

Data are presented with the S.E.M. and respective sample size. Data analysis and graphs prepared using GraphPad Prism 4.0. Desitometric analysis was done for Western blots using Image J. P values calculated as indicated in the Fig. legends; $P<0.05$ was considered statistically significant using non-paired, 2 tailed student-t test.

CHAPTER 3 SNAREs ARE INVOLVED IN

CYTOKINE RELEASE FROM A HUMAN

SYNOVIAL CELL LINE (SW982)

3.1 BACKGROUND

RA and OA are chronic diseases marked by inflammation in the lining of the joint (i.e. the synovium) and destruction of cartilage and bone. The inner lining of the joint consists of the synovium located between the joint capsule and the joint cavity. Synovium is also important for maintaining proper joint function by providing the structural support and supplying the necessary nutrients to the surrounding cartilage. Synovial membrane is divided into two compartments – the outer layer (subintima) and the inner layer (intima). The inner layer is mainly composed of two cell types, specialized macrophages (macrophage-like synovial cells) and fibroblast-like synoviocytes (FLS), which are important in maintaining the internal joint homeostasis (Dasuri et al., 2004; Chang et al., 2010). FLS are cells of mesenchymal origin that display many characteristics common to fibroblasts, such as expression of several types of collagens and protein vimentin, a part of cytoskeletal filaments (Ospelt et al., 2004; Bartok and Firestein, 2010). Synoviocytes contribute to the local production of cytokines, small molecule mediators of inflammation, and proteolytic enzymes that degrade the extracellular matrix (Ospelt et al., 2004; Bartok and Firestein, 2010). Synoviocytes are one of the important cells in the progression of arthritis due to their increased secretion of cytokines after onset of disease.

SNAREs are involved in release of cytokines or pain peptides in neuronal and non-neuronal cells (Stow et al., 2006; Stow et al., 2009). In this chapter human synovial cell line (SW982) was used to study inhibition of cytokine release, by using lentiviral shRNA to knockdown (KD) SNAREs. SNAP-23 and VAMP-3 were required for release of cytokines in SW982 cells. Even though, these cells have BoNT/A receptor, SV2A/C, exposed to chimera BA or DA, failed to truncate VAMP-3. Because SV2 was not expressed on the cell surface but located intracellularly, the toxins were unable to bind the receptor and become internalized (see Results later). This problem was overcome by employing digitonin permeabilisation of SW982 cells to deliver a novel BoNT mutant, LC/E400(K224D), and exclusively truncate SNAP-23.

3.2 RESULTS

3.2.1 Human synovial cell line (SW982) mostly contains fibroblast-like cells

SW982 cells were routinely cultured in T-150 flasks and grown in RPMI1640 with 2 mM L-glutamine, 10% fetal bovine serum (FBS) and 1% Pen-Strep at 37 °C, 5% CO_2. Labelling of all the cells with a fibroblast-specific vimentin antibody, and counterstaining with a nuclear marker, DAPI (Fig. 3-1B) established that FLS, spindle shaped cells of variable size, are the major constituents in cultured SW982 (Fig. 3-1A). Immunostaining for CD68, a macrophage-specific marker, proved negative (data not shown).
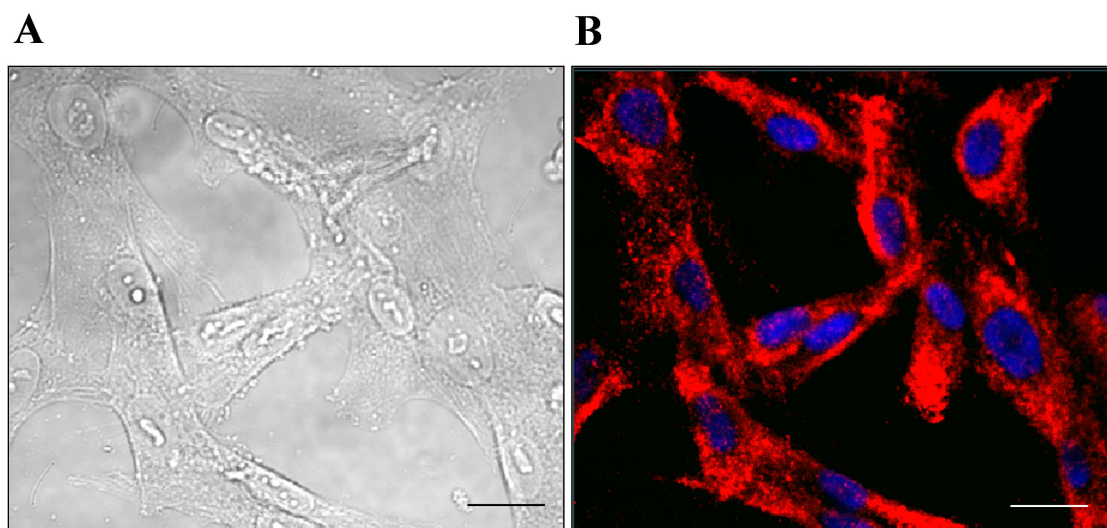
Fig. 3-1. Human synovial cells mainly contain fibroblast-like cells.

A) Bright field view of fibroblast-like synoviocytes, 4-5 days old (passage 5). B) Merged confocal microscopic image showing the fibroblast-cell marker, vimentin (red), expressed in all the cells counterstained with DAPI (blue). Alexa flour-labelled goat anti-rabbit 568 (1:1500) was used as secondary antibody. Scale for A and B is 20 μm.

3.2.2 Human synovial cells contain certain SNAREs and synaptic vesicle protein 2

In seeking a molecular basis for exocytosis of cytokines from SW982, their complement of SNAREs was assessed in comparison to other secretory cells [mouse macrophage cell line, (RAW264.7) and rat cerebellar granule neurons (rCGNs)].

Western blotting of cell lysates using isoform-specific antibodies revealed that, in contrast to RAW264.7 which contain SNAP-23, VAMP-3, -7, -8, and syntaxin 2-6, SW982 express a somewhat lower level of syntaxin-3 and similar amounts of SNAP-23, VAMP-3, syntaxin-2 and higher levels of syntaxin-4 with little or no syntaxin-5 or 6 and VAMP-7 or -8 (Fig. 3-2A). SNAP-25, syntaxin-1 and VAMP-2 characteristic of neurons were hardly detectable in SW982 but, as expected, enriched in rCGNs (Fig. 3-2B). Interestingly, synaptic vesicle protein 2 (SV2) isoforms A and C — key proteins for Ca^{2+}-regulated transmitter release in neuronal and endocrine cells (Schivell et al., 2005; Chang and Sudhof, 2009) —were also found in SW982, but not the Ca^{2+}-sensor, synaptotagmin I or II, which (except for SV2C) occur (Chapter 2.1.2), in rCGNs (Fig. 3-2B). Thus, it was warranted to establish if the SNAREs present in SW982 contribute to the release of cytokines.
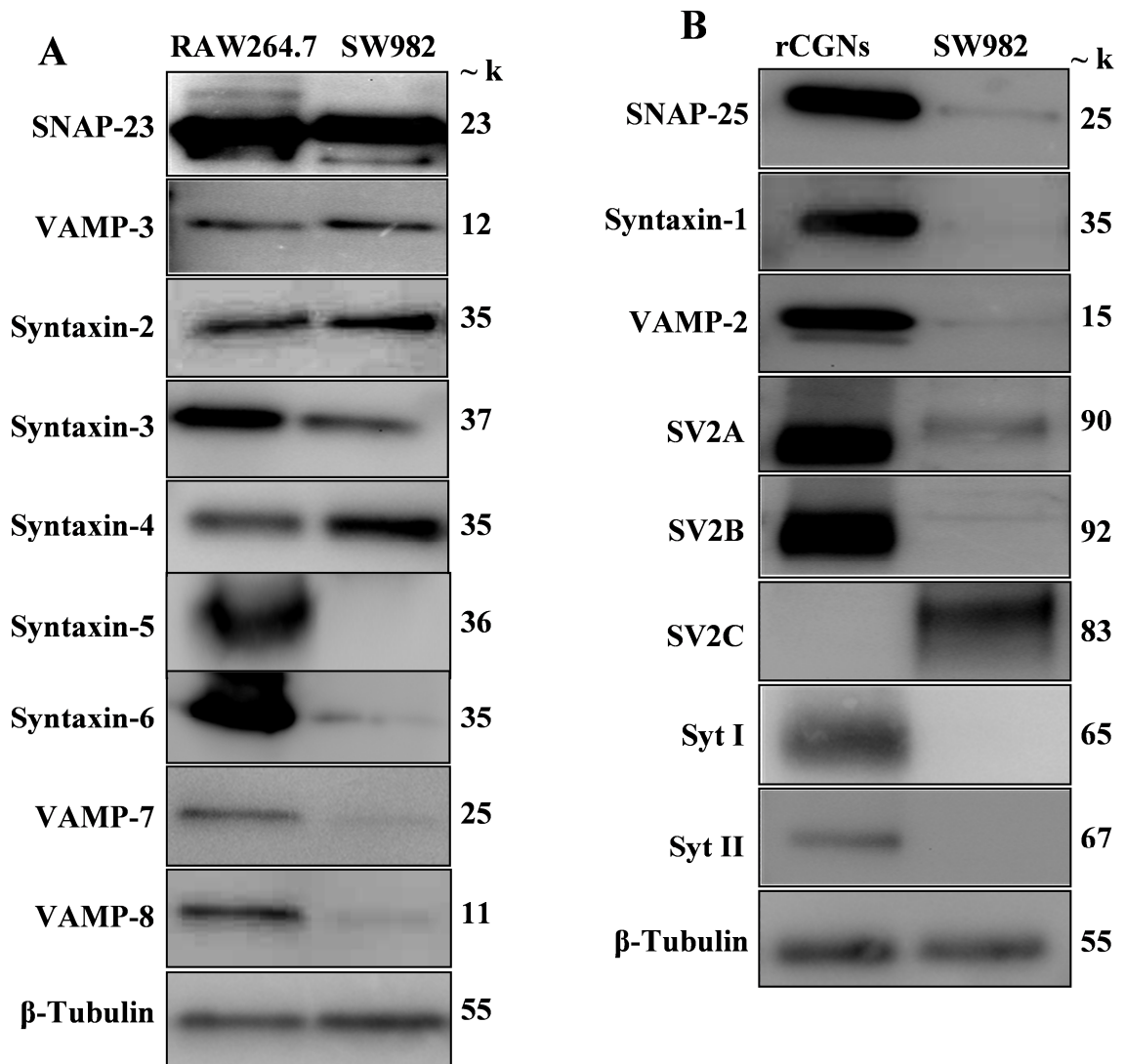
Fig. 3-2. Immuno-blots of human synovial cells demonstrate the presence of SNAREs and SV2 isoforms.

A) Western blots demonstrating that SNAP-23, VAMP-3, syntaxin 2-4 and traces of syntaxin-6 and VAMP-8 are expressed in SW982 cells; these proteins plus a relatively small amount of VAMP-7 were also detected in a RAW264.7. B) Detection in SW982 of only traces of SNAP-25, syntaxin-1, VAMP-2, a relatively higher level of SV2C than SV2A and a lack of SV2B plus synaptotagmin (Syt) I and II, compared to the complement of these protein in rCGNs, with the exception of SV2C. Equal amount of protein was loaded in each lane for all the blots and β–tubulin acted as a loading control; approximate sizes of the bands are indicated.

3.2.3 IL-1β induces the release of cytokines from SW982 in a Ca^{2+}-dependent manner

Although elevated $[K^+]$ is known to elicit transmitter release from excitatory cells (Meng et al., 2007), the levels of IL-6 secretion triggered in 3.5 and 60 mM $[K^+]$ from SW982 after 4 h incubation were similar; K^+-depolarisation induced release was unaffected by the absence of extracellular Ca^{2+} and presence of EGTA (Fig. 3-3A). On the other hand, a 4 h incubation of the cells with an established effective concentration (100 ng/ml) of the pro-inflammatory factor, IL-1β (Tsuji et al., 1999), together with 60 mM $[K^+]$ and 2.5mM Ca^{2+} (Chapter 2.1.12), elicited a ~3.5-fold increase in the release of IL-6 over the Ca^{2+}-free level (Fig. 3-3A). A cell viability assay performed after 4 h incubation with LK or HK buffer, with or without external Ca^{2+} and IL-1β, showed that the cells had not died (Fig. 3-3A, lower panel), and representative image galleries of cells after each treatment showed that they had not detached (Fig. 3-3C). Incubation for 20 h, rather than 4 h, with IL-1β in culture medium which contained Ca^{2+} gave a ~10-fold increment of IL-6 release (Fig. 3-3B), suggestive of the time course of this cytokine release induced by IL-1β alone needs longer than 4 h. These results indicate the importance of IL-1β in stimulating cytokine release from SW982 cells.
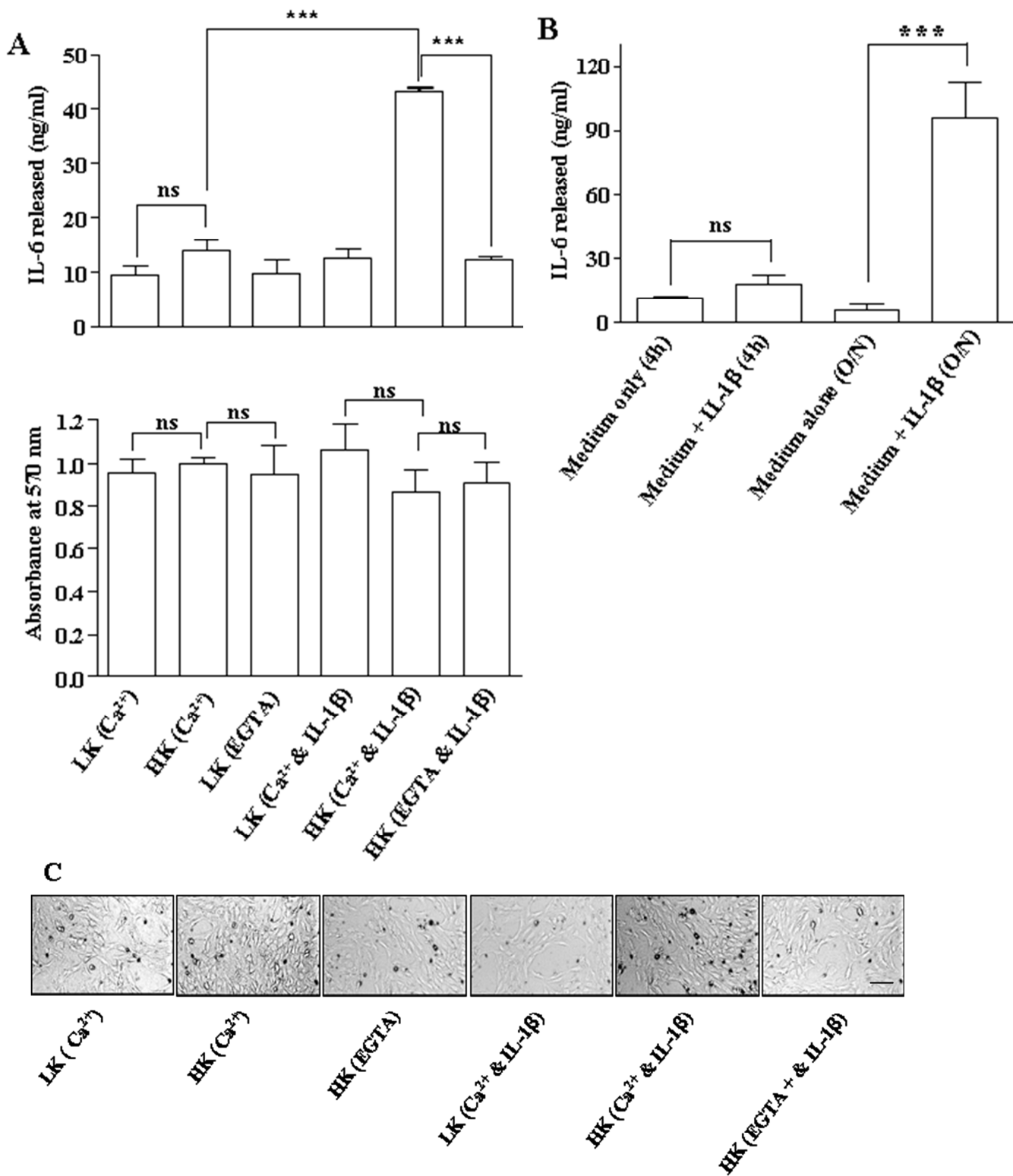
Fig. 3-3. IL-1β-induced IL-6 release by SW982 requires external Ca²⁺.

A upper) A 4 h incubation of the cells with a high [K⁺] buffer (HK) in the presence or absence of extracellular Ca²⁺ gave minimal stimulation of IL-6 release, whereas the additional application of IL-1β (100 ng/ml) in HK with Ca²⁺ yielded a ~3.5-fold increase over the basal value without extracellular Ca²⁺. A lower) A cell viability assay using MTT showed no cell death occurred after a 4 h-incubation in HK or LK

buffer, with or without external Ca^{2+} and IL-1β. B) Incubation of SW982 for 20 h in the culture medium containing Ca^{2+} and IL-1β (100 ng/ml) elicited ~10-fold more release of IL-6 over that for medium alone; however, incubation for 4 h with medium and IL-1β did not yield significant release of IL-6. C) Representative gallery images showing cells were not detached after each treatment for 4 h. Data represented as mean ± S.E.M.; n = 3 for each experiment; p < 0.05 considered statistically significant, ***p < 0.001; scale bar 100 μm.

3.2.4 SNAP-23 is required for IL-1β-induced release of IL-6 and TNF-α from SW982: KD of SNAP-23 enhances peri-nuclear distribution of SV2

To examine the involvement of SNAP-23 in the release of cytokines from SW982, KD of this protein was achieved by culturing the cells with specific shRNA lentiviral particles (Table 2-1) before Western blotting of the total cell lysates. Immunoblot analysis showed that the KD cells had a substantially reduced content of SNAP-23 (Fig. 3-4A); its quantitation in KD and control, relative to β-tubulin as an internal standard, yielded a reduction of ~80% (Fig. 3-4B). The extensive KD of SNAP-23 was confirmed by immuno-cytochemical visualisation (Fig. 3-4E). Specificity of the KD was confirmed by the observed absence of any significant changes in the levels of VAMP-3 or syntaxin 2-4 (Fig. 3-4A). Notably, the release of TNF-α and IL-6 elicited by IL-1β overnight was decreased by ~50% and ~55%, respectively, from the cells after KD of SNAP-23 (Fig. 3-4C, D); likewise, a ~55% decrease in IL-6 release was observed when assayed after a 4 h treatment with IL-1β together with HK (Fig. 3-4D). Therefore, SNAP-23 contributes to IL-6 and TNF-α release from SW982. Interestingly, total SV2, detected with an isoform non-specific antibody, displayed a diffuse pattern in control cells, but had a striking peri-nuclear distribution in SNAP-23 KD cells (Fig. 3-4E). Because this protein occurs on secretory vesicles, this accumulation suggests that in SNAP-23 KD cells is impaired (Fig. 3-4E). A stable cell line of SNAP-23 KD was successfully established using lentiviral shRNA.
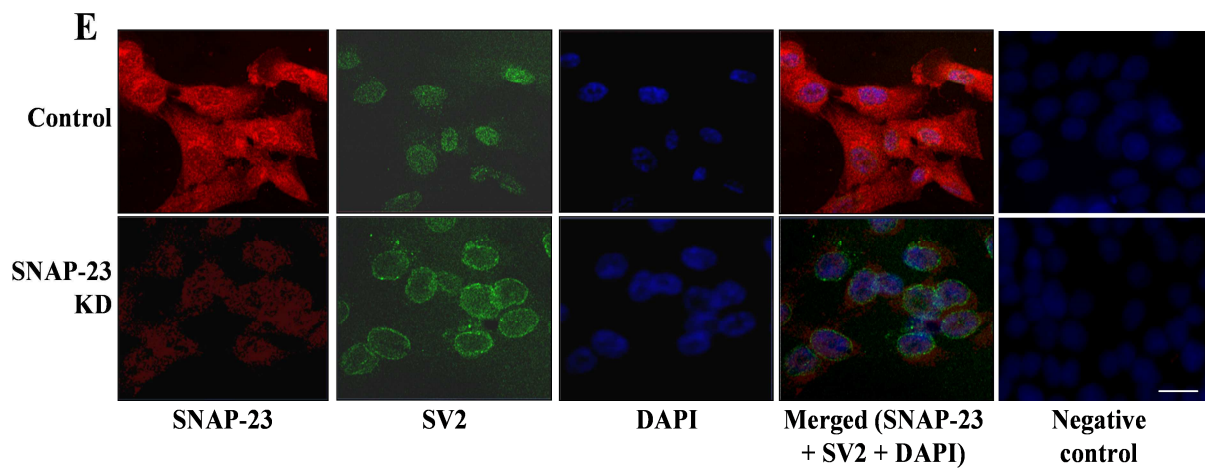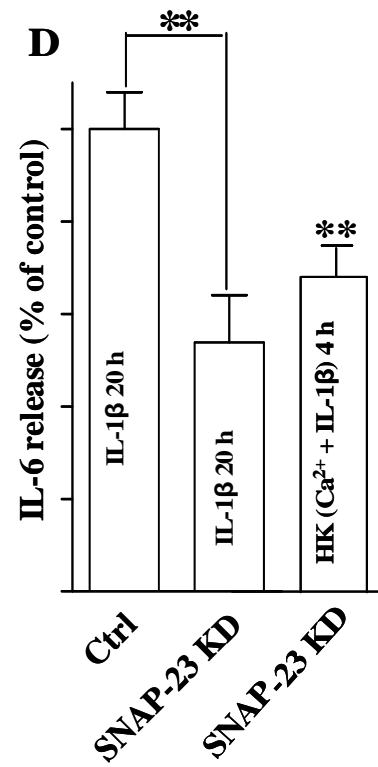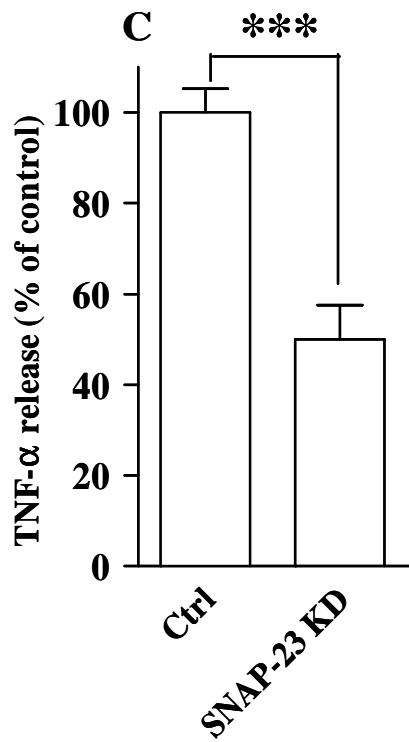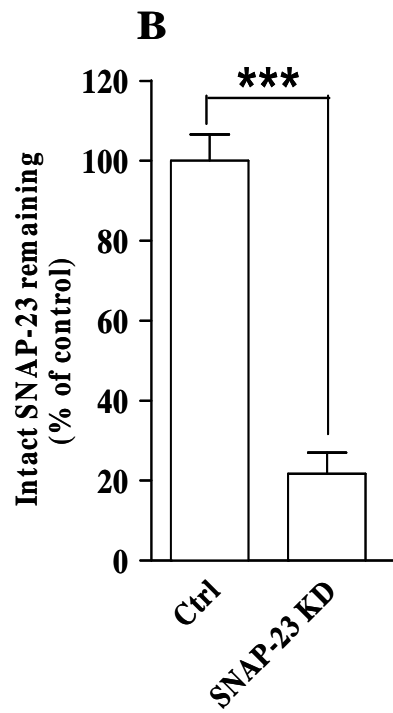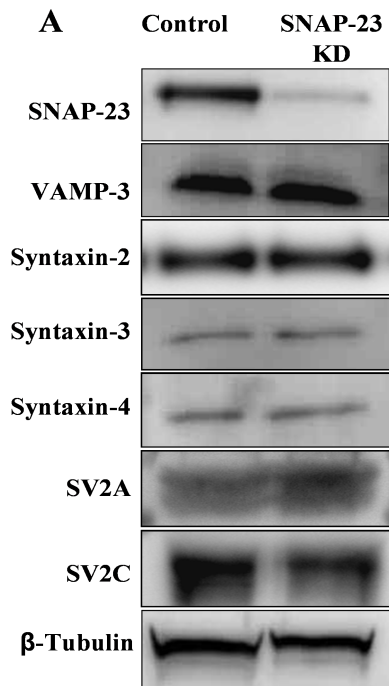
Fig. 3-4. Specific KD of SNAP-23 greatly reduced IL-1β mediated release of IL-6 and TNF-α from SW982 as well as enhancing peri-nuclear distribution of SV2. *A) Western blots of SNAREs and SV2A/C in lysates of control and SNAP-23 KD cells (60 µg/lane) demonstrating that the level of SNAP-23 only was significantly reduced after its KD compared to the control. B) % KD of SNAP-23 relative to the control was calculated using β-tubulin as an internal reference. After overnight incubation in the presence of IL-1β (100 ng/ml), the extents of inhibition of evoked release of TNF-α C) and IL-6 D) from KD cells were calculated relative to those for the control. Data are mean ± S.E.M. from n = 3, p < 0.05 considered statistically significant, **p < 0.01, ***p < 0.001. E) Confocal microscopy images reveal that SV2 acquired a pronounced peri-nuclear distribution in KD SW982, whereas in controls its distribution appeared more diffuse. Alexa flour-tagged goat anti-rabbit 568, (1:1500) and donkey anti-mouse 488 (1:1500) were used as secondary antibodies, with nuclei stained by DAPI. The scale bar is 10 µm.*

3.2.5 KD of VAMP-3, but not syntaxin-4, decreased IL-1β-induced release of

IL-6 and TNF-α from cultured SW982

To ascertain if VAMP-3 is needed for exocytosis of cytokines, its content in SW982 was decreased by ~75% after transient KD (Table 2-2), calculated using β-tubulin as an internal control (Fig. 3-5A and B). No Change in expression of other SNAREs were observed after VAMP-3 KD (Fig. 3-5A). Accordingly, there were respective decreases of ~55% and ~60% with IL-1β stimulated release of TNF-α (Fig. 3-5C) and IL-6 (Fig. 3-5D) from VAMP-3 KD cells. These convergent findings highlight the functional importance in exocytosis of SNAP-23 and VAMP-3. A different set of results was obtained for syntaxin. The transient KD of syntaxin-4 (Table 2-5) to ~50% observed (Fig. 3-5E, F) failed to reduce the stimulated release of TNF-α (Fig. 3-5G) or IL-6 (Fig. 3-5H) compared to controls). Residual syntaxin-4 and/or other isoforms (i.e. 2 and 3) might have compensated for the reduction of syntaxin-4 achieved. To investigate role of syntaxin-2 or 3 in release of cytokines, their KD was achieved.
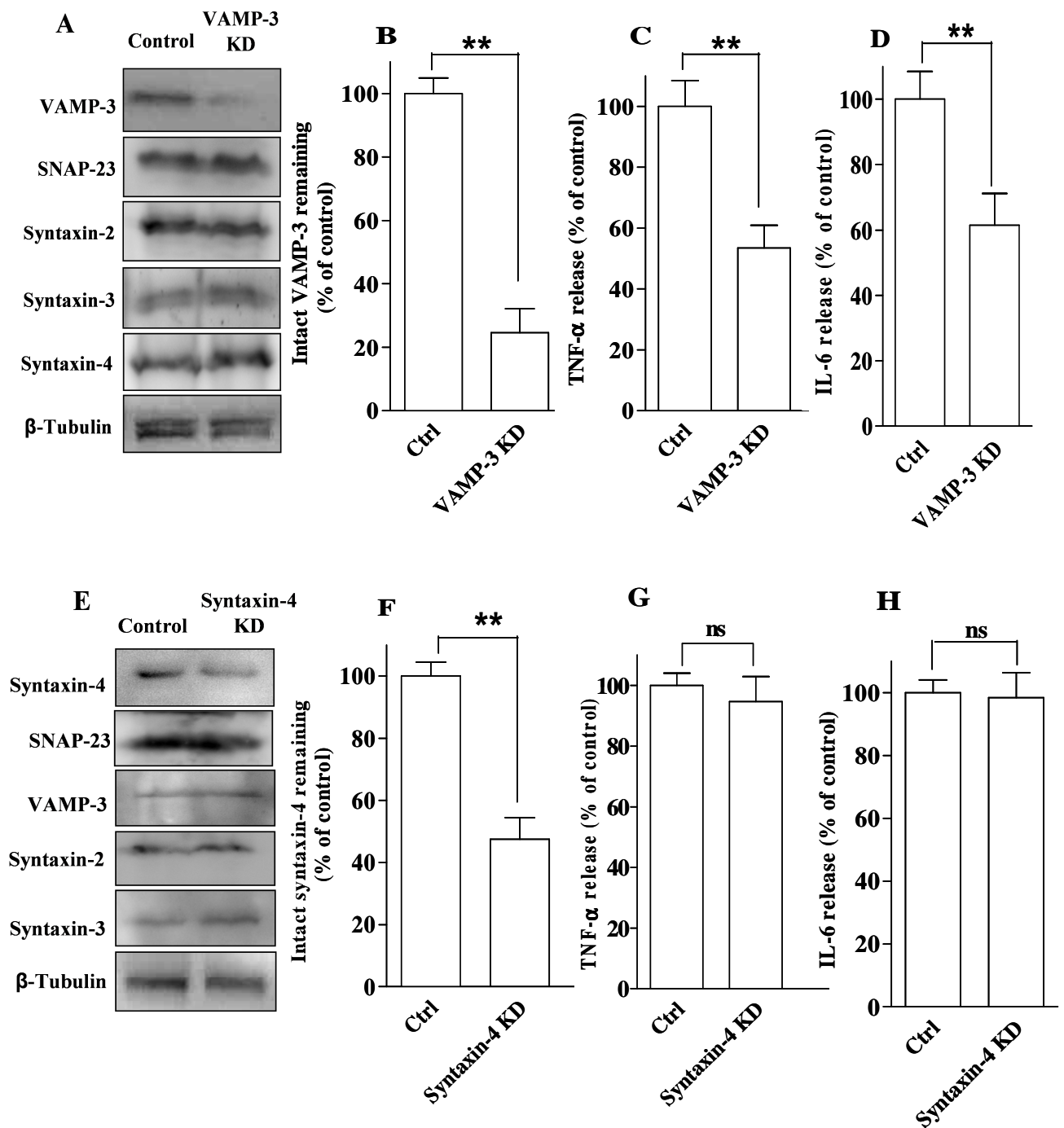
Fig. 3-5. KD of VAMP-3, but not syntaxin-4, significantly decreased the IL-1β stimulated release of IL-6 and TNF-α from SW982 cells.

A) Immunoblotting revealed that VAMP-3 was diminished in the KD cells after densitometric scanning and calculation of its level relative to that in the control B), using β-tubulin as a reference. Cells were incubated overnight with IL-1β (100 ng/ml) in medium before collecting the supernatant for quantifying the amounts of TNF-α and IL-6. VAMP-3 KD caused significant reductions in the release of both cytokines, TNF-α C) and IL-6 D), relative to that for non-treated control. E,F)

64

Western blot analysis showed ~50% KD of syntaxin-4, calculated as in B.) Overnight stimulation with IL-1β (100 ng/ml) failed to inhibit the release of TNF-α G) or IL-6 H) after KD of syntaxin-4. The results are expressed as mean ± S.E.M., n = 3, p < 0.05 considered statistically significant, **p < 0.01.

3.2.6 Non-targeted lentiviral shRNA particles failed to KD any SNAREs

To confirm specificity of above mentioned SNAREs KD with shRNA, SW982 cells were transduced with non-targeted lentiviral particles. The this non-targeted lentiviral particles could not KD any SNAREs (Fig. 3-6A) as well as inhibit release of TNF-α (Fig. 3-6B) and IL-6 (Fig. 3-6C), confirming specificity of shRNA used in these experiments.
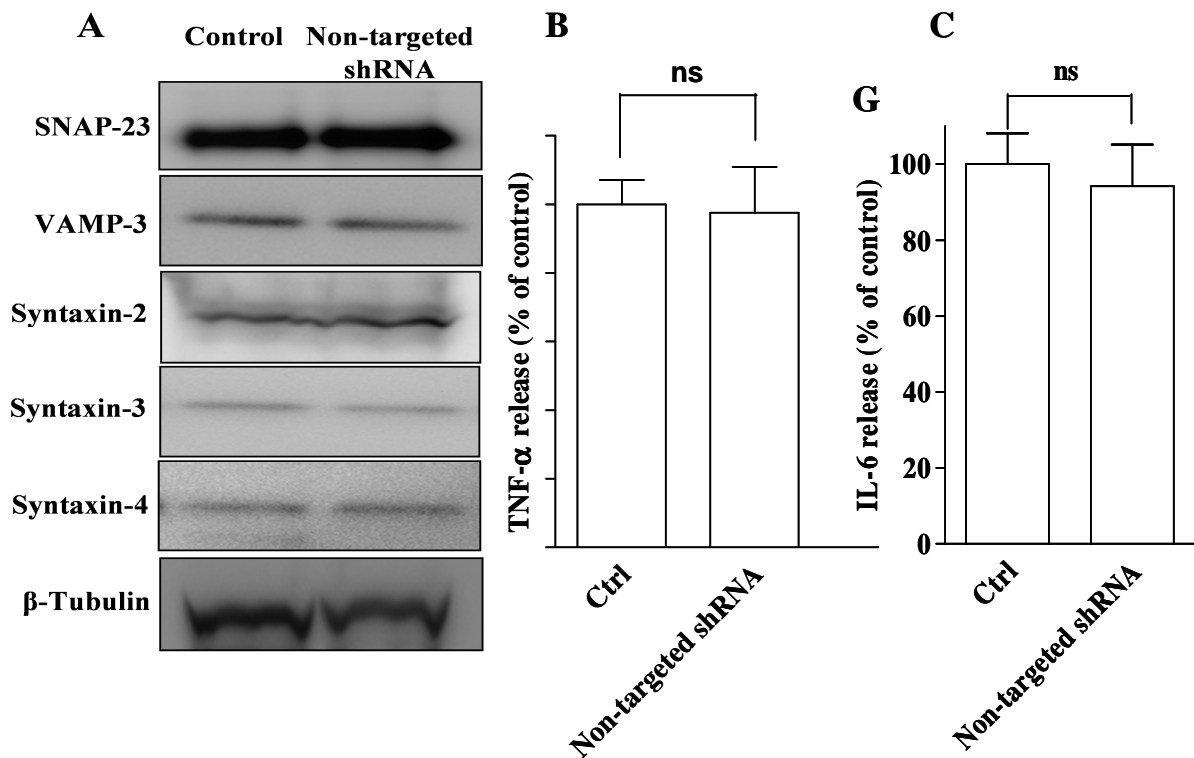
Fig. 3-6. The non-targeted lentiviral shRNA failed to KD SNAREs and inhibit release of cytokines.

A) Western blotting showing non-targeted shRNA could not KD SNAP-23, VAMP-3, Syntaxin-2, 3 or 4, control used as reference. B, C) Cell culture supernatant was collected after stimulation with IL-1β (100 ng/ml) for 20 h . The non-targeted shRNA did not inhibited TNF-α and IL-6 release. The results were expressed mean ± S.E.M., n=3.

3.2.7 Syntaxin-2 is not involved in release of cytokines (TNF- α and IL-6)

SW982 cells were transduced with shRNA (Table 2-3) for 10 days and then untransduced cells were removed by adding puromycin (5 µM) for 3-5 days. Cells were then stimulated with IL-1β (100 ng/ml) for 20 h before harvesting for Western blot analysis. The transient knock down of syntaxin-2 was achieved by ~ 60% when compared to control cells, without altering expression of other SNAREs (Fig. 3-7A, B). KD of syntaxin-2 did not alter expression of other SNAREs (Fig. 3-7A). The release of TNF-α (Fig. 3-7C) and IL-6 (Fig. 3-7D) was not reduced when compared to control. This is suggesting that syntaxin-3 might be involved in release of cytokines.
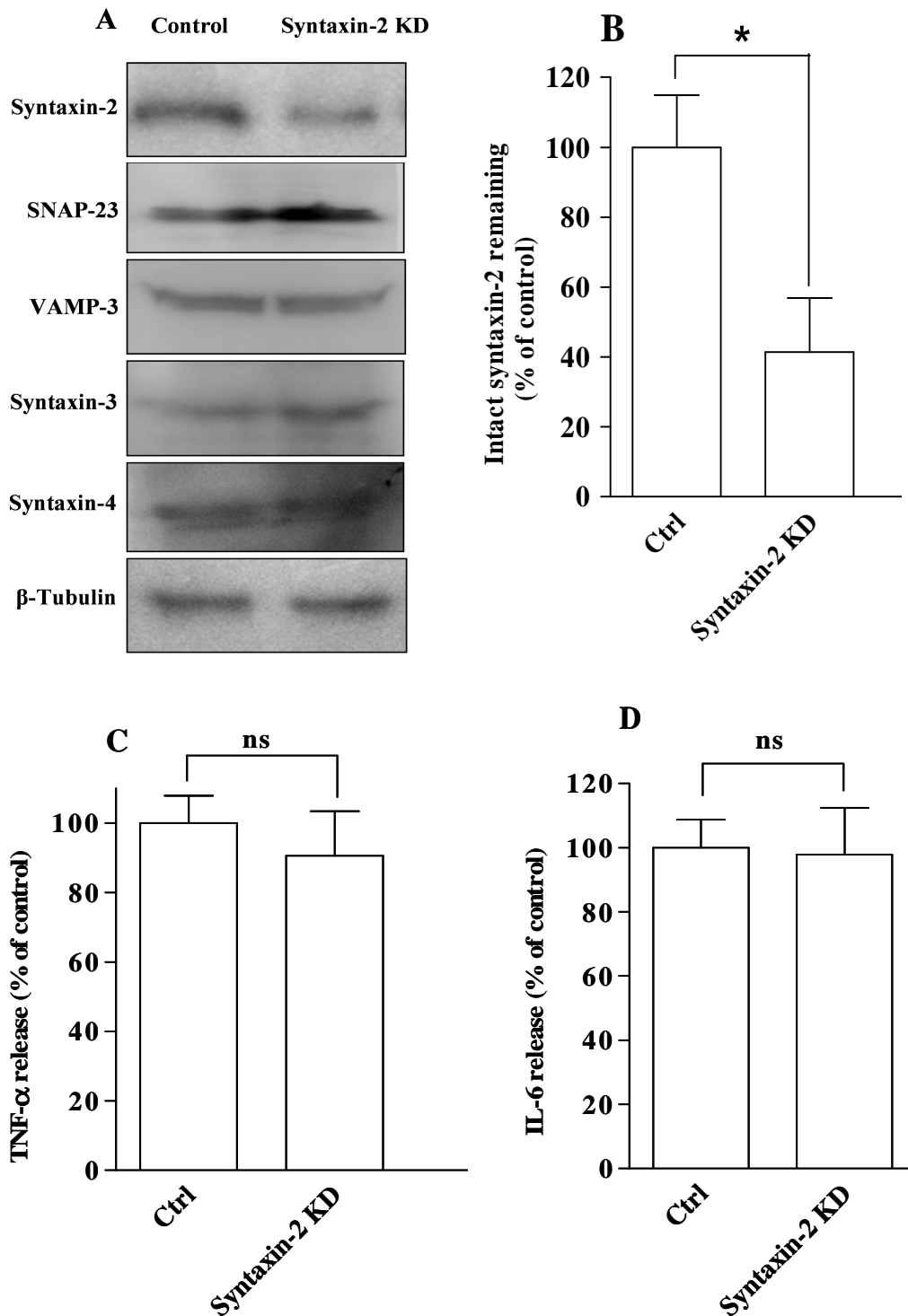
Fig. 3-7. KD of syntaxin-2 failed to reduce release of cytokines (TNF-α and IL-6).
A) Immunoblot was significantly reduced levels of syntaxin-2 compared to the control without altering other SNAREs. B) % KD of syntaxin-2 relative to the control was calculated using β-tubulin as an internal control. The KD of syntaxin-2 failed to inhibition of evoked release of TNF-α C) and IL-6 D). The results are expressed as mean ± S.E.M., n = 3, p < 0.05 considered statistically significant, *p < 0.05.

3.2.8 Knocking down syntaxin-3 did not alter cytokine release

SW982 cells were plated on 24-well plate and incubated overnight. After, incubation cells were infected with syntaxin-3 lentiviral shRNA (Table 2-4) for 10 days. Non-infected cells were died because of addition of puromycin (5 μM). Cells further incubated for another 4-5 days, before stimulating with IL-1β (100 ng/ml) for 20 h. The cell culture supernatant was collected and cells were recovered for immunoblot analysis. Western blot showed that ~50% KD was achieved (Fig. 3-8 A, B). The levels of other SNARE proteins were not affected after syntaxin-3 KD (Fig. 3-8A). The evoked release of TNF-α (Fig. 3-8C) and IL-6 (Fig. 3-8D) were not inhibited after syntaxin-3 KD.
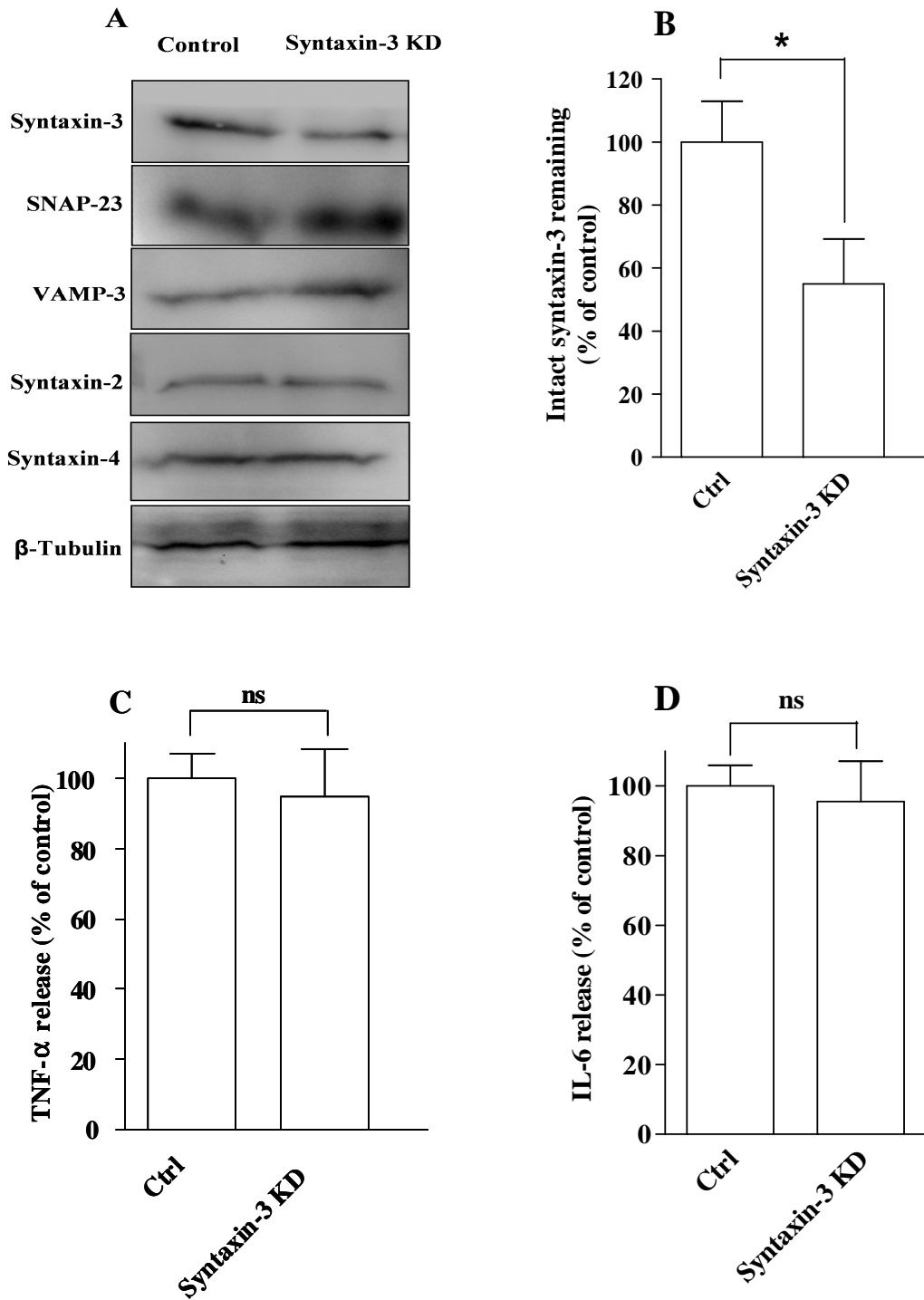
Fig. 3-8. *No decrease in release of cytokines (TNF- α and IL-6) was observed after KD of syntaxin-3.*

A) Western blot demonstrated decreased expression of syntaxin-3, unaffected levels of other SNAREs. B) % knock down of syntaxin-3 compared to control was analysed. β-tubulin served as internal control. IL-1β (100 ng/ml) stimulated release of TNF-α C) and IL-6 D) was not inhibited after KD of syntaxin-3. The results are expressed as mean ± S.E.M., n = 3, p < 0.05 considered statistically significant, *p < 0.05.

3.2.9 Formation of SDS-resistant SNARE complexes was decreased by KD of SNAP-23

Ca^{2+}-dependant membrane fusion requires formation of stable SNARE complex(es) and these are resistant to denaturation by SDS at temperatures up to ~80°C (Hayashi et al., 1994). In order to identify the SNARE partners participating in formation of such complex(es), 2-D electrophoresis (Chapter 2.1.8) was performed. Proteins from the cells were extracted by LDS and applied to the first dimensional gel (data not shown) without boiling; gel strips were cut and solubilised in LDS sample buffer, boiled, and applied to the second dimensional SDS-PAGE (Fig. 3-9A). Because SNAP-23 and VAMP-3 were found to contribute to the exocytosis of cytokines in SW982 cells, their participation in the formation of SDS-resistant SNARE complex(es) was investigated. In IL-1β-stimulated wild type (WT) SW982 cells, the majority of SNAP-23, VAMP-3 and syntaxin-2 did not occur in SDS-resistant complex(es) (Fig. 3-9A); this is shown by their electrophoretic migrations being unchanged by boiling and matching the mobilities known for their molecular masses. However, some SNAP-23 was retained in complex(es), presumably with other SNAREs, ranging in Mr of ~49 to ~272 k (Fig. 3-9A); complex(es) of Mr > 69 k displayed weak signal for VAMP-3 (Fig. 3-9A), with the intensity corresponding to that of SNAP-23 especially at Mr > 137 k. In contrast, IL-1β-treated cells in which SNAP-23 was stably knocked down showed only a minute amount of SNAP-23 in the free form and even less in complex(es) (Fig. 3-9B). Although an abundance of free VAMP-3 and syntaxin-2 remained, there was little if any complexed. These observations are suggestive of SNAP-23, VAMP-3 and syntaxin-2 forming SNARE complex(es) in normal cells which could contribute to evoked release of cytokines (c.f. Fig.. 3-3 and 3-4). Diminishing SNAP-23 caused abolishment of its partner, VAMP-3 and syntaxin-2 from SDS-resistant SNARE complex(es). Using co-immunoprecipitation, confirmatory evidence was obtained for SNAP-23 complex(es) containing VAMP-3, and VAMP-3 forming complex(es) with syntaxin-2, but hardly with syntaxin-3 and -4(Fig. 3-9C).

A

Molecular mass (kDa) before boiling	272	193	137	98	69	49	35	25	17
	193	137	98	69	49	35	25	17	12

B

C
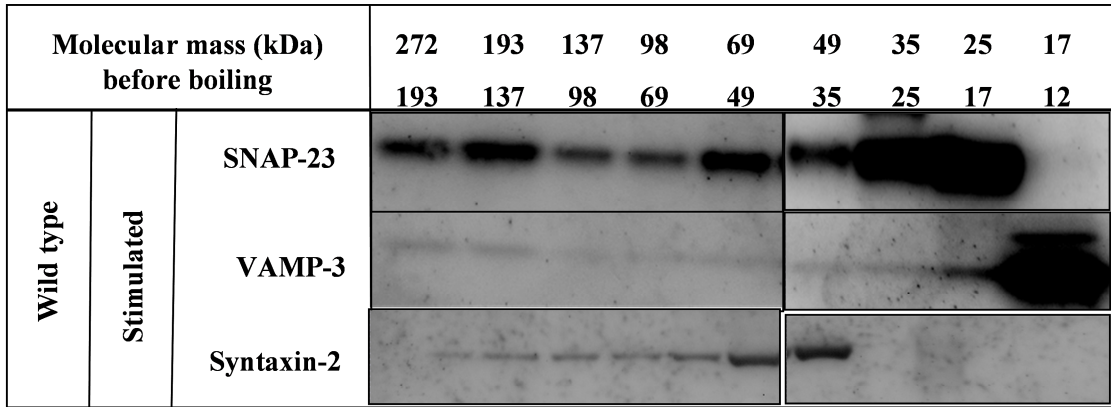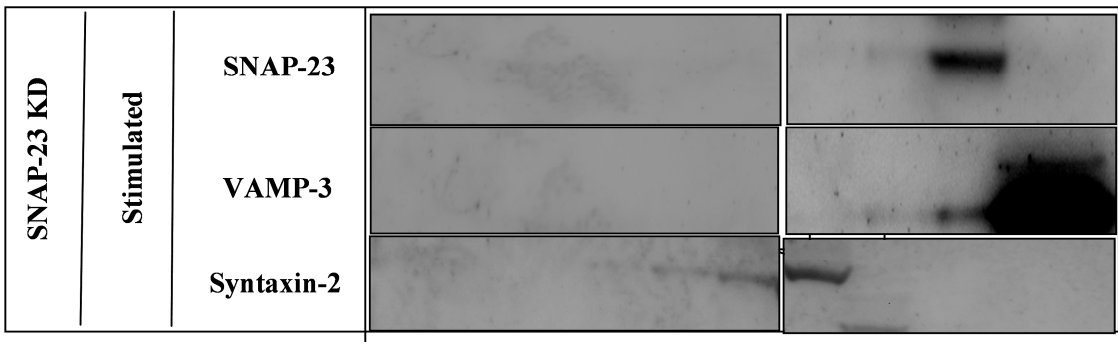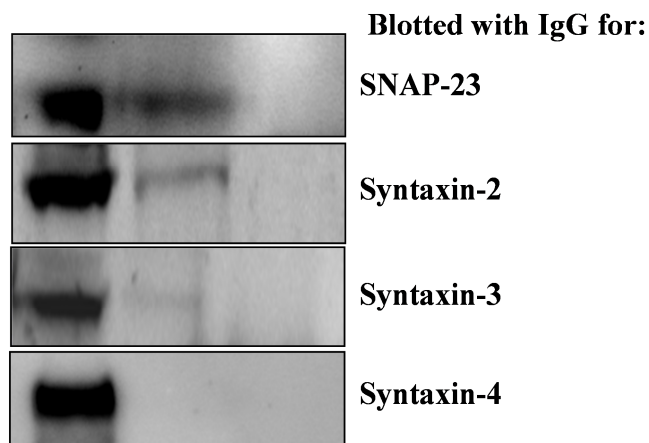
Fig. 3-9. **KD of SNAP-23 lowered the formation of SDS-resistant SNARE complexes in SW982**

Control and SNAP-23 KD SW982 cells were solubilised in LDS buffer without boiling and the proteins separated on precast 4-12% gels by SDS-PAGE. Gel sections containing the separated proteins were excised according to migration distances and extracted by boiling in LDS sample buffer before re-electrophoresis and immuno-blotting with antibodies specific for SNAP-23, VAMP-3 and syntaxin-2. A) SNAP-23

formed complex(es) with VAMP-3and syntaxin-2 in control cells after IL-1β (100 ng/ml) stimulation for 20 h. Note that the proteins in higher molecular weight are in complexes, while free forms of SNAREs are present at lower molecular weight. B) KD of SNAP-23 resulted in minimal formation of complex(es) with VAMP-3 and syntaxin-2 under stimulation conditions. C) VAMP-3 complex(es) with SNAP-23 or syntaxin-2 in stimulated control SW982. Total lysate (50 ug input) and 50% of the eluted protein were subjected to SDS-PAGE. Only the lower halves of the gels are shown because of excessive staining of the rabbit IgG that overlapped the SNARE complex(es). Note that SNAP23 associated with VAMP-3 was readily detected by Western blotting, confirming the result of panel A.

3.2.10 IL-1β stimulation significantly increased the expression of SNAP-23 and IL-6 in control cells whereas weaker signals were seen after SNAP-23 KD

Identical numbers of control or SNAP-23 KD cells were treated with IL-1β overnight before being lysed in LDS sample buffer and subjected to SDS-PAGE and Western blotting (Fig. 3-10A, B). Notably, IL-1β raised the expression of IL-6 and to a lesser extent SNAP-23 in control cells (Fig. 3-10A); quantities of their levels revealed respective increment of 2.8 ($\pm$ 0.04; $P < 0.01$; n = 3) and 1.3 ($\pm$ 0.05; $P < 0.05$; n = 3) fold.. Interestingly, IL-1β treatment did not induce such a change ($P>0.05$) the content of these two proteins in the SNAP-23 KD and normal cells (Fig. 3-10B). Moreover, confocal microscopy (Chapter 2.1.13) demonstrated an increased expression of IL-6 in the peri-nuclear region of control cells after stimulation with IL-1β overnight (Fig. 3-10C); in stark contrast, SNAP-23 in the KD cells only gave a very weak signal for IL-6 under both conditions, consistent with the finding in Fig. 3-4D, though a striking clustered distribution of IL-6 was seen in the stimulated cells (Fig. 3-10C). These cumulative findings indicate that SNAP-23 contributes to the trafficking of vesicles and secretion of IL-6 in human synovial cells.
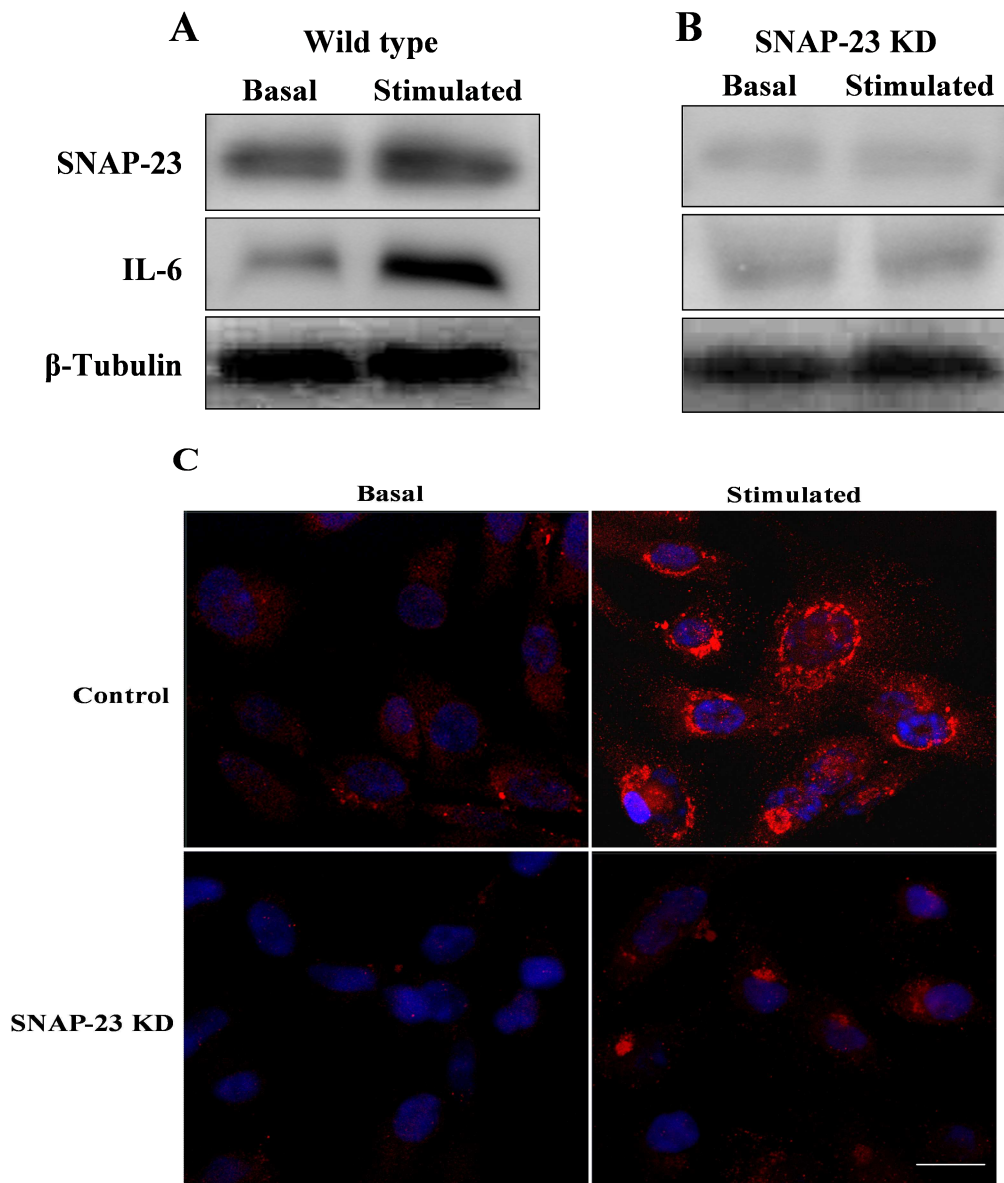
Fig. 3-10. Stimulation with IL-1β raised the levels of SNAP-23 and IL-6 in control SW982 but weaker signals were seen after SNAP-23 KD.

A) Western blotting of the wild type cells stimulated with IL-1β (100 ng/ml) showed increased expression of SNAP-23 and IL-6, relative to their contents under basal conditions. B) In SNAP-23 KD cells, no significant calculated changes were found in the levels of SNAP-23 and IL-6 under basal or stimulated conditions. β-tubulin acted as an internal standard for A and B. C) Confocal micrographs showing an increased occurrence of IL-6 at peri-nuclear region in IL-1β (100 ng/ml) stimulated control cells whereas the non-stimulated control displayed very weak staining for IL-6. Notably, the SNAP-23 KD cells exhibited very weak signals under basal and stimulated conditions, with some clustering near the nuclei in the latter. Alexa flour-labelled goat anti-rabbit 568 (1:1500) was used as a secondary antibody. The scale for images is 20 μm.

3.2.11 SNAP-23 KD abolished the filamentous-like distribution of IL-1 receptor but not its apparent surface content

To search for possible changes in the surface level of IL-1 receptor upon KD of SNAP-23, WT and SNAP-23 KD cells were stimulated with IL-1β (100 ng/ml) for 20 h. Total proteins and biotinylated cell surface IL-1 receptors (Chapter 2.1.10) were isolated from the cells, extracted in 2 x LDS sample buffer and separated by SDS-PAGE for Western blot analysis. Notably, in the stimulated and SNAP-23 KD cells, no change in total and surface content of IL-1R was observed, compared to non-stimulated WT (Fig. 3-11B). Thus, it is concluded that although the distribution pattern of IL-1 receptor on the SNAP-23 KD cells seemed to be changed, this did not alter its surface expression or total membrane content (Fig. 3-11 A).

A

WT   IL-1 receptor + DAPI   SNAP-23 KD

20 µm   20 µm

B

WT   SNAP-23 KD

−   +   −   +   Stimulation

IL-1R (Total)

IL-1R (Surface biotinylated)

β-Tubulin
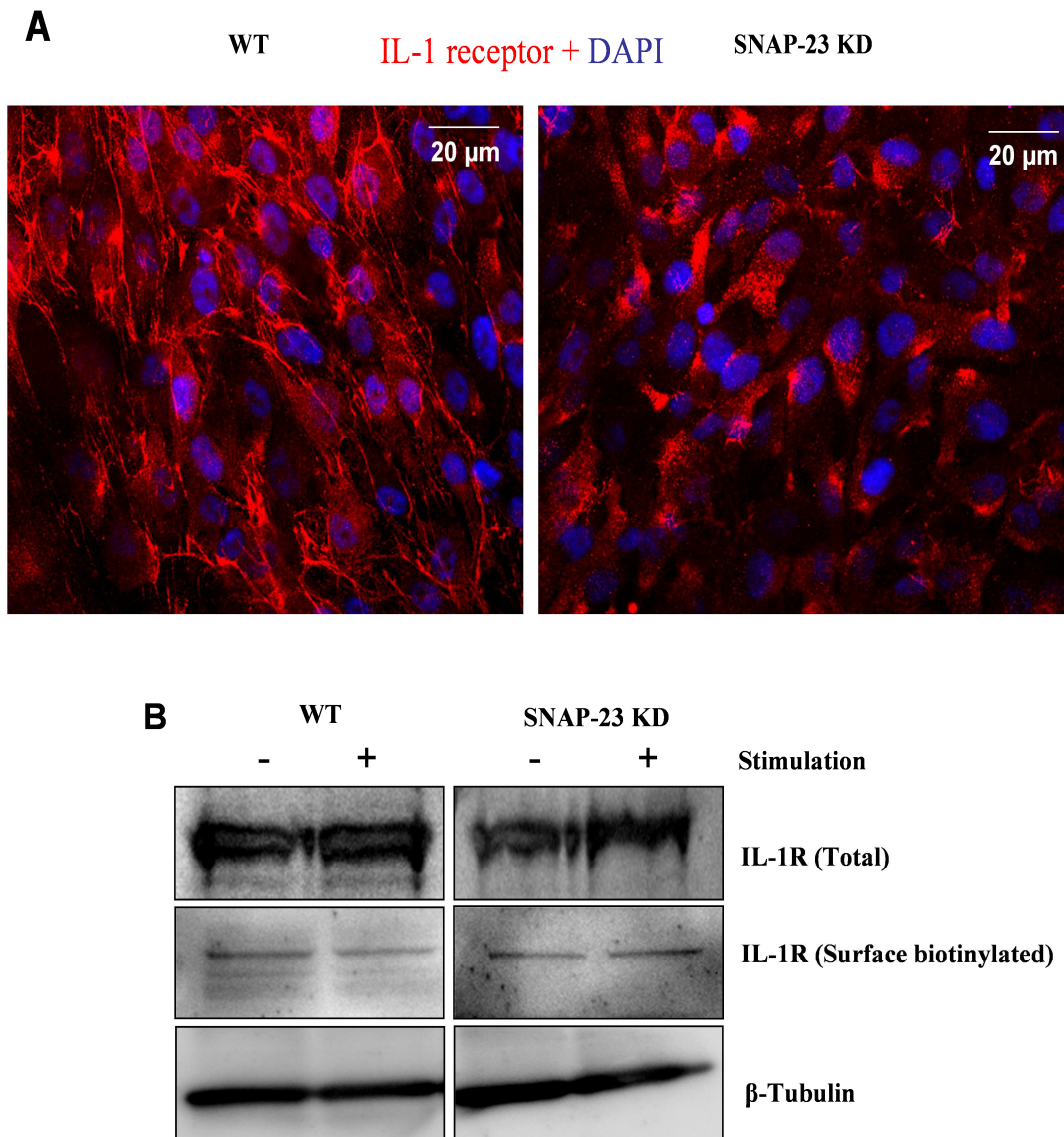
Fig. 3-11. Peri-nuclear accumulation of IL-1 receptor and lack of filamentous distribution resulted from SNAP-23 KD in SW982 cells.

A) WT SW982 and SNAP-23 KD cells were stimulated 20 h with IL-1β before being fixed, permeabilized, and labelled with IL-1 receptor rabbit antibody at 4°C for 16 h. Goat anti-rabbit Alexa 594 was applied as the fluorescent secondary antibody. Nuclei were stained with DAPI. Confocal images showing, that compared to control SW982 cells, the distribution of IL-1 receptor on the cell bodies and filaments was changed in SNAP-23 KD, showing a decreased expression on the cell body surface and filaments and an accumulation of IL-1 receptor near nuclei. Scales are indicated. B) IL-1β did not alter the cell surface content of IL-1 receptor in WT and SNAP-23 KD SW982 cells. Top panel shows total IL-1 receptor expression in whole cell extracts. Western blots of the surface expressed biotinylated IL-1 receptor with or without IL-1β

stimulation are illustrated in the middle panel. ß-tubulin was used as internal control for biotinylated samples (bottom panel). Notably, KD of SNAP-23 in SW982 cells did not alter the level of surface IL-1 receptor in the presence or absence of IL-1ß.

3.2.12 Cleavage of SNAP-23 by LC/E400(K224D) mutant

Modification of BoNT to truncate SNAREs in non-neuronal cells by retargeting the catalytic activity of BoNT has been developed to extend therapeutic application. In order to target non-neuronal SNARE proteins, targeted position 224 within the catalytic site of BoNT-E, which specifically cleaves the neuronal SNARE, SNAP-25. In addition to cleaving SNAP-25, the engineered BoNT-E (K224D) cleaved non-neuronal SNAP-23, at a similar rate to that at which the wild-type toxin cleaves its native target (Chen and Barbieri, 2009). In SW982 cells, EA (mutant) did not get into cells itself though SV2 is present.

The delivery of LC/E400(K224D) in SW982 cells was performed by digitonin permeabilisation over 30 mins in presence of LC/E400(K224D); cells were then washed with DMEM containing 10% FBS for 3 times and incubated overnight at 37°C. The partial cleavage of SNAP-23 found at 1000nM concentration of LC/E400(K224D) (Fig. 3-12). The VAMP-3 served as loading control.
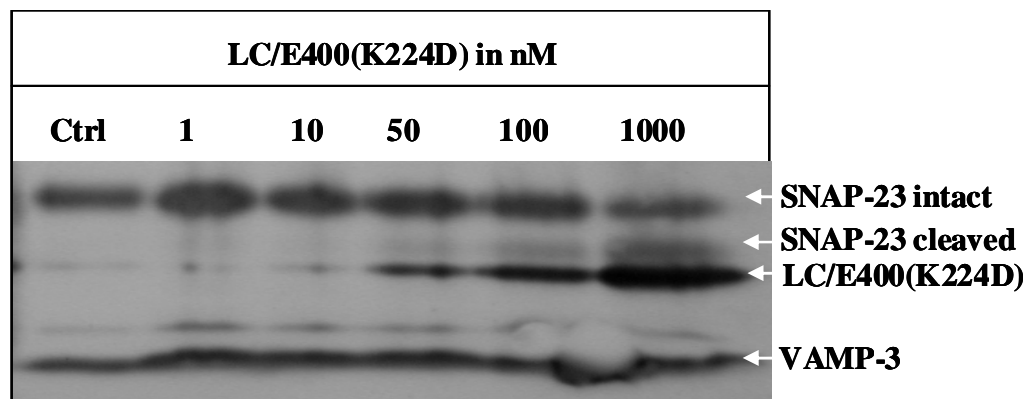
Fig. 3-12. SNAP-23 is partially proteolysed by LC/E400(K224D) in digitonin-permeabilized cells.

The permeabilisation of cells was achieved by digitonin (40 μM) in complete medium for 30 min in presence of LC/E400(K224D). After 30mins, cells washed 3 times with 1X PBS and harvested for western blot analysis. The truncation of SNAP-23 observed with 50, 100 and 1000 nM. The antibody against LC/E400(K224D) used to confirm presence of LC/E.

3.3 DISCUSSION

The importance of synoviocytes in arthritis disease progression is elucidated in this chapter. It is known that synoviocytes contributes to joint inflammation by producing cytokines upon disease onset (von Banchet et al., 2007). However, the SNAREs proteins are involved in exocytosis of cytokines and other pain mediators. Previous study demonstrated that, recruitment of SNAP-23 to granule membranes in rat peritoneal cells is implicated as an essential prerequisite for mediator release from mast cells (Murray et al., 2005). SNAREs are shown to be involved in exocytosis of cytokines and other mediators in cells, such as neutrophiles, mast cells, macrophages and platelets (Logan et al., 2003). It is very interesting to investigate whether SNAREs proteins are required in exocytosis of cytokines in synoviocytes.

This study provides the first evidence for the presence of particular SNAREs in a SW982 cells, and the involvement of SNAP-23 and VAMP-3 but not syntaxin-2, -3, or -4 in exocytosis of cytokines. During necrosis and cell lysis in pathological stages of RA and OA, there is enhanced exocytosis of IL-6 and TNF-α induced by IL-1β (Houssiau, 1995; Schaible et al., 2006; Lacy and Stow, 2011). IL-1β is one of the most critical pro-inflammatory factors that are released by many innate immune-cells, and contributes to inflammatory pain hypersensitivity. In fact, the generation and propagation of arthritis could involve sequential release of multiple inflammatory cytokines which act through a positive feed-back cascade involving surrounding cells (Houssiau, 1995; Choy and Panayi, 2001; Feldmann, 2001; Schaible et al., 2006; Kinne et al., 2007). Our finding of increased secretion of IL-6 and TNF-α upon incubation of SW982 with IL-1β is reminiscent of their co-release from lipopolysaccharides (LPS)-treated macrophages (Manderson et al., 2007; Lacy and Stow, 2011). Overnight stimulation of the normal SW982 with IL-1β resulted in increased expression of SNAP-23 and IL-6, which indicates up-regulation of SNAP-23 is required to meet the demand for the increased cytokine trafficking/secretion; a similar finding was reported for immune cells upon lipopolysaccharides treatment (Han et al., 2009; Lacy and Stow, 2011). Furthermore, convincing evidence for the involvement of SNAP-23 and VAMP-3 in the exocytosis was obtained because their KD did not reduce the levels of other SNAREs, but decreased the secretion of IL-6 and TNF-α to similar extents. The remaining release can reasonably be attributed to the residual levels of SNAP-23 and VAMP-3 after KD or, perhaps, the participation

77

of other unidentified SNARE isoforms, and even non-classical secretion pathways (Stanley and Lacy, 2010). The simultaneous participation of both SNAP-23 and VAMP-3 in the co-release of IL-6 and TNF-α from SW982 cells is an interesting feature, because the intracellular trafficking pathways for IL-6 and TNF-α in other cell types, i.e. macrophages, overlap but with some divergence. For example, in macrophages after synthesis of these cytokines in the endoplasmic reticulum (ER), they co-accumulate in the Golgi complex(es) before sorting. The membrane-bound TNF-α is delivered by recycling endosomes to phagocytic cups or the plasma membrane for secretion. IL-6 which lacks a transmembrane domain could be secreted directly, though KD of VAMP-3 does affect the secretion of TNF-α in macrophages (Murray et al., 2005; Manderson et al., 2007). This clearly supports the notion that cytokine secretion can be tailored to the needs of inflammatory systems, through variant SNARE-dependent pathways (Stow et al., 2009). Notably, TNF-α release from secretory granules in mast cells also requires SNAP-23 (Stanley and Lacy, 2010), similar to our finding in SW982. KD of the syntaxin-2,-3 or -4 present in SW982 did not impair the IL-1β-stimulated release of IL-6 and TNF-α, though trace amounts of isoforms -2 and -3 were co-immunoprecipitated with VAMP-3. This lack of inhibition of exocytosis is presumably due to incomplete and less extensive KD than that of SNAP-23 and VAMP-3, and/or any other isoforms possibly present, compensating for their function. In macrophages, multiple syntaxin isoforms (4, 6 and 7) are implicated in TNF-α release (Stanley and Lacy, 2010).

KD of SNAP-23 significantly reduced the amount of SDS-resistant complex(es) formed between SNAP-23, VAMP-3 and synatxin-2 but did not affect surface content of IL-1 receptor though the filamentous-like distribution was disappeared. As such complex(es) are known to be essential for transport of TNF-α vesicles and membrane fusion (McMahon and Sudhof, 1995; Pagan et al., 2003), their decrease appears to underlie the reduced exocytosis of IL-6 from SNAP-23 KD cells. It is well knows that Ca^{2+} binding to its sensor which triggers exocytosis of vesicles by SNARE complex(es) assembly (Chen et al., 1999).

External Ca^{2+} was found to be required for cytokine release as incubation with IL-1β in the presence of extracellular Ca^{2+} enhanced this release and did not affect survival of the SW982 cells (~95% of cells were viable). Consistent with the Ca^{2+}-dependence of cytokine release, voltage-dependent Ca^{2+} channels, mainly L-type, occur in SW982 (Kochukov et al., 2006). Also, carrier membrane proteins

(SCAMPs) have been implicated in the Ca^{2+} regulation of cytokine trafficking in immune cells (Han et al., 2009). SCAMPs directly bind to Ca^{2+} sensor in immune cells; thus, these proteins have potential roles in cooperation with the SNARE machinery in Ca^{2+}-regulated exocytosis of cytokines (Han et al., 2009). The observed ability of IL-1β to increase K^+-stimulated release of IL-6, ~3.5-fold over the basal in 4 h, and its inhibition upon depleting SNAP-23 reaffirms a need for extracellular Ca^{2+} in SNARE-mediated cytokine release in SW982. The lack of significant IL-6 release after 4 h incubation compared to 20 h might suggest only a portion of release was collected during shorter time and the release requires longer time of stimulation.

Our interesting finding of peri-nuclear localisation of SV2 protein after SNAP-23 KD, but not in normal cells, suggests participation of the former in the transportation of cytokines from this locus, presumably trans-Golgi or ER regions (unfortunately, suitable paired antibodies were not available for counter-staining). Although the role of SV2 in regulating the expression and trafficking of the Ca^{2+} sensor protein, synaptotagmin, has been well documented (Chang and Sudhof, 2009), nothing is known about the function of this trans-membrane protein in non-neuronal cells except for its location on secretory vesicles visualized by immuno-electron microscopy (Feany et al., 1993). Nevertheless, the enhanced occurrence of SV2 in the peri-nuclear region in SNAP-23 KD cells implicates this protein in the package and delivery of cytokines to the cell surface. IL-6 is also visualised in the peri-nuclear area in both control and SNAP-23 KD cells after overnight stimulation with IL-1β. This is in agreement with the finding in macrophages where LPS or interferon (IFN) increases IL-6 expression in peri-nuclear Golgi complex 2-fold (Manderson et al., 2007). IL-β stimulated wild type cells showed increased expression of SNAP-23 and IL-6, but not in SNAP-23KD cells. It is also interesting that in SW982, SV2 located intracellularly and it does not serve as the protein acceptor for BoNT/A, unlike in the neuronal cells (Dong et al., 2006). Mutated LC/E400(K224D) developed, which can cleave human SNAP-23 (Chen and Barbieri, 2009), did not get into cells. Though successful delivery of LC/E400(K224D) into HeLa cells to inhibit IL-8 and mucin secretion supports a role for LC/E400(K224D) as a research tool and, also, shows the potential for therapy to regulate human hypersecretion diseases such as asthma and inflammatory diseases (Chen and Barbieri, 2009). LC/E400(K224D) was delivered into SW982 cells by permeabilisation cleaved SNAP-23.

Because of the importance of synovial cells in the propagation of inflammatory response in RA and OA, the finding herein of SNAREs involvement in the release of cytokines could aid the development of novel and effective therapeutics. It is known that BoNTs cleave SNAREs and, subsequently, block the release of cell mediators (Dolly et al., 2011; Dolly and O'Connell, 2012). Accordingly, SNAP-23 is inactivated by a mutant of type /E light chain which reduces the release of cytokines from HeLa cells (Chen and Barbieri, 2009); likewise, VAMP-3 is cleaved by /D and blocks TNF-α release from human monocytes (Imamura et al., 1989). Notably, some serotypes of BoNTs have been used successfully to alleviate inflammatory pain symptoms in RA and OA (Mahowald et al., 2006; Singh et al., 2009b; Singh et al., 2009a; Chou et al., 2010), and in chronic arthritis models (Krug et al., 2009; Anderson et al., 2010). Consistent with our demonstrated presence of SV2 isoforms (receptors for BoNT/A, /D, /E /F and tetanus toxins) (Hayashi et al., 1994; Mahrhold et al., 2006; Schaible et al., 2006; Fu et al., 2009; Yeh et al., 2010; Peng et al., 2011; Wang et al., 2012) in rat cultured synoviocytes, these cells are susceptible to BoNT chimera /BA (Wang et al., 2012), generated by substituting the HC/A (C-terminal half of BoNT/A heavy chain) into BoNT/B. BA delivers the type B protease via the BoNT/A acceptor into synoviocytes and cleaves the requisite isoforms of VAMP . Future work could attempt to specifically target synoviocytes, macrophages and sensory neurons using BoNT chimeric strategy (Wang et al., 2008; Meng et al., 2009; Somm et al., 2012) by switching the wide-spectrum binding domain to a cell-type unique ligand (Somm et al., 2012).

In conclusion, particular SNAREs and SV2 present in SW982 cells have been identified; KD of SNAP-23 or VAMP-3 impaired release of IL-6 and TNF-α upon stimulation with IL-1β, implicating these SNAREs in the exocytosis of cytokines.

CHAPTER 4 VAMP-8 IS REQUIRED FOR THE RELEASE OF CYTOKINES FROM RAT SYNOVIOCYTES

4.1 BACKGROUND

As part of the investigation of BoNT as therapeutic agent in rat models of arthritis, rat synoviocytes (rSCs) were first used to measure the expression of BoNT receptors, SNAREs, their truncation, native or chimeric BoNTs and inhibition of the release of cytokines.

Synoviocytes were isolated from rat knee joint synovium and cultured using DMEM containing FBS. The synovium is the central area of pathology in a number of inflammatory joint diseases, including RA and OA. The type A synoviocyte has cell surface markers identifying it as being from macrophage lineage derived from blood monocytes while the type B is of fibroblast lineage are intimal fibroblasts which are derived locally (Smith et al., 2003; Smith, 2011).

Rat synoviocytes were found to express the receptor SV2A for BoNT/A and /D but not that for BoNT/B-synaptotagmin I/II for BoNT/B, moreover, SNAP-25 is absent, thereby, precluding the use of BoNT/A or /E with these cells. To truncate VAMP-3, BA or DA chimaeras were generated by substituting HC/A by its counterparts from BoNT/B or /D; these exhibited high specific activity, delivered the BoNT/B or /D protease via the BoNT/A acceptor into synoviocytes (Wang et al., 2012). In the present study, these novel hybrid BoNTs truncated VAMP-3 in synoviocytes but failed to inhibit release of cytokines (TNF-α and IL-6), suggesting involvement of other isoform(s) of VAMP. Because these cells express VAMP-8, knockdown of VAMP-8 was carried out and shown to it result in inhibition of the release of cytokines.

4.2 RESULTS

4.2.1 Construction and expression of BoNT/BA or DA chimaeras

Both chimeras were engineered and expressed by Dr. Jiafu Wang. The BA and DA (Fig. 4-1) were generated by ligation of the corresponding genes generated by PCR for LC.H_N/B or LC.H_N/D and HC/A via a linker encoding two extra residues (DI) into pET29a to create an expression vector containing the BA or DA insert (Chapter 2.1.5). Both chimeras contain two thrombin-cleavage sites generated by PCR, using suitable primers followed by self-ligation. One site is in the loop region to facilitate specific nicking, whereas extra nucleotides were also added to encode a thrombin consensus site for cleaving the C-terminal His_6 tag. All of the DNA sequences were verified and each new single chain (SC) gene was transformed into *E. coli* BL21.DE3 cells, expressed and the protein purified by IMAC (immobilized metal-affinity chromatography, Chapter 2.1.19). The IMAC purification of chimaera BA or DA was gel-filtered into 20 mM sodium phosphate buffer (pH 5.8) and further purified on a UNO S1 column, followed by washing with 100 mM NaCl and elution with a stepwise gradient (up to 1 M NaCl in the phosphate buffer). After buffer exchanging the eluted toxin into 20 mM Hepes and 145 mM NaCl (pH 7.8), purified SC toxin was either stored at −80°C or nicked by biotinylated thrombin (1 unit/mg for 1 h at 22°C) followed by removal of the thrombin by Streptavidin agarose, using the manufacturer's protocol before storage (Wang et al., 2012).
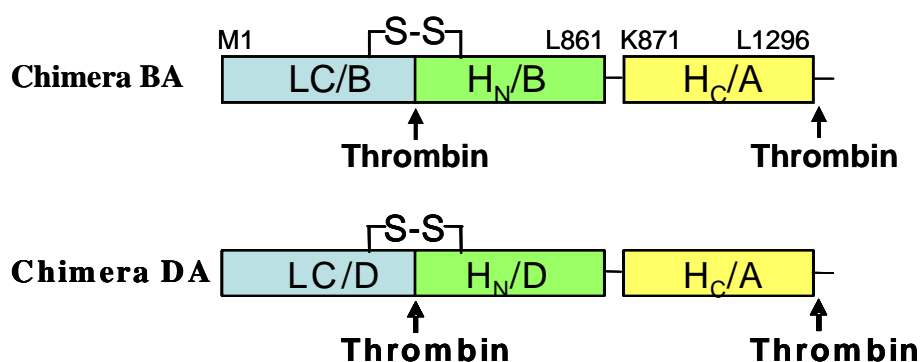
Fig. 4-1. Schematic of chimera BA and DA.

Chimera BA or DA were generated by ligating the relevant fragments of the BoNT/B or /D gene (blue and green, respectively), encoding LC-H_N/B or /D, to the SV2-binding domain (HC) of BoNT/A (yellow) via a linker encoding two extra residues (DI). Both constructs were tagged with His_6 to facilitate purification.

It was necessary to verify that the HC substitution of BoNT/B did not in any way hinder protease function, using an assay with a model synthetic substrate (Table 4-1). Chimera BA showed protease activities comparable to their parent toxin (BoNT/B) demonstrating that these were not altered by the binding domains being swapped. Therefore, any differences found later between the performance of this chimaera and the parent could be ascribed to the translocation and/or acceptor-binding domain (Table 4-1). In the terms of specific neurotoxicity (Chapter 2.1.18), no significant difference between BoNT/B and chimera BA.

Table 4-1. Proteolytic activities and mouse lethalities of DC chimaera and parental toxin.

Toxin	EC_{50} nM for cleavage of GFP–VAMP2$_{(2–94)}$-His$_6$	mLD_{50}units/mg
BoNT/B	2.72 ± 2.08 (n=5)	7×10^8
Chimera BA	3.81 ± 2.18 (n=5)	6×10^8
Chimera DA	ND	6×10^7

Proteolytic activities of chimeric and parental DC toxins were determined using model substrates (13.5 μM GFP–VAMP2(2–94)–His6). Values represent the amount of each toxin needed to cleave 50% of substrate within 30 min at 37°C. The lowest dose of toxin that killed 50% of a group of four mice within 4 days after intra-peritoneal injection is defined as 1 mLD_{50} unit. DC, di-chain; GFP, green fluorescent protein; ND, not determined; His$_6$, histidine tag.

4.2.2 Synoviocytes isolated from rat knee joint

Synovium was isolated from rat knee joint as shown (Fig. 4-2). Briefly, knee joint was separated from tibia and fibula and then cut open patella surrounded by synovium (Hyc et al., 2007). Rat synovial cells (rSCs) were dissociated from synovial membrane by digesting with collagenase and plated onto 24-well plate. For all experiments, cells were used between passage number 4-12. Purity of rSC cultures was confirmed by fibroblast-specific vimetin staining. Cultures were found to be consisting of ~95% of fibroblasts and free from macrophages.
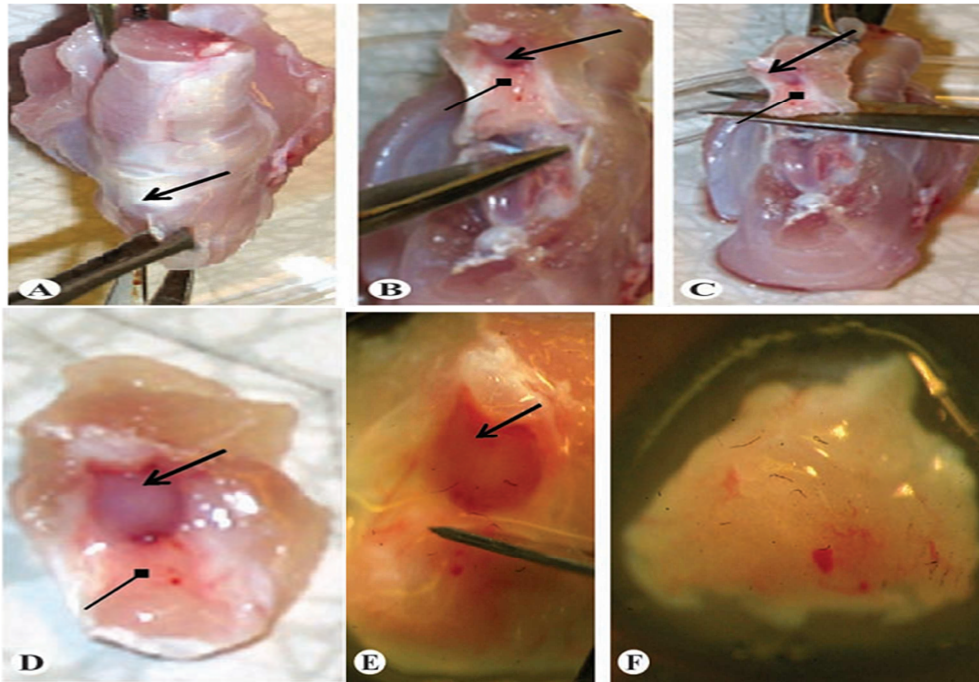
Fig. 4-2. Preparation of synovial membrane from rat knee joint.
(Hyc et al., 2007)

A) Showing knee joint cut from tibia and fibula using scissors and removal of skin with scalpel, B) knee joint was opened from one end C) the patella was exposed by removing the upper tissue of joint, D) the patella with surrounding synovium E) further dissection of synovium F) synovium is separated from patella. Open arrow – patella and rhomboidal arrow synovium.

4.2.3 Culture of rCGNs and rTGNs

rCGNs and rTGNs were cultured as described in Chapter 2.1.3. Phase contrast micrographs revealed that rCGNs and rTGNs (Fig 4.3) neuronal cells are distinguished by round, phase-bright cell bodies with extended fine fibres and cultures were free from non-neuronal cells. All neuronal cultures were used for experiments at 7 days *in vitro* (see later).

rCGNs rTGNs
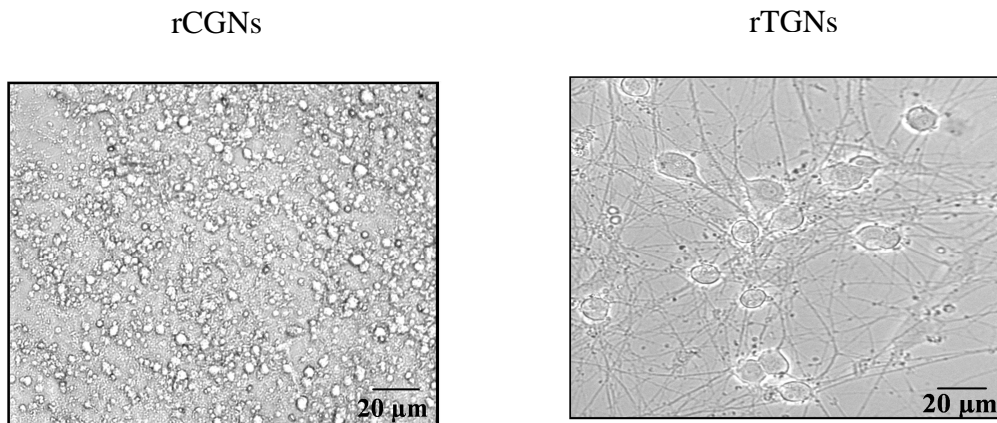
Fig. 4.3 Culture of rCGNs and TGNs.

Neurons were isolated from rat cerebelli or trigeminal ganglia and cultured using 24-well plate. Bright field images of rCGNs and rTGNs viewed using phase-contrast show round cell bodies and neurite outgrowth.

4.2.4 rSCs contain SNAREs and BoNT/A receptor

To investigate the involvement of SNAREs in release of cytokines from synoviocytes, cells were isolated from rat knee joint, and the total cell lysate analysed for SNAREs and receptors for BoNT/A. Western blotting revealed the presence of SNAP-23, VAMP-2, -3, -8 and lesser amount of syntaxin-1 (Fig. 4-4A) and SV2A (Fig. 4-4B). Thus, it was warranted to establish if the SNAREs present in rSCs contribute to the release of cytokines.
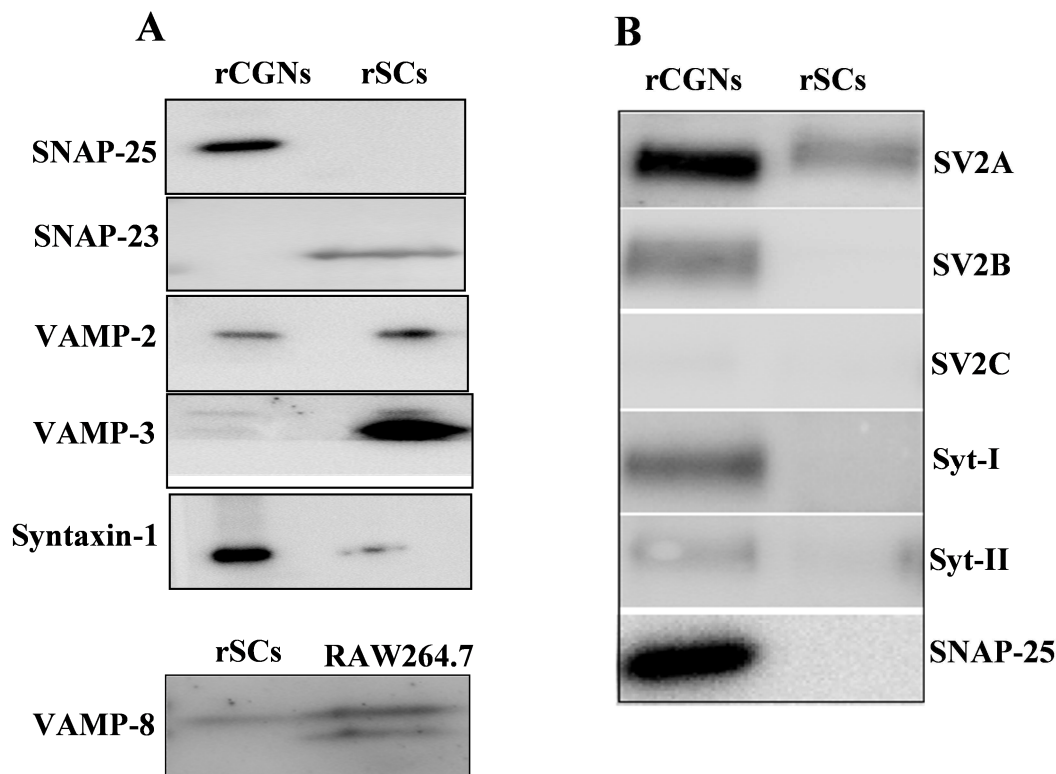
Fig. 4-4. Demonstration of SNAREs and BoNT receptor in rSCs.

A) Immuno-blot demonstrating the presence of SNAP-23, VAMP-2, -3 and -8 and B) SV2A in rSCs. An equal amount of protein was loaded into each lane for all the blots; the approximate sizes of the bands are indicated.

4.2.5 BoNT DA and BA chimeras truncated VAMP-2 in cultured rTGNs and rCGNs

To assessing the novel chimera-DA and BA toxins undergo the multiple steps of binding, translocation and cleavage of their respective substrates *in situ*, they were incubated with rTGNs and rCGNs (Chapter 2.1.3) for 24 h and cleavage of VAMP-2 was monitored by immuno-blotting. In rTGNs, chimera DA caused a dose dependent cleavage of VAMP-2 (Fig. 4-5A). Western blotting of rCGNs lysates for VAMP-2 cleavage showed BA matched the activity of /B (Fig. 4-5B).
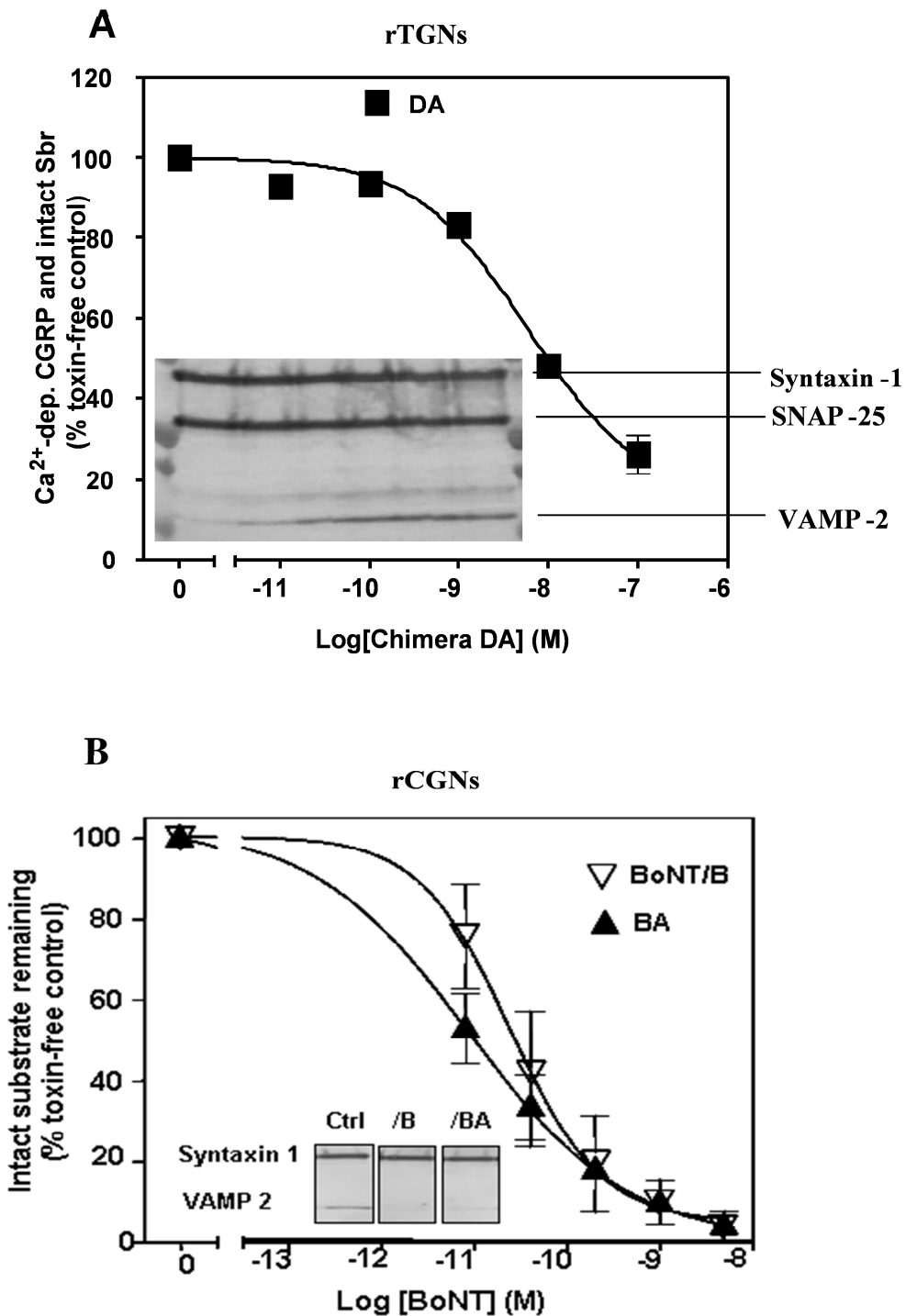
Fig. 4-5. Both BoNT chimeras potently and specifically cleaved their requisite substrate in intact cultured neurons.

Rat TGNs at 7 days in vitro were incubated with chimera-DA A) and rCGNs were treated with chimera-BA or BoNT/B B) for 24 h in culture medium, washed and solubilised in SDS sample buffer. Equal amounts of protein were subjected to SDS-PAGE, under non-reducing conditions, and Western blotting. The proportions of intact VAMP-2 remaining were calculated relative to an internal un-cleaved syntaxin-

1 control in the same lane, before calculating their intensities as a % of the signal observed in toxin-free control lanes.

4.2.6 Chimera DA and BA cleaved VAMP-3 after successful delivery into rSCs through /A binding receptor, SV2

Because rSCs express the protein receptor SV2A for /A, chimera DA was used to cleave VAMP-3. The cells were plated onto 24-well plate and incubated for 20h before adding DA (100 nM) in presence of lipopolysaccharide (LPS, 50 μg/ml); after overnight incubation at 37°C, the cells were harvested for immuno-blot analysis. DA cleaved VAMP-3 in presence of LPS (Fig. 4-6A). LPS was used because it sensitizes cells to secrete cytokines and thus, should stimulate the exocytosis-coupled endocytosis. Densitometric analysis revealed that ~45% of VAMP-3 got truncated (Fig. 4-6B). Where BoNT/A, /B or BA (100 nM) were added to cells in presence of substance P (1 μM) and incubated for 24 h; unlike /B and /A, BA cleaved VAMP-3 (Fig. 4-6C). The densitometric analysis show ~60% cleavage of VAMP-3 (Fig. 4-6D). BoNT/B failed to cleave VAMP-3 due to a lack of its synaptotagmin receptor in these cells; because there is no SNAP-25 in these cells, /A did not give any cleavage (Fig 4-6C).
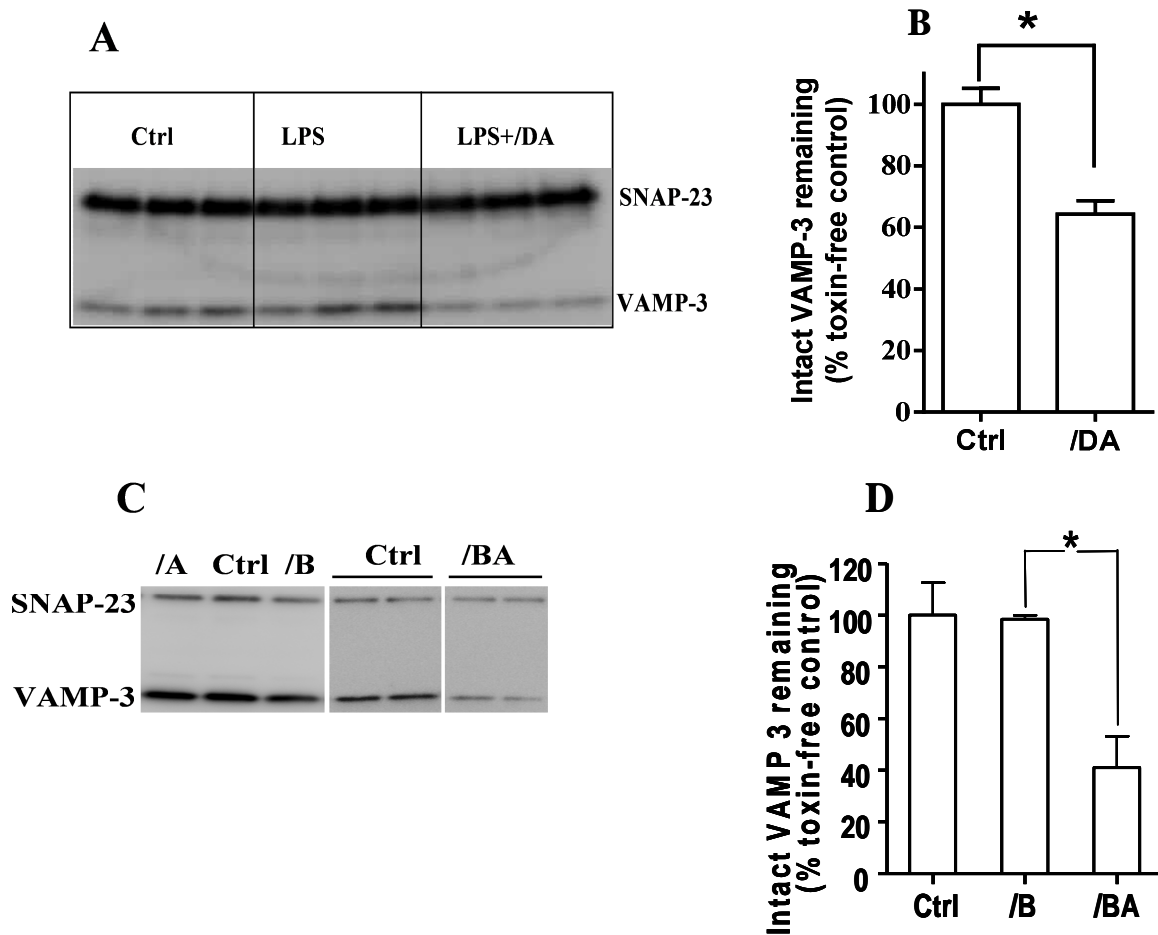
Fig. 4-6. Chimera DA and BA entered cultured rSCs and cleaved VAMP-3, unlike their parents which failed to truncate their respective substrates.

rSCs were incubated at 37°C for 24 h with or without 100 nM of /DA with LPS (50 μg/ml) and B/A in the presence of 1 μM substance P in culture medium. Cells were washed and harvested in SDS sample buffer. Solubilised proteins were subjected to SDS-PAGE and Western blotting using the antibodies indicated. A) Immuno-blots showing cleavage of VAMP-3 by DA (triplicate lanes); no change occurred in two controls: medium alone and the latter containing LPS. B) The amount of intact VAMP-3 left after toxin treatment. C) Representative blots indicating that BoNT/A, relative to the non-toxin treated control (Ctrl), failed to truncate SNAP-23 but chimera BA cleaved VAMP-3 (duplicate lanes) unlike /B. D) The proportions of VAMP-3 remaining intact after treatment with 100 nM of either chimera BA or /B were calculated (± S.E.M.; n = 3) relative to the uncleaved SNAP-23, internal standard.

4.2.7 Truncation of VAMP-3 by chimera DA or BA failed to inhibit release of TNF-α and IL-6 indicating VAMP-8 may be required for exocytosis of cytokines

rSCs were incubated for 24h at 37°C with 100 nM of DA in presence of LPS (50 µg/ml), /BA(100 nM) in presence of substance P (1 µM) or BoNT/B. Cells were washed twice with PBS and stimulated with IL-1β (100 ng/ml) in complete medium for 20 h to release cytokines. Notably, IL-1β stimulated release of IL-6 (Fig. 4-7A) and TNF-α (Fig. 4-7B) was not inhibited by either toxin. Because VAMP-3 cleavage was shown by Western blot analysis but no blockade of cytokines release, the isoform, VAMP-8 present in rSCs may be functional. This possibility was next examined.
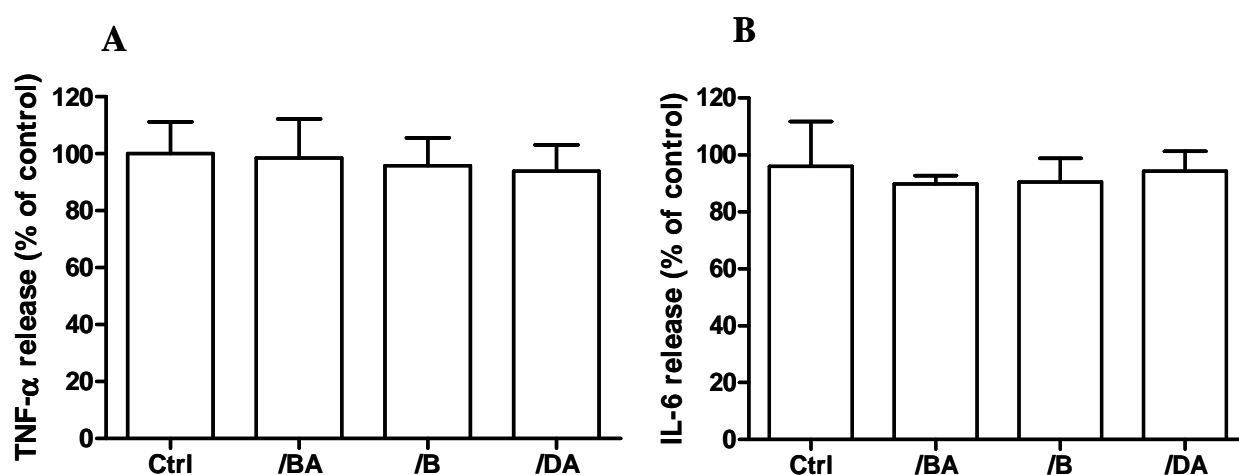
Fig. 4-7. ELISA for IL-6 and TNF-α in cell culture supernatant.

Cells exposed for 24 h to BA plus substance P, DA in presence of LPS or BoNT/B. Cell culture supernatants were collected after stimulating cells with IL-1β (100 ng/ml). Cytokine release was assayed using commercial ELISA kit for IL-6 A) and TNF-α B), while the cells were subjected to Western blot analysis. Notably, no significant difference was detected between toxin-treated and control cells. Data plotted are Mean ± S.E.M.; n=3.

4.2.8 VAMP-8 is required for the release of cytokines (IL-6 and TNF-α) from rSCs

Synoviocytes isolated from rat synovium were incubated with VAMP-8 lentiviral shRNA (Table 2-6) for 15 days, and half of the growth medium changed every 6-7 days. The rSCs were further incubated in the presence of puromycin (5 µM) for 4-5

days to kill off the non-transduced cells. For evoked release of TNF-α and IL-6, cells were stimulated with IL-1β (100 ng/ml) for 20 h before collecting cell supernatants for ELISA and cells for Western blot analysis. shRNA caused ~50% KD of VAMP-8 whilst not affecting expression of SNAP-23 (Fig. 4-8A, B), reduced by ~35% the release of TNF-α (Fig. 4-8C) and ~30% of IL-6 (Fig. 4-8D). This finding indicates that VAMP-8 is required for release of cytokines from rSCs.
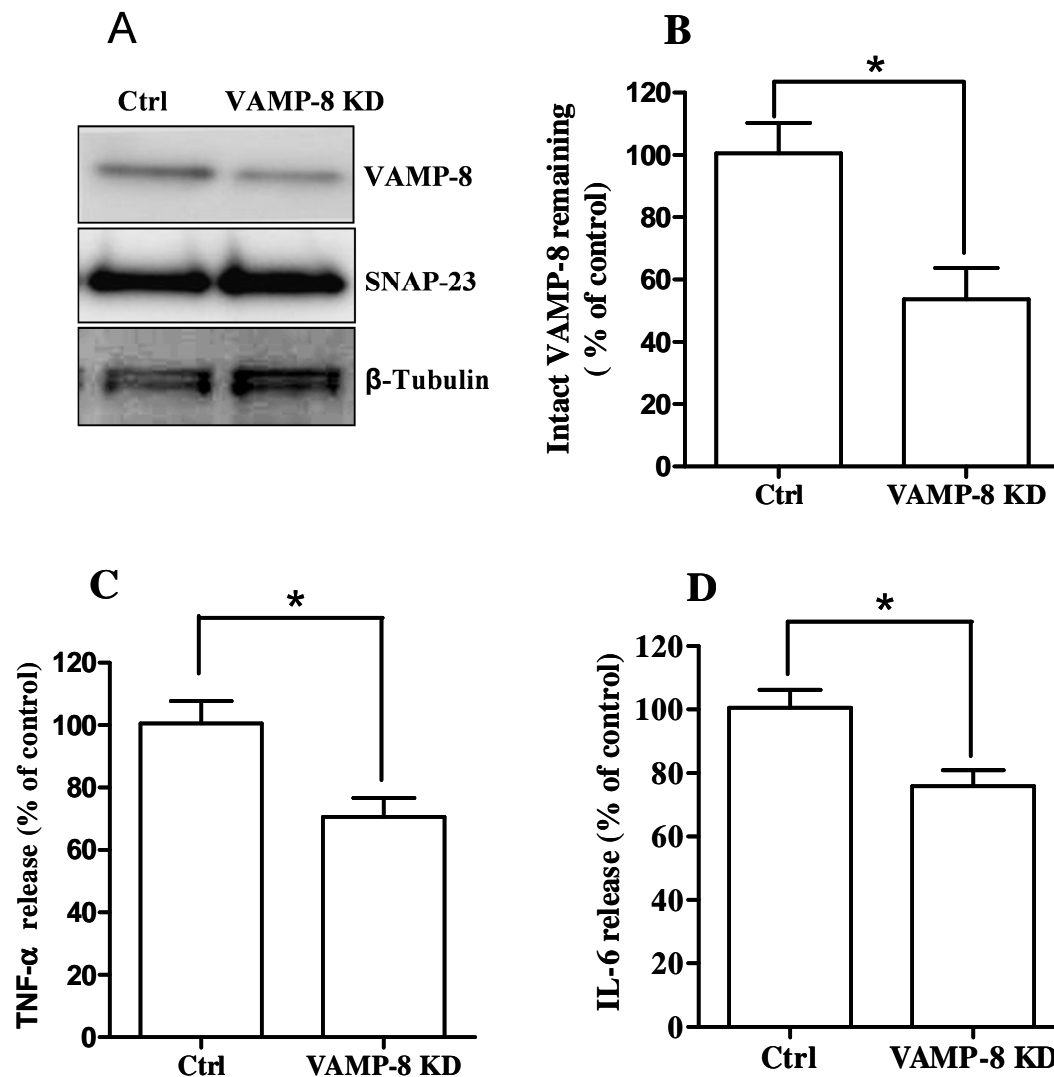
Fig. 4-8. KD of VAMP-8 reduced cytokine release from rSCs.

VAMP-8 KD was achieved by incubating the cells (5 x 10^4 cells/well in 24-well plate) with lentiviral shRNA (20 MOI) for 7-8 days. A and B) Immunoblot analysis was done to calculate percentage of KD compared to a virus-free control. No change in expression of SNAP-23 was observed. C and D) KD of VAMP-8 resulted in reduction of the release of cytokines, TNF-α and IL-6. The data represents mean ± S.E.M., n=3, p<0.05 considered as significant.

4.3 DISCUSSION

VAMP-3 had been shown to be involved in release of cytokines from human synoviocytes (Chapter 3), additional experiments were performed to ascertain if this is also the case for rSCs. From our previous findings, chimera EA successfully entered nociceptive neurons and inhibited CGRP release (Meng et al., 2009). Thus, it was warranted to engineer chimeric BoNTs to target non-neuronal cells like synoviocytes. As rSCs were found to express SNAP-23, VAMP-3 (but not SNAP-25) and SV2A receptor for BoNT/A (but not but not Syt I or II making them inaccessible to /B), chimeras BA and DA were used. These toxins utilised the binding domain of BoNT/A to enter synoviocytes and cleave VAMP-3. Cleavage of VAMP-3 occurred following stimulation by LPS or substance P, a pain mediator involved in the development of arthritis (Wang et al., 2012). Although truncation of VAMP-3 could not inhibit release of IL-6 and TNF-α from rSCs, this could be due to limited extent of truncation of VAMP-3 (~50%); for example in SW982, ~75% KD of VAMP-3 resulted in 50-55% inhibition of IL-6 and TNF-α release (Chapter 3). Our collective observations suggest that BA or DA could offer an advantage of counteracting the symptoms of arthritis at two points: directly upstream on the neuronal component like BoNT/A and, indirectly, on synoviocytes.

Interestingly, VAMP-8 KD resulted in reduction of the secretion of cytokines from rSCs, unlike human synoviocytes. It has been reported that mast cells requires VAMP-8 for histamine release (Sander et al., 2008)**.** These findings indicate that VAMP-8 is required for release of cytokines from rSCs instead of VAMP-3. However, VAMP-8 could not be detected in human synoviocytes instead; VAMP-3 participated in the release of cytokines (Chapter 3). It is notable that in mouse macrophages, TNF-α was found to co-localize with VAMP-8-positive vesicle, and in VAMP8-deficient macrophages, TNF-α release was inhibited but VAMP-3 is also required for this process (Stow et al., 2009; Pushparaj and Tay, 2013). Interestingly, VAMP-8 is necessary for the release of protein-containing granules in response to FcγRI-mediated secretion in mouse mast cells (Puri and Roche, 2008; Lacy and Stow, 2011). Furthermore, VAMP-8 has been shown to regulate the release of TNF-α and β-hexosaminidase from macrophages. KD of VAMP-8 results in decreasing evoked hypersecretion of mucin in human airway epithelial cell cultures (Jones et al., 2012). Unlike VAMP-8 silencing, KD of VAMP-2 or VAMP-3 did not affect this mucin

secretion (Jones et al., 2011; Jones et al., 2012). Previously reported in human mast cells, VAMP-8 is involved in the release of CXCL8 but not of CCL2, CCL3, or CCL4 (Frank et al., 2011).

Different species were found to use distinct isoforms of VAMP. For example, in human platelets, VAMP-3 is required for alpha granules and dense-granules secretion and VAMP-8 for secretion of dense granules but not alpha granules (Polgar et al., 2002). Also, we demonstrated that VAMP-3 can be used in human synoviocytes to release cytokines.

CHAPTER 5 EVALUATION OF TARGETED BIO-THERAPEUTIC IN CYTOKINE AND NEUROPEPTIDE-RELEASING CELLS

5.1 BACKGROUND

Arthritis is the bane of millions of lives. Though it comes in many forms, their common theme is inflammation of the tissues around joints. Treatment is merely palliative: anti-inflammatory drugs, painkillers or both (Feldmann, 2001; Emery, 2006). Unfortunately, the majority of sufferers do not respond to currently available, non-additive medicines; also, commonly used analgesics are short-acting, and cause unwanted adverse effects which raise serious problems for repeated use over long periods. Thus, there is a huge unmet need for more effective, long-acting treatments. Immune cells like macrophages, synoviocytes and mast cells release cytokines (TNF-α and IL-6) and, thereby, induce inflammation in mainly joints in disease conditions (Houssiau, 1995; Feldmann, 2001). It is now apparent that RA and OA pain involve substantial changes in the nociceptive (pain) system at all levels of the neuraxis, including the peripheral neurons and the central nervous system (Konttinen et al., 2006). Both TNF-α and IL-6 potently stimulates joint nociceptors resulting in the secretion of SP and CGRP. Recent studies showed that intra-articular injection of BoNT/A or /B into humans or murine models of arthritis reduces the associated pain, reaffirming the neuronal input in the pathogenesis of arthritis (Mahowald et al., 2009; Singh et al., 2009b; Singh et al., 2009a). BoNT inhibit regulated exocytosis, specifically the release of neurotransmitters at the neuromuscular junction. These toxins cleave SNAREs, proteins involved in the fusion of synaptic vesicles with the plasma membrane (Dolly and Aoki, 2006). Therefore, resulting the inhibition of the release of acetylcholine at the neuromuscular junction. BoNTs are synthesized as single-chain polypeptides of ~150 kDa and subsequently cleaved to DC forms, in which the light (LC) and heavy chains (HC) are linked by a single disulphide and non-covalent bond. The 50-kDa LC acts as a zinc-dependent endopeptidase (Dolly and Aoki, 2006). The heavy chain contains two functional domains, each of ~50 kDa. The N-terminal half (H_N) acts as a translocation domain, known to form membrane ion channels; as the C-terminal half (H_C) mediates acceptor binding, it plays a key role targeting cells and the binding leads to internalization of the toxin into neurons. The HC further comprises two sub-domains: the extreme carboxy-sub-domain, HCC, and the proximal HCN sub-domain (Foster et al., 2006; Foster, 2009). Although the SNARE proteins and their role in secretion were first identified in neuronal cells, the SNARE complex is ubiquitous. It is well established that SNARE proteins are

expressed and participates in secretion from many cell types, including eosinophils, neutrophils, synoviocytes, macrophages, and mast cells (Stow et al., 2006; Stow et al., 2009). Our previous study (Chapter 3), demonstrated that knocking down SNAP-23 or VAMP-3 using lentiviral shRNAs inhibited the release of TNF-α and IL-6 from SW982 cells. Although the SNARE inactivating toxins have the ability to suppress exocytosis; their full therapeutic potential has not been reached because of the lack of the acceptor on non-neuronal cells. This can be circumvented by engineering BoNT to generate recombinant derivative, endowed with ability to target cytokine-releasing cells and sensory neurons (but not motor neurons) for treating chronic inflammatory pain. Two novel ligands were selected to deliver protease domain of BoNT/D into both of the above mentioned cells with the aim of inhibiting the release of cytokines and pain peptides by truncating VAMP isoforms; this raised the exciting project of novel therapeutics for inflammatory as well as neuropathic pain. In this study the targeted bio-therapeutics were created by recombinantly fusing the genes encoding LC/D and translocation domain (H_N), with or without H_{CN} to targeting ligands. The latter were selected to specifically bind receptors expressed on cells involved in arthritis (sensory neurons and cytokine-releasing cells) and, hopefully, culminate in translocation of LC and subsequent block of exocytosis. A total of 3 candidates were developed using 2 different ligands. One of these was found to enter both cell types and translocate the protease domain of BoNT/D, as reflected by cleavage of its substrate VAMP. As expected, the release of cytokines and a pain peptides from synoviocytes or macrophages and rDRGS was inhibited. The control non-liganded protein (LC.H_N/D), did not cleave VAMP or cause any inhibition, confirming the targeting by the ligand.

5.2 RESULTS

5.2.1 RAW264.7 cells contain SNARE proteins but not BoNT acceptors

To investigate expression of SNAREs and BoNT receptors in RAW264.7 cells were subjected to Western blot analysis and using antibodies specific for SNAP-23, SNAP-25, VAMP-2/3, syntaxin-1, SV2 A/B/C or synaptotagmin I/II. RAW264.7 expresses SNAP-23 and VAMP-3 (Fig. 5-1A) but not the SNAP-25, VAMP-2, syntaxin-1, SV2 A/B/C, synaptotagmin I/II (Fig. 5-1B). Because of lack of BoNT receptors in macrophages, it was necessary to develop targeted BoNT-based bio-therapeutics.
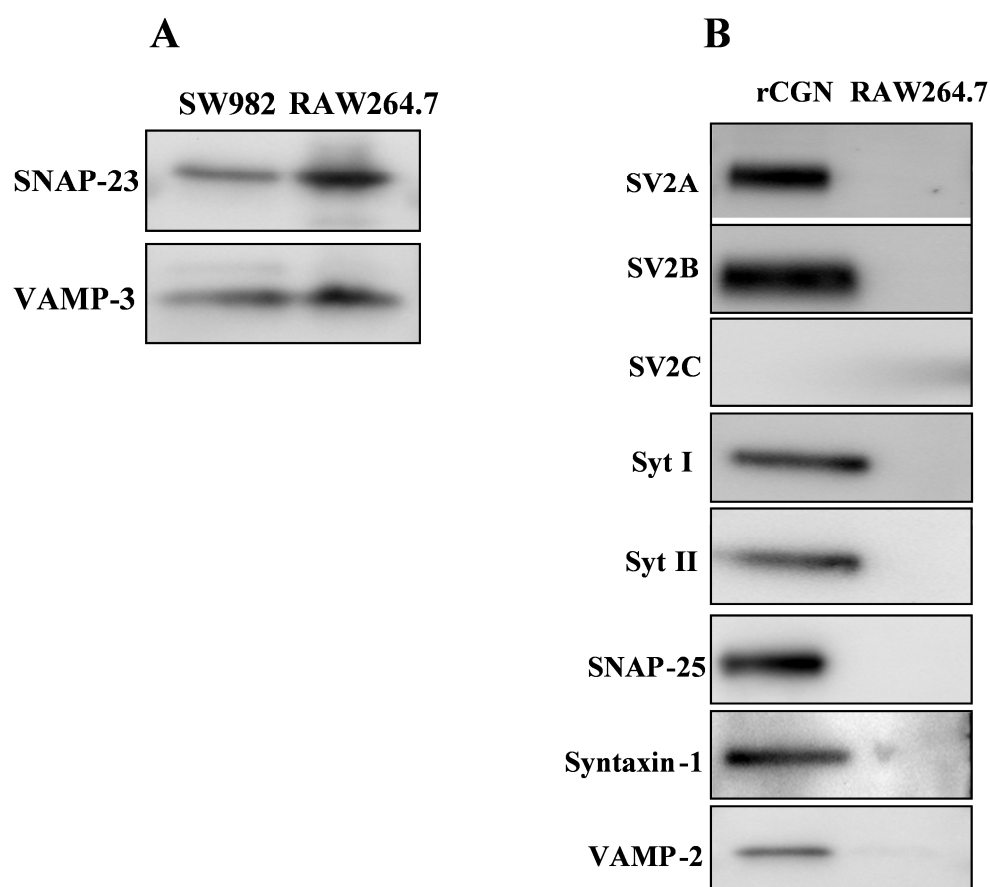
Fig. 5-1. RAW264.7 contains SNAP-23 and VAMP-3 but lacks BoNT acceptor
RAW264.7 were harvested, solubilised in LDS sample buffer and separated on SDS-PAGE before doing immunoblot analysis. Antibodies specific for each SNARE and BoNT receptors were used. SNAP-23 and VAMP-3, but not other SNAREs or BoNT acceptors detected. SW982 and rCGN served as positive controls.

5.2.2 Construction, expression and purification of targeted bio-therapeutics

A total of 3 targeting proteins containing 2 different ligands were engineered by Dr. Jiafu Wang. The first BoNT/DΔH$_{CC}$-TL consists of LC and translocation (H$_N$) and Hc$_N$ (C-terminal subdomain of Hc) of BoNT/D and ligand 1 (TL-1). The second BoNT/DΔH$_C$-TL-1, lacks the Hc$_N$ of /D. The third BoNT/DΔH$_C$-TL2, abbreviated as ARA-7 contains LC.H$_N$/D and targeting ligand 2 (Fig. 5-2A); a non-targeted version (Fig. 5.2B) acted as a control.

These targeted proteins were expressed in BL21.*DE3* strain, using auto-induction medium, and purified by IMAC only (Chapter 2.1.19). SDS-PAGE followed by protein staining revealed that these therapeutics were expressed and purified as SC form, which were fully nicked to DC by thrombin (1 mg toxin/unit at 22ºC for 2 h) (Fig. 5.2C). A protein of ~115 kDa was eluted by imidazole, as demonstrated by SDS-PAGE and Coomassie Blue staining. The resultant recombinants gave a single band of ~115 kDa upon SDS-PAGE followed by Coomassie blue staining in either the absence or presence of DTT (Fig. 5-2C). Control protein (LC.H$_N$/D) was also expressed and purified as non-targeting protein (Fig. 5-2B).
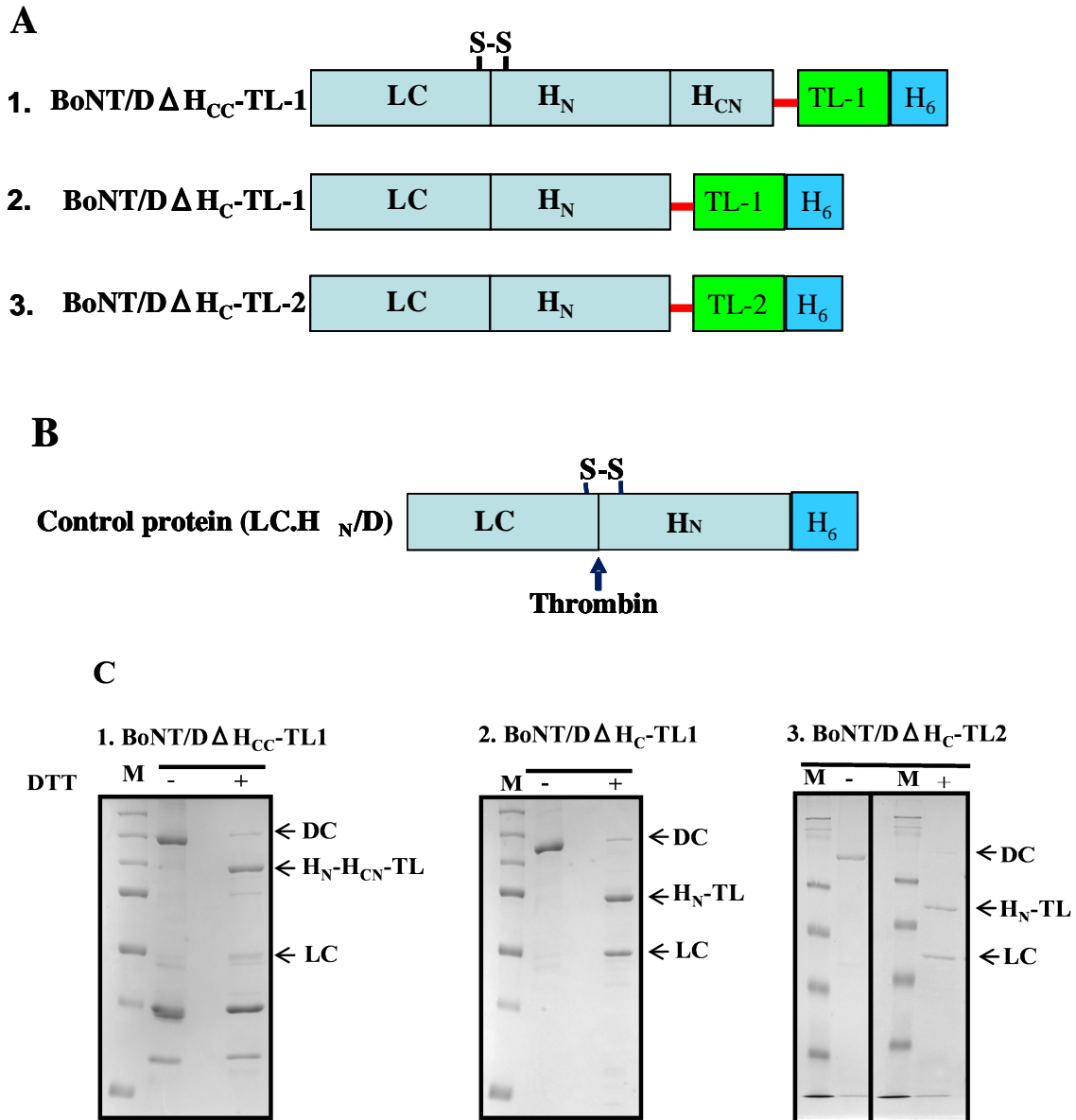
Fig. 5-2. Schematics of engineered bio-therapeutics; expression of SC and conversion of the purified to DC forms by nicking and simultaneous tag removal.

A) Showing the composition of the three targeted constructs. B) Control protein (LC.H_N/D) was engineered by deleting HC domain from BoNT/D. (C) The purified recombinant therapeutics were incubated with thrombin. Aliquots were analyzed by SDS-PAGE in the absence or presence of 25 mM DTT, followed by Coomassie Blue staining. Arrows indicate the positions of the DC, LC, H_N-TL, H_N-H_{CN}-TL. Abbreviations: H_{CN}, N-terminal subdomain of Hc; H_N, translocation domain; LC, catalytic light chain; S-S , disulphide bond; TL, Targeted ligand (TL) 1 or 2; M, standard proteins.

5.2.3 BoNT/DΔH$_{CC}$-TL1 protein cleaved VAMP-3 and inhibited release of cytokines (IL-6 and TNF-α) from mouse macrophage cell line (RAW264.7) but only at high concentration

RAW264.7 were incubated with differrent concentrations of BoNT/DΔH$_{CC}$-TL1 for 48 h before being washed and stimulated by LPS (100 ng/ml) + IFN-γ (500 pg/ml) over 6 h to release cytokines. As shown by Western blot analysis, the first targeted therapeutic significantly cleaved VAMP-3 ~ 50% at 100 nM concentration (Fig. 5-3A); this resulted in inhibition of evoked release of TNF- α and IL-6 by ~65% and ~55% respectively, compared to non-treated control (Fig. 5-3B).

A

BoNT/DΔH$_{CC}$-TL1

0	10	50	100	(nM)

Syntaxin-4

VAMP-3

B
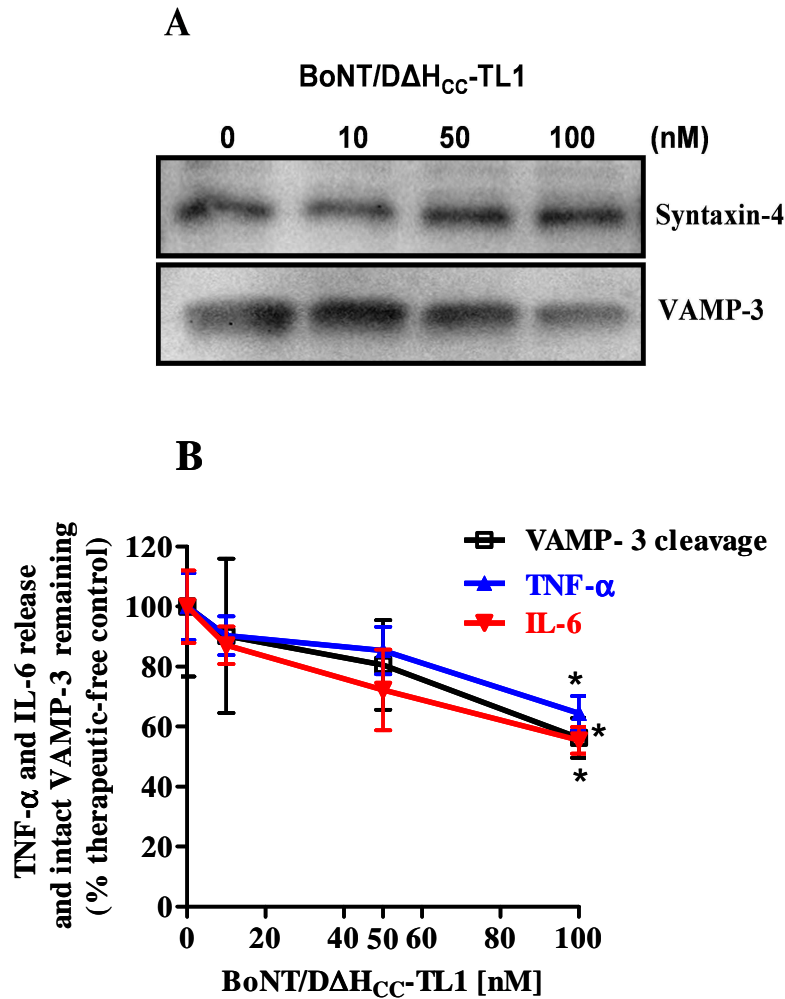
Fig. 5-3. BoNT/DΔH$_{CC}$-TL1 cleaved VAMP-3 in macrophages and decreased release of cytokines.

A) The cells were harvested after stimulation and proteins separated on SDS-PAGE for Western blotting which shows cleavage of VAMP-3 by increased concentration of the therapeutic. Syntaxin-4 served as internal control. B) The cells were stimulated with LPS (100 ng/ml) + IFN-γ (500 pg/ml) for 6h before collecting the supernatants for ELISA. The graph represents cleavage of VAMP-3 and inhibition of release of both cytokines (TNF-α and IL-6). Densitometric analysis using Image J was done to calculate % of cleavage of VAMP-3 relative to control. The amounts of release of TNF-α and IL-6 were calculated relative to non-treated controls. Data plotted as % of control. The data represents mean ± S.E.M, n = 3, *p <0.05 considered as significant.

5.2.4 BoNT/DΔH$_C$-TL1 did not give significant cleavage of VAMP-3 and failed to inhibit the release of cytokines from mouse macrophage cell line (RAW264.7)

Cells were intoxicated with for BoNT/DΔH$_C$-TL1 48 h before stimulation with LPS (100 ng/ml) + IFN-γ (500 pg/ml) for 6h. The Western blotting showed that it failed to truncate VAMP-3 at any concentration tested (Fig. 5-4A); accordingly, the release of cytokines (TNF-α and IL-6) was not inhibited by this treatment (Fig. 5-5B).
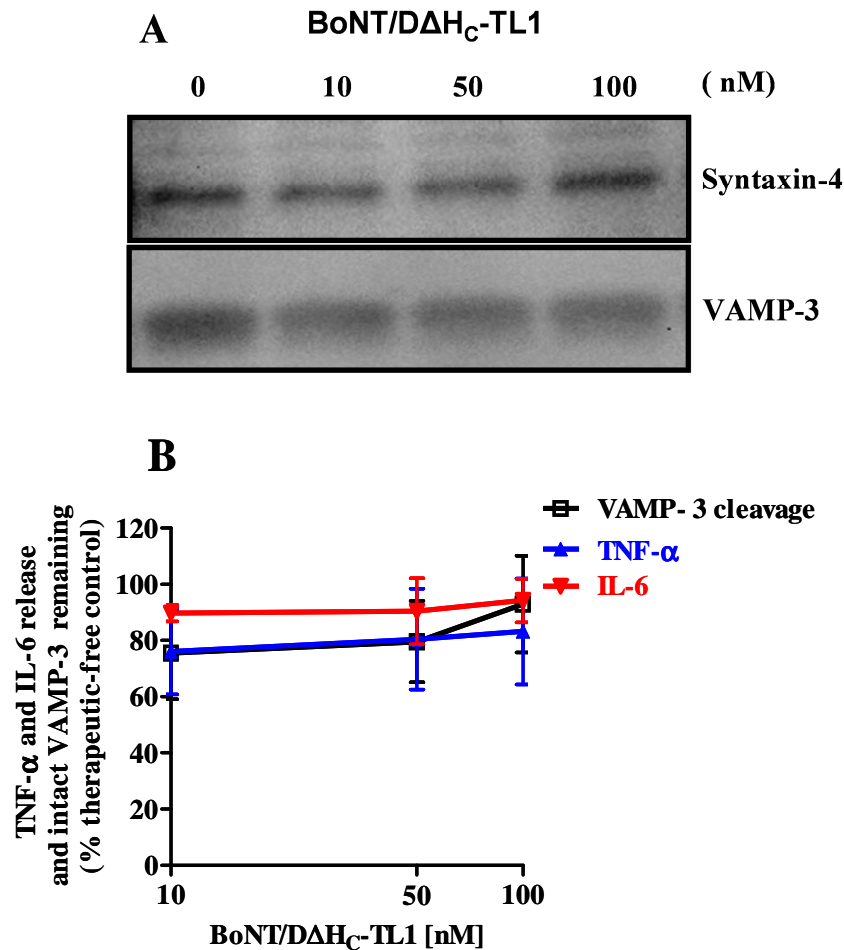
Fig. 5-4. BoNT/DΔH$_C$-TL1 did not truncate VAMP-3 or decrease the release of cytokines from RAW264.7

A) Immunoblot revealing the absence of VAMP-3 cleavage by BoNT/DΔH$_C$-TL-1; syntaxin-4 acts as a loading control. Densitometric analysis was done to measure % of cleavage of VAMP-3. B) The stimulated release of cytokines, TNF-α and IL-6 was not affected by this protein even at 100 nM concentration. Data presented as mean ± S.E.M, n=3.

5.2.5 BoNT/DΔH$_C$-TL2 (ARA-7) entered cultured RAW264.7 cells, cleaved VAMP-3 and blocked the release of cytokines, unlike its control protein

Mouse macrophages were incubated with its various concentrations of ARA-7 for 48 h and then stimulated by LPS (100 ng/ml) + IFN-γ (500 pg/ml) for 6 h for to release cytokines before cells harvested for Western blot analysis. ARA-7 dose-dependently cleaved VAMP-3 with EC$_{50}$ of ~10 nM (Fig. 5-5A, B), after calculating the percentage of VAMP-3 cleavage relative to non-treated control using densitometry scanning and Image J analysis. Further experiments were carried out to test this therapeutic on other inflammatory cell lines like synoviocytes (SW982). To verify specificity of ARA-7 for VAMP cleavage, the control Protein (LC.H$_N$/D) which is devoid of a TL was used as control. Cells were incubated with LC.H$_N$/D same as before for 48h and the evoked release of cytokines analysed by ELISA. LC.H$_N$/D failed to cleave VAMP-3 (Fig. 5-5C) and decrease the release of TNF-α and IL-6 (Fig. 5-5D).
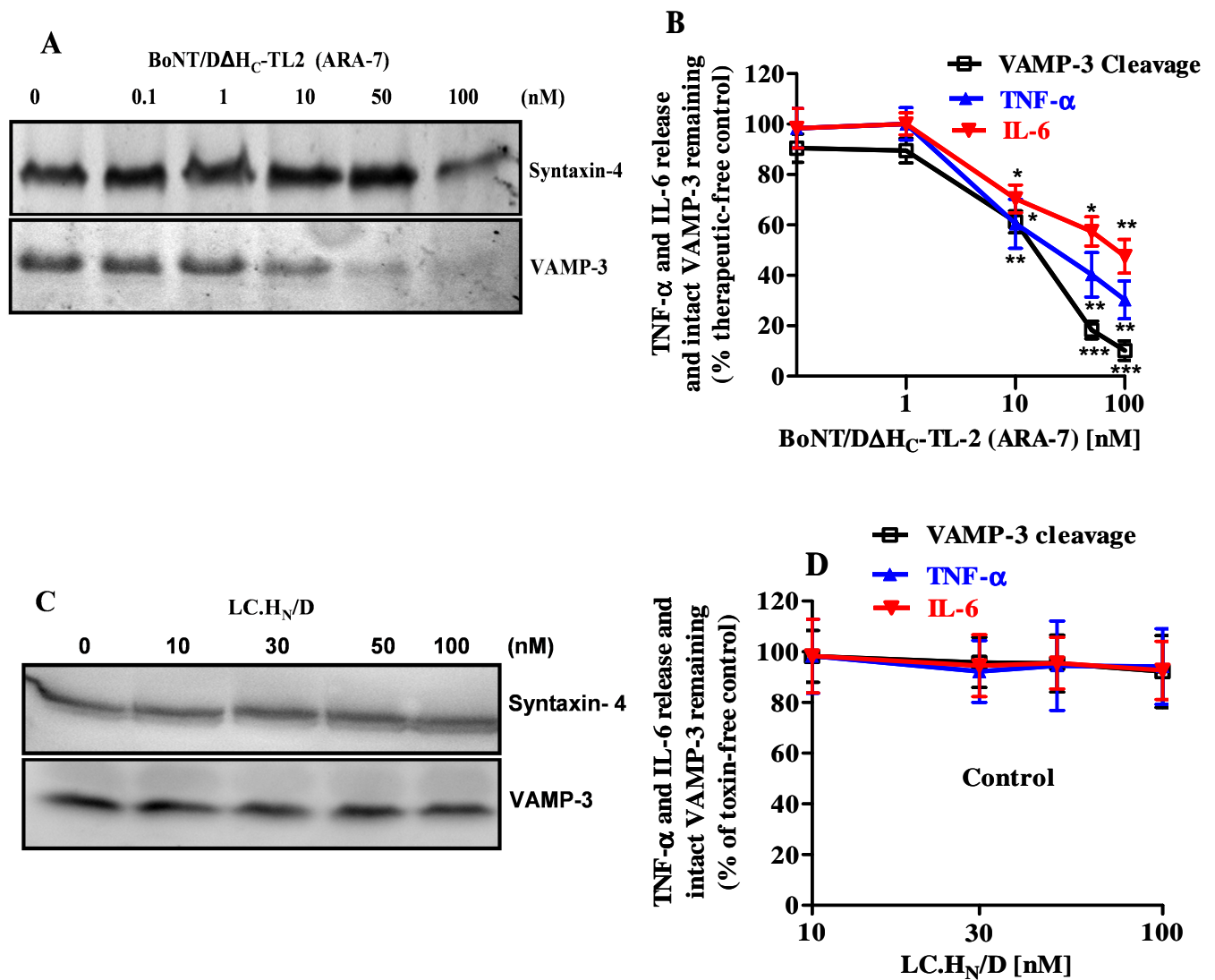
Fig. 5-5. ARA-7 cleaved VAMP-3 and inhibited release of cytokines from RAW264.7, unlike its control protein (LC.H_N/D)

A) Cells were harvested for SDS-PAGE and immunoblotting. ARA-7 dose-dependently cleaved VAMP-3; extent of VAMP-3 cleavage of VAMP-3 were calculated relative to its non-treated control. B) The cells were stimulated with LPS (100 ng/ml) + IFN-γ (500 pg/ml) for 6 h before collecting cell culture supernatants for ELISA. C) Control protein (LC.H_N/D) did not cleave VAMP-3 or reduce cytokine release (D). Data presented as mean ± S.E.M, n = 3, p < 0.05 considered statistically significant,*P<0.05, **p < 0.01, ***p < 0.001 when compared to non-toxin treated control.

5.2.6 ARA-7, but not LC.H$_N$/D, truncated VAMP-3 dose-dependently in a human synovial cell line (SW982) and reduced the release of cytokines

Human synovial cells were plated at density of 5 x 10^4 per well in 24-well plate. After overnight incubation, the cells were incubated with different concentration of ARA-7 for 48 h., stimulated with IL-1β (100 ng/ml) for 20 h before immunoblot analysis of the cell lysates. ARA-7 cleaved VAMP-3 in a dose-dependent manner (Fig. 5-6A) and reduced the release of TNF-α and IL-6 (Fig. 5-6B). The EC$_{50}$ for VAMP-3 cleavage was found to be ~10nM (Fig. 5-6B).

When SW982 cells were treated with control protein (LC.H$_N$/D) for 48h and stimulated as before no cleavage of VAMP-3 or alternation in the release of TNF-α and IL-6 were observed (Fig. 5-6C, D), demonstrating ARA-7 specifically enters into the cells and cleaves VAMP-3.
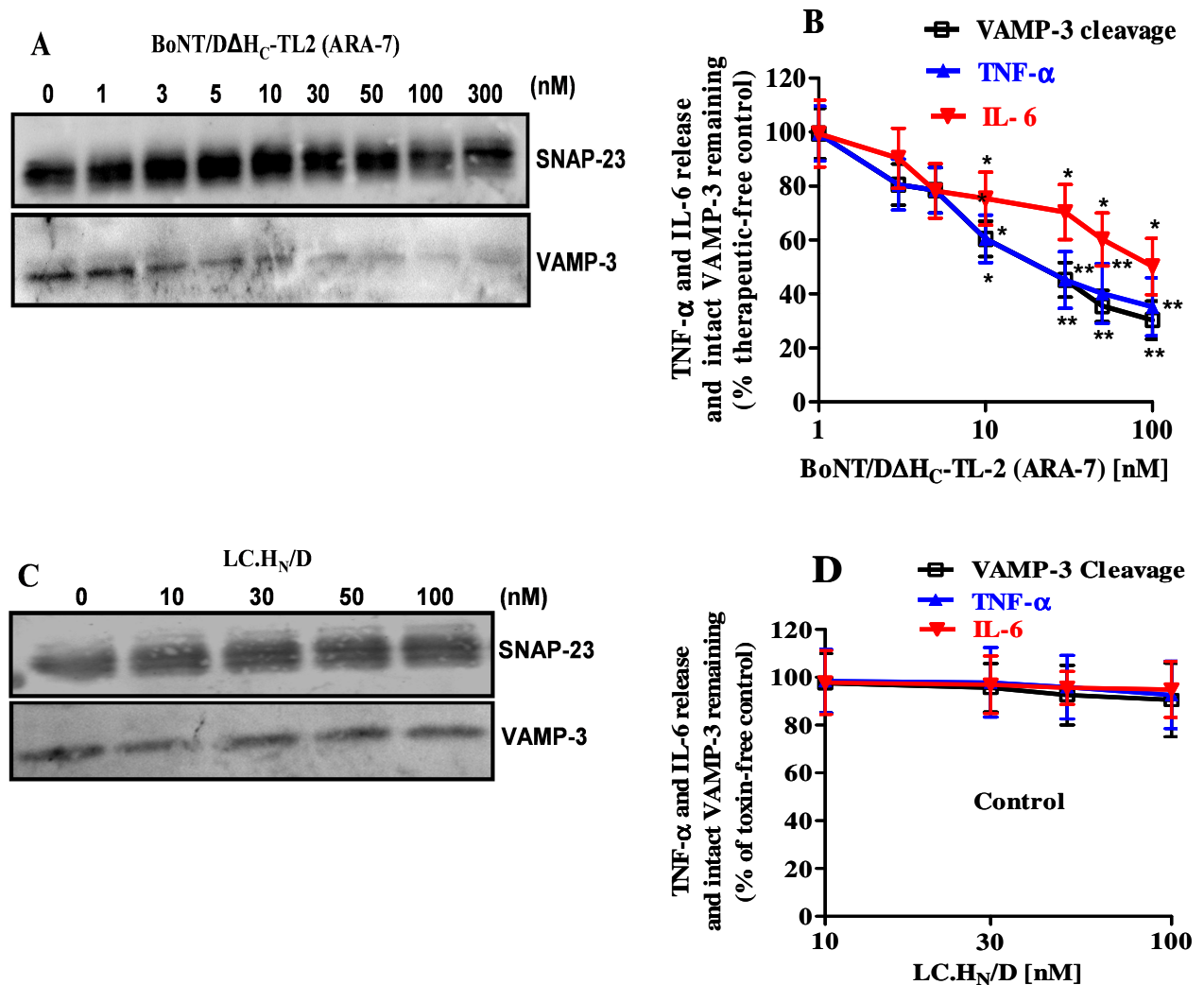
Fig. 5-6. Unlike control protein, ARA-7 truncated VAMP-3 in SW982 cells and inhibited release of cytokines in a dose-dependent fashion

A) Immunoblots demonstrating cleavage of VAMP-3 by ARA-7, which was calculated relative to non-treated control using SNAP-23 as a loading control. B) The cell culture supernatants after stimulation with IL-1β (100 ng/ml) for 20 h were assayed for release of cytokines (TNF-α and IL-6). Both cytokines were reduced by ARA-7 at >10nM. C) The control protein (LC.H$_N$/D) did not truncate VAMP-3 and D) failed to inhibit the release of TNF-α and IL-6. Data presented as mean ± S.E.M., n=3, p < 0.05 considered statistically significant,*P<0.05, **p < 0.01, ***p < 0.001.

5.2.7 ARA-7 did not affect the viability of cultured macrophages or synoviocytes

Equal number of cells were plated on 24-well plate and incubated overnight; ARA-7 was then added incubation continued for 48 h, before MTT assay of cell viability. Cell culture supernatants were removed, MTT (Chapter 2.1.14) was added to wells and

incubated for 4h. Absorbance was measured after 4h. SW982 (Fig. 5-7A) and RAW264.7 (Fig. 5-7B) cells did not died or become detached when ARA-7 treatment for 48h, demonstrating its the lack of toxicity.

A SW982

B RAW264.7

BoNT/DΔH$_C$ (ARA-7) (nM)

BoNT/DΔH$_C$ (ARA-7) (nM)
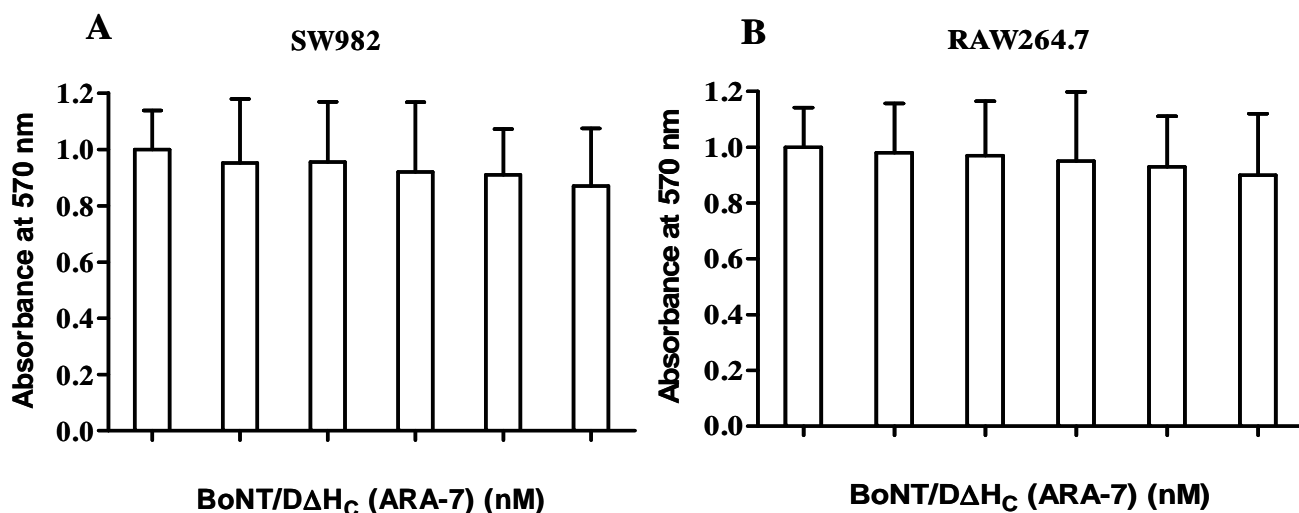
Fig. 5-7. Viability of SW982 and RAW264.7 cells were not affected by incubation with ARA-7.

A) SW982 and B) RAW264.7 cells were exposed to ARA-7 for 48h. No cell death was observed after at any ARA-7 concentrations. Data presented mean ± S.E.M, n=3.

5.2.8 BoNT/DΔH$_C$-TL2 (ARA-7) cleaved VAMP-2 in rDRGs and decreased release of substance P

To assess ability of the therapeutic to undergo the receptor binding, translocation and cleavage VAMP, it was incubated with rDRGs for 24 h and cleavage of VAMP-2 monitored by immunoblotting. The rDRGs were incubated with various concentrations of ARA-7 for 24 h, before being stimulated by 60 mM [K$^+$] and 2.5mM [Ca^{2+}] for 10 min. The amounts of substance P released under basal and stimulated conditions were quantified by ELISA. ARA-7 successfully entered rDRGs, cleaved VAMP-2 with EC$_{50}$ ~30nM (Fig. 5-8A). Consistently the evoked release of substance P was decreased by ARA-7 with IC$_{50}$ ~30nM (Fig. 5-8B). On the other hand, control protein (LC.H$_N$/D) similarly exposed to rDRGS failed to cleave VAMP-2 (Fig. 5-8C), confirming ARA-7 specifically enters into neurons and truncates VAMP-2 through the TL.

A BoNT/DΔH$_C$-TL2 (ARA-7)

0 1 3 5 10 30 50 100 (nM)

SNAP-25

VAMP-2

B

Substance P
VAMP-2 cleavage

C LC.H$_N$/D

0 10 50 100 (nM)

SNAP- 25
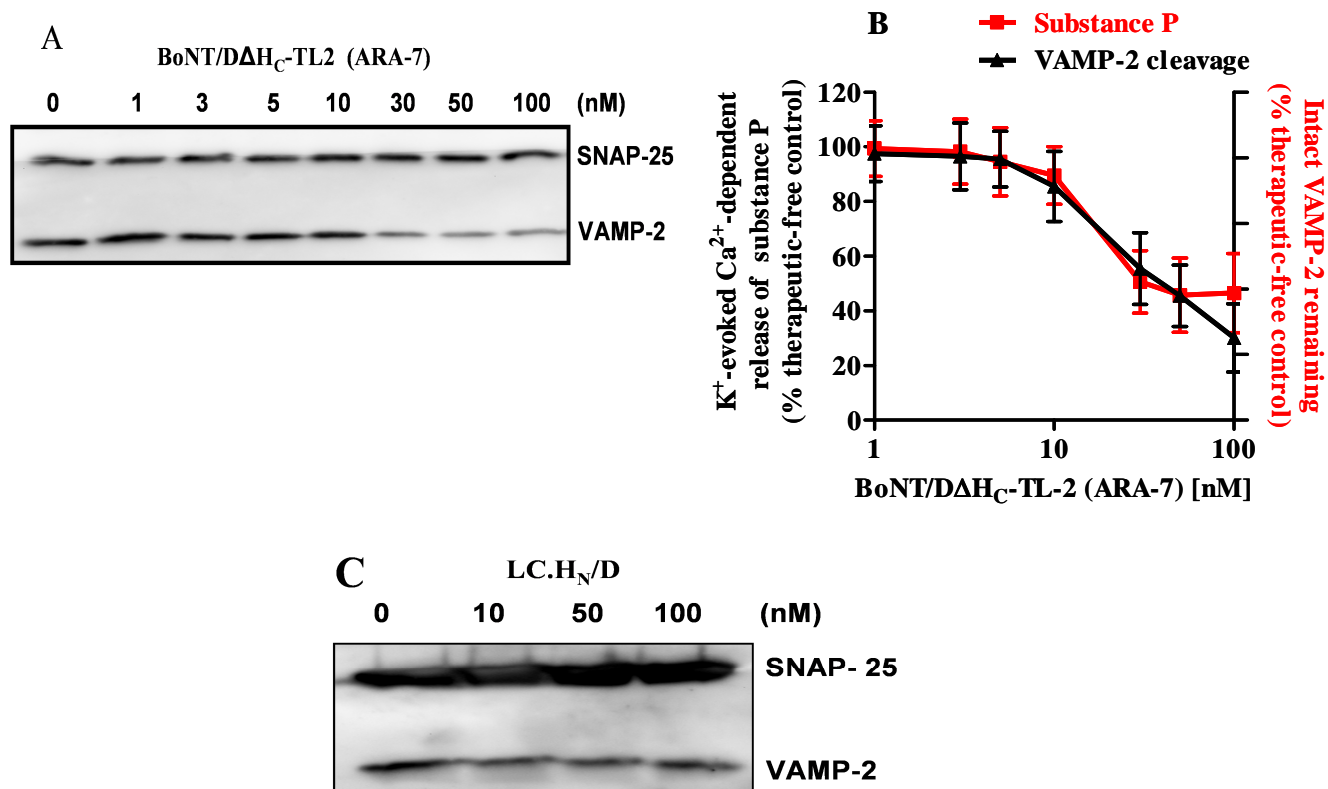
VAMP-2

Fig. 5-8. ARA-7 truncated VAMP-2 in rDRGs and inhibited the release of substance P.

rDRGs were exposed to ARA-7 and release of substance P was assayed over 10 min. Cells were then solubilised in SDS-sample buffer and equal volumes subjected to SDS-PAGE and Western blotting, using an antibody that recognises VAMP-2 or SNAP-25. The proportion of intact VAMP-2 remaining was calculated relative to an internal SNAP-25 control, using digital images of the gels. (A) Immunoblot showing the cleavage by the therapeutic of VAMP-2; SNAP-25 served as internal control. (B) Dose-response blockade of substance P release evoked by 60 mM K^+. C) Control protein (LC.H$_N$/D) did not cleave VAMP-2. Data represented mean ± S.E.M., n=2, p<0.05 considered significant.

5.3 DISCUSSION

This study aimed to selectively target the endopeptidase activity of BoNTs to specific cell types. In this chapter, targeted SNARE-inactivating endopeptidases were developed to selectively target synoviocytes, macrophages and nociceptive sensory neurons. Initial work consisted identification of ligands that had greatest selectivity to target cells of interest; conjugate its gene to that of the core therapeutic (LC.H$_N$) and express the fusion protein in *E. coli*. The purified products were then applied to synoviocytes, macrophages or sensory neurons to demonstrate their cleavage of intracellular SNARE and blockade of release.

Vesicle fusion with the plasma membrane involving the SNARE complex represents a universal mechanism for exocytosis in eukaryotic cells. BoNTs potently inhibits neurotransmitter release at the neuromuscular junction by proteolysis of specific components of the vesicle docking/fusion complex (Dolly and Aoki, 2006). Their mechanism of action of entails distinct phases, includes binding to cell surface acceptor, internalisation, endosomal release and cleavage of SNARE involved in fusion of exocytotic vesicles, which disable release of neurotransmitter (Montal, 2009, , 2010). However, many non-neuronal cells lack BoNT acceptor, so there was an unmet need to engineer recombinantly targeted biotherapeutic variants. Disease-modifying antirheumatic drugs (DMARDs) have long been used to slow the progression of joint destruction in patients with RA and OA. However, these synthetic agents fail to significantly improve the course of RA and OA in a substantial number of patients, and they are associated with considerable toxicity (Breedveld and Combe, 2011). Moreover, many patients do not respond adequately to these treatments or other available drugs. Intra-articular injection of BoNT/A reduced pain in patients with chronic arthritis who were less responded with other available drugs as well as in mouse models of arthritis alleviated pain (Mahowald et al., 2006). Off-target side effects can occasionally occur with conventional BoNT therapy. To overcome these shortcomings, new therapeutics to treat arthritis with little or no side effects would be highly desirable. A recombinant chimeric protein composed of the growth hormone–releasing hormone (GHRH) coupled to LH$_N$ of BoNT/D, specifically bind to GHRH receptor on pituitary somatotrophs, cleaved VAMP-2 and reduced secretion of growth hormone (GH), offering a potential treatment for hyper secretion of pituitary GH (Leggett et al., 2013). A recombinant fusion protein consisting of the LCH$_N$-

fragment of BoNT/C_1 and epidermal growth factor (EGF) was able to inhibit secretion of mucus from epithelial cells (Foster et al., 2006).

Synoviocytes, macrophages and sensory neurons are involved in progression of arthritis by secreting cytokines and neuropeptides and inhibition of these pain-mediators by novel targeted bio-therapeutics could prove very beneficial. In this study, a H_C domain of BoNT/D substituted with a ligand was engineered to target to desired cell type harnessing the receptor for that particular ligand. A LC/D was chosen because it has advantage over LC/B in that it can cleave all three isoforms of VAMP (1, 2, and 3). We selected two different ligands to engineer targeted bio-therapeutics. Binding of ligand to receptor on cell surface enabled translocation of LC/D into cell cytoplasm and resulted in cleavage of VAMP. Cytokines produced by immune cells stimulate sensory nerves which innervate the knee joint. This bio-therapeutic was able to truncate VAMP in synoviocytes and macrophages and dose-dependently inhibited release of cytokines. BoNT/DΔH_{CC}-TL-1 proved less potent in macrophages cleaved VAMP-3 at higher concentration. The another molecule, BoNT/DΔH_C-TL1 was unable to truncate VAMP-3 in macrophages. These two less active molecules may result from a lower abundance of TL-1 receptor in these cells and/or inadequate efficiency. The most effective and promising therapeutics was BoNT/DΔH_C-TL2 (ARA-7), which cleaved VAMP-2/3 in macrophages, synoviocytes and rDRGS at very low concentration. ARA-7 is the most potent in cleaving VAMP may be due to a higher expression of its receptor on the cell surface. A dose-response study revealed that EC_{50} for ARA-7 is ~10 nM in macrophages and synoviocytes. Control protein (LC.H_N/D) without targeted ligand failed to cleave VAMP in all cell types tested confirming this bio-therapeutic specifically bind to its receptor and subsequently become internalised LC/D into cell cytosol. Most importantly, both targeted and control protein did not effect on cell viability.

This investigation also confirmed findings from Chapter 3, where VAMP-3 KD was achieved with lentiviral shRNAs resulted in blockade of release of cytokines from SW982 cells. Consistently, antibody-mediated delivery of BoNT/B into macrophages cleaved VAMP-3 and decreased release of TNF-α (Yeh et al., 2011). Although, KD of VAMP-3 found to reduce release of cytokines from macrophages (Murray et al., 2005; Stow et al., 2006; Stow et al., 2009), similar results were obtained here for synoviocytes and macrophages which are involved in arthritic pain.

Another advantage of this therapeutic is that it enter into the sensory neurons and cleaves VAMP-2, resulting in inhibition of substance P release. This ability to block secretion from both sensory neurons and inflammatory cells is particularly important painful situations, where it is known that multiple mediators are involved in the sensation of pain and associated inflammation. The importance of this novel bio-therapeutic is that it can be used to truncate VAMP in neuronal and non-neuronal cells and block release of cytokines and pain peptides from sensory neurons and inflammatory cells both of which mediate arthritic pain.

This prototype therapeutic would have more beneficial for the medical application the native neurotoxins, while removing the inherent toxicity (natural BoNT/A with 2.5×10^8 median lethal doses [MLD_{50}] per mg) and offering a much-improved therapeutic window by only targeting non-neuronal cells and sensory neurons.

CHAPTER 6 PRODUCTION OF LENTIVIRAL PARTICLES EXPRESSING LC/D AND EVALUATION OF ITS INHIBITION OF THE RELEASE OF CYTOKINES FROM INFLAMMATORY CELLS

6.1 BACKGROUND

KD of the expression of SNAP-23 or VAMP-3 in synoviocytes by lentiviral shRNA results in reduction of the release of TNF-α and IL-6 and truncation of VAMP by engineered bio-therapeutic in synoviocytes, macrophages or sensory neurons decreased the secretion of both cytokines and neuropeptide (substance P) highlighting the importance of these SNARES for exocytosis of cytokines.

Viral vectors have been successfully used for delivering therapeutics. Adeno–associated virus vectors can express a cleavage-resistant mutant of SNAP-25 in rats which diminish neuromuscular paralysis by BoNT/A. (Raghunath et al., 2008). Lentiviral particles (LVs) mediated blockade of nuclear factor κB (NF-κB activity) in spinal glial cells attenuates pain in a chronic constriction injury (CCI) model in rats (Meunier et al., 2007). Thus, this chapter focuses on engineering and production of capable of infecting synoviocytes and macrophages, lentiviral particles expressing LC/D cleaving VAMP and hopefully block the release of pain peptides and cytokines. Such virus could be used *in-vitro* to truncate VAMP in neurons and/or non-neuronal cells as well as *in vivo* to potentially attenuate pain behaviour in animal models.

LVs belongs to the genus of Retroviridae family which includes the human pathogen human immunodeficiency virus (HIV). Replication-incompetent vector particles derived from lentiviruses have been shown to mediate transfer and expression of heterologous genes (transgenes) into a variety of cells including e.g. macrophages, synoviocytes, lymphocytes and nerve cells (Jurgens et al., 2012). In addition to use in *ex vivo* cell transduction, LVs could be useful for gene delivery *in vivo*. Furthermore, LVs may allow for long-term expression of transgene, as the transcript silencing observed with other retroviral vectors is less frequent with LV and as such may provide a means more prolonged clinical management of chronic diseases (Tiscornia et al., 2006; Jurgens et al., 2012).

The virions are roughly 100 nm in diameter, spherical and the outer layer is a lipid envelope displaying viral glycoproteins (Fig. 6-1). Each particle contains two copies of the linear viral RNA genome (~ 10 kb) which contains three essential genes, gag, pol and env. The pol gene encodes three viral enzymes: the protease, reverse transcriptase (RT), and integrase. The gag gene encodes structural proteins: the capsid, matrix, and nucleocapsid. The Env gene encodes the envelope glycoproteins of the virus (Akhtar et al., 2013). After the retrovirus enters the target cell, the viral

genome is converted into double-stranded DNA by RT. Proviral genome is then integrated into that of the target cell by the integrase. Viral long terminal repeats (LTRs) are important for the initiation of viral DNA synthesis, integration and regulation of viral transcription (Akhtar et al., 2013). In addition, there are a number of *cis*-acting elements required during viral life cycle; the TAT activation region (Jurgens et al., 2012; Akhtar et al., 2013), splice donor and acceptor sites, packaging and dimerization signal (Ψ), Rev-responsive element (RRE) as well as the central and terminal polypurine tracts (PPT) during viral life cycle. To produce replication-defective vector particles, all dispensable genes have to be eliminated from HIV-1 genome; the cis-acting sequences are required for viral production (Yu et al., 2011; Sakuma et al., 2012).
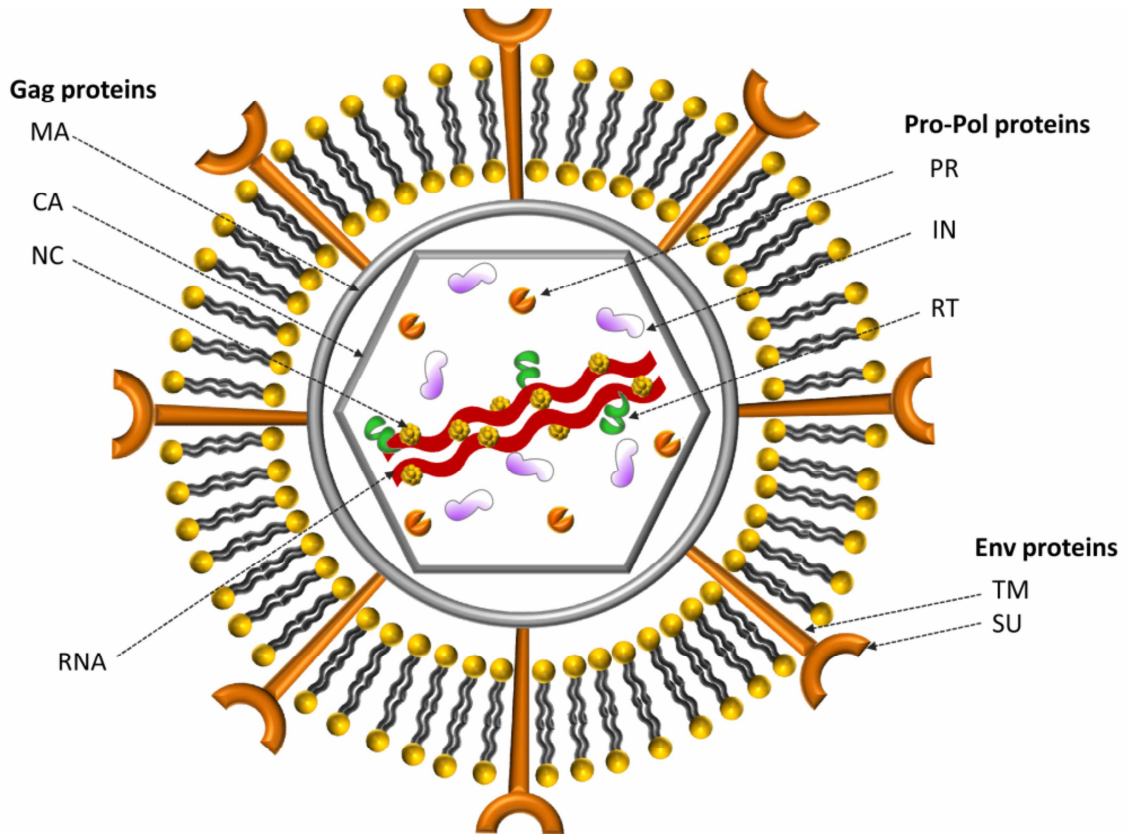
*Fig. 6-1. Structure of wild type LV (http://www.niaid.nih.gov/factsheets/how
hiv.htm).*

*LVs are double stranded RNA enveloped viruses mainly characterized by the ability to
"reverse-transcribe" their genome from RNA to DNA. Virions measure ~100 nm in
diameter and contain a dimeric genome of identical positive RNA strands complexed
with the nucleocapsid (NC) proteins. The genome is enclosed in a protein capsid (CA)
that also contains enzymatic proteins, namely the reverse transcriptase (RT), the
integrase (IN) and proteases (PR), required for viral infection. The matrix proteins
(MA) form a layer outside of the capsid core that interacts with the envelope and a
lipid bilayer derived from the host cellular membrane, which surrounds the viral core
particle (Coffin JM, 1997). Anchored in this bilayer are the viral envelope
glycoproteins (Env) responsible for recognizing specific receptors on the host cell and
initiating the infection process. Envelope proteins are formed from two subunits, the
transmembrane (TM) that anchors the protein to the lipid membrane and the surface
(SU) which binds to cellular receptors.*

For the production of LVs, a second-generation LV vector system was used, which
consists of plasmids, psPAX2 (Fig. 6-2), pMD2.G (Fig. 6-3) and pWPI (Fig. 6-4).

116
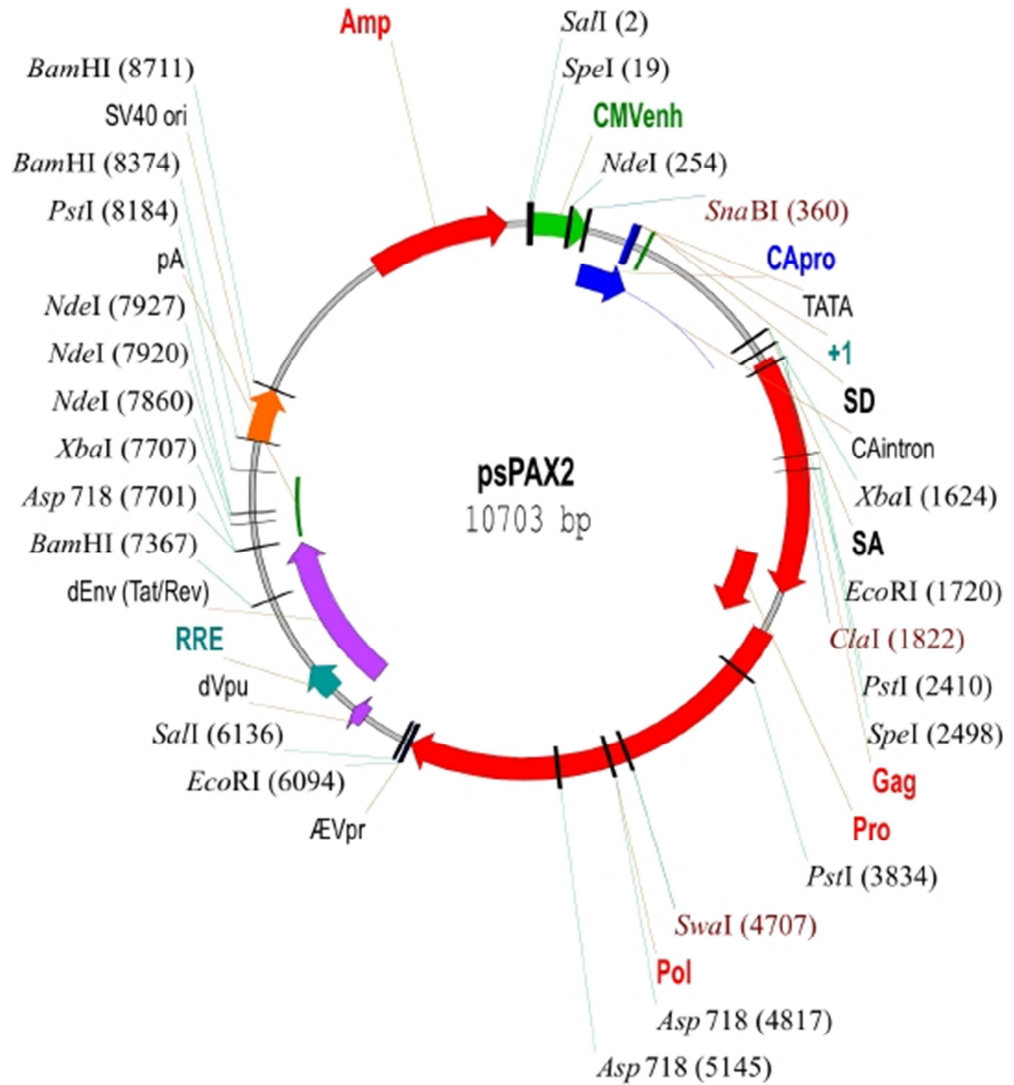
Fig. 6-2. Packaging vector (psPAX2) vector map (Source-Addgene).

GAG – group specific antigen; Pro – protease; POL –polymerase; dVpu. dVpr and dENV – deleted viral protein U, viral protein R and envelope proteins; pA sequence, polyadenylation.
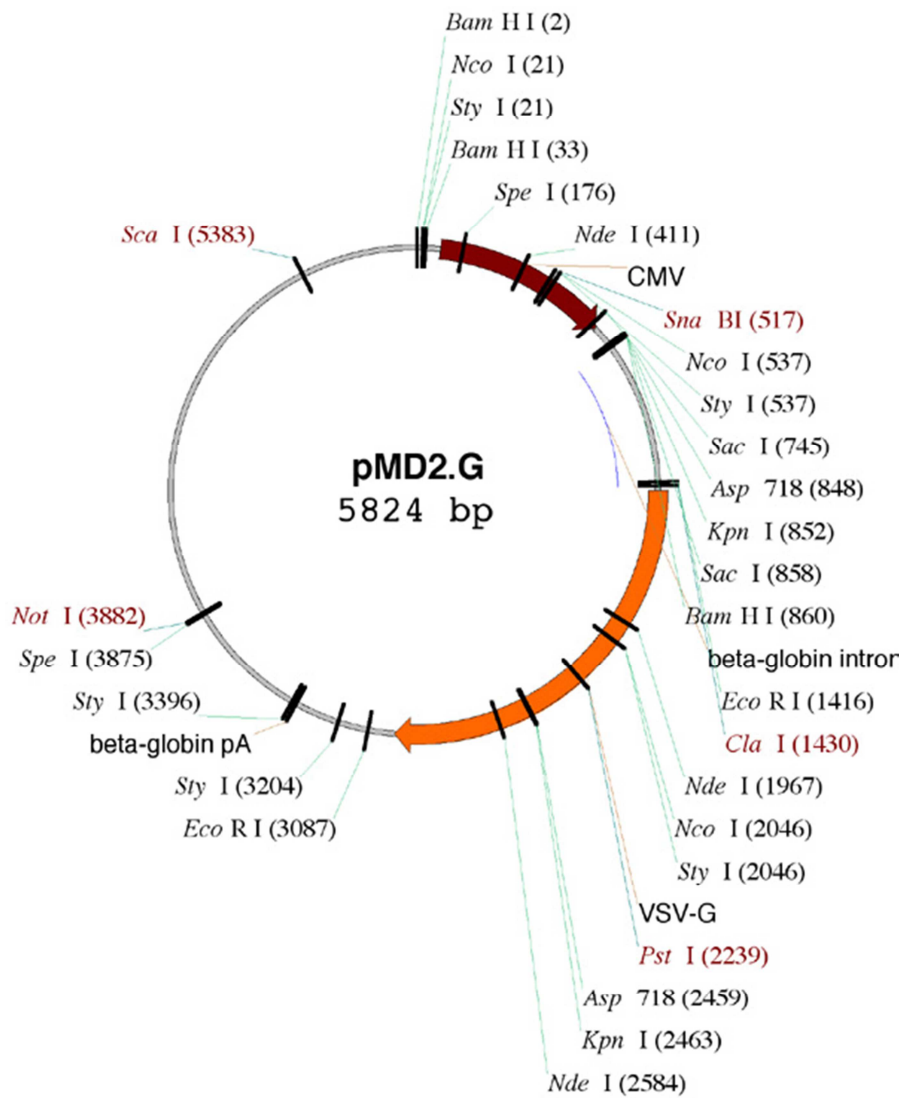
Fig. 6-3. Envelope vector plasmid (pMD2.G) map (Source-Addgene).

This diagram of pMD2.G show its important constituents and unique restriction site.
AMP – beta-lactamase gene; CMV – cytomegalovirus promoter; VSV-G, vesicular
stomatitis virus-G; beta-globin pA –globin poly-adenylation site.
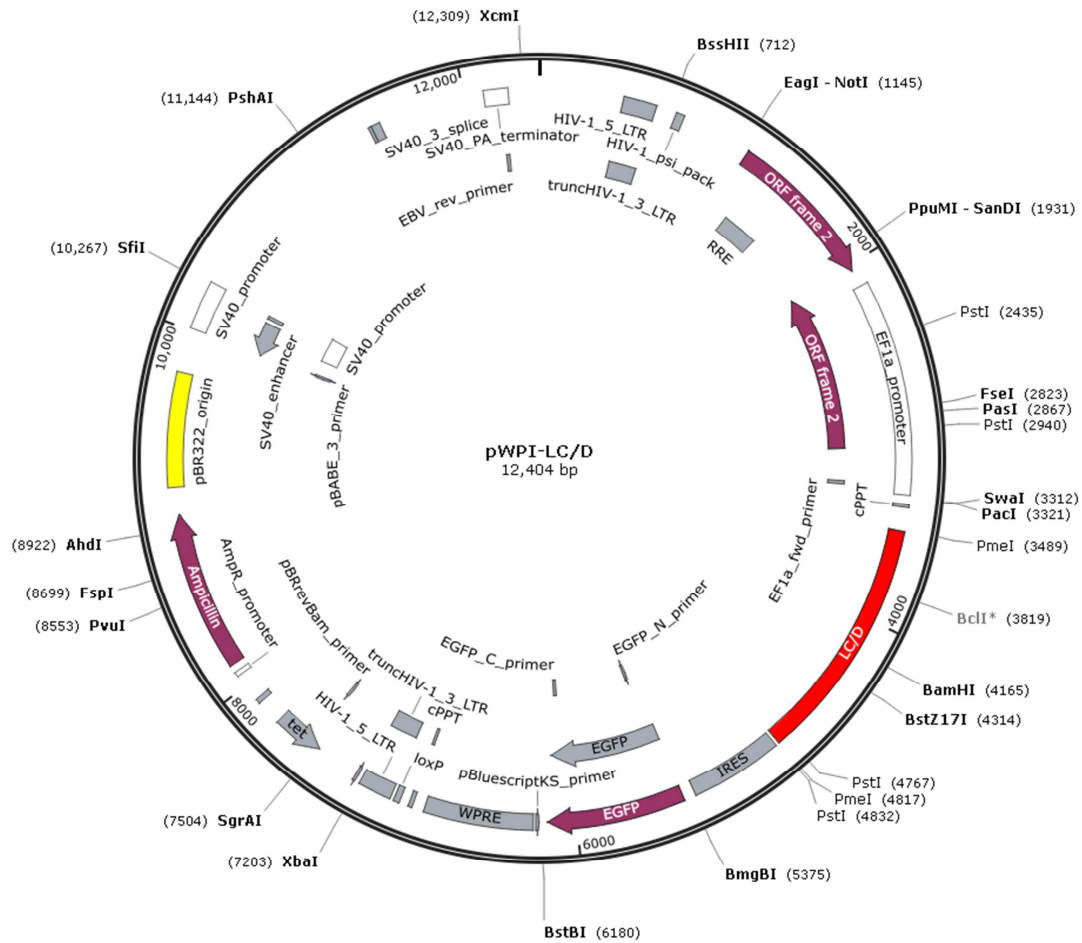
Fig. 6-4. Transfer vector (pWPI-LC/D) vector map (Designed by Dr. Jiafu Wang).
The transfer vector construct, pWPI-LC/D, containing the essential cis-acting sequences and LC/D insert (red). LTR – Long terminal repeats; RRE – rev responsive element; cPPT – central poly-purine tract; EF1 – elongation factor 1 promoter; EGFP, enhanced green fluorescent protein.

The transfer vector (pWPI), containing cis-acting sequences required for genomic RNA production, was used to clone LC/D. All three plasmid were co-transfected into Lenti-X 293T and viral particles released in the supernatant. High-titre viral preparations were obtained by ultracentrifugation. Both LVs, concentrated and supernatant were used to transduce synoviocytes and macrophages with objective of cleaving VAMP-3.

6.2 RESULTS

6.2.1 Schematic of vectors used to produce LVs

The requisite vectors, psPAX2, pMD2.G and pWPI-LC/D were used to produce LVs. Replication-deficient LVs encoding green fluorescent protein (GFP) as reporter gene were pseudotyped with the vesicular stomatitis virus glycoprotein (VSV-G). The packaging vector (psPAX2) contain promoter, gag, pol gene (Fig. 6-5A). The pol gene encodes three viral enzymes: the protease, reverse transcriptase, and integrase, and a gag gene encodes the structural proteins: the capsid, matrix, and nucleocapsid and rev for reverse transcription. The envelope vector consists of VSV-G and cytomegalovirus (CMV) region with a poly A tail (Fig. 6-5B). A transfer vector (pWPI) containing a promoter and protease domain from BoNT/D (LC/D) as well as IRES sequence for the co-expression of GFP was constructed by Dr. Jiafu Wang (Fig. 6-5C). All three vectors were used for producing LV particles.

A psPAX2 (packaging vector): Promotor | GAG | POL | TAT | REV

B pMD2.G (envelope vector): VSV-G | CMV | polyA

C pWPI-LC/D (transfer vector): LTR | Promotor | LC/D | LTR
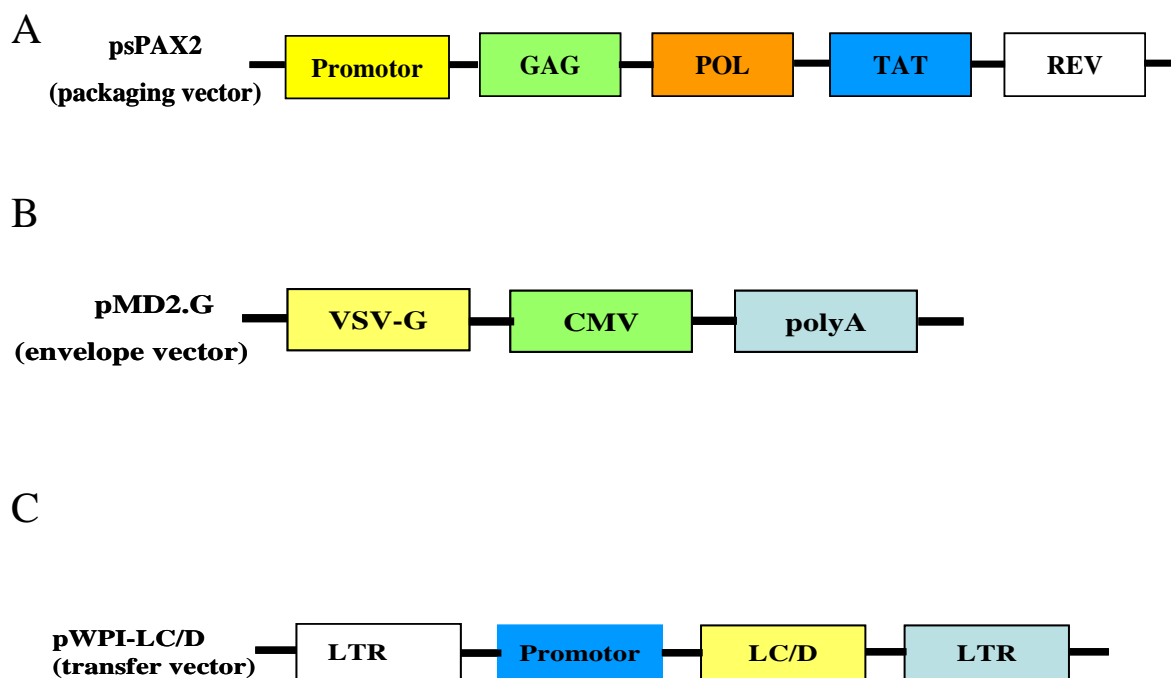
Fig. 6-5. Schematic of LV vectors.

A) psPAX2 with promoter, GAG, POL,TAT and REV gene; B) envelope vector (pMD2.G) consisting of VSV-G, CMV and poly A and C) transfer vector with LC/D and non-neuronal promoter incorporated.

GAG, group-specific antigen; POL, reverse transcriptase; REV, regulator of expression of virion proteins; TAT, trans-activator of transcription; VSV-G, Vesicular stomatitis virus-envelope glycoprotein; CMV, Cytomegalovirus envelope protein gene; poly-A, polyadenylation; LC/D, light chain of BoNT/D.

6.2.2 Validation of vectors by restriction digestion

To check the quality of vectors prepared on a large-scale, all 3 were digested using specific restriction enzyme which cuts plasmids at particular sequences in the gene. Correct sizes of gene fragment were revealed when separated by agarose gel electrophoresis. pWPI containing LC/D was digested with Pme-1 and Pst-1 which gave a band at ~8 Kb. While psPAX2 with Sal-I and pMD2.G with ECoR-I digestion

gave right size restriction fragments. Thus, all vectors gave the expected restriction patterns suggesting free from contamination with other plasmid (Fig. 6-6).
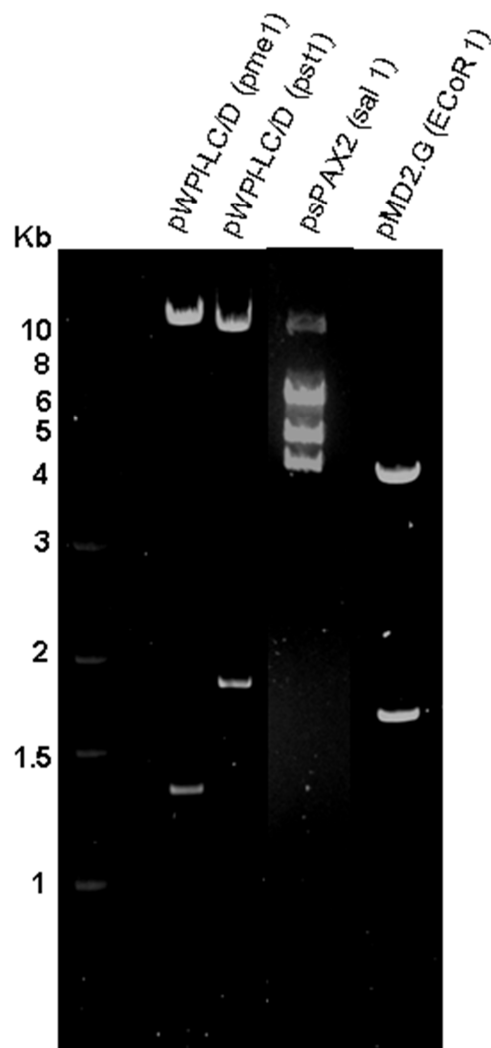
Fig. 6-6. Restriction digestion of vectors.

All 3 vectors, psPAX2, pMD2.G and pWPI-LC/D were enzymatically digested with the specific enzyme as shown in Fig.. After addition of enzyme in buffer, DNAs were incubated for 3h at 37 ^0C and then separated on 1% agarose containing ethidium bromide. A 1 Kb ladder was used to identify size of each band. Kb= kilobases. Pme-I digestion released the insert LC/D (~1.3 Kb) from the transfer vector pWPI.

6.2.3 Successful co-transfection of three vectors in Lenti-293T cells resulted in production of LVs expressing LC/D

To produce lentiviral particles, Lenti-293T cells were plated onto 6 x 15 cm poly L-lysine coated petri-plates to give 80-90% confluency and incubated overnight. Cells were then transfected with all three plasmids, psPAX2, pMD2.G and pWPI-LC/D (see Chapter 2.1.15 for transfection protocol) and incubated for 24 h before collecting the cell culture supernatant over 4 days by changing the medium daily. Supernatant containing LVs were filtered and aliquoted or concentrated by ultracentrifugation (as described in Chapter 2.1.15). As transfer vector contains a GFP marker gene, the expressed GFP signal was used to calculate transfection efficiency by counting the fluorescent cells relative to the total. In fact, ~90% of cells were transfected with lentiviral vectors after 40 h (Fig. 6-7).
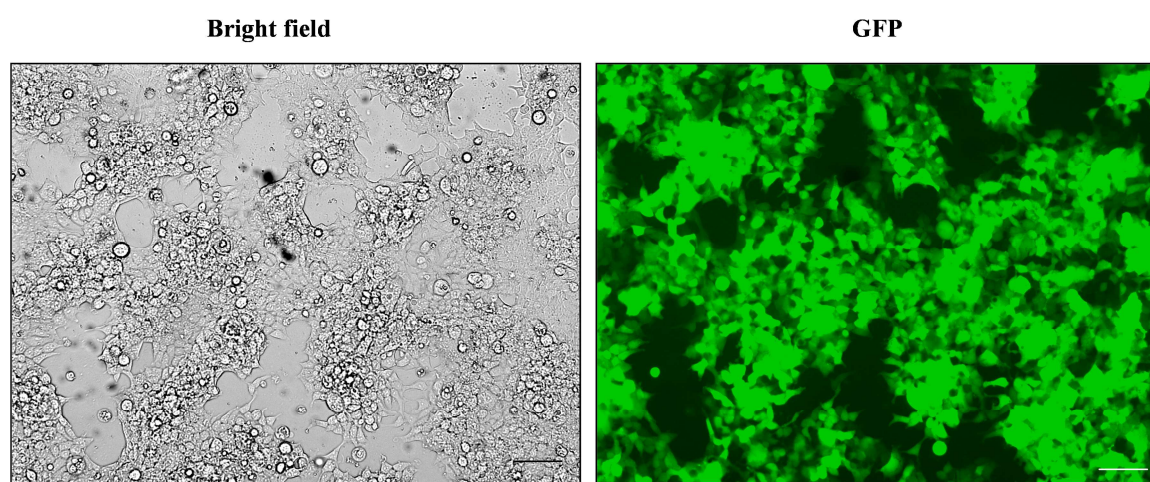
Bright field	GFP

Fig. 6-7. GFP signal indicated successful transfection.
Lenti-293T cells were transfected with psPAX2, pMD2.G and pWPI-LC/D and incubated for 24 h. Images taken under bright field and fluorescent mode after 48 h of transfection. The detected GFP signal confirmed that transfection had been achieved. Scale bar indicates 100 μm.

6.2.4 LC/D expressed by LVs cleaved VAMP-3 in human synovial cell line (SW982)

SW982 cells were plated on to 24-well plate and incubated overnight at 37 ^{O}C with 5% CO_2 before being transduced with 20 or 40 μl of concentrated or 1:2, 1:5 of non-

concentrated LVs (cell culture supernatant) and incubated for 3 days without changing the medium. Cells were then harvested for immunoblot analysis. As expected, concentrated LVs more extensively cleaved VAMP-3 (almost complete) than the non-concentrated virus (Fig. 6-8).

1. **Control (lacking LVs)**
2. **20 µl of concentrated LVs**
3. **40 µl of concentrated LVs**
4. **1:2 dilution of non-concentrated LVs**
5. **1:5 dilution of non-concentrated LVs**
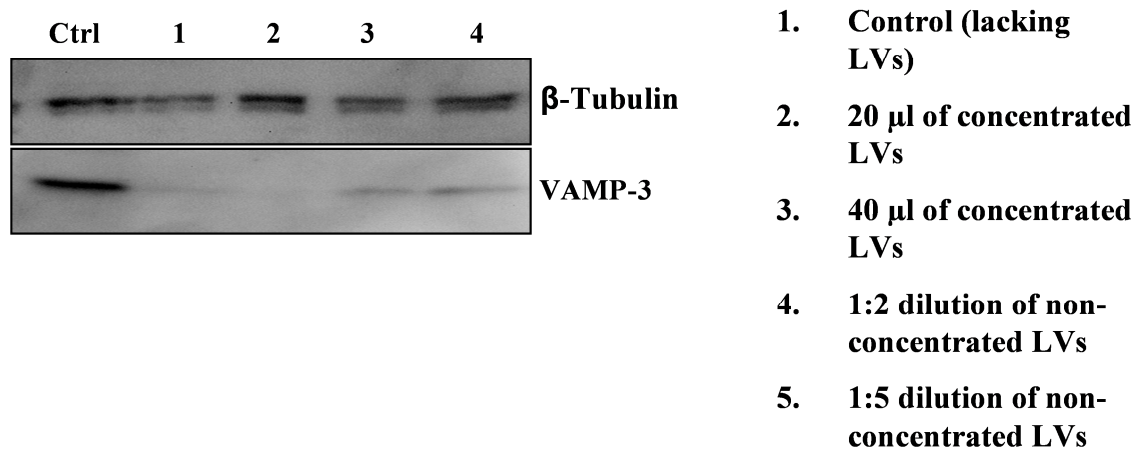
Fig. 6-8. Lentiviral particles expressing LC/D cleaved VAMP-3 in SW982 cells.
The cells were transduced with the amounts of lentiviral particles indicated, washed twice with PBS before being collected for Western blot analysis. β-tubulin served as internal control.

6.2.5 Cleavage of VAMP-3 by LVs expressing LC/D resulted in blockade of the release of cytokines from SW982 cells

Equal number of SW982 cells were plated onto 24-well plate and incubated overnight at 37 ^{O}C, infected with concentrated or non-concentrated LVs and incubated further for 3 days before collecting lysate for Western blot analysis. Concentrated LVs gave complete cleavage of VAMP-3 (~ 80%) compared to non-concentrated LVs (Fig. 6-9A and B). Truncation of VAMP-3 resulted in inhibition of the IL-1β evoked release of TNF-α ~60% (Fig. 6-9C) and IL-6 ~50% (Fig. 6-9D) with both concentrated and non-concentrated LVs.

A

Ctrl 1 2 3

β-Tubulin

VAMP-3

B

Intact VAMP-3 remaining (% of control)

C

Evoked TNF-α release (% of control)

D

Evoked IL-6 release (% of control)

1. **20 μl of concentrated LVs**
2. **1:2 dilution of non-concentrated LVs**
3. **1:5 dilution of non-concentrated LVs**
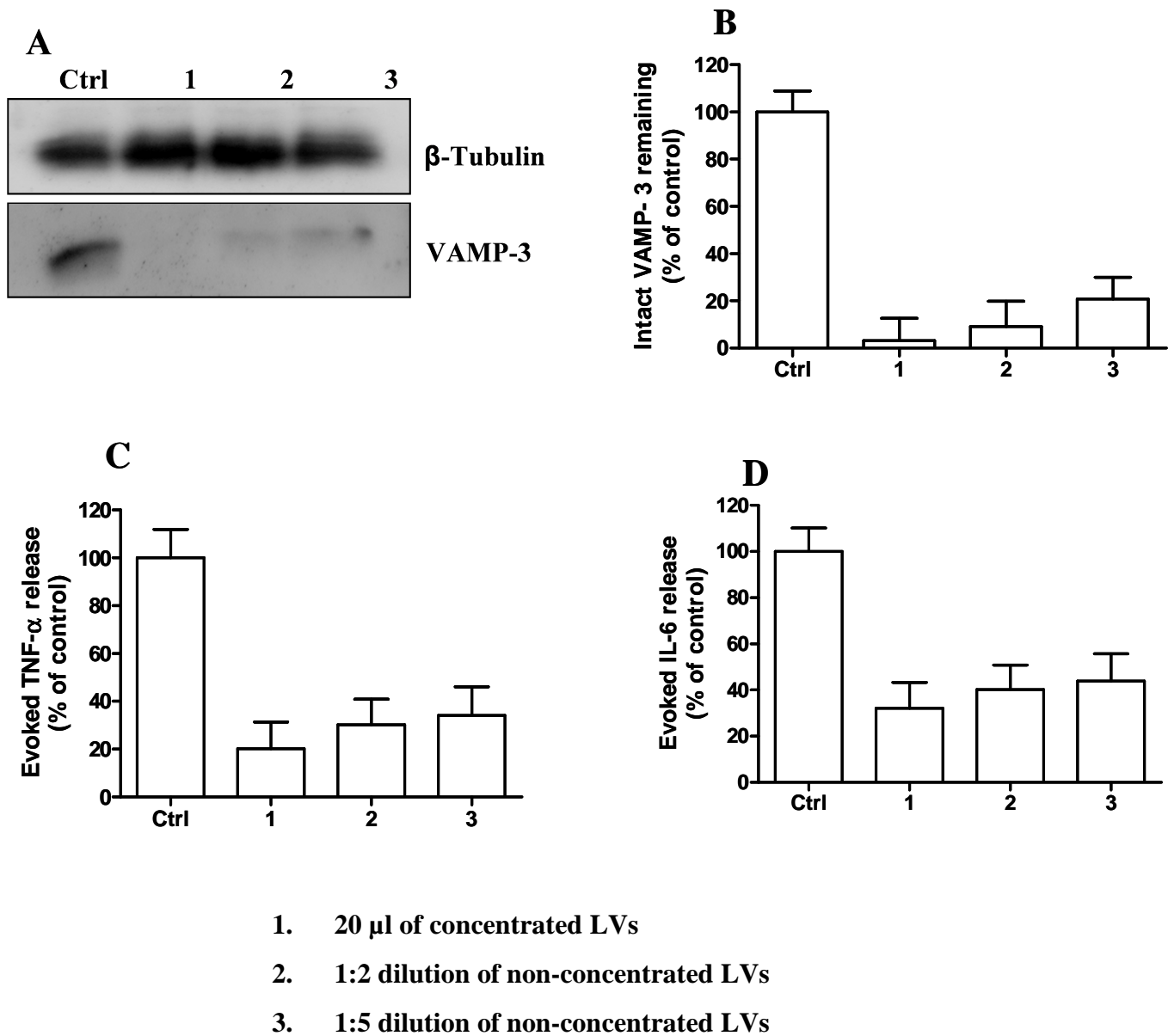
Fig. 6-9. LVs expressing LC/D cleaved VAMP-3 and inhibited release of cytokines in SW982 cells.

Cells were transfected with LVs and lysate harvested after 3 days. A) Immunoblot revealing cleavage of VAMP-3 with both concentrated and non-concentrated LVs. B) Densitometric analysis showing truncation of VAMP-3 by concentrated and un-concentrated LVs. Due to cleavage of VAMP-3, IL-1β-evoked release of TNF-α (C) and IL-6 (D) was inhibited. Data represented as mean ± S.E.M, n=2.

6.2.6 In RAW264.7 cells, LVs expressing LC/D inhibited cytokine release by truncating VAMP-3

In order to further investigate whether LVs expressing LC/D would enter and cleave VAMP-3 and inhibit cytokine release, RAW264.7 cells were transduced with LVs and incubated for 3 days. A cell lysate and cell culture supernatant was collected for immunoblot and ELISA assays. LVs; concentrated (20 µl) and non-concentrated (1:2 and 1:5 dilution), infected macrophages and cleaved VAMP-3 (Fig. 6-10A). Both concentrated and non-concentrated LVs gave ~ 50% cleavage of VAMP-3 in macrophages (Fig. 6-10B) and this was accompanied by inhibition of LPS (100 ng/ml) + IFN-Y(500 pg/ml) stimulated release ~ 40% of TNF-α (Fig. 6-10C) and IL-6 (Fig. 6-10D).

A

Ctrl   1   2   3

β-Tubulin

VAMP-3

B

Intact VAMP-3 remaining (% of control)

C

Evoked TNF-α release (% of control)

D

Evoked IL-6 release (% of control)

1. **20 μl of concentrated LVs**

2. **1:2 dilution of non-concentrated LVs**

3. **1:5 dilution of non-concentrated LVs**
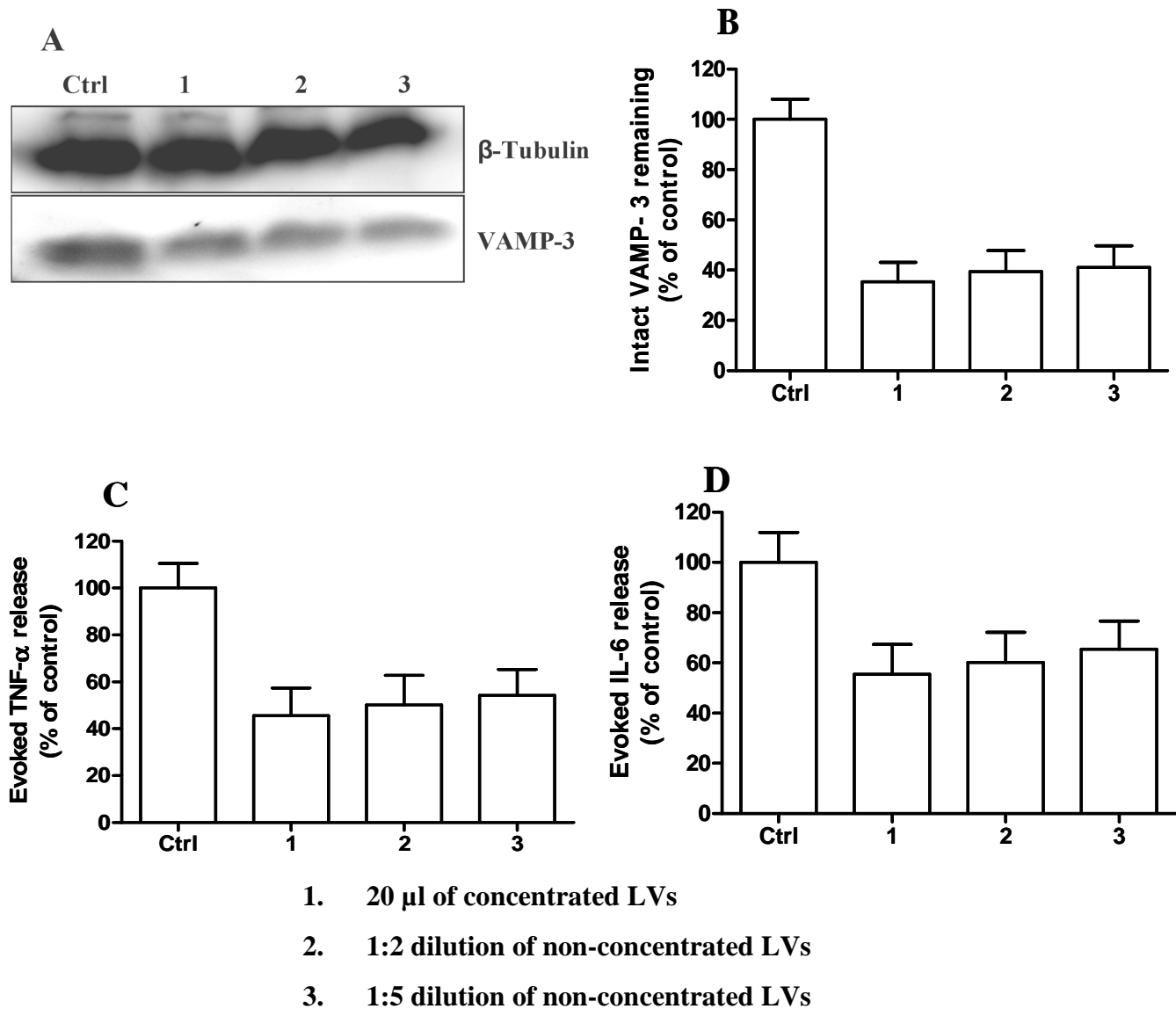
Fig. 6-10. LVs truncated VAMP-3 and blocked the release of cytokines from RAW264.7 cells.

A) Cells were transduced with LVs caused cleavage of VAMP-3. B) VAMP-3 cleavage was found with both concentrated and non-concentrated LVs. Non-treated cells served as control. Stimulated release of TNF-α (C) and IL-6 (D) compared to control after VAMP-3 truncation was plotted. Data represented as mean ± S.E.M., n=2.

6.3 DISCUSSION

Targeted delivery and expression of ameliorative genes in neuronal and non-neuronal cells are highly relevant for basic research and front-line medical advancement (Nanou and Azzouz, 2009). Numerous disease-modifying drugs for treating OA and RA have been proposed, focusing largely on antagonising production or activity of inflammatory mediators. Intra-articular drug delivery is compromised by the presence of a highly efficient lymphatic system that rapidly eliminates molecules from the synovial cavity, requiring frequent administration of the drug (Levick, 1980; Allen et al., 2010). Therapeutic gene transfer via LVs is a valuable approach over other traditional anti-inflammatory treatments because it has the potential to allow the production of factors over extended periods compared with the application of molecules with short pharmacological half-lives. LVs was selected because of larger cloning capacity and easier production of high titres (Connolly, 2002; Wu et al., 2007; Federici et al., 2009). LV vectors can deliver exogenous gene *in vitro* and *in vivo* in neuronal and non-neuronal cells (Gouze et al., 2002; Gouze et al., 2003; Van den Haute et al., 2003; Peluffo et al., 2013). Our previous use of lentiviral shRNA and targeted bio-therapeutics, KD or cleavage of VAMP-2/3 resulted in inhibition of the release of cytokines or pain peptides from synoviocytes, macrophages and sensory neurons (Chapter 3 and 5). A recombinant form of full-length inactive BoNT/B (BoTIM/B) fused with core streptavidin (CS-BoTIM/B)-guided lentiviral transduction with the expression BoNT/A- or /E- cleavage resistant SNAP-25, attenuated the effect by BoNT/A or /E in spinal cord neurons (O'Leary et al., 2011). Thus, it was warranted to develop LVs expressing LC/D to knockdown VAMP in synoviocytes, macrophages and sensory neurons.

To minimize the possibility of generating replication-competent virus through recombination, a three-plasmid expression system was used, consisting of an packaging plasmid, a vector plasmid containing viral integrase and promoter-driven transgene, and a plasmid expressing the surface VSV-G glycoprotein. To enhance the safety of this system further, a self-inactivating (SIN) lentivirus vector has been introduced. The U3 region of the 5' LTR was replaced with the CMV promoter, and the U3 region of the 3' LTR (containing TATA box and transcription-factor binding sites) was deleted. In addition, inclusion of polyadenylation sequence in the U5 region of the 3' LTR increases vector titres (Miyoshi et al., 1998; Kafri et al., 1999; Cockrell

and Kafri, 2007; Akhtar et al., 2013). All three plasmids (psPAX2, pMD2.G and pWPI-LC/D) showed correct gene sequence. LVs expressing LC/D were successfully produced and its activity demonstrated by cleavage of VAMP-3 in human synoviocytes. Both concentrated and non-concentrated LVs truncated VAMP-3 in human synoviocytes and macrophages, blocked the release of cytokines, reaffirming previous finding that VAMP-3 is required for exocytosis of TNF-α and IL-6. Although, co-expression of GFP in LVs infected cells provided somewhat evidence for viral infection efficiency, the titre of LVs is to be determined by p24 ELISA kit. Further experiments need to be carried out to completely characterise LVs and its activity in inflammatory cells.

CHAPTER 7 GENERAL DISCUSSION

AND FUTURE ASPECTS

7.1 A REQUIREMENT FOR SNAP-23 AND VAMP-3 IN THE EXOCYTOSIS OF CYTOKINES FROM HUMAN SYNOVIOCYTES BUT VAMP-8 IN RAT

The current available drugs are not very effective to treat arthritis. So, there is unmet need of new potent and longer acting therapeutics to combat arthritic pain. Synoviocytes, microphages and sensory neurons are involved in the progression of arthritis by producing cytokines and neuropeptides. SNAREs comprise distinct families of conserved membrane-associated proteins which facilitates membrane fusion exocytosis in eukaryotes. They are found throughout the secretory pathways and participates in number of membrane-trafficking events, including trafficking of cargo-containing vesicles, compartmental organisation and organelle fusion (Han et al., 2009; Stanley and Lacy, 2010). New BoNT-based targeted bio-therapeutics and lentiviral particles expressing LC/D were engineered in the current studies to block release of pain mediators from inflammatory cells and sensory neurons.

In this study, KD of SNAP-23 or VAMP-3 inhibited release of TNF-α and IL-6 from SW982. However, KD of syntaxin-2, -3 or -4 failed to reduce secretion, suggesting involvement of other syntaxin isoforms. SNAP-23 and VAMP-3 containing SDS-resistant SNARE complexes were detected; also co-immunoprecipitation identified VAMP-3 as a constituent of the complex with SNAP-23 and to a lesser extent to syntaxin-2 or -3 but not with -4. Even though syntaxin-2 or -3 formed complex with VAMP-3 did not alter the release of cytokines, may be because of other syntaxin isoforms involved in secretion of cytokines which were not investigated in SW982. A peri-nuclear localisation of SV2 protein after KD of SNAP-23 was observed, but not in normal cells, suggesting participation of the former in the transportation of cytokines from this locus, presumably trans-Golgi or ER regions. Even though SW982 cells express SV2 receptor, /EA failed to enter. To overcome this problem, access of novel BoNT LC/E400(K224D) mutant was achieved with digitonin permeabilisation; this resulted specific cleavage of SNAP-23. Although KD of SNAP-23 blocked release of cytokines, it did not affect the surface content of IL-1 receptor; its filamentous-like distribution disappeared, suggesting IL-1 receptor trafficking is not affected (Chapter 3). IL-1 receptor expression was not altered after SNAP-23 KD, showing IL-1β can bind to receptor and internalise.

Novel BoNT-based chimeras BA and DA were engineered were internalised by binding to SV2 receptor, translocated LC/B or LC/D into the cytosol and cleaved VAMP in rCGNs, rTGNs and rSCs. BA and DA cleaved VAMP-3 in rSCs, but did not inhibited cytokine release; however, KD of VAMP-8 blocked release of cytokines, suggesting that it fulfils this function in these cells instead of VAMP-3 in SW982 (Chapter 4). Recombinant chimera (EA) of BoNT/A and BoNT/E was bound to SV2C expressed in rTGNs and cleaved SNAP-25, indicates that /A binding domain (HC) mediated uptake of the active /E protease (Meng et al., 2009). Such recombinant BoNTs can be engineered to deliver LC into the non-neuronal cells which express SV2.

Even though synoviocytes expresses BoNT/A receptor, it was difficult to cleave SNAREs using native BoNTs. To overcome these difficulties, BoNT chimeric strategy by switching the wide-spectrum binding domain to a cell-type unique ligand and LVs expressing LC/D was achieved.

7.2 TARGETED BIO-THERAPEUTIC AND LVs EXPRESSING LC/D BLOCKED THE RELEASE OF CYTOKINES AND/OR PAIN PEPTIDES BY CLEAVING AND KD OF VAMP, RESPECTIVELY

As previously shown that SNAP-23 and VAMP-3 required for exocytosis of cytokines, a novel BoNT-based targeted bio-therapeutic with a unique ligand was engineered, which specifically binds to receptors on the cells of interest, gets internalised and cleaves its substrate. A chemical conjugate of *E. cristagalli* lectin and recombinant LH(N)/A or LC/A of BoNT/A conjugated to SP cleave SNAP-25 and inhibit neuropeptide release from rDRGs and other neuronal cells (Duggan et al., 2002; Mustafa et al., 2013). However, chemical conjugation is problematic not reproducible and the products usually display lower activity. Use of targeted bio-therapeutics overcomes these difficulties, because these can be engineered and expressed recombinantly as stable and active fusions. It has been reported that a fusion of LH(N)-domains of BoNT/C1 and epidermal growth factor (EGF) inhibits secretion of mucus from epithelial cells (Foster et al., 2006). In this project three proteins with two different ligand were developed; ARA-7 proved to be most promising therapeutic, cleaving VAMP at low concentration with an EC_{50} ~10 nM.

ARA-7 cleaved VAMP not only in macrophages and synoviocytes but also in sensory neurons and reduced release of cytokines or a pain peptide, suggesting it could be used to decrease inflammatory as well as neuropathic pain. A control protein (LC.HN/D) without the ligand failed to cleave VAMP presumably due to lack of binding/internalisation (Chapter 5). As reported previously, BoNTs can be used to alleviate arthritic pain in patients, these bio-therapeutic can be used to reduce inflammation by specifically targeting inflammatory cells and sensory neurons which are involved in pain.

In an alternative approach, replication-defective LVs have been used to deliver therapeutic gene due to their intrinsic ability to integrate into the host genome, resulting in expression of gene. LVs expressing LC/D were developed in the laboratory to target neuronal and non-neuronal cells; these cleaved VAMP-3 in synoviocytes and macrophages which lead to a blockade of cytokine release (Chapter 6).

As both therapeutics successfully truncated VAMP and blocked release of a pain mediators, it is warranted to evaluate these in other inflammatory cells like mast, lymphocytes, primary human synoviocytes and chondrocytes which are also involved in arthritic pain and in rat models of arthritis. Further studies can be carried out based on these findings by engineering novel therapeutics with other ligands like TLRs (Toll-like receptors) which are expressed on inflammatory and sensory neurons. The existence of several toxin serotypes with different SNARE substrates/cleavage sites and have a potential to create chimeric toxins to treat pain. These therapeutics can be further tested in animal models of inflammatory and neuropathic pain and based on the results of these pre-clinical studies.

BIBLIOGRAPHY

Abeles AM, Pillinger MH (2006) The role of the synovial fibroblast in rheumatoid arthritis: cartilage destruction and the regulation of matrix metalloproteinases. Bull NYU Hosp Jt Dis 64:20-24.

Ahlback S (1968) Osteoarthrosis of the knee. A radiographic investigation. Acta Radiol Diagn (Stockh):Suppl 277:277-272.

Akhtar J, Wang Z, Zhang ZP, Bi MM (2013) Lentiviral-mediated RNA interference targeting stathmin1 gene in human gastric cancer cells inhibits proliferation in vitro and tumor growth in vivo. J Transl Med 11:212.

Allen KD, Adams SB, Setton LA (2010) Evaluating intra-articular drug delivery for the treatment of osteoarthritis in a rat model. Tissue Eng Part B Rev 16:81-92.

Altman R, Asch E, Bloch D, Bole G, Borenstein D, Brandt K, Christy W, Cooke TD, Greenwald R, Hochberg M, et al. (1986) Development of criteria for the classification and reporting of osteoarthritis. Classification of osteoarthritis of the knee. Diagnostic and Therapeutic Criteria Committee of the American Rheumatism Association. Arthritis Rheum 29:1039-1049.

Anderson S, Krug H, Dorman C, McGarraugh P, Frizelle S, Mahowald M (2010) Analgesic effects of intra-articular botulinum toxin Type B in a murine model of chronic degenerative knee arthritis pain. J Pain Res 3:161-168.

Aoki KR (2003) Pharmacology and immunology of botulinum toxin type A. Clin Dermatol 21:476-480.

Aoki KR, Francis J (2011) Updates on the antinociceptive mechanism hypothesis of botulinum toxin A. Parkinsonism Relat Disord 17 Suppl 1:S28-33.

Arend WP, Dayer JM (1990) Cytokines and cytokine inhibitors or antagonists in rheumatoid arthritis. Arthritis Rheum 33:305-315.

Arnett FC, Edworthy SM, Bloch DA, McShane DJ, Fries JF, Cooper NS, Healey LA, Kaplan SR, Liang MH, Luthra HS, et al. (1988) The American Rheumatism Association 1987 revised criteria for the classification of rheumatoid arthritis. Arthritis Rheum 31:315-324.

Arnon SS, Schechter R, Inglesby TV, Henderson DA, Bartlett JG, Ascher MS, Eitzen E, Fine AD, Hauer J, Layton M, Lillibridge S, Osterholm MT, O'Toole T, Parker G, Perl TM, Russell PK, Swerdlow DL, Tonat K (2001) Botulinum

toxin as a biological weapon: medical and public health management. JAMA 285:1059-1070.

Barrera P, Joosten LA, den Broeder AA, van de Putte LB, van Riel PL, van den Berg WB (2001) Effects of treatment with a fully human anti-tumour necrosis factor alpha monoclonal antibody on the local and systemic homeostasis of interleukin 1 and TNFalpha in patients with rheumatoid arthritis. Ann Rheum Dis 60:660-669.

Bartok B, Firestein GS (2010) Fibroblast-like synoviocytes: key effector cells in rheumatoid arthritis. Immunol Rev 233:233-255.

Bazan JF, Timans JC, Kastelein RA (1996) A newly defined interleukin-1? Nature 379:591.

Bidlack JM (2000) Detection and function of opioid receptors on cells from the immune system. Clin Diagn Lab Immunol 7:719-723.

Bileviciute I, Lundeberg T, Ekblom A, Theodorsson E (1993) Bilateral changes of substance P-, neurokinin A-, calcitonin gene-related peptide- and neuropeptide Y-like immunoreactivity in rat knee joint synovial fluid during acute monoarthritis. Neurosci Lett 153:37-40.

Bingham B, Ajit SK, Blake DR, Samad TA (2009) The molecular basis of pain and its clinical implications in rheumatology. Nat Clin Pract Rheumatol 5:28-37.

Binz T, Sikorra S, Mahrhold S (2010) Clostridial neurotoxins: mechanism of SNARE cleavage and outlook on potential substrate specificity reengineering. Toxins (Basel) 2:665-682.

Bonica JJ (1991) History of pain concepts and pain therapy. Mt Sinai J Med 58:191-202.

Boon AJ, Smith J, Dahm DL, Sorenson EJ, Larson DR, Fitz-Gibbon PD, Dykstra DD, Singh JA (2010) Efficacy of intra-articular botulinum toxin type A in painful knee osteoarthritis: a pilot study. PM R 2:268-276.

Bowes J, Barton A (2008) Recent advances in the genetics of RA susceptibility. Rheumatology (Oxford) 47:399-402.

Bradley JR (2008) TNF-mediated inflammatory disease. J Pathol 214:149-160.

Braun T, Zwerina J (2011) Positive regulators of osteoclastogenesis and bone resorption in rheumatoid arthritis. Arthritis Res Ther 13:235.

Breedveld FC, Combe B (2011) Understanding emerging treatment paradigms in rheumatoid arthritis. Arthritis Res Ther 13 Suppl 1:S3.

Breivik H, Collett B, Ventafridda V, Cohen R, Gallacher D (2006) Survey of chronic pain in Europe: prevalence, impact on daily life, and treatment. Eur J Pain 10:287-333.

Brennan FM, Maini RN, Feldmann M (1992) TNF alpha--a pivotal role in rheumatoid arthritis? Br J Rheumatol 31:293-298.

Bromley M, Woolley DE (1984) Chondroclasts and osteoclasts at subchondral sites of erosion in the rheumatoid joint. Arthritis Rheum 27:968-975.

Brown H (2000) Advances in anti-arthritic agents. 24-25 January 2000, London, UK. IDrugs 3:386-391.

Bugatti S, Codullo V, Caporali R, Montecucco C (2007) B cells in rheumatoid arthritis. Autoimmun Rev 7:137-142.

Burkey TH, Hingtgen CM, Vasko MR (2004) Isolation and culture of sensory neurons from the dorsal-root ganglia of embryonic or adult rats. Methods Mol Med 99:189-202.

Burmester GR, Blanco R, Charles-Schoeman C, Wollenhaupt J, Zerbini C, Benda B, Gruben D, Wallenstein G, Krishnaswami S, Zwillich SH, Koncz T, Soma K, Bradley J, Mebus C (2013) Tofacitinib (CP-690,550) in combination with methotrexate in patients with active rheumatoid arthritis with an inadequate response to tumour necrosis factor inhibitors: a randomised phase 3 trial. Lancet 381:451-460.

Caporali R, Pallavicini FB, Filippini M, Gorla R, Marchesoni A, Favalli EG, Sarzi-Puttini P, Atzeni F, Montecucco C (2009) Treatment of rheumatoid arthritis with anti-TNF-alpha agents: a reappraisal. Autoimmun Rev 8:274-280.

Chang SK, Gu Z, Brenner MB (2010) Fibroblast-like synoviocytes in inflammatory arthritis pathology: the emerging role of cadherin-11. Immunol Rev 233:256-266.

Chang WP, Sudhof TC (2009) SV2 renders primed synaptic vesicles competent for Ca2+ -induced exocytosis. J Neurosci 29:883-897.

Chen S, Barbieri JT (2009) Engineering botulinum neurotoxin to extend therapeutic intervention. Proc Natl Acad Sci U S A 106:9180-9184.

Chen YA, Scales SJ, Patel SM, Doung YC, Scheller RH (1999) SNARE complex formation is triggered by Ca2+ and drives membrane fusion. Cell 97:165-174.

Chiu IM, von Hehn CA, Woolf CJ (2012) Neurogenic inflammation and the peripheral nervous system in host defense and immunopathology. Nat Neurosci 15:1063-1067.

Chou CL, Lee SH, Lu SY, Tsai KL, Ho CY, Lai HC (2010) Therapeutic effects of intra-articular botulinum neurotoxin in advanced knee osteoarthritis. J Chin Med Assoc 73:573-580.

Choy EH, Panayi GS (2001) Cytokine pathways and joint inflammation in rheumatoid arthritis. N Engl J Med 344:907-916.

Chu CQ, Field M, Feldmann M, Maini RN (1991) Localization of tumor necrosis factor alpha in synovial tissues and at the cartilage-pannus junction in patients with rheumatoid arthritis. Arthritis Rheum 34:1125-1132.

Cockrell AS, Kafri T (2007) Gene delivery by lentivirus vectors. Mol Biotechnol 36:184-204.

Coffin JM HS, Varmus HE (1997) Retroviruses. Cold Spring Harbor (NY).

Colmegna I, Ohata BR, Menard HA (2012) Current understanding of rheumatoid arthritis therapy. Clin Pharmacol Ther 91:607-620.

Connolly JB (2002) Lentiviruses in gene therapy clinical research. Gene Ther 9:1730-1734.

Cope AP, Aderka D, Doherty M, Engelmann H, Gibbons D, Jones AC, Brennan FM, Maini RN, Wallach D, Feldmann M (1992) Increased levels of soluble tumor necrosis factor receptors in the sera and synovial fluid of patients with rheumatic diseases. Arthritis Rheum 35:1160-1169.

Cruwys SC, Garrett NE, Kidd BL (1995) Sensory denervation with capsaicin attenuates inflammation and nociception in arthritic rats. Neurosci Lett 193:205-207.

Curtis JR, Singh JA (2011) Use of biologics in rheumatoid arthritis: current and emerging paradigms of care. Clin Ther 33:679-707.

Curtis JR, Singh JA (2011) Use of biologics in rheumatoid arthritis: current and emerging paradigms of care. Clin Ther 33:679-707.

Dasuri K, Antonovici M, Chen K, Wong K, Standing K, Ens W, El-Gabalawy H, Wilkins JA (2004) The synovial proteome: analysis of fibroblast-like synoviocytes. Arthritis Res Ther 6:R161-168.

De Silva D, Mitchell MD, Keelan JA (2010) Inhibition of choriodecidual cytokine production and inflammatory gene expression by selective I-kappaB kinase (IKK) inhibitors. Br J Pharmacol 160:1808-1822.

Dieppe PA, Lohmander LS (2005) Pathogenesis and management of pain in osteoarthritis. Lancet 365:965-973.

Dolly JO, Aoki KR (2006) The structure and mode of action of different botulinum toxins. Eur J Neurol 13 Suppl 4:1-9.

Dolly JO, O'Connell MA (2012) Neurotherapeutics to inhibit exocytosis from sensory neurons for the control of chronic pain. Curr Opin Pharmacol 12:100-108.

Dolly JO, Wang J, Zurawski TH, Meng J (2011) Novel therapeutics based on recombinant botulinum neurotoxins to normalize the release of transmitters and pain mediators. FEBS J 278:4454-4466.

Dolly JO, Wang J, Zurawski TH, Meng J (2011) Novel therapeutics based on recombinant botulinum neurotoxins to normalize the release of transmitters and pain mediators. Febs J 278:4454-4466.

Dolly JO, Lawrence GW, Meng J, Wang J, Ovsepian SV (2009) Neuro-exocytosis: botulinum toxins as inhibitory probes and versatile therapeutics. Curr Opin Pharmacol 9:326-335.

Dong M, Yeh F, Tepp WH, Dean C, Johnson EA, Janz R, Chapman ER (2006) SV2 is the protein receptor for botulinum neurotoxin A. Science 312:592-596.

Duggan MJ, Quinn CP, Chaddock JA, Purkiss JR, Alexander FC, Doward S, Fooks SJ, Friis LM, Hall YH, Kirby ER, Leeds N, Moulsdale HJ, Dickenson A, Green GM, Rahman W, Suzuki R, Shone CC, Foster KA (2002) Inhibition of release of neurotransmitters from rat dorsal root ganglia by a novel conjugate of a Clostridium botulinum toxin A endopeptidase fragment and Erythrina cristagalli lectin. J Biol Chem 277:34846-34852.

Edwards CJ, Arden NK, Fisher D, Saperia JC, Reading I, Van Staa TP, Cooper C (2005) The changing use of disease-modifying anti-rheumatic drugs in individuals with rheumatoid arthritis from the United Kingdom General Practice Research Database. Rheumatology (Oxford) 44:1394-1398.

Edwards JC (2000) Fibroblast biology. Development and differentiation of synovial fibroblasts in arthritis. Arthritis Res 2:344-347.

Emery P (2006) Treatment of rheumatoid arthritis. BMJ 332:152-155.

Emery P, Keystone E, Tony HP, Cantagrel A, van Vollenhoven R, Sanchez A, Alecock E, Lee J, Kremer J (2008) IL-6 receptor inhibition with tocilizumab improves treatment outcomes in patients with rheumatoid arthritis refractory to anti-tumour necrosis factor biologicals: results from a 24-week multicentre randomised placebo-controlled trial. Ann Rheum Dis 67:1516-1523.

Erbguth FJ (2004) Historical notes on botulism, Clostridium botulinum, botulinum toxin, and the idea of the therapeutic use of the toxin. Mov Disord 19 Suppl 8:S2-6.

Feany MB, Yee AG, Delvy ML, Buckley KM (1993) The synaptic vesicle proteins SV2, synaptotagmin and synaptophysin are sorted to separate cellular compartments in CHO fibroblasts. J Cell Biol 123:575-584.

Federici T, Kutner R, Zhang XY, Kuroda H, Tordo N, Boulis NM, Reiser J (2009) Comparative analysis of HIV-1-based lentiviral vectors bearing lyssavirus glycoproteins for neuronal gene transfer. Genet Vaccines Ther 7:1.

Feldmann M (2001) Pathogenesis of arthritis: recent research progress. Nat Immunol 2:771-773.

Fernandes JC, Martel-Pelletier J, Pelletier JP (2002) The role of cytokines in osteoarthritis pathophysiology. Biorheology 39:237-246.

Fleischmann RM, Tesser J, Schiff MH, Schechtman J, Burmester GR, Bennett R, Modafferi D, Zhou L, Bell D, Appleton B (2006) Safety of extended treatment with anakinra in patients with rheumatoid arthritis. Ann Rheum Dis 65:1006-1012.

Flynn TC, Clark RE, 2nd (2003) Botulinum toxin type B (MYOBLOC) versus botulinum toxin type A (BOTOX) frontalis study: rate of onset and radius of diffusion. Dermatol Surg 29:519-522; discussion 522.

Foster KA (2009) Engineered toxins: new therapeutics. Toxicon 54:587-592.

Foster KA, Adams EJ, Durose L, Cruttwell CJ, Marks E, Shone CC, Chaddock JA, Cox CL, Heaton C, Sutton JM, Wayne J, Alexander FC, Rogers DF (2006) Re-engineering the target specificity of Clostridial neurotoxins - a route to novel therapeutics. Neurotox Res 9:101-107.

Frank SP, Thon KP, Bischoff SC, Lorentz A (2011) SNAP-23 and syntaxin-3 are required for chemokine release by mature human mast cells. Mol Immunol 49:353-358.

Fu Z, Chen C, Barbieri JT, Kim JJ, Baldwin MR (2009) Glycosylated SV2 and gangliosides as dual receptors for botulinum neurotoxin serotype F. Biochemistry 48:5631-5641.

Fujimoto M, Serada S, Mihara M, Uchiyama Y, Yoshida H, Koike N, Ohsugi Y, Nishikawa T, Ripley B, Kimura A, Kishimoto T, Naka T (2008) Interleukin-6 blockade suppresses autoimmune arthritis in mice by the inhibition of inflammatory Th17 responses. Arthritis Rheum 58:3710-3719.

Glick EN (1967) Asymmetrical rheumatoid arthritis after poliomyelitis. Br Med J 3:26-28.

Goldring SR, Gravallese EM (2000) Pathogenesis of bone erosions in rheumatoid arthritis. Curr Opin Rheumatol 12:195-199.

Gottschalk A, Smith DS (2001) New concepts in acute pain therapy: preemptive analgesia. Am Fam Physician 63:1979-1984.

Gouze E, Pawliuk R, Pilapil C, Gouze JN, Fleet C, Palmer GD, Evans CH, Leboulch P, Ghivizzani SC (2002) In vivo gene delivery to synovium by lentiviral vectors. Mol Ther 5:397-404.

Gouze E, Pawliuk R, Gouze JN, Pilapil C, Fleet C, Palmer GD, Evans CH, Leboulch P, Ghivizzani SC (2003) Lentiviral-mediated gene delivery to synovium: potent intra-articular expression with amplification by inflammation. Mol Ther 7:460-466.

Gravallese EM, Harada Y, Wang JT, Gorn AH, Thornhill TS, Goldring SR (1998) Identification of cell types responsible for bone resorption in rheumatoid arthritis and juvenile rheumatoid arthritis. Am J Pathol 152:943-951.

Gregersen PK (1999) Genetics of rheumatoid arthritis: confronting complexity. Arthritis Res 1:37-44.

Grubb BD (2004) Activation of sensory neurons in the arthritic joint. Novartis Found Symp 260:28-36; discussion 36-48, 100-104, 277-109.

Han C, Chen T, Yang M, Li N, Liu H, Cao X (2009) Human SCAMP5, a novel secretory carrier membrane protein, facilitates calcium-triggered cytokine secretion by interaction with SNARE machinery. J Immunol 182:2986-2996.

Hayashi T, McMahon H, Yamasaki S, Binz T, Hata Y, Sudhof TC, Niemann H (1994) Synaptic vesicle membrane fusion complex: action of clostridial neurotoxins on assembly. Embo J 13:5051-5061.

Heppelmann B (1997) Anatomy and histology of joint innervation. J Peripher Nerv Syst 2:5-16.

Houssiau FA (1995) Cytokines in rheumatoid arthritis. Clin Rheumatol 14 Suppl 2:10-13.

Houssiau FA, Devogelaer JP, Van Damme J, de Deuxchaisnes CN, Van Snick J (1988) Interleukin-6 in synovial fluid and serum of patients with rheumatoid arthritis and other inflammatory arthritides. Arthritis Rheum 31:784-788.

Hyc A, Osiecka-Iwan A, Dziunycz P, Moskalewski S (2007) Preparation of rat synovial membrane for studies of cytokine secretion. Folia Histochem Cytobiol 45:57-60.

Imamura K, Spriggs D, Ohno T, Kufe D (1989) Effects of botulinum toxin type D on secretion of tumor necrosis factor from human monocytes. Mol Cell Biol 9:2239-2243.

Jahn R (2004) Principles of exocytosis and membrane fusion. Ann N Y Acad Sci 1014:170-178.

Jahn R, Lang T, Sudhof TC (2003) Membrane fusion. Cell 112:519-533.

Jones LC, Moussa L, Fulcher ML, Zhu Y, Hudson EJ, O'Neal WK, Randell SH, Lazarowski ER, Boucher RC, Kreda SM (2011) VAMP8 is a vesicle SNARE that regulates mucin secretion in airway goblet cells. J Physiol 590:545-562.

Jones LC, Moussa L, Fulcher ML, Zhu Y, Hudson EJ, Oâ€™Neal WK, Randell SH, Lazarowski ER, Boucher RC, Kreda SM (2012) VAMP8 is a vesicle SNARE that regulates mucin secretion in airway goblet cells. The Journal of Physiology 590:545-562.

Julius D (2013) TRP channels and pain. Annu Rev Cell Dev Biol 29:355-384.

Jurgens CK, Young KR, Madden VJ, Johnson PR, Johnston RE (2012) A novel self-replicating chimeric lentivirus-like particle. J Virol 86:246-261.

Kafri T, van Praag H, Ouyang L, Gage FH, Verma IM (1999) A packaging cell line for lentivirus vectors. J Virol 73:576-584.

Kane D, Lockhart JC, Balint PV, Mann C, Ferrell WR, McInnes IB (2005) Protective effect of sensory denervation in inflammatory arthritis (evidence of regulatory neuroimmune pathways in the arthritic joint). Ann Rheum Dis 64:325-327.

Kidd BL, Langford RM, Wodehouse T (2007) Arthritis and pain. Current approaches in the treatment of arthritic pain. Arthritis Res Ther 9:214.

Kinne RW, Stuhlmuller B, Burmester GR (2007) Cells of the synovium in rheumatoid arthritis. Macrophages. Arthritis Res Ther 9:224.

Knoop J, Steultjens MP, van der Leeden M, van der Esch M, Thorstensson CA, Roorda LD, Lems WF, Dekker J (2011) Proprioception in knee osteoarthritis: a narrative review. Osteoarthritis Cartilage 19:381-388.

Kobayashi I, Ziff M (1975) Electron microscopic studies of the cartilage-pannus junction in rheumatoid arthritis. Arthritis Rheum 18:475-483.

Koch AE, Kunkel SL, Strieter RM (1995) Cytokines in rheumatoid arthritis. J Investig Med 43:28-38.

Kochukov MY, McNearney TA, Fu Y, Westlund KN (2006) Thermosensitive TRP ion channels mediate cytosolic calcium response in human synoviocytes. Am J Physiol Cell Physiol 291:C424-432.

Konttinen YT, Tiainen VM, Gomez-Barrena E, Hukkanen M, Salo J (2006) Innervation of the joint and role of neuropeptides. Ann N Y Acad Sci 1069:149-154.

Krug HE, Frizelle S, McGarraugh P, Mahowald ML (2009) Pain behavior measures to quantitate joint pain and response to neurotoxin treatment in murine models of arthritis. Pain Med 10:1218-1228.

Lacy DB, Tepp W, Cohen AC, DasGupta BR, Stevens RC (1998) Crystal structure of botulinum neurotoxin type A and implications for toxicity. Nat Struct Biol 5:898-902.

Lacy P, Stow JL (2011) Cytokine release from innate immune cells: association with diverse membrane trafficking pathways. Blood 118:9-18.

Lawrence GW, Dolly JO (2002) Ca2+-induced changes in SNAREs and synaptotagmin I correlate with triggered exocytosis from chromaffin cells: insights gleaned into the signal transduction using trypsin and botulinum toxins. J Cell Sci 115:2791-2800.

Le Loet X, Nordstrom D, Rodriguez M, Rubbert A, Sarzi-Puttini P, Wouters JM, Woolley JM, Wright N, Lawrence C, Appleton B (2008) Effect of anakinra on functional status in patients with active rheumatoid arthritis receiving concomitant therapy with traditional disease modifying antirheumatic drugs: evidence from the OMEGA Trial. J Rheumatol 35:1538-1544.

Leggett J, Harper E, Waite E, Marks P, Martinez A, Lightman S (2013) GHRH Receptor-Targeted Botulinum Neurotoxin Selectively Inhibits Pulsatile GH Secretion in Male Rats. Endocrinology 154:3305-3318.

Levick JR (1980) Contributions of the lymphatic and microvascular systems to fluid absorption from the synovial cavity of the rabbit knee. J Physiol 306:445-461.

Logan MR, Odemuyiwa SO, Moqbel R (2003) Understanding exocytosis in immune and inflammatory cells: the molecular basis of mediator secretion. J Allergy Clin Immunol 111:923-932; quiz 933.

Lundy SK, Sarkar S, Tesmer LA, Fox DA (2007) Cells of the synovium in rheumatoid arthritis. T lymphocytes. Arthritis Res Ther 9:202.

Mahowald ML, Singh JA, Dykstra D (2006) Long term effects of intra-articular botulinum toxin A for refractory joint pain. Neurotox Res 9:179-188.

Mahowald ML, Krug HE, Singh JA, Dykstra D (2009) Intra-articular Botulinum Toxin Type A: a new approach to treat arthritis joint pain. Toxicon 54:658-667.

Mahrhold S, Rummel A, Bigalke H, Davletov B, Binz T (2006) The synaptic vesicle protein 2C mediates the uptake of botulinum neurotoxin A into phrenic nerves. FEBS Lett 580:2011-2014.

Maisey EA, Wadsworth JD, Poulain B, Shone CC, Melling J, Gibbs P, Tauc L, Dolly JO (1988) Involvement of the constituent chains of botulinum neurotoxins A and B in the blockade of neurotransmitter release. Eur J Biochem 177:683-691.

Malemud CJ (2007) Growth hormone, VEGF and FGF: involvement in rheumatoid arthritis. Clin Chim Acta 375:10-19.

Manderson AP, Kay JG, Hammond LA, Brown DL, Stow JL (2007) Subcompartments of the macrophage recycling endosome direct the differential secretion of IL-6 and TNFalpha. J Cell Biol 178:57-69.

Mapp PI, Terenghi G, Walsh DA, Chen ST, Cruwys SC, Garrett N, Kidd BL, Polak JM, Blake DR (1993) Monoarthritis in the rat knee induces bilateral and time-dependent changes in substance P and calcitonin gene-related peptide immunoreactivity in the spinal cord. Neuroscience 57:1091-1096.

March CJ, Mosley B, Larsen A, Cerretti DP, Braedt G, Price V, Gillis S, Henney CS, Kronheim SR, Grabstein K, et al. (1985) Cloning, sequence and expression of two distinct human interleukin-1 complementary DNAs. Nature 315:641-647.

McDougall JJ (2006) Arthritis and pain. Neurogenic origin of joint pain. Arthritis Res Ther 8:220.

McMahon HT, Sudhof TC (1995) Synaptic core complex of synaptobrevin, syntaxin, and SNAP25 forms high affinity alpha-SNAP binding site. J Biol Chem 270:2213-2217.

Melzack R (1993) Pain: past, present and future. Can J Exp Psychol 47:615-629.

Meng J, Wang J, Lawrence G, Dolly JO (2007) Synaptobrevin I mediates exocytosis of CGRP from sensory neurons and inhibition by botulinum toxins reflects their anti-nociceptive potential. J Cell Sci 120:2864-2874.

Meng J, Ovsepian SV, Wang J, Pickering M, Sasse A, Aoki KR, Lawrence GW, Dolly JO (2009) Activation of TRPV1 mediates calcitonin gene-related peptide release, which excites trigeminal sensory neurons and is attenuated by a retargeted botulinum toxin with anti-nociceptive potential. J Neurosci 29:4981-4992.

Merskey H (1978) Diagnosis of the patient with chronic pain. J Human Stress 4:3-7.

Meunier A, Latremoliere A, Dominguez E, Mauborgne A, Philippe S, Hamon M, Mallet J, Benoliel JJ, Pohl M (2007) Lentiviral-mediated targeted NF-kappaB blockade in dorsal spinal cord glia attenuates sciatic nerve injury-induced neuropathic pain in the rat. Mol Ther 15:687-697.

Miller LE, Justen HP, Scholmerich J, Straub RH (2000) The loss of sympathetic nerve fibers in the synovial tissue of patients with rheumatoid arthritis is accompanied by increased norepinephrine release from synovial macrophages. FASEB J 14:2097-2107.

Miyoshi H, Blomer U, Takahashi M, Gage FH, Verma IM (1998) Development of a self-inactivating lentivirus vector. J Virol 72:8150-8157.

Moayedi M, Davis KD (2013) Theories of pain: from specificity to gate control. J Neurophysiol 109:5-12.

Montal M (2009) Translocation of botulinum neurotoxin light chain protease by the heavy chain protein-conducting channel. Toxicon 54:565-569.

Montal M (2010) Botulinum neurotoxin: a marvel of protein design. Annu Rev Biochem 79:591-617.

Montecucco C, Rossetto O, Caccin P, Rigoni M, Carli L, Morbiato L, Muraro L, Paoli M (2009) Different mechanisms of inhibition of nerve terminals by botulinum and snake presynaptic neurotoxins. Toxicon 54:561-564.

Montes-Sandoval L (1999) An analysis of the concept of pain. J Adv Nurs 29:935-941.

Moskowitz RW, Kelly MA, Lewallen DG (2004) Understanding osteoarthritis of the knee--causes and effects. Am J Orthop (Belle Mead NJ) 33:5-9.

Mugnier B, Bouvenot G (2000) [Anti-TNF-alpha monoclonal antibodies in the treatment of rheumatoid arthritis]. Rev Med Interne 21:854-862.

Mulherin D, Fitzgerald O, Bresnihan B (1996) Synovial tissue macrophage populations and articular damage in rheumatoid arthritis. Arthritis Rheum 39:115-124.

Murray RZ, Kay JG, Sangermani DG, Stow JL (2005) A role for the phagosome in cytokine secretion. Science 310:1492-1495.

Mustafa G, Anderson EM, Bokrand-Donatelli Y, Neubert JK, Caudle RM (2013) Anti-nociceptive effect of a conjugate of substance P and light chain of botulinum neurotoxin type A. Pain.

Nanou A, Azzouz M (2009) Gene therapy for neurodegenerative diseases based on lentiviral vectors. Prog Brain Res 175:187-200.

Naumann M, So Y, Argoff CE, Childers MK, Dykstra DD, Gronseth GS, Jabbari B, Kaufmann HC, Schurch B, Silberstein SD, Simpson DM (2008) Assessment: Botulinum neurotoxin in the treatment of autonomic disorders and pain (an evidence-based review): report of the Therapeutics and Technology Assessment Subcommittee of the American Academy of Neurology. Neurology 70:1707-1714.

Navarro-Millan I, Singh JA, Curtis JR (2012) Systematic review of tocilizumab for rheumatoid arthritis: a new biologic agent targeting the interleukin-6 receptor. Clin Ther 34:788-802 e783.

Niu X, He D, Deng S, Li W, Xi Y, Xie C, Jiang T, Zhang JZ, Dong C, Chen G (2011) Regulatory immune responses induced by IL-1 receptor antagonist in rheumatoid arthritis. Mol Immunol 49:290-296.

O'Connell JX (2000) Pathology of the synovium. Am J Clin Pathol 114:773-784.

O'Leary VB, Ovsepian SV, Raghunath A, Huo Q, Lawrence GW, Smith L, Dolly JO (2011) Innocuous full-length botulinum neurotoxin targets and promotes the expression of lentiviral vectors in central and autonomic neurons. Gene Ther 18:656-665.

Ospelt C, Neidhart M, Gay RE, Gay S (2004) Synovial activation in rheumatoid arthritis. Front Biosci 9:2323-2334.

Otero M, Goldring MB (2007) Cells of the synovium in rheumatoid arthritis. Chondrocytes. Arthritis Res Ther 9:220.

Pagan JK, Wylie FG, Joseph S, Widberg C, Bryant NJ, James DE, Stow JL (2003) The t-SNARE syntaxin 4 is regulated during macrophage activation to function in membrane traffic and cytokine secretion. Curr Biol 13:156-160.

Peluffo H, Foster E, Ahmed SG, Lago N, Hutson TH, Moon L, Yip P, Wanisch K, Caraballo-Miralles V, Olmos G, Llado J, McMahon SB, Yanez-Munoz RJ (2013) Efficient gene expression from integration-deficient lentiviral vectors in the spinal cord. Gene Ther 20:645-657.

Peng L, Tepp WH, Johnson EA, Dong M (2011) Botulinum neurotoxin D uses synaptic vesicle protein SV2 and gangliosides as receptors. PLoS Pathog 7:e1002008.

Polgar J, Chung SH, Reed GL (2002) Vesicle-associated membrane protein 3 (VAMP-3) and VAMP-8 are present in human platelets and are required for granule secretion. Blood 100:1081-1083.

Prevoo ML, van 't Hof MA, Kuper HH, van Leeuwen MA, van de Putte LB, van Riel PL (1995) Modified disease activity scores that include twenty-eight-joint counts. Development and validation in a prospective longitudinal study of patients with rheumatoid arthritis. Arthritis Rheum 38:44-48.

Puri N, Roche PA (2008) Mast cells possess distinct secretory granule subsets whose exocytosis is regulated by different SNARE isoforms. Proc Natl Acad Sci U S A 105:2580-2585.

Pushparaj PN, Tay HK (2013) Retraction: VAMP8 is essential in anaphylatoxin-induced degranulation, TNF-alpha secretion, peritonitis, and systemic inflammation. J Immunol 190:3007.

Raghunath A, Perez-Branguli F, Smith L, Dolly JO (2008) Adeno-associated virus transfer of a gene encoding SNAP-25 resistant to botulinum toxin A attenuates neuromuscular paralysis associated with botulism. J Neurosci 28:3683-3688.

Ranoux D, Attal N, Morain F, Bouhassira D (2008) Botulinum toxin type A induces direct analgesic effects in chronic neuropathic pain. Ann Neurol 64:274-283.

Rantapaa-Dahlqvist S (2005) Diagnostic and prognostic significance of autoantibodies in early rheumatoid arthritis. Scand J Rheumatol 34:83-96.

Riedel W, Neeck G (2001) Nociception, pain, and antinociception: current concepts. Z Rheumatol 60:404-415.

Roth-Isigkeit A, Thyen U, Stoven H, Schwarzenberger J, Schmucker P (2005) Pain among children and adolescents: restrictions in daily living and triggering factors. Pediatrics 115:e152-162.

Ruiz Garcia V, Jobanputra P, Burls A, Cabello JB, Galvez Munoz JG, Saiz Cuenca ES, Fry-Smith A (2011) Certolizumab pegol (CDP870) for rheumatoid arthritis in adults. Cochrane Database Syst Rev:CD007649.

Saag KG, Teng GG, Patkar NM, Anuntiyo J, Finney C, Curtis JR, Paulus HE, Mudano A, Pisu M, Elkins-Melton M, Outman R, Allison JJ, Suarez Almazor M, Bridges SL, Jr., Chatham WW, Hochberg M, MacLean C, Mikuls T, Moreland LW, O'Dell J, Turkiewicz AM, Furst DE (2008) American College of Rheumatology 2008 recommendations for the use of nonbiologic and biologic disease-modifying antirheumatic drugs in rheumatoid arthritis. Arthritis Rheum 59:762-784.

Saito T, Koshino T (2000) Distribution of neuropeptides in synovium of the knee with osteoarthritis. Clin Orthop Relat Res:172-182.

Sakuma T, Barry MA, Ikeda Y (2012) Lentiviral vectors: basic to translational. Biochem J 443:603-618.

Samuel EP (1952) The autonomic and somatic innervation of the articular capsule. Anat Rec 113:53-70.

Sander LE, Frank SP, Bolat S, Blank U, Galli T, Bigalke H, Bischoff SC, Lorentz A (2008) Vesicle associated membrane protein (VAMP)-7 and VAMP-8, but not VAMP-2 or VAMP-3, are required for activation-induced degranulation of mature human mast cells. Eur J Immunol 38:855-863.

Saxne T, Palladino MA, Jr., Heinegard D, Talal N, Wollheim FA (1988) Detection of tumor necrosis factor alpha but not tumor necrosis factor beta in rheumatoid arthritis synovial fluid and serum. Arthritis Rheum 31:1041-1045.

Scales SJ, Bock JB, Scheller RH (2000) The specifics of membrane fusion. Nature 407:144-146.

Schaible HG (2007) [Pathophysiology of pain]. Orthopade 36:8, 10-12, 14-16.

Schaible HG, Schmelz M, Tegeder I (2006) Pathophysiology and treatment of pain in joint disease. Adv Drug Deliv Rev 58:323-342.

Schivell AE, Mochida S, Kensel-Hammes P, Custer KL, Bajjalieh SM (2005) SV2A and SV2C contain a unique synaptotagmin-binding site. Mol Cell Neurosci 29:56-64.

Scholz J, Woolf CJ (2007) The neuropathic pain triad: neurons, immune cells and glia. Nat Neurosci 10:1361-1368.

Senolt L, Vencovsky J, Pavelka K, Ospelt C, Gay S (2009) Prospective new biological therapies for rheumatoid arthritis. Autoimmun Rev 9:102-107.

Sibilia J, Gottenberg JE, Mariette X (2008) Rituximab: a new therapeutic alternative in rheumatoid arthritis. Joint Bone Spine 75:526-532.

Singh JA, Mahowald ML, Noorbaloochi S (2009a) Intra-articular botulinum toxin A for refractory shoulder pain: a randomized, double-blinded, placebo-controlled trial. Transl Res 153:205-216.

Singh JA, Mahowald ML, Kushnaryov A, Goelz E, Dykstra D (2009b) Repeat injections of intra-articular botulinum toxin a for the treatment of chronic arthritis joint pain. J Clin Rheumatol 15:35-38.

Skoglund S (1956) Anatomical and physiological studies of knee joint innervation in the cat. Acta Physiol Scand Suppl 36:1-101.

Smith BH, Elliott AM, Chambers WA, Smith WC, Hannaford PC, Penny K (2001) The impact of chronic pain in the community. Fam Pract 18:292-299.

Smith HS, Audette J, Royal MA (2002) Botulinum toxin in pain management of soft tissue syndromes. Clin J Pain 18:S147-154.

Smith MD (2011) The normal synovium. Open Rheumatol J 5:100-106.

Smith MD, Barg E, Weedon H, Papengelis V, Smeets T, Tak PP, Kraan M, Coleman M, Ahern MJ (2003) Microarchitecture and protective mechanisms in synovial tissue from clinically and arthroscopically normal knee joints. Ann Rheum Dis 62:303-307.

Somm E, Bonnet N, Martinez A, Marks PM, Cadd VA, Elliott M, Toulotte A, Ferrari SL, Rizzoli R, Huppi PS, Harper E, Melmed S, Jones R, Aubert ML (2012) A botulinum toxin-derived targeted secretion inhibitor downregulates the GH/IGF1 axis. J Clin Invest 122:3295-3306.

Stanley AC, Lacy P (2010) Pathways for cytokine secretion. Physiology (Bethesda) 25:218-229.

Stow JL, Manderson AP, Murray RZ (2006) SNAREing immunity: the role of SNAREs in the immune system. Nat Rev Immunol 6:919-929.

Stow JL, Low PC, Offenhauser C, Sangermani D (2009) Cytokine secretion in macrophages and other cells: pathways and mediators. Immunobiology 214:601-612.

Symmons DP (2003) Environmental factors and the outcome of rheumatoid arthritis. Best Pract Res Clin Rheumatol 17:717-727.

Tak PP, Bresnihan B (2000) The pathogenesis and prevention of joint damage in rheumatoid arthritis: advances from synovial biopsy and tissue analysis. Arthritis Rheum 43:2619-2633.

Thompson M, Bywaters EG (1962) Unilateral rheumatoid arthritis following hemiplegia. Ann Rheum Dis 21:370-377.

Tiscornia G, Singer O, Verma IM (2006) Production and purification of lentiviral vectors. Nat Protoc 1:241-245.

Tsuji F, Oki K, Senda T, Horiuchi M, Mita S (1999) Effects of mitogen-activated protein kinase inhibitors or phosphodiesterase inhibitors on interleukin-1-induced cytokines production in synovium-derived cells. Immunol Lett 68:275-279.

Tugwell P, Singh JA, Wells GA (2011) Biologicals for rheumatoid arthritis. Bmj 343:d4027.

Van den Haute C, Eggermont K, Nuttin B, Debyser Z, Baekelandt V (2003) Lentiviral vector-mediated delivery of short hairpin RNA results in persistent knockdown of gene expression in mouse brain. Hum Gene Ther 14:1799-1807.

Van Snick J (1990) Interleukin-6: an overview. Annu Rev Immunol 8:253-278.

von Banchet GS, Richter J, Huckel M, Rose C, Brauer R, Schaible HG (2007) Fibroblast-like synovial cells from normal and inflamed knee joints differently affect the expression of pain-related receptors in sensory neurones: a co-culture study. Arthritis Res Ther 9:R6.

Wallberg-Jonsson S, Ohman ML, Dahlqvist SR (1997) Cardiovascular morbidity and mortality in patients with seropositive rheumatoid arthritis in Northern Sweden. J Rheumatol 24:445-451.

Wang J, Zurawski TH, Bodeker MO, Meng J, Boddul S, Aoki KR, Dolly JO (2012) Longer-acting and highly potent chimaeric inhibitors of excessive exocytosis created with domains from botulinum neurotoxin A and B. Biochem J 444:59-67.

Wang J, Meng J, Lawrence GW, Zurawski TH, Sasse A, Bodeker MO, Gilmore MA, Fernandez-Salas E, Francis J, Steward LE, Aoki KR, Dolly JO (2008) Novel chimeras of botulinum neurotoxins A and E unveil contributions from the binding, translocation, and protease domains to their functional characteristics. J Biol Chem 283:16993-17002.

Weidler C, Holzer C, Harbuz M, Hofbauer R, Angele P, Scholmerich J, Straub RH (2005) Low density of sympathetic nerve fibres and increased density of brain derived neurotrophic factor positive cells in RA synovium. Ann Rheum Dis 64:13-20.

Welch MJ, Purkiss JR, Foster KA (2000) Sensitivity of embryonic rat dorsal root ganglia neurons to Clostridium botulinum neurotoxins. Toxicon 38:245-258.

Wong HY (1993) Neural mechanisms of joint pain. Ann Acad Med Singapore 22:646-650.

Woolf CJ (2010) What is this thing called pain? J Clin Invest 120:3742-3744.

Woolf CJ (2011) Central sensitization: implications for the diagnosis and treatment of pain. Pain 152:S2-15.

Woolley DE, Crossley MJ, Evanson JM (1977) Collagenase at sites of cartilage erosion in the rheumatoid joint. Arthritis Rheum 20:1231-1239.

Wu Y, Beddall MH, Marsh JW (2007) Rev-dependent lentiviral expression vector. Retrovirology 4:12.

Yamazaki T, Yokoyama T, Akatsu H, Tukiyama T, Tokiwa T (2003) Phenotypic characterization of a human synovial sarcoma cell line, SW982, and its response to dexamethasone. In Vitro Cell Dev Biol Anim 39:337-339.

Yeh FL, Zhu Y, Tepp WH, Johnson EA, Bertics PJ, Chapman ER (2011) Retargeted clostridial neurotoxins as novel agents for treating chronic diseases. Biochemistry 50:10419-10421.

Yeh FL, Dong M, Yao J, Tepp WH, Lin G, Johnson EA, Chapman ER (2010) SV2 mediates entry of tetanus neurotoxin into central neurons. PLoS Pathog 6:e1001207.

Yu H, Fischer G, Jia G, Reiser J, Park F, Hogan QH (2011) Lentiviral gene transfer into the dorsal root ganglion of adult rats. Mol Pain 7:63.

Appendix 1

Company	Country	Web
Abcam Ltd.	UK	www.abcam.com
Amersham GE Healthcare	UK	www.amersham.com
Biosciences	Ireland	www.biosciences.ie
Gibco	Ireland	www.biosciences.ie
Invitrogen	Ireland	www.biosciences.ie
Jackson ImmunoResearch Europe	UK	www.jacksonimmunoresearch.com
Harlan, UK	UK	www.harlan.com
MabTech AB	Sweden	www.mabtech.com
Millipore	Ireland	www.millipore.ie
Pierce (order through Medical Supply Company Ltd.)	Ireland	www.medical-supply.ie
Santacruz Biotech.	Ireland	www.scbt.ie
Sigma-Aldrich	Ireland	www.sigmaaldrich.com
Synaptic Systems	Germany	www.sysy.com
Trinity college, Dublin Bio-Resources Dept.	Ireland	www.tcd.ie/BioResources
SPI-BIO/Cayman chemical company	USA	www.caymanchem.com

Appendix 2

Buffers and Solutions

Phosphate buffered Saline (PBS): 10 mM $NaH_2PO_4.2H_2O$; 1.8 mM KH_2PO_4; 137 mM NaCl; 2.7 mM KCl

Tris buffered saline (TBS): 150 mM NaCl; 50 mM Tris-HCl pH 7.4

TBS/Tween: 50 mM Tris; 150 mM NaCl; 0.05% Tween-20

2x HBS for transfection: 50mM HEPES; 280mM NaCl; 1.5mM NaH_2PO_4

$CaCl_2$ for transfection: 0.25M $CaCl_2.2H2O$

MOPs running buffer: 250mM MOPs; 250mM Tris; 5mM EDTA; 0.1% SDS

Western transfer buffer: 25mM Tris-base; 190mM Glycine; 100ml Methanol; and 900ml H_2O

Lysis buffer: 20 mM HEPES- pH 7.4; 150 mM NaCl; 1mM $MgCl_2$; 1mM EGTA; 0.1% Triton X-100

BJ www.biochemj.org

This is a data-enriched, interactive PDF that provides the gateway to a world of information when opened in Utopia Documents.
Download FREE software now
utopia

BJ Cell

Longer-acting and highly potent chimaeric inhibitors of excessive exocytosis created with domains from botulinum neurotoxin A and B

Jiafu WANG*, Tomas H. ZURAWSKI*, MacDara O. BODEKER*, Jianghui MENG*, Sanjay BODDUL*, K. Roger AOKI† and J. Oliver DOLLY*[1]

*International Centre for Neurotherapeutics, Dublin City University, Glasnevin, Dublin 9, Ireland, and †Allergan, P.O. Box 19534, Irvine, CA 9262, U.S.A.

Various human neurogenic hyper-excitability disorders are successfully treated with type A or B BoNT (botulinum neurotoxin). The BoNT/A complex is widely used because of its longer-lasting benefits; also, autonomic side-effects are more often reported for BoNT/B. To establish if this distinct effect of BoNT/B could be exploited therapeutically, BoNT/A was modified so that it would bind the more abundant BoNT/B acceptor in rodents while retaining its desirable persistent action. The advantageous protease and translocation domain of BoNT/A were recombinantly combined with the acceptor-binding moiety of type B [H_C/B (C-terminal half of BoNT/B heavy chain)], creating the chimaera AB. This purified protein bound the BoNT/B acceptor, displayed enhanced capability relative to type A for intraneuronally delivering its protease, cleaved SNAP-25 (synaptosome-associated protein of 25 kDa) and induced a more prolonged neuromuscular paralysis than BoNT/A in mice. The BA chimaera, generated by substituting H_C/A (C-terminal half of BoNT/A heavy chain) into BoNT/B, exhibited an extremely high specific activity, delivered the BoNT/B protease via the BoNT/A acceptor into neurons, or fibroblast-like synoviocytes that lack SNAP-25, cleaving the requisite isoforms of VAMP (vesicle-associated membrane protein). Both chimaeras inhibited neurotransmission in murine bladder smooth muscle. BA has the unique ability to reduce exocytosis from non-neuronal cells expressing the BoNT/A-acceptor and utilising VAMP, but not SNAP-25, in exocytosis.

Key words: clostridial neurotoxins, drug design, duration of action, exocytosis, protein chimaeras, soluble N-ethylmaleimide-sensitive fusion protein-attachment protein receptor (SNARE).

INTRODUCTION

Hyper-excitability disorders of cholinergically innervated skeletal and smooth muscles are treatable with BoNTs (botulinum neurotoxins) [1]. There are seven serotypes of BoNT/(A–G), from *Clostridium botulinum*, consisting of a LC (light chain) protease which is linked to a HC (heavy chain) through a disulphide and non-covalent bonds. H_C (C-terminal half of HC) binds to its specific acceptors expressed on susceptible neurons, whereas H_N (N-terminal half of HC) forms a channel that allows the attached LC to translocate from 'endosomal-like' membrane vesicles into the cytosol. Thereafter, the LC cleaves intracellular SNAREs (soluble N-ethylmaleimide-sensitive fusion protein-attachment protein receptor) and negates their roles in neurotransmitter release (reviewed in [2,3]). BoNT/A binds SV2 (synaptic vesicle protein 2) isoforms [4,5] and removes nine amino acids from the C-terminus of SNAP-25 (synaptosome-associated protein of 25 kDa) resulting in a very prolonged neuroparalysis, one of the key features that underlies its widespread and effective treatment for various disorders of muscles (e.g. dystonias, dysphonias, spasticity, over-active bladder and certain gastrointestinal conditions) and glands (hyper-hydrosis and sialorrhea) due to their overly-active cholinergic nerves [1]. Syt (synaptotagmin) I and II plus gangliosides serve as acceptors for BoNT/B [6–8]. There is a higher content of Syts in rat synaptic vesicles than SV2 [9], and murine motor nerve endings possess a higher density of binding sites for BoNT/B than BoNT/A [10]. After internalization, VAMP (vesicle-associated membrane protein) is cleaved by BoNT/B

[11]; its complex with haemagglutinin is sometimes injected intramuscularly into patients not responding to BoNT/A, but much higher doses are required [12,13]. Neurologists have noticed that patients given BoNT/B tended to show autonomic side-effects (e.g. dry mouth, accommodation difficulties, dryness of eyes and reduced sweating) [14,15], an interesting finding in relation to SytI being mainly expressed in rat peripheral autonomic and sensory neurons rather than motor endplates [16]. Hence, it seemed warranted to evaluate if a novel therapeutic could be engineered that encompasses the most advantageous properties of BoNT/A (e.g. its long-lived LC protease [17]), the more abundant BoNT/B acceptors in rodents and the, apparently, more pronounced action of BoNT/B on autonomic cholinergic nerves innervating secretory glands. One strategy for such an attractive improvement entailed creating the chimaera AB by replacing the C-terminal acceptor binding domain of BoNT/A (H_C/A) with its counterpart H_C/B. In a complementary approach, the acceptor binding domain of BoNT/B was replaced with its counterpart from BoNT/A in order to establish if the resultant protein has new therapeutic potential by delivering its VAMP-cleaving protease into BoNT/B-insensitive cells.

In the present study, the chimaera AB was constructed by protein engineering to harness the LC/A protease, including the contiguous translocation domain (H_N) of BoNT/A together with the H_C of BoNT/B. For its counterpart, BA, H_C/A was combined with the VAMP-cleaving LC protease and H_N/B. Both chimaeras were readily expressed in *Escherichia coli* as SC (single chain) His_6-tagged proteins, completely purified and converted readily

Biochemical Journal

into their disulfide-linked DC (di-chain) forms by controlled proteolysis. AB was found to enter cultured neurons efficiently cleaving SNAP-25, and to block synaptic transmission in mouse phrenic nerve-muscle like BoNT/A. Most importantly, it produced a more extended neuromuscular paralysis than BoNT/A in mice. BA exhibited all the functional characteristics of BoNT/B, and with an exceptionally high specific neurotoxicity. An observed ability of BA to cleave VAMP in non-neuronal cells highlights its therapeutic potential for normalizing secretion from cells expressing the acceptor for BoNT/A (SV2), but not that for BoNT/B (SytI and II), and requiring VAMP for exocytosis.

EXPERIMENTAL

Materials

Suppliers of reagents for production of chimaeric proteins were listed previously [18]. Custom-made antibodies specific for LC/A, LC/B or BoNT/A were prepared by Zymed Laboratories; anti-BoNT/B IgG antibody was from Metabiologics. Natural purified BoNTs were purchased from List Laboratories (BoNT/A in the DC form) and Metabiologics (BoNT/B); the latter SC was proteolytically nicked to DC with TrypZean (8 μg/mg toxin for 40 min at 22°C). Mouse SytII cDNA clone was obtained from ImaGenes. Unless specified, all other reagents were from Sigma.

Animals

Female Tyler's Ordinary mice were purchased from Harlan UK and Sprague–Dawley rats were bred in an approved Bioresource Unit at Dublin City University. All experimental procedures involving animals were approved by the Institutional Ethics Committee and licensed by the Irish Government, Department of Health and Children.

Construction of BoNT AB and BA chimaeras

The cloning and expression of all BoNT variants were performed in accordance with European Union regulations, registered in Ireland with the Environmental Protection Agency and notified to the Health and Safety Authority. Codon-optimized genes encoding the SC of either BoNT/A or BoNT/B were synthesized and their sequences verified. Gene fragments encoding the LC plus the H_N of BoNT/A (LC.H_N/A) and that for the BoNT/B-binding domain (H_C/B) were produced by PCR and cloned into pET29a vector to generate the chimaera AB (Figure 1A, upper panel). Nucleotides encoding a 9-residue linker (ELGGGGSEL) were inserted between the H_N and H_C to improve protein folding. The chimaera BA (see Figure 1A, lower panel) was, likewise, generated by ligation of the corresponding genes generated by PCR for LC.H_N/B and H_C/A via a linker encoding two extra residues (DI) into pET29a to create an expression vector containing the BA insert. This construct, unlike AB, contains two thrombin-cleavage sites generated by PCR using suitable primers followed by self-ligation. One site is in the loop region to facilitate specific nicking, whereas extra nucleotides were also added to encode a thrombin consensus site for cleaving the C-terminal His$_6$ tag (Figure 1A, lower panel), a strategy successfully used before [19].

Expression and purification of the chimaeric neurotoxins

All of the DNA sequences were verified and each new SC gene was transformed into *E. coli* BL21.DE3 cells, expressed and the protein purified by IMAC (immobilized metal-affinity chromatography) as described previously [18]. The resultant AB chimaera was buffer exchanged into 50 mM Tris/HCl (pH 8.1)
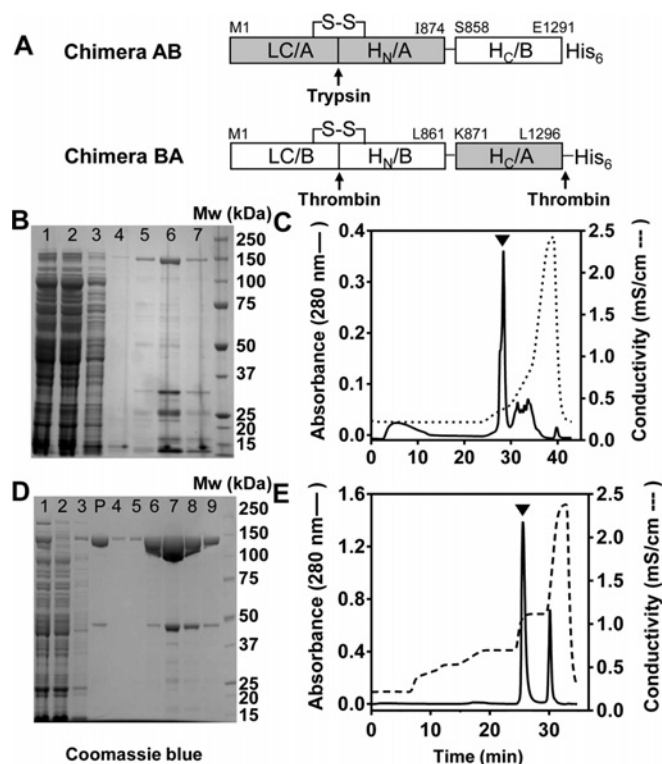
Figure 1   Arrangements of the functional domains in the BoNT chimaeras AB and BA, their expression and purification

(**A**) Chimaera AB was generated by ligating the relevant fragments of the BoNT/A gene (grey), encoding LC-H_N/A, to the Syt-binding domain (H_C) of BoNT/B (white) via a linker of nine inserted residues (ELGGGGSEL). For creating chimaera BA, the requisite domains were swapped as for AB; LC-H_N/B (white) was fused to SV2-binding subdomain (H_C) of BoNT/A (grey) via a linker encoding two extra residues (DI). Both constructs were tagged with His$_6$ to facilitate purification. Please note that the BoNT/A sequence used for AB includes a trypsin nicking site in the loop, whereas the BA construct has two thrombin cleavage sites inserted, one in a specially engineered nicking loop of BoNT/B and a second designed for tag removal. The numbers indicate amino acid positions in sequences of parental toxins (GenBank® accession numbers AF488749 and M81186). After expression in *E. coli* as SC proteins, AB (**B**) and BA (**D**) were purified by IMAC, followed by anion- or cation-exchange chromatography (**C** and **E**) and analysed by SDS/PAGE, under reducing conditions with protein staining. (**B** and **D**) Lane 1, cleared lysate; lane 2, flow-through from IMAC; lane 3, washes; and lanes 4–9, eluted fractions. Lane P in (**D**) shows the pooled eluates from IMAC. Molecular masses are shown on the right-hand side in kDa. (**C** and **E**) The eluted peak from ion-exchange chromatography of each is highlighted (▼). mS, milli-Siemens.

and further purified on a UNO Q1 column; after washing with 30 mM NaCl, elution was achieved with a stepwise gradient (up to 1 M NaCl in 50 mM Tris/HCl). Pooled fractions containing pure SC were either stored at −80°C or proteolytically nicked by TrypZean (1 μg/mg of toxin for 1 h at 22°C) before the addition of trypsin inhibitor (100 μg/mg of toxin) and storage (as for the SC). Material from the IMAC purification of chimaera BA was gel-filtered into 20 mM sodium phosphate buffer (pH 5.8) and further purified on a UNO S1 column, followed by washing with 100 mM NaCl and elution with a stepwise gradient (up to 1 M NaCl in the phosphate buffer). After buffer exchanging the eluted toxin into 20 mM Hepes and 145 mM NaCl (pH 7.8), purified SC toxin was either stored at −80°C or nicked by biotinylated thrombin (1 unit/mg for 1 h at 22°C) followed by removal of the thrombin by Streptavidin agarose, using the manufacturer's protocol before storage. The chimaeras were analysed by SDS/PAGE (4–12% precast Bis-Tris gel, Invitrogen) and Western blotting at each stage, as described previously [18]. Note that all assays were performed using their DC forms.

Protease activities of new BoNT variants

A model recombinant substrate for assay of SNAP-25 cleavage by BoNT/A and the chimaera AB was used as described previously [18,20]. For analysis of VAMP2 cleavage by BoNT/B and chimaera BA, DNA-encoding GFP (green fluorescent protein) was fused to nucleotides encoding rat VAMP2 (residues 2–94) and a His_6 tag. The GFP–VAMP2$_{(2-94)}$–His_6 fusion protein, expressed in *E. coli* and purified by IMAC, acted as substrate in the fluorescence assay following an established protocol [18,20].

In vitro acceptor-binding assay

GST (glutathione transferase)-tagged intra-luminal fragments of acceptors for BoNT/A [GST–rat SV2C$_{(454-579)}$] [21] and BoNT/B [GST–mouse SytII$_{(1-63)}$–His_6] were expressed/purified as described previously [18] and employed for measuring the binding characteristics of the two chimaeras. GST–SytII$_{(1-63)}$–His_6 was generated from the mouse *SytII* gene using PCR, cloned into the pET-41a vector (Novagen) and expressed in *E. coli* cells (BL21.DE3). The binding assay was performed as described previously [4,21]. Briefly, the proteins ($\sim 100\ \mu$g) were immobilized using 100 μl of slurry of glutathione Sepharose-4B Fast Flow resin (GE Healthcare) and incubated with 100 nM of each toxin in total volume of 100 μl of binding buffer [50 mM Tris/HCl, 150 mM NaCl and 0.5 % Triton X-100 (pH 7.6)]. Beads were then collected by centrifugation (500 $\boldsymbol{g}$ for 5 min at 4°C) and washed five times with >10 bed volumes of the same buffer for 15 min at 4°C. Bound proteins were eluted from the washed beads by adding SDS sample buffer. Less than 5 % of bound material was subjected to electrophoresis on 4–12 % precast Bis-Tris gels (Invitrogen). Toxins were detected by Western blotting with the antibodies indicated.

Cell-based SNARE cleavage assay

Preparation and maintenance of rat CGNs (cerebellar granule neurons) followed standard methods [17]. After 7 days *in vitro*, the cells were exposed for 24 h at 37°C to a series of toxin concentrations. Spinal neurons were prepared from mouse spinal cords removed at gestation day 13, as described previously [18]. Cultures were exposed to 400 pM of toxin in stimulation buffer [18] for the time indicated, washed twice with toxin-free medium and incubated for a further 20 h before harvesting. Fibroblast-like synoviocytes were prepared from the knee joint synovium of Sprague–Dawley rats (8–10-weeks-old), as reported previously [22,23]. After four passages, the cells were incubated at 37°C for 20 h with or without 100 nM toxin in the presence of 1 μM substance P in complete DMEM (Dulbecco's modified Eagle's medium) [22,23]. The cells were washed twice before harvesting, solubilization in SDS sample buffer and SDS/PAGE (12% precast Bis-Tris gel) followed by Western blotting; cleavage of endogenous SNAREs was quantified as described previously [17,24].

Neuromuscular paralytic activities and lethalities of BoNTs

Mouse phrenic-nerve hemi-diaphragms were set up as described previously [18]. The whole bladder was removed from freshly decapitated rats or mice, processed and stimulated, as established by others [25]. The times taken for each toxin, at a range of concentrations, to reach 50 % paralysis were recorded. For clarity, data for a single representative concentration have been plotted. Comparison of the recovery times from neuromuscular paralysis *in vivo* was based on the DAS (digit abduction score) assay [18,26]. For each BoNT, the TD$_{max.}$ (maximal tolerated dose)

was established [18]; ten mice per sample were injected with the doses summarized in the Figure legends. Toxins' lethalities were determined using a LD$_{50}$ assay after intraperitoneal injection into mice as described previously [27]. Groups of four mice were used for each concentration; specific neurotoxicities are expressed as the number of mLD$_{50}$ (mouse LD$_{50}$) units/mg of toxin.

## Statistical analysis and data presentation

Average data are presented with the S.E.M. and relevant sample size. All calculations and graphs were done using GraphPad Prism 4.0 and *P* values calculated as indicated in the Figure legends; $P < 0.05$ was considered statistically significant.

RESULTS

Inter-changing functional domains between BoNT/A and BoNT/B generated chimaera AB and BA with unaltered levels of the requisite protease activities

It was highly desirable to create a therapeutic encompassing the most advantageous features of the two clinically used serotypes, BoNT/A and BoNT/B. In the first instance, the long-acting LC/A protease and associated translocation moiety (H$_N$) was combined recombinantly with the binding domain of BoNT/B, H$_C$/B, which targets the relatively abundant acceptors, SytI and II in rodents (see the Introduction section). This chimaera AB (LC.H$_N$/A–H$_C$/B) was created by fusing portions of the genes encoding the protease and translocation domains of BoNT/A with the C-terminal acceptor-binding moiety of BoNT/B, on the basis of their crystal structures [28,29]. A linker of nine exogenous residues between the H$_N$/A and H$_C$/B domains was added to facilitate protein folding and functioning of these moieties (Figure 1A, upper panel). Generation of the counterpart chimaera was achieved in a similar manner. In this case, DNA encoding the LC.H$_N$ of BoNT/B was fused to the sequence for the H$_C$/A, creating a contiguous open reading frame for the BA chimaera (Figure 1A, lower panel). In the present study, the native loop of BoNT/B was partially substituted with a specific consensus sequence and a six-residue non-structured linker for efficient cleavage by thrombin. Both proteins were C-terminally tagged with His$_6$ for affinity purification; a C-terminal recognition site for thrombin was also introduced in chimaera BA to facilitate tag removal.

Both chimaeric toxins were successfully expressed in *E. coli* and purified from the lysed bacteria to ⩽80 % purity by IMAC via their His$_6$ tag. Following elution with imidazole, proteins of the expected size (~ 150 kDa) were detected by SDS/PAGE and Coomassie Blue staining, together with contaminants of lower molecular mass (Figures 1B and 1D). Nearly all impurities were removed by subsequent ion-exchange chromatography; chimaera AB was eluted from an anion-exchange column at ⩾70 mM NaCl (~ 1 mg of pure toxin per litre of culture) (Figure 1C), whereas BA could be readily purified using cation-exchange chromatography (Figure 1E), eluting at ⩾180 mM NaCl, with a typical yield of ~ 8 mg of pure toxin per litre of culture. SDS/PAGE analysis of peak fractions, followed by protein staining, revealed a single band of expected size for both chimaera AB (Figure 2A) and BA (Figure 2C) in the presence or absence of DTT (dithiothreitol). Controlled nicking of chimaera AB with TrypZean resulted in near-complete proteolysis of SC to a disulfide-linked DC (Figure 2A). Virtually all of chimaera BA was nicked with thrombin (Figure 2C). The appearance of HC and LC from both chimaeras in the presence of reducing agent not only confirms
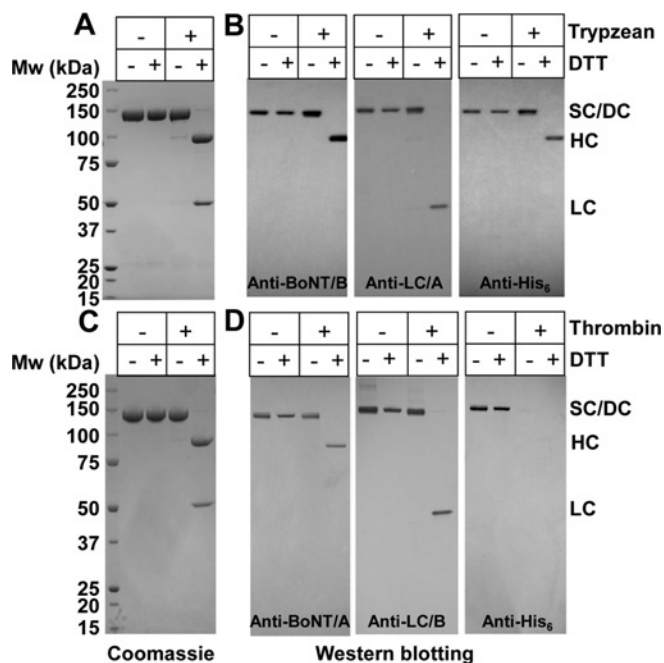
Figure 2   Activation of SC chimaeric BoNTs by specific proteolytic nicking

Pure SC chimaera AB (**A** and **B**) and BA (**C** and **D**) were efficiently converted to DC forms by incubation with TrypZean and thrombin respectively (see the Experimental section). Aliquots were analysed by SDS/PAGE in the absence and presence of DTT, followed by either protein staining (**A** and **C**) or Western blotting using the antibodies indicated (**B** and **D**). Arrows indicate the position of the SC, DC, HC and LC. Molecular masses are shown on the left-hand side in kDa.

efficient nicking, but also indicates that the inter-chain disulfide bond had been successfully formed in each (Figures 2A and 2C). Presence of the requisite functional domains in AB and BA was confirmed by Western blotting, using specific IgGs (Figures 2B and 2D). Unlike visualization of His$_6$ in the SC and DC of chimaera AB, and in the HC in the presence of DTT (Figure 2B), this signal could not be detected in BA after treatment with thrombin, confirming complete removal of the tag (Figure 2D).

It was necessary to verify that the H$_C$ substitution of BoNT/A and BoNT/B did not in any way hinder protease function, using an assay with two model synthetic substrates (see the Experimental section and [18]). Both chimaeras showed protease activities comparable with their parents (Table 1), demonstrating that these were not altered by the binding domains being swapped. Therefore, any differences between the performance of chimaeras and their parents could be ascribed to the translocation and/or acceptor-binding domain.

Chimaera AB specifically binds to a BoNT/B acceptor, SytII, whereas BA interacts with SV2C, the acceptor for BoNT/A

Previous studies established that the binding of BoNT/B to SytI and II leads to uptake into cells, whereas the entry of BoNT/A is mediated by SV2 (see the Introduction section). To ensure successful delivery of LC/B via the BoNT/A-binding domain and of LC/A via the acceptor for H$_C$/B, it was first necessary to ascertain if both chimaeras had acquired the ability to bind the acceptors dictated by their H$_C$ domains. Evaluating their binding in a pull-down assay utilized purified intra-luminal fragments of acceptors for BoNT/A [GST–rat SV2C$_{(454–579)}$] or BoNT/B [GST–mouse SytII$_{(1–63)}$–His$_6$]. SytII rather than I was chosen because the former has been confirmed to be present at the neuromuscular
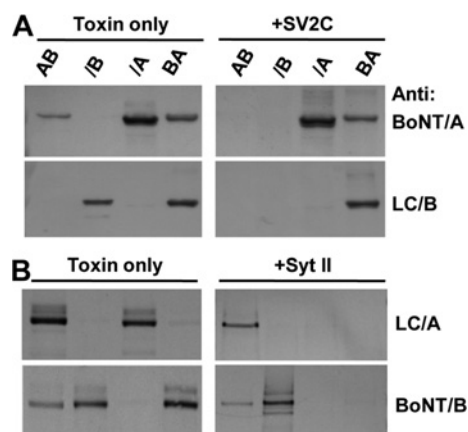
Figure 3   Exclusive interaction of chimaera AB with SytII and BA with SV2C *in vitro*

Binding assays were performed using GST-tagged recombinantly expressed and purified intraluminal fragments of acceptors for BoNT/A [GST–rat SV2C$_{(454–579)}$] and BoNT/B [GST–mouse SytII$_{(1–63)}$]. Each protein ($\sim$100 μg) was immobilized on to 100 μl of glutathione–Sepharose-4B matrix; the beads were incubated with 100 nM of toxin. After washing, bound proteins were eluted by SDS sample buffer under non-reducing conditions and subjected to electrophoresis. Toxins were detected with specific antibodies as indicated.

junction and does not require the presence of gangliosides for BoNT binding [6,8,30]. Binding to the protein acceptors was established by confirming the specificities of antibodies used for detecting the toxins (Figures 3A and 3B, left-hand panels). As expected, the BoNT/A acceptor pulled down only toxins containing H$_C$/A (BoNT/A and BA) (Figure 3A, right-hand panel). This interaction has to be attributed to the binding of H$_C$/A to SV2C as this is the only domain shared by these two toxins. The binding also appears to be specific as H$_C$/B-containing toxins (BoNT/B and AB) were not detected (Figure 3A, right-hand panel). In other experiments, where the toxins were pulled down using the BoNT/B acceptor, only BoNT/B and chimaera AB were found to bind to the SytII fragment (Figure 3B, right-hand panel). This reaffirms that acceptor binding can be mediated through the H$_C$/B in BoNT/B or chimaera AB. Neither chimaera nor parental BoNTs displayed any binding to GST–agarose (results not shown).

AB and BA cleave their requisite SNAREs, SNAP-25 and VAMP, in neurons and block transmission in both skeletal and smooth muscles

To assess the toxins' abilities to undergo the multiple steps of binding, translocation and cleavage of their respective substrates *in situ*, they were incubated with rat cultured CGNs for 24 h and cleavage of SNAP-25 and VAMP2 was monitored by immunoblotting. Chimaera AB and BoNT/A proved equipotent, with the ratio between intact and cleaved SNAP-25 being the same for both of these BoNT/A protease-containing toxins (Figure 4A). Immunoprobing of cell lysates for VAMP2 cleavage showed BA matched the activity of BoNT/B (Figure 4B). As the cause of death by BoNT is asphyxiation due to blockade of neurotransmission in the diaphragm, uptake of these toxins into the phrenic nerve was examined. Both chimaeras took similar times to paralyse mouse nerve hemi-diaphragms as their parental toxins (Figure 4C). Hence successful delivery of the respective LCs into motor neurons, via different acceptors, followed by translocation to the cytosol had occurred. The versatility of these chimaeras was assessed in the autonomic nervous system. BA and AB

Table 1 Proteolytic activities and mouse lethalities of DC chimaeras and parental toxins

Toxin	EC_{50} (nM) for cleavage of GFP–SNAP-25$_{(134-206)}$–His$_6$ or GFP–VAMP2$_{(2-94)}$-His$_6$*	mLD$_{50}$ units/mg‡
BoNT/A	0.57 ± 0.11 ($n = 5$)	3×10^8
Chimaera AB	0.53 ± 0.10 ($n = 3$)	0.3×10^8§
BoNT/B	2.72 ± 2.08 ($n = 5$)†	7×10^8
Chimaera BA	3.81 ± 2.18 ($n = 5$)†	6×10^8

*Proteolytic activities of chimaeric and parental DC toxins were determined using model substrates (13.5 μM GFP–SNAP-25$_{(134-206)}$–His$_6$ or 13.5 μM GFP–VAMP2$_{(2-94)}$–His$_6$). Values represent the amount of each toxin needed to cleave 50 % of substrate within 30 min at 37°C.

†There are no significant differences between BoNT/B and chimaera BA ($P > 0.05$ using unpaired Student's t test).

‡The lowest dose of toxin that killed 50 % of a group of four mice within 4 days after intraperitoneal injection was 1 mLD$_{50}$ unit.

§A similar value was obtained for AB devoid of the His$_6$ tag.
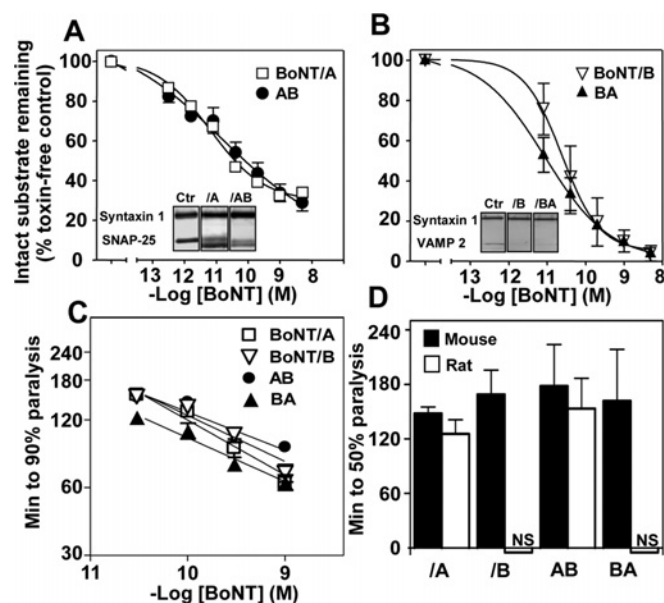
Figure 4 Both chimaeras potently and specifically cleave their requisite substrates in intact cultured neurons and block neuromuscular transmission *in vitro*

(**A** and **B**) Rat CGNs at 7 days *in vitro* were incubated with each toxin for 24 h in culture medium, washed and solubilized in SDS/PAGE, under non-reducing conditions, and Western blotting. The proportions of remaining intact SNAP-25 (**A**) or VAMP2 (**B**) were calculated relative to an internal uncleaved syntaxin control in the same lane, before calculating their intensities as the percentage of the signal observed in toxin-free control lanes. Insets: immunoblots demonstrating cleavage of SNAP-25 by 1 nM of BoNT/A or AB (**A**) and VAMP2 by 1 nM BoNT/B or BA (**B**). Both chimaeras blocked transmission in mouse phrenic-nerve hemi-diaphragm (**C**); times required for 90 % reduction of the starting tension were calculated. (**D**) Toxins (1 nM) were also added to stabilized electrically stimulated mouse or rat bladder strips and the times taken to reach 50 % reduction were determined after subtracting the decline due to fatigue. Results are means ± S.E.M., $n \geqslant 3$. Ctr, control; NS, not sensitive. In some cases symbols overlap, and some error bars are encompassed by the symbols.

displayed characteristics comparable with the parental toxins when tested on mouse bladder strips; 1 nM of each achieved 50 % paralysis within 3 h (Figure 4D). Contraction of bladder from rat was inhibited only by BoNT/A but not BoNT/B (Figure 4D), observations reflected by their chimaeras where only AB induced muscle paralysis. An insensitivity of rat bladder to BoNT/B or BA may be attributable to the known non-susceptibility of VAMP1 to cleavage [11]; this observation suggests an apparent preferential use of isoform 1 for neurotransmission in smooth muscle rather than an absence of the Syt acceptors (see the Discussion section).

Unique characteristics of BA offering potential for new therapeutic avenues

The neurotoxicity of chimaera BA, measured by intraperitoneal injection into mice, gave a very high value (6×10^8 mLD$_{50}$/mg), 20-fold greater than that for AB (Table 1). Such findings could indicate more optimal folding and/or interactive compatibility of the constituent domains of BA than is the case for AB, even though the latter contains a linker which does slightly improve the potency (results not shown). Special features of this new chimaera could allow additional unexplored applications in the treatment of diseases. Such prospects are exemplified by attempts to cleave the particular SNARE isoforms found in fibroblast-like synoviocytes, with the possibility of reducing their exocytosis of cytokines and, in that way, alleviating symptoms of arthritis [31,32]. These cells were found by Western blotting to contain VAMP3 and SNAP-23 (synaptosome-associated protein of 23 kDa) rather than SNAP-25 (Figures 5A and 5C); SNAP-23 is not cleaved by BoNT/A (Figure 5A). Despite VAMP3 being a substrate for BoNT/B, the latter failed to cleave this target in the synoviocytes (Figures 5A and 5B); encouragingly, 100 nM BA cleaved $\sim$60 % of VAMP3 in the presence of substance P (Figure 5A and 5B), a pain mediator whose level is known to be elevated under arthritic conditions [33]. These contrasting findings are explained by the demonstrated presence of the BoNT/A acceptor, SV2A, in these cells and an absence of SytI and II, in contrast with their occurrence in CGNs (Figure 5C). This example highlights the utility of BA which could be applicable to other non-neuronal cells lacking SNAP-25, but possessing the SV2, the BoNT/A acceptor, and utilising VAMP(1–3) in exocytosis.

AB enhanced the delivery of LC into spinal cord neurons and induced longer neuromuscular paralysis than BoNT/A *in vivo*

It was hypothesized that the expression of a higher content of Syt I/II than SV2 in rat synaptic vesicles [9], and a higher density of binding sites for BoNT/B than BoNT/A in murine motor nerve endings [10], would allow more uptake of AB than BoNT/A which, in turn, might culminate in an extension of the duration of action. Mouse spinal cord neurons were used initially for addressing this possibility. These cultured neurons were briefly bathed in stimulation buffer containing 400 pM toxin for selected periods, followed by extensive washing; subsequent incubation for 20 h allowed extrapolation of the amounts of toxin bound from the extents of SNARE cleavage. Under this paradigm, there seemed to be less binding of BoNT/A than BoNT/B over short times as reflected in a minor fraction of SNAP-25 being cleaved (Figure 6A), compared with the extent of VAMP2 disappearance due to BoNT/B (Figure 6B). There was only enough of BoNT/A bound to the acceptor in 5 min to truncate $\sim$10 % of SNAP-25
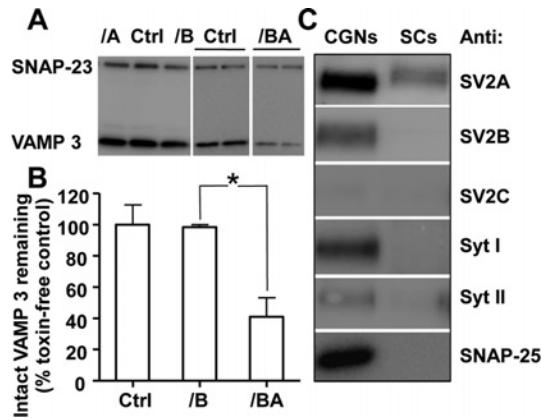
Figure 5   Chimaera BA enters rat cultured synoviocytes and cleaves VAMP 3, unlike BoNT/B which fails to cleave its substrate

Synovial cells (SCs) were incubated at 37°C for 20 h with or without 100 nM of each toxin in the presence of 1 μM substance P in culture medium. Cells were washed and harvested in SDS sample buffer. Solubilized proteins were subjected to SDS/PAGE and Western blotting using the antibodies indicated. (**A**) Representative blots indicating that chimaera BA cleaved VAMP3 (duplicate lanes) unlike BoNT/B; as expected, SNAP-23 was not cleaved by BoNT/A. (**B**) The proportions of VAMP 3 remaining intact after treatment with 100 nM of either chimaera BA or BoNT/B were calculated ($\pm$ S.E.M., $n = 3$) relative to the uncleaved SNAP-23, internal standard. * $P < 0.05$, BoNT/B compared with BA using unpaired Student's t test. (**C**) Immunoblots from non-toxin treated samples demonstrating the presence of SV2A in synovial cells and the absence of SV2B, SV2C, SytI, SytII and SNAP-25. Cell lysates from rat cultured CGNs were used as neuronal controls. Ctrl, control.

after incubation for 20 h (Figure 6A), whereas BoNT/B caused cleavage of over 80% of VAMP2 (Figure 6B). AB cleaved significantly more SNAP-25 than BoNT/A (Figure 6A), even though it possesses the same protease, more closely reflecting the binding time course of BoNT/B. As the AB chimaera shares the same protease and H_N regions as its BoNT/A parent, it is reasonable to deduce that these differences are attributable to acceptor H_C-mediated binding. This deduction was reinforced by comparing BA with BoNT/A. Even though BA contains the VAMP2-cleaving LC/B, shown to cause significant cleavage when part of BoNT/B (Figure 6B), the protease activity of this chimaera deduced from this assay was significantly retarded, registering ~10% cleavage after 5 min of binding compared with BoNT/B, which cleaved ~80% of VAMP2 (Figure 6B). Again, their near-identical protease activities towards recombinant VAMP2 substrate (Table 1) rule out any of these differences being derived from LC.

The above-noted enhanced acceptor-binding capabilities of AB compared with BoNT/A in spinal cord neurons might alter the persistence of its neuromuscular paralysis *in vivo*. Therefore, this was measured using the DAS assay in mice (Figure 6C). The $TD_{max.}$ of each toxin was established empirically (Figure 6C, inset) to avoid any local and systemic side-effects [18]. As found previously [18], full muscle paralysis (DAS = 4) was observed in mice injected with $TD_{max.}$ of BoNT/A, lasting up to 28 days (when DAS = 0). The amount of BoNT/B that could be injected without inducing systemic effects was limited by its high LD_{50} value and when the smaller permitted amount of BoNT/B (1.5 units/~2 pg) was injected intramuscularly, near-complete paralysis ensued within 2 days and full recovery occurred by day 14 (Figure 6C). Chimaera BA containing LC/B proved to be highly effective in inducing muscle weakening; again the limiting dose (1.5 units/~2 pg) injected caused paralysis followed by recovery within ~10 days. On the other hand, the neuromuscular paralysis induced by chimaera AB (6 units/200 pg) outlasted that
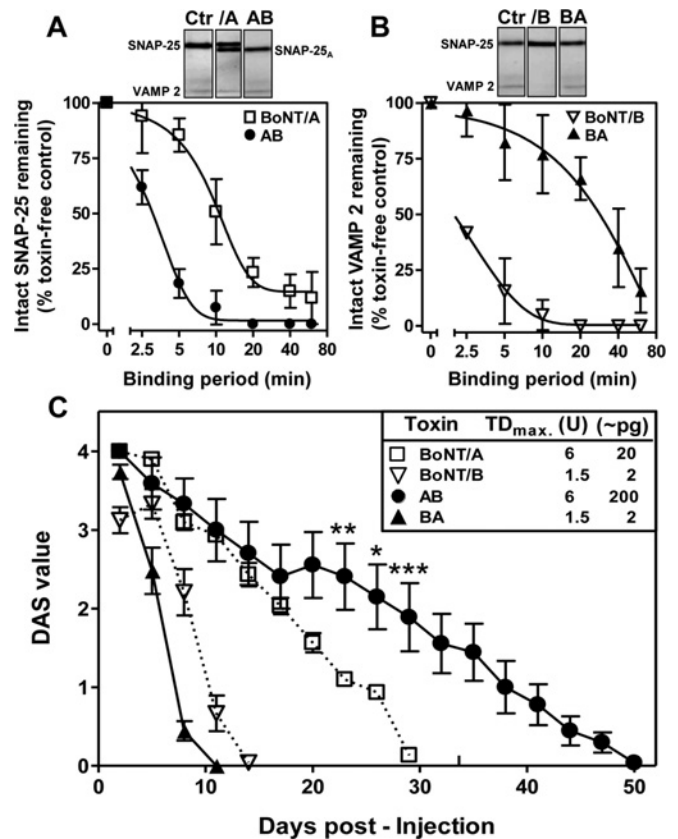
Figure 6   Cleavage of SNAREs by the chimaeras in spinal cord neurons approximates to that of the parental toxins providing their H_C: AB induces the longest neuroparalysis *in vivo*

To assess the binding capabilities of chimaeric toxins and the parents, mouse spinal cord neurons were briefly bathed in stimulation buffer containing 400 pM of each. After the times indicated, cells were washed, medium was replaced and cells were cultured for a further 20 h before assaying for cleavage of SNAP-25 (**A**) or VAMP 2 (**B**) as before. The remaining intact substrate was calculated relative to an internal syntaxin control. The upper panels of (**A**) and (**B**) are representative blots of samples exposed to the toxins for 10 min. (**C**) Duration of paralytic action *in vivo* was monitored after injecting toxin (5 μl) unilaterally into mouse gastrocnemius muscle by determining the level of paralysis using the DAS scale (0 = normal; 4 = maximal reduction in digit abduction). Inset, the dose of each toxin determined for inducing a total loss of toe spread reflex without causing systemic effects [$TD_{max.}$ as units (mLD$_{50}$ intraperitoneal units) and protein quantity used]. Motor impairment was limited to the toxin-treated limb. AB was compared with BoNT/A using a two-way ANOVA followed by post-hoc Bonferroni test for comparison of individual time points where these two could be compared (*$P < 0.05$, **$P < 0.01$, ***$P < 0.001$). Note that a few symbols overlap, and some error bars are encompassed by the symbols. Results are means $\pm$ S.E.M., $n = 10$. Ctr, control.

of the other toxins tested in rodents, exceeding the previously published record set by the clinically used type A complex [34]. This result seems to support the hypothesis that the more efficient binding of AB, apparently facilitated by a greater abundance of SytI/II acceptors, lengthens the duration of neuromuscular paralysis (up to 50 days) in this test system.

These collective findings demonstrate clearly that BoNT chimaeras can be constructed through recombination of functional domains from different serotypes and, also, highlight how these can be expressed efficiently, simply purified to homogeneity, and readily converted into active DC forms. Both proteins retained functional characteristics of their parents; most importantly, AB displays a persistent BoNT/A-like property, but of even longer duration, in mice, whereas BA has the potential to substitute for BoNT/B because of its high specific neurotoxicity and demonstrated ability to deliver LC/B into cells insensitive to BoNT/B, but susceptible to VAMP cleavage.

DISCUSSION

Engineered BoNTs with potential as improved and more versatile inhibitors of exocytosis

Development of novel forms of BoNTs with extended duration of paralytic activity and wider applications is very desirable for treating human neurogenic hyper-activity disorders. For the first time, it is shown in the present study that the duration of BoNT/A can be extended substantially in a murine model by replacing the acceptor-binding domain with its counterpart from BoNT/B, resulting in the chimaera AB. Due to utilizing a different acceptor to initiate entry, it could provide an additional and/or improved form active on certain neuron types. On the other hand, BA, which harnesses the binding domain of BoNT/A, can enter neurons, block neuromuscular transmission and has an extremely high potency, giving a similar duration of neuroparalysis as BoNT/B. Its ability to target an alternative SNARE in BoNT/A-sensitive neurons, or other cells, creates the exciting potential for being an innovative therapeutic applicable to cells whose exocytosis involves VAMP, but not SNAP-25 (see below).

Chimaera AB causes the most persistent neuromuscular weakening in a mouse model

Proof of principle was obtained for generating a longer-lasting chimaeric neurotoxin by selectively combining the most advantageous domains of two BoNTs, based on an understanding of their multi-step mechanisms of action. As BoNT/A causes the most prolonged muscle weakness in human therapy, LC/A was selected for this purpose, as the life-times of LCs determine durations of action [17,18,35,36]. Murine motor endplates possess more acceptors for ^{125}I-labelled BoNT/B than BoNT/A [10], consistent with findings from a proteomic demonstration that more copies of Syt than SV2 are present on small synaptic clear vesicles from rat brain [9]. Additionally, evidence from rat cultured neurons suggests that SytI and II can accumulate at the cell surface, forming a stockpile of acceptor available for binding H_C/B, which is not the case for SV2C, whose distribution is skewed towards the synaptic vesicle rather than the cell surface [37,38]. Recently, *in-vitro*-translated ^{35}S-labelled H_C/B was reported to have a higher affinity for rat brain synaptosomes than H_C/A, although the sensitivity of motor nerve endings was not measured [39]. Transfer of BoNT/B acceptor-binding domain to BoNT/A could, it was speculated, allow delivery of more BoNT/A protease to the rodent nerve terminals and, thereby, cause an extended duration of its action. Moreover, as BoNT/B appears to show a more pronounced action on autonomic cholinergic nerves in human secretory glands (see the Introduction section), transfer of this feature to BoNT/A could increase its scope for targeting the BoNT/A long-lived protease to certain nerve types. For these purposes, the engineered AB, expressed in *E. coli* as a SC and purified to homogeneity, followed by activation by controlled proteolysis, was shown to retain characteristics of the respective functional domains from BoNT/A and BoNT/B, i.e. binding the luminal portion of murine SytII, entering into neurons, cleaving SNAP-25 and blocking nerve–muscle transmission.

Experiments on time-dependency of acceptor binding to murine spinal neurons indicated that AB does, indeed, deliver its LC more efficiently than BoNT/A into the cytosol, as reflected by a greater extent of SNAP-25 cleavage at each time tested. This difference may underlie the notably prolonged neuroparalysis resulting from AB, which even exceeds that of BoNT/A. Such an extended action of AB seems to be due to binding to distinct acceptors via its modified H_C domain. Notably, chimaera AB is equipotent to native BoNT/A in blocking neurotransmission in mouse hemi-

diaphragm *in vitro*, but it exhibits much lower specific toxicity in a mouse lethality assay. This could be due to fact that the *in vitro* assay only reflects the speed of onset of neuroparalysis, rather than true potency. Therefore, the recent report of a 4-fold greater potency on the diaphragm for the SC of chimaera AB compared with SC BoNT/A [39], may not necessarily translate into a higher specific lethality *in vivo*; no comparative biological data for BoNT/A were provided [39]. Nevertheless, ~ 1.7-fold increase in the duration of muscle weakness in mice observed for AB relative to BoNT/A could further extend the therapeutic action in patients as the time courses observed in mice are known to be far longer in humans. Although ethical issues pose difficulties, it will be necessary eventually to evaluate AB in humans, especially as human SytII was recently excluded as a high-affinity acceptor for BoNT/B due to a single amino acid difference in the interaction site compared with the rodent protein [40], which leaves Syt I as the protein constituent of the acceptor for mediating entry of the toxin into motor endings in humans. This and the lower specific neurotoxicity of AB compared with BoNT/A may require injection of a higher protein dose, which could increase the possibility of triggering the production of neutralising antibodies. It may be possible to overcome the latter by protein engineering an improved version of the toxin via site-directed mutagenesis in its binding site for human SytII, thereby raising the affinity for the acceptor, as suggested previously [40]. The duration of action of AB on autonomic neurons should also be evaluated, as the autonomic side-effects reported for BoNT/B could be due to the higher abundance of SytI in autonomic neurons as shown in rodents [16] or by the higher amounts injected.

BA offers scope for attenuating secretion from a variety of cell types (e.g. fibroblast-like synoviocytes) via two sites of action

Notably, both BA and BoNT/B gave a much shorter duration of neuromuscular paralysis than BoNT/A, further confirming that the protease life-time determines the normal duration of action, as reported previously [17,18,35,36]. Nevertheless, BA proved as effective as BoNT/B in cleaving VAMP in cultured neurons and inhibiting neuromuscular transmission; of special note is its extremely high specific neurotoxicity. These attractive features highlight that BA was properly folded in *E. coli*, forming all of the fully functional multiple domains. As BA targets LC/B to BoNT/A-susceptible neurons by binding to SV2 rather than Syt in humans, it has the potential to be applied as an alternative to BoNT/B, but with much lower doses required. Moreover, because BA targets VAMP, it could complement BoNT/A-based neurotherapy. The further utility of BA has been highlighted with synoviocytes, that express BoNT/A-acceptor SV2A but not SytI or II (making them inaccessible to BoNT/B), in which cleavage of VAMP3 occurred following stimulation by substance P, a pain mediator in the development of arthritis [33]. BoNT/A also can reduce arthritis-associated pain in humans, an effect most probably mediated through direct inhibition of peripheral nociceptive nerve activation and thereby prevents sensitization [41]. Our collective observations suggest that BA could offer an advantage of counteracting the symptoms of arthritis at two points: directly upstream at the neuronal component like BoNT/A and, indirectly, in synoviocytes.

Involvement of VAMP 1 isoform in exocytosis from autonomic nerves revealed by BoNT chimaeras

The therapeutic effectiveness of BoNT/A in autonomic cholinergic diseases (reviewed in [42]) prompted evaluation of

the performance of these chimaeras in the bladder. Although neuroparalysis observed in mouse bladder confirmed their functionality, reminiscent of that of their parents, experiments on rat bladder implicated VAMP1 in neurotransmission. The observation that BoNT/B had no effect on rat bladder suggested that there might be a BoNT/B-insensitive VAMP 1 [11] mediating transmitter release or a lack of the acceptor for BoNT/B. The latter notion was excluded because chimaera AB blocked the transmission like BoNT/A, establishing the presence of the Syt I/II acceptor, as it successfully delivered the LC/A protease culminating in paralysis. Likewise, the inability of BA to block transmission in the rat bladder reaffirmed the notion that insensitivity to BoNT/B in rat is due to the resistant VAMP1 mediating transmitter release, as demonstrated for sensory neurons [24] and motor endplates [43].

AUTHOR CONTRIBUTION

Jiafu Wang designed and manufactured the AB and BA chimaeras. Jiafu Wang, Tomas Zurawski, MacDara Bodeker, Jianghui Meng and Sanjay Boddul performed experimental procedures. Jiafu Wang, Tomas Zurawski and MacDara Bodeker prepared the paper; Roger Aoki and Oliver Dolly edited the paper prior to submission.

FUNDING

REFERENCES

1 Ward, A. B. and Barnes, M. P. (2007) Clinical Uses of Botulinum Toxins. Cambridge University Press, Cambridge

2 Dolly, J. O., Wang, J., Zurawski, T. H. and Meng, J. (2011) Novel therapeutics based on recombinant botulinum neurotoxins to normalize the release of transmitters and pain mediators. FEBS J. **278**, 4454–4466

3 Dolly, J. O., Lawrence, G. W., Meng, J., Wang, J. and Ovsepian, S. V. (2009) Neuro-exocytosis: botulinum toxins as inhibitory probes and versatile therapeutics. Curr. Opin. Pharmacol. **9**, 326–335

4 Dong, M., Yeh, F., Tepp, W. H., Dean, C., Johnson, E. A., Janz, R. and Chapman, E. R. (2006) SV2 is the protein receptor for botulinum neurotoxin A. Science **312**, 592–596

5 Mahrhold, S., Rummel, A., Bigalke, H., Davletov, B. and Binz, T. (2006) The synaptic vesicle protein 2C mediates the uptake of botulinum neurotoxin A into phrenic nerves. FEBS Lett. **580**, 2011–2014

6 Nishiki, T., Tokuyama, Y., Kamata, Y., Nemoto, Y., Yoshida, A., Sato, K., Sekiguchi, M., Takahashi, M. and Kozaki, S. (1996) The high-affinity binding of Clostridium botulinum type B neurotoxin to synaptotagmin II associated with gangliosides G_{T1b}/G_{D1a}. FEBS Lett. **378**, 253–257

7 Nishiki, T., Kamata, Y., Nemoto, Y., Omori, A., Ito, T., Takahashi, M. and Kozaki, S. (1994) Identification of protein receptor for Clostridium botulinum type B neurotoxin in rat brain synaptosomes. J. Biol. Chem. **269**, 10498–10503

8 Dong, M., Richards, D. A., Goodnough, M. C., Tepp, W. H., Johnson, E. A. and Chapman, E. R. (2003) Synaptotagmins I and II mediate entry of botulinum neurotoxin B into cells. J. Cell Biol. **162**, 1293–1303

9 Takamori, S., Holt, M., Stenius, K., Lemke, E. A., Gronborg, M., Riedel, D., Urlaub, H., Schenck, S., Brugger, B., Ringler, B. et al. (2006) Molecular anatomy of a trafficking organelle. Cell **127**, 831–846

10 Black, J. D. and Dolly, J. O. (1986) Interaction of 125I-labeled botulinum neurotoxins with nerve terminals. I. Ultrastructural autoradiographic localization and quantitation of distinct membrane acceptors for types A and B on motor nerves. J. Cell Biol. **103**, 521–534

11 Schiavo, G., Benfenati, F., Poulain, B., Rossetto, O., Polverino de Laureto, P., DasGupta, B. R. and Montecucco, C. (1992) Tetanus and botulinum-B neurotoxins block neurotransmitter release by proteolytic cleavage of synaptobrevin. Nature **359**, 832–835

12 Kranz, G., Paul, A., Voller, B., Posch, M., Windischberger, C., Auff, E. and Sycha, T. (2011) Long-term efficacy and respective potencies of botulinum toxin A and B: a randomized, double-blind study. Br. J. Dermatol. **164**, 176–181

13 Sloop, R. R., Cole, B. A. and Escutin, R. O. (1997) Human response to botulinum toxin injection: type B compared with type A. Neurology **49**, 189–194

14 Dressler, D. and Benecke, R. (2004) Autonomic side effects of botulinum toxin type B therapy. Adv. Neurol. **94**, 315–320

15 Lew, M. F., Adornato, B. T., Duane, D. D., Dykstra, D. D., Factor, S. A., Massey, J. M., Brin, M. F., Jankovic, J., Rodnitzky, R. L., Singer, C. et al. (1997) Botulinum toxin type B: a double-blind, placebo-controlled, safety and efficacy study in cervical dystonia. Neurology **49**, 701–707

16 Li, J. Y., Jahn, R. and Dahlstrom, A. (1994) Synaptotagmin I is present mainly in autonomic and sensory neurons of the rat peripheral nervous system. Neuroscience **63**, 837–850

17 Foran, P. G., Mohammed, N., Lisk, G. O., Nagwaney, S., Lawrence, G. W., Johnson, E., Smith, L., Aoki, K. R. and Dolly, J. O. (2003) Evaluation of the therapeutic usefulness of botulinum neurotoxin B, C1, E, and F compared with the long lasting type A. Basis for distinct durations of inhibition of exocytosis in central neurons. J. Biol. Chem. **278**, 1363–1371

18 Wang, J., Meng, J., Lawrence, G. W., Zurawski, T. H., Sasse, A., Bodeker, M. O., Gilmore, M. A., Fernandez-Salas, E., Francis, J., Steward, L. E. et al. (2008) Novel chimeras of botulinum neurotoxins A and E unveil contributions from the binding, translocation, and protease domains to their functional characteristics. J. Biol. Chem. **283**, 16993–17002

19 Wang, J., Zurawski, T. H., Meng, J., Lawrence, G., Olango, W. M., Finn, D. P., Wheeler, L. and Dolly, J. O. (2011) A dileucine in the protease of botulinum toxin A underlies its long-lived neuroparalysis: transfer of longevity to a novel potential therapeutic. J. Biol. Chem. **286**, 6375–6385

20 Williams, D., Steward, L. E., Gilmore, M. A., Okawa, Y., Webber, J. A. and Aoki, K.-R. (2006) GFP–SNAP25 fluorescence release assay of BoNT proteolytic activity. Neurotox. Res. **9**, 239

21 Meng, J., Ovsepian, S. V., Wang, J., Pickering, M., Sasse, A., Aoki, K. R., Lawrence, G. W. and Dolly, J. O. (2009) Activation of TRPV1 mediates calcitonin gene-related peptide release, which excites trigeminal sensory neurons and is attenuated by a retargeted botulinum toxin with anti-nociceptive potential. J. Neurosci. **29**, 4981–4992

22 Hyc, A., Osiecka-Iwan, A., Dziunycz, P. and Moskalewski, S. (2007) Preparation of rat synovial membrane for studies of cytokine secretion. Folia Histochem. Cytobiol. **45**, 57–60

23 Ozturk, A. M., Yam, A., Chin, S. I., Heong, T. S., Helvacioglu, F. and Tan, A. (2008) Synovial cell culture and tissue engineering of a tendon synovial cell biomembrane. J. Biomed. Mater. Res. A. **84**, 1120–1126

24 Meng, J., Wang, J., Lawrence, G. and Dolly, J. O. (2007) Synaptobrevin I mediates exocytosis of CGRP from sensory neurons and inhibition by botulinum toxins reflects their anti-nociceptive potential. J. Cell Sci. **120**, 2864–2874

25 Quinn, T., Collins, C. and Baird, A. W. (2004) Mechanisms of neurokinin A- and substance P-induced contractions in rat detrusor smooth muscle in vitro. BJU Int. **94**, 651–657

26 Aoki, K. R. (2001) A comparison of the safety margins of botulinum neurotoxin serotypes A, B, and F in mice. Toxicon **39**, 1815–1820

27 Maisey, E. A., Wadsworth, J. D., Poulain, B., Shone, C. C., Melling, J., Gibbs, P., Tauc, L. and Dolly, J. O. (1988) Involvement of the constituent chains of botulinum neurotoxins A and B in the blockade of neurotransmitter release. Eur. J. Biochem. **177**, 683–691

28 Lacy, D. B., Tepp, W., Cohen, A. C., DasGupta, B. R. and Stevens, R. C. (1998) Crystal structure of botulinum neurotoxin type A and implications for toxicity. Nat. Struct. Biol. **5**, 898–902

29 Swaminathan, S. and Eswaramoorthy, S. (2000) Structural analysis of the catalytic and binding sites of Clostridium botulinum neurotoxin B. Nat. Struct. Biol. **7**, 693–699

30 Jin, R., Rummel, A., Binz, T. and Brunger, A. T. (2006) Botulinum neurotoxin B recognizes its protein receptor with high affinity and specificity. Nature **444**, 1092–1095

31 Stow, J. L., Manderson, A. P. and Murray, R. Z. (2006) SNAREing immunity: the role of SNAREs in the immune system. Nat. Rev. Immunol. **6**, 919–929

32 Noss, E. H. and Brenner, M. B. (2008) The role and therapeutic implications of fibroblast-like synoviocytes in inflammation and cartilage erosion in rheumatoid arthritis. Immunol. Rev. **223**, 252–270

33 Lotz, M., Carson, D. A. and Vaughan, J. H. (1987) Substance P activation of rheumatoid synoviocytes: neural pathway in pathogenesis of arthritis. Science **235**, 893–895

34 Aoki, K. R. (2002) Botulinum neurotoxin serotypes A and B preparations have different safety margins in preclinical models of muscle weakening efficacy and systemic safety. Toxicon **40**, 923–928

35 Adler, M., Keller, J. E., Sheridan, R. E. and Deshpande, S. S. (2001) Persistence of botulinum neurotoxin A demonstrated by sequential administration of serotypes A and E in rat EDL muscle. Toxicon **39**, 233–243

36 Keller, J. E., Neale, E. A., Oyler, G. and Adler, M. (1999) Persistence of botulinum neurotoxin action in cultured spinal cord cells. FEBS Lett. **456**, 137–142

37 Taubenblatt, P., Dedieu, J. C., Gulik-Krzywicki, T. and Morel, N. (1999) VAMP (synaptobrevin) is present in the plasma membrane of nerve terminals. J. Cell Sci. **112**, 3559–3567

38 Fernandez-Alfonso, T., Kwan, R. and Ryan, T. A. (2006) Synaptic vesicles interchange their membrane proteins with a large surface reservoir during recycling. Neuron **51**, 179–186

39 Rummel, A., Mahrhold, S., Bigalke, H. and Binz, T. (2011) Exchange of the H_{CC} domain mediating double receptor recognition improves the pharmacodynamic properties of botulinum neurotoxin. FEBS J. **278**, 4506–4515

40 Strotmeier, J., Willjes, G., Binz, T. and Rummel, A. (2012) Human synaptotagmin-II is not a high affinity receptor for botulinum neurotoxin B and G: increased therapeutic dosage and immunogenicity. FEBS Lett. **586**, 310–313

41 Mahowald, M. L., Krug, H. E., Singh, J. A. and Dykstra, D. (2009) Intra-articular botulinum toxin type A: a new approach to treat arthritis joint pain. Toxicon **54**, 658–667

42 Brisinda, G., Caddedu, F. and Maria, G. (2007) Bladder and bowel indications. In Clinicial Uses of Botulinum Toxins (Ward, A. B. and Barnes, M. P., eds), pp. 282–327, Cambridge University Press, Cambridge

43 Liu, Y., Sugiura, Y. and Lin, W. (2011) The role of synaptobrevin1/VAMP1 in Ca^{2+}-triggered neurotransmitter release at the mouse neuromuscular junction. J. Physiol. **589**, 1603–1618

SNAP-23 and VAMP-3 contribute to the release of IL-6 and TNFα from a human synovial sarcoma cell line

Sanjay V. Boddul, Jianghui Meng, James Oliver Dolly and Jiafu Wang

International Centre for Neurotherapeutics, Dublin City University, Ireland

Fibroblast-like synoviocytes are important mediators of inflammatory joint damage in arthritis through the release of cytokines, but it is unknown whether their exocytosis from these particular cells is SNARE-dependent. Here, the complement of soluble N-ethylmaleimide-sensitive factor attachment protein receptors (SNAREs) in human synovial sarcoma cells (SW982) was examined with respect to the secretion of interleukin-6 (IL-6) and tumour necrosis factor α (TNFα), before and after knockdown of a synaptosome-associated protein of molecular mass 23 kDa (SNAP-23) or the vesicle-associated membrane protein 3 (VAMP-3). Wild-type SW982 cells expressed SNAP-23, VAMP-3, syntaxin isoforms 2–4 and synaptic vesicle protein 2C (SV2C). These cells showed Ca^{2+}-dependent secretion of IL-6 and TNFα when stimulated by interleukin-1β (IL-1β) or in combination with K^+ depolarization. Specific knockdown of SNAP-23 or VAMP-3 decreased the exocytosis of IL-6 and TNFα; the reduced expression of SNAP-23 caused accumulation of SV2 in the peri-nuclear area. A monoclonal antibody specific for VAMP-3 precipitated SNAP-23 and syntaxin-2 (and syntaxin-3 to a lesser extent). The formation of SDS-resistant complexes by SNAP-23 and VAMP-3 was reduced upon knockdown of SNAP-23. Although the syntaxin isoforms 2, 3 and 4 are expressed in SW982 cells, knockdown of each did not affect the release of cytokines. Collectively, these results show that SNAP-23 and VAMP-3 participate in IL-1β-induced Ca^{2+}-dependent release of IL-6 and TNFα from SW982 cells.

Structured digital abstract

- VAMP-3 physically interacts with syntaxin 2 and SNAP-23 by anti-bait coimmunoprecipitation (View interaction)

Introduction

Arthritic pain is a common and widespread condition that severely affects the functional performance of sufferers, resulting in a poor quality of life [1]. Joint pain may result from many types of injuries or abnormalities, the most frequent being rheumatoid and osteoarthritis [2,3]. Approximately 1% of humans have rheumatoid arthritis, an inflammatory autoimmune disease of the joints. It mainly affects the synovium, cartilage and sub-chondral bone, but also has systemic effects, leading to increased co-morbidity and mortality, particularly due to cardiovascular disease [4,5]. Osteoarthritis occurs in 10% of the

population, and is caused by an imbalance in cartilage metabolism, i.e. levels of synthesis versus destruction, which leads to a progressive loss of the tissue; additionally, inflammation of the synovium and damage to the sub-chondral bone may occur. Many mediators are involved in both rheumatoid arthritis and osteoarthritis, including cytokines, growth factors, matrix metalloproteinases and chondro-degradative enzymes [6]. Macrophages and fibroblast-like synovial cells represent the predominant cell types in the inflamed synovium [7], being largely responsible for joint destruction via attachment to the cartilage and secretion of cytokines and matrix metalloproteinases [7,8]; osteoclasts also participate in the breakdown of cartilage [9,10].

Secreted cytokines and chemokines profoundly alter bodily responses to cellular damage or invasive pathogens. Pro-inflammatory cytokines such as tumour necrosis factor α (TNFα) and interleukin-1β (IL-1β), interleukin-6 (IL-6) and interleukin-15, among others, are involved in the pathogenesis and inflammatory processes in rheumatoid arthritis and osteoarthritis. Synoviocytes contribute to joint inflammation by producing cytokines after onset of the disease [11–13]; although secretion of cytokines has been widely studied, little is known about the precise molecular components involved in these particular cells. In yeast and mammalian cells, soluble *N*-ethylmaleimide-sensitive factor attachment protein receptors (SNAREs) drive membrane fusion and exocytosis, as well as contributing to membrane/protein targeting and delivery [14,15]. Botulinum neurotoxins (BoNTs) inhibit SNARE-dependent release of substance P, calcitonin gene-related peptide and glutamate, which are the important mediators of arthritic pain [16–18]. A broad spectrum of factors, including immune and pain mediators are stored in pre-formed granules of granulocytes (neutrophils, eosinophils and mast cells) [15]. Cytokine release from macrophages may be inhibited by delivering BoNT/B, using a targeting antibody, and the toxin's protease truncating vesicle-associated membrane protein isoform 3 (VAMP-3) [19]. Stimulated release of vesicular contents requires membrane fusion, which involves particular SNAREs present on the granules and plasma membrane [15,20,21]. For example, recruitment of a synaptosome-associated protein of molecular mass 23 kDa (SNAP-23) to granule membranes in rat peritoneal cells is as an essential prerequisite for release of mediators from mast cells [15,21]. Moreover, members of the SNARE family mediate membrane fusion of TNFα transport vesicles [15]. Previous studies have shown that cytokines synthesized by various immune cells co-localize with certain Rab proteins and SNAREs, and are translocated to the plasmalemma in response to extracellular stimuli [22–25].

In view of the involvement of synoviocytes in arthritic conditions, we wished to establish whether SNAREs mediate exocytosis of cytokines from cultured synoviocytes. Knockdown of SNAP-23 or VAMP-3 using lentiviral particles encoding short hairpin RNA (shRNA) demonstrated their involvement in the secretion of IL-6 and TNFα stimulated by IL-1β, whereas knockdown of syntaxin isoforms 2, 3 or 4 was ineffective. Our novel findings suggest that these proteins are potential targets for therapeutic agents to alleviate the symptoms of arthritis.

Results

Human synovial sarcoma cells contain certain SNAREs and synaptic vesicle protein 2

Inflammatory cytokines are known to be released from SW982 cells, a line derived from human synovial sarcoma [26,27]. Cultured SW982 cells mainly contained fibroblast-like, spindle-shaped cells of variable size, visualized by labelling with a vimentin fibroblast-specific antibody and counter-staining using the nuclear marker 4′,6-diamidino-2-phenylindole (DAPI) (data not shown). To determine the molecular basis for exocytosis of cytokines from SW982 cells, their complement of SNAREs was assessed in comparison to other secretory cells (mouse macrophage cell line RAW264.7 and rat cerebellar granule neurons). Western blotting of cell lysates using isoform-specific antibodies revealed that, in contrast to RAW264.7 cells which contain SNAP-23, VAMP-3, -7 and -8, and syntaxin isoforms 2–6, SW982 cells express a somewhat lower level of syntaxin-3, similar amounts of SNAP-23, VAMP-3, syntaxin-2 and higher levels of syntaxin-4, but with little or no syntaxin isoform 5 or 6 or vesicle-associated membrane proteins VAMP-7 or -8 (Fig. 1A). Expression of SNAP-25, syntaxin-1 and VAMP-2, which is characteristic of neurons, was hardly detectable in SW982 cells, but, as expected, was enriched in rat cerebellar granule neurons (Fig. 1B). Interestingly, synaptic vesicle protein 2 (SV2) isoforms A and C, which are key proteins for Ca^{2+}-regulated transmitter release in neuronal and endocrine cells [28,29], were also found in SW982 cells. The latter do not possess the Ca^{2+} sensors synaptotagmin I or II, all of which except SV2C are expressed in rat cerebellar granule neurons (Fig. 1B). Thus, we wished to establish whether the SNAREs present in SW982 cells contribute to the release of cytokines.

Fig. 1. Human synovial sarcoma cells contain SNAREs and SV2 isoforms. (A) Western blots demonstrating that SNAP-23, VAMP-3, syntaxin isoforms 2–4 and traces of syntaxin-6 and VAMP-8 are expressed in SW982 cells; these proteins plus a relatively small amount of VAMP-7 and -8 were also detected in a mouse microphage cell line (RAW264.7). (B) Traces of SNAP-25, syntaxin-1 and VAMP-2, a higher level of SV2C than SV2A and a lack of SV2B and synaptotagmins I and II (Syt I and Syt II), were observed in SW982 cells compared to rat cerebellar granule neurons, with the exception of SV2C. Note that the antibodies used recognize human, mouse and rat antigens, although the difference in reactivity for the various species is not unknown. An equal amount of protein was loaded in each lane for all blots, with β-tubulin acting as a loading control; approximate sizes of the bands are indicated (k).
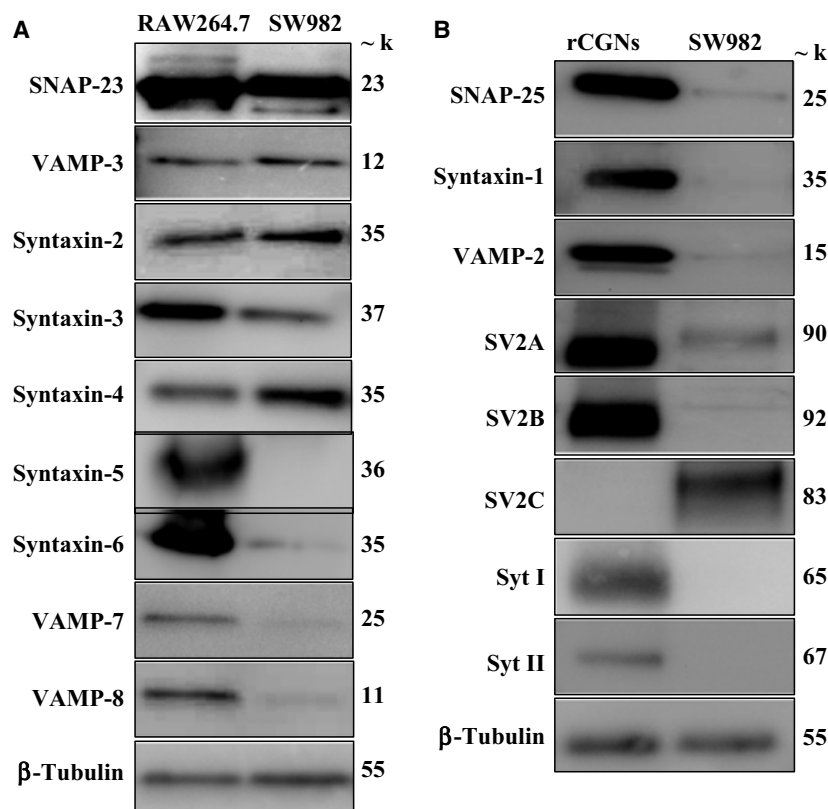
IL-1β induces the release of cytokines from SW982 cells in a Ca^{2+}-dependent manner

Although elevated [K$^+$] is known to elicit transmitter release from excitatory cells [18], the levels of IL-6 secretion from SW982 cells in LK buffer containing 3.5 or HK containing 60 mM [K$^+$] after 4 h incubation were similar; K$^+$ depolarization-induced release was unaffected by the absence of extracellular Ca^{2+} and presence of EGTA (Fig. 2A, top panel). On the other hand, 4 h incubation of the cells with an established effective concentration (100 ng·mL^{-1}) of the pro-inflammatory factor IL-1β [26], together with 60 mM [K$^+$] and 2.5 mM Ca^{2+}, elicited an approximately 3.5-fold increase in the release of IL-6 over the Ca^{2+}-free level (Fig. 2A, top panel). A cell viability assay performed after 4 h incubation in medium containing 3.5 or 60 mM [K$^+$], with or without external Ca^{2+} and IL-1β, demonstrated that the cells had not died (Fig. 2A, bottom panel), and representative images of cells after each treatment showed that they had not detached (Fig. 2C). Incubation for 20 h, rather than 4 h, with IL-1β in culture medium that contained Ca^{2+} gave a approximately 10-fold increase in IL-6 release (Fig. 2B), indicating that induction of release of this cytokine by IL-1β alone requires longer than

4 h. These results highlight the importance of IL-1β in stimulating cytokine release from SW982 cells.

SNAP-23 is required for IL-1β-induced release of IL-6 and TNFα from cultured SW982 cells: knockdown of SNAP-23 enhances peri-nuclear distribution of SV2

To examine the involvement of SNAP-23 in the release of cytokines from SW982 cells, knockdown of this protein was achieved by incubating the cells with specific shRNA lentiviral particles. Western blotting of total cell lysates showed that the knockdown resulted in a substantially reduced content of SNAP-23 (Fig. 3A); specificity of this knockdown was confirmed by the absence of any significant changes in the levels of VAMP-3 or syntaxin isoforms 2–4 (Fig. 3A). Quantification of the SNAP-23 content relative to β-tubulin as an internal standard showed a decrease of approximately 80% (Fig. 3B), with no change in a negative control treated with non-targeted lentiviral particles (Fig. 3C). This result was confirmed by immunocytochemical visualization of SNAP-23 in knockdown and normal cells (Fig. 3H); negative controls did not show any signal for SNAP-23 (Fig. 3H). Notably, SNAP-23 knockdown
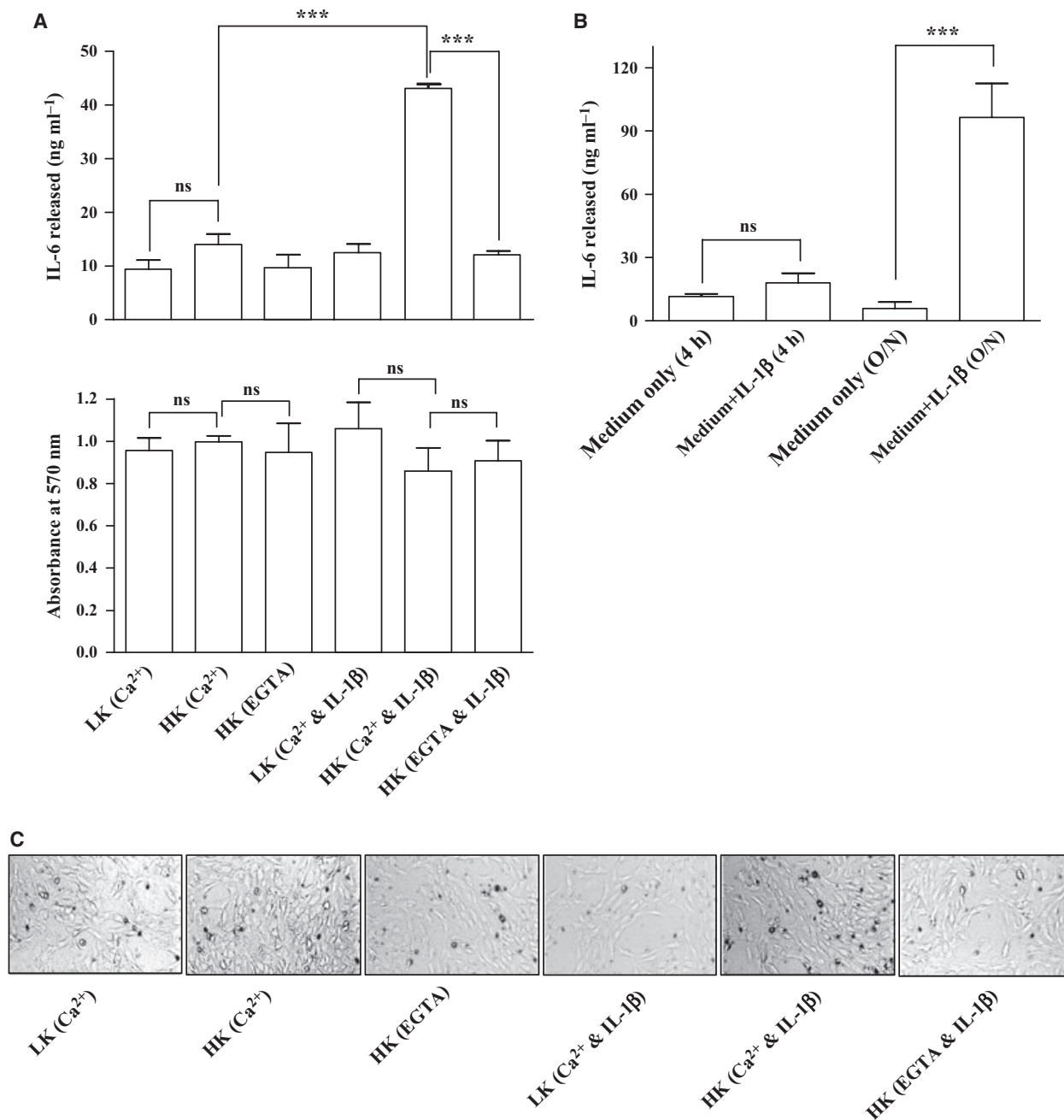
Fig. 2. IL-1β-induced IL-6 release from SW982 cells requires external Ca^{2+}. (A, top panel) A 4 h incubation of the cells with high [K$^+$] buffer (HK) in the presence or absence of extracellular Ca^{2+} resulted in minimal stimulation of IL-6 release, but addition of IL-1β (100 ng·mL^{-1}) in HK with Ca^{2+} yielded an approximately 3.5-fold increase over the basal value without extracellular Ca^{2+}. (A, bottom panel) Cell viability assay using methylthiazolyldiphenyl tetrazolium bromide, showed that no cell death occurred after a 4 h incubation in HK or LK buffer (medium containing 3.5 or 60 mM [K$^+$]), with or without external Ca^{2+} and IL-1β. (B) Incubation of SW982 cells for 20 h in culture medium containing Ca^{2+} and IL-1β (100 ng·mL^{-1}) elicited an approximately 10-fold higher release of IL-6 compared with medium alone; however, incubation for 4 h with medium and IL-1β did not result in a significant release of IL-6. (C) Representative images showing that cells were not detached after treatment for 4 h. Values are means and SEM ($n = 3$) for each experiment; asterisks indicate statistically significant differences (***$P < 0.001$). Scale bar = 100 μm.

decreased the release of TNFα and IL-6 elicited by IL-1β during a 20 h incubation by approximately 50% and 55%, respectively (Fig. 3D,E); likewise, an approximately 55% reduction in IL-6 release was observed after a 4 h treatment with IL-1β in medium containing 60 mM $[K^+]$ (Fig. 3E). As expected, the control lentiviral particles failed to inhibit release of TNFα and IL-6 (Fig. 3F,G). These collective findings show that the IL-1β-induced release of IL-6 and TNFα from SW982 cells involves SNAP-23. Interestingly, SV2 detected using an antibody reactive to all its isoforms [30] displayed a diffuse pattern in control cells but co-localized to a significant extent with IL-6 around the peri-nuclear area, presumably the endoplasmic reticulum and the Golgi apparatus (Fig. 3I). Strikingly, knockdown of the expression of SNAP-23 led to an accumulation of the SV2 signal around the peri-nuclear region (Fig. 3H). Because SV2 is a synaptic vesicle protein, such accumulation suggests that vesicle trafficking in SNAP-23 knockdown cells is impaired.

Knockdown of VAMP-3, but not syntaxin isoforms 2, 3 or 4, reduces IL-1β-induced release of IL-6 and TNFα from cultured SW982 cells

The content of VAMP-3 in SW982 cells decreased by approximately 80% after transient knockdown, calculated using β-tubulin as an internal control (Fig. 4A, B), without any significant alteration in the levels of other SNAREs in these cells or in a negative control treated with non-targeted lentiviral particles (Fig. 4A; cf Fig. 3C). Accordingly, there were reductions of approximately 55% and 60% in IL-1β-stimulated release of TNFα and IL-6, respectively, from VAMP-3 knockdown cells (Fig. 4C,D). These results highlight the functional importance of SNAP-23 and VAMP-3 in exocytosis of these two cytokines.

Experiments with syntaxin isoforms 2–4 yielded contrasting results. Transient knockdown of syntaxin-4 to approximately 50% (Fig. 4E) was achieved without a change in the levels of other SNARE proteins (Fig. 4E), but there were no alterations in protein levels in cells treated with the non-targeted lentiviral particles (cf Fig. 3C). Notably, syntaxin-4 knockdown did not reduce the stimulated release of TNFα or IL-6 compared to controls (Fig. 4G,H). Moreover, transient knockdown of syntaxin-2 by approximately 60% compared to control cells, without altering the expression of other SNAREs (Fig 5A,B), did not significantly inhibit release of TNFα and IL-6 (Fig. 5C,D). Likewise, knockdown of syntaxin-3 by approximately 50% (Fig. 6A,B) did not reduce the release of TNFα and IL-6 (Fig. 6C,D). Attempted knockdown of VAMP-3
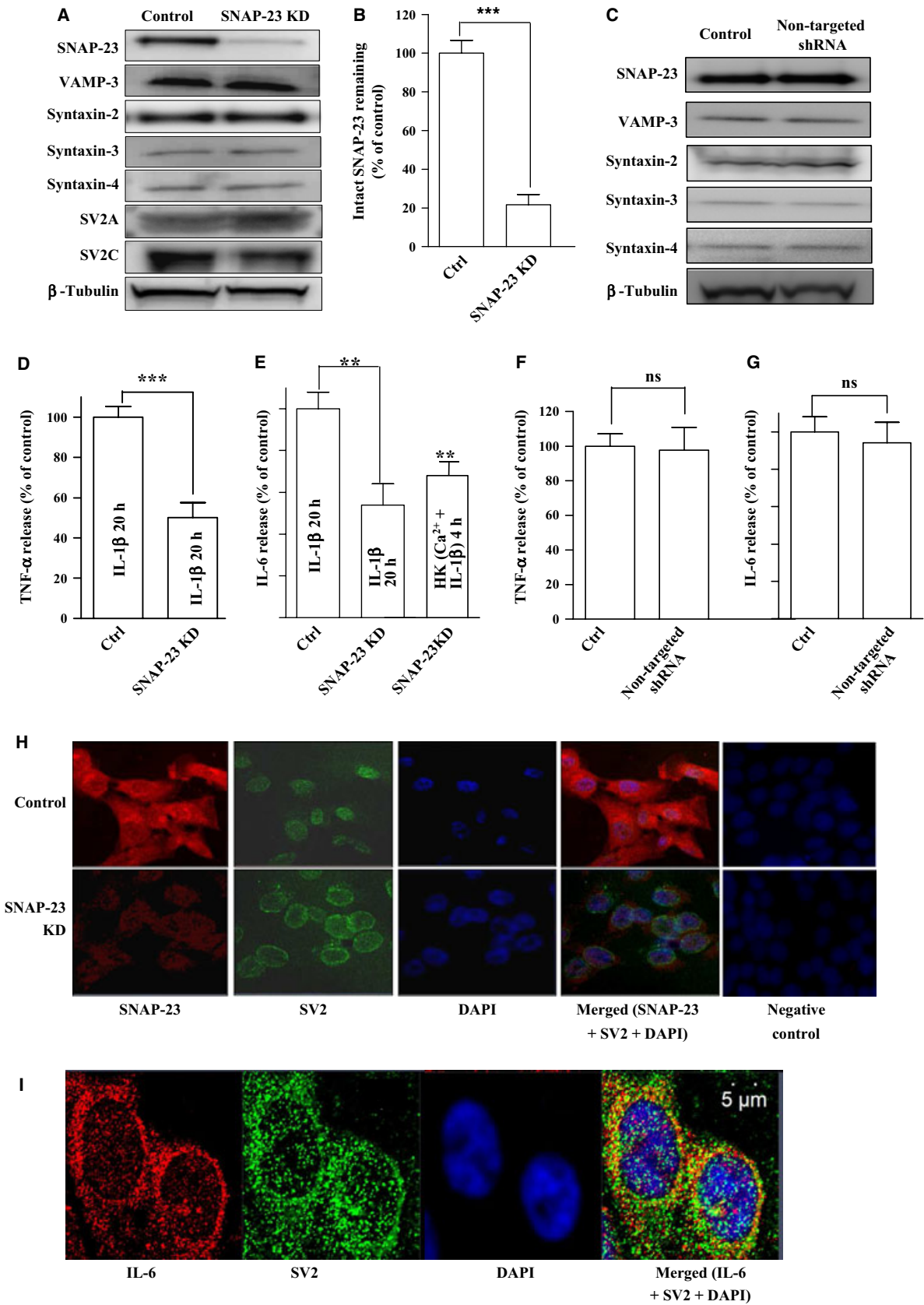
in stable SNAP-23-deficient cells caused extensive cell death, precluding further investigation.

Formation of SDS-resistant SNARE complexes is decreased by knockdown of SNAP-23

Ca^{2+}-dependent membrane fusion requires formation of stable SNARE complexes, and these are resistant to denaturation by SDS at temperatures up to approximately 80 °C [31]. In order to identify the SNARE partners participating in formation of such complexes, 2D electrophoresis was performed. Proteins were extracted from the cells using lithium dodecyl sulfate (LDS) and subjected to the first-dimension SDS/PAGE (data not shown) without boiling; gel strips were cut and solubilized in LDS sample buffer, boiled, and applied to second-dimension SDS/PAGE (Fig. 7A). Because SNAP-23 and VAMP-3 were found to contribute to exocytosis of cytokines in SW982 cells, attention was focused on their participation in the formation of SDS-resistant SNARE complexes. Notably, in IL-1β-stimulated wild-type SW982 cells, the majority of SNAP-23 and VAMP-3 was not present in SDS-resistant complexes (Fig. 7A), as indicated by the fact that their electrophoretic migrations were unchanged by boiling and matched the mobilities known for their molecular masses. However, some SNAP-23 was retained in complexes, presumably with other SNAREs with molecular masses ranging from approximately 49 to approximately 272 kDa (Fig. 7A); those with molecular mass > 69 kDa displayed weak signals for VAMP-3 (Fig. 7A), with the increment in intensities corresponding to those for SNAP-23 especially at a molecular mass > 137 kDa. In contrast, IL-1β-treated cells in which SNAP-23 was stably knocked down showed only a very small amount of SNAP-23, in the free form and even less in complexes (Fig. 7B). Although an abundance of free VAMP-3 remained, little if any was complexed. These observations suggest that SNAP-23 and VAMP-3 form SNARE complexes in normal cells that may contribute to evoked release of cytokines (cf Figs 3 and 4). A decrease in SNAP-23 excluded its partner, VAMP-3, from SDS-resistant SNARE complexes. Co-immunoprecipitation provided confirmatory evidence of SNAP-23 complexes containing VAMP-3 and syntaxin-2; syntaxin-3 was hardly detectable and syntaxin-4 was absent (Fig. 7C).

SNAP-23 knockdown abolishes the filamentous-like distribution of the IL-1 receptor but not its apparent surface content

Confocal immunofluorescence microscopy of intact synoviocytes labelled with a polyclonal IgG specific for

A

SNAP-23
VAMP-3
Syntaxin-2
Syntaxin-3
Syntaxin-4
SV2A
SV2C
β-Tubulin

Control   SNAP-23 KD

B

Intact SNAP-23 remaining (% of control)

***

Ctrl   SNAP-23 KD

C

SNAP-23
VAMP-3
Syntaxin-2
Syntaxin-3
Syntaxin-4
β-Tubulin

Control   Non-targeted shRNA

D

TNF-α release (% of control)

***

IL-1β 20 h   IL-1β 20 h
Ctrl   SNAP-23 KD

E

IL-6 release (% of control)

**   **

IL-1β 20 h   IL-1β 20 h   HK (Ca²⁺ + IL-1β) 4 h
Ctrl   SNAP-23 KD   SNAP-23KD

F

TNF-α release (% of control)

ns

Ctrl   Non-targeted shRNA

G

IL-6 release (% of control)

ns

Ctrl   Non-targeted shRNA

H

Control

SNAP-23 KD

SNAP-23   SV2   DAPI   Merged (SNAP-23 + SV2 + DAPI)   Negative control

I

5 µm

IL-6   SV2   DAPI   Merged (IL-6 + SV2 + DAPI)

the IL-1 receptor (IL-1R) revealed that SNAP-23 knockdown decreased the filamentous-like staining of IL-1R to a clustered pattern close to the nuclei, compared to wild-type cells (Fig. 8A). To assess possible changes in the surface level of IL-1R upon knockdown of SNAP-23, wild-type and SNAP-23 knockdown cells were stimulated with IL-1β (100 ng·mL^{-1}) for 20 h. Total proteins and biotinylated cell-surface IL-1Rs were extracted from cells in 2 x LDS sample buffer, and separated by SDS/PAGE for western blot analysis. In stimulated and SNAP-23 knockdown cells, no change in total and surface content of IL-1R was observed, compared to non-stimulated wild-type (Fig. 8B). Thus, although the distribution pattern of IL-1R on SNAP-23 knockdown cells appeared to be altered, this did not alter its surface expression or total membrane content.

Discussion

This study provides evidence for the presence of particular SNAREs and SV2 in a human synovial sarcoma cell line, and the involvement of SNAP-23 and VAMP-3 but not syntaxin isoforms 2, 3 or 4 in the exocytosis of cytokines. There is enhanced exocytosis of IL-6 and TNFα induced by IL-1β during necrotic form of cell death in rheumatoid arthritis and osteoarthritis [32,33]. IL-1β is one of the most critical pro-inflammatory factors that are released by innate immune cells, and contributes to inflammatory pain hypersensitivity. In fact, the generation and progression of arthritis appears to involve sequential secretion of multiple inflammatory cytokines that act through a positive feedback cascade involving the surrounding cells [4,8,11,32,33]. SW982 cells were chosen for this investigation because these are fibroblast-like synovial cells, although their morphology is mixed in culture [34]. Our finding of increased secretion of IL-6 and TNFα upon incubation of SW982 cells with IL-1β is reminiscent of their release from lipopolysaccharide-treated macrophages [35,36]. Furthermore, there is convincing evidence for the involvement of SNAP-23 and VAMP-3 in their exocytosis, because their knockdown did not reduce the levels of other SNAREs but decreased the secretion of IL-6 and TNFα to similar extents. The remaining release may be attributed to residual levels of SNAP-23 and VAMP-3 after knockdown, or, perhaps, participation of other unidentified SNARE isoforms and even non-classical secretion pathways [37]. The simultaneous participation of both SNAP-23 and VAMP-3 in the release of IL-6 and TNFα from SW982 cells is an interesting feature, because the intracellular trafficking pathways for IL-6 and TNFα in other cell types (i.e. macrophages) overlap but with some divergence. For example, in macrophages, after synthesis of these cytokines in the endoplasmic reticulum, they accumulate in Golgi complexes before sorting. The membrane-bound TNFα is delivered by recycling endosomes to phagocytic cups or the plasma membrane for secretion, whereas IL-6, which lacks a transmembrane domain, may be secreted directly; however, knockdown of VAMP-3 affects secretion of both cytokines from macrophages [24,35]. Our findings support the notion that cytokine secretion may be tailored to the needs of inflammatory systems through variant SNARE-dependent pathways [21]. Notably, TNFα release from secretory granules in mast cells also requires SNAP-23 [37], similar to our finding in SW982 cells. Knockdown of the syntaxin isoforms 2, 3 or 4 present in SW982 cells did not impair IL-1β-stimulated release of IL-6 or TNFα, although trace amounts of isoforms 2 and 3 co-immunoprecipitated with VAMP-3 (Fig. 7C). This lack of inhibition of exocytosis

Fig. 3. Selective knockdown of SNAP-23 greatly reduces IL-1β-mediated release of IL-6 and TNFα from SW982 cells as well as enhancing peri-nuclear distribution of SV2. (A) Western blots of SNAREs and SV2A/C in lysates of control and SNAP-23 knockdown cells (60 μg per lane), demonstrating that the level of SNAP-23 only was significantly reduced compared to the control. (B) Percentage knockdown of SNAP-23 relative to the control was calculated using β-tubulin as an internal standard. (C) As expected, use of non-targeted shRNA did not alter the level of SNAP-23 or other proteins monitored. (D,E) After 20 h incubation with IL-1β (100 ng·mL^{-1}) in complete medium, the extent of inhibition of induced release of TNFα (D) and IL-6 (E) from knockdown cells was calculated relative to those for the control. The reduction in IL-6 release after 4 h stimulation by IL-1β (100 ng·mL^{-1}) in medium containing 60 mM [K$^+$] (HK) is also shown (E). In contrast, no significant difference in release of the two cytokines was seen in cells treated similarly but with non-targeted viral particles (F,G). (H) Fluorescence images showing that SV2 adopted a pronounced peri-nuclear distribution in SW982 cells after knockdown of SNAP-23, whereas its distribution was more diffuse in controls. Alexa Fluor 568-tagged goat anti-rabbit (1:1500) and Alexa Fluor 488-tagged donkey anti-mouse (1:1500) were used as secondary antibodies, with nuclei staining using DAPI. Negative controls, treated in the same way except that primary antibodies were omitted, failed to yield any positive signals for SV2 or SNAP-23. Scale bar = 10 μm. (I) Confocal microscopic images of control SW982 cells show that SV2 and IL-6 have a diffuse distribution pattern but co-localize around peri-nuclear areas. Values are means and SEM (*n* = 3) for each experiment; asterisks indicate statistically significant differences (**$P < 0.01$, ***$p < 0.001$).
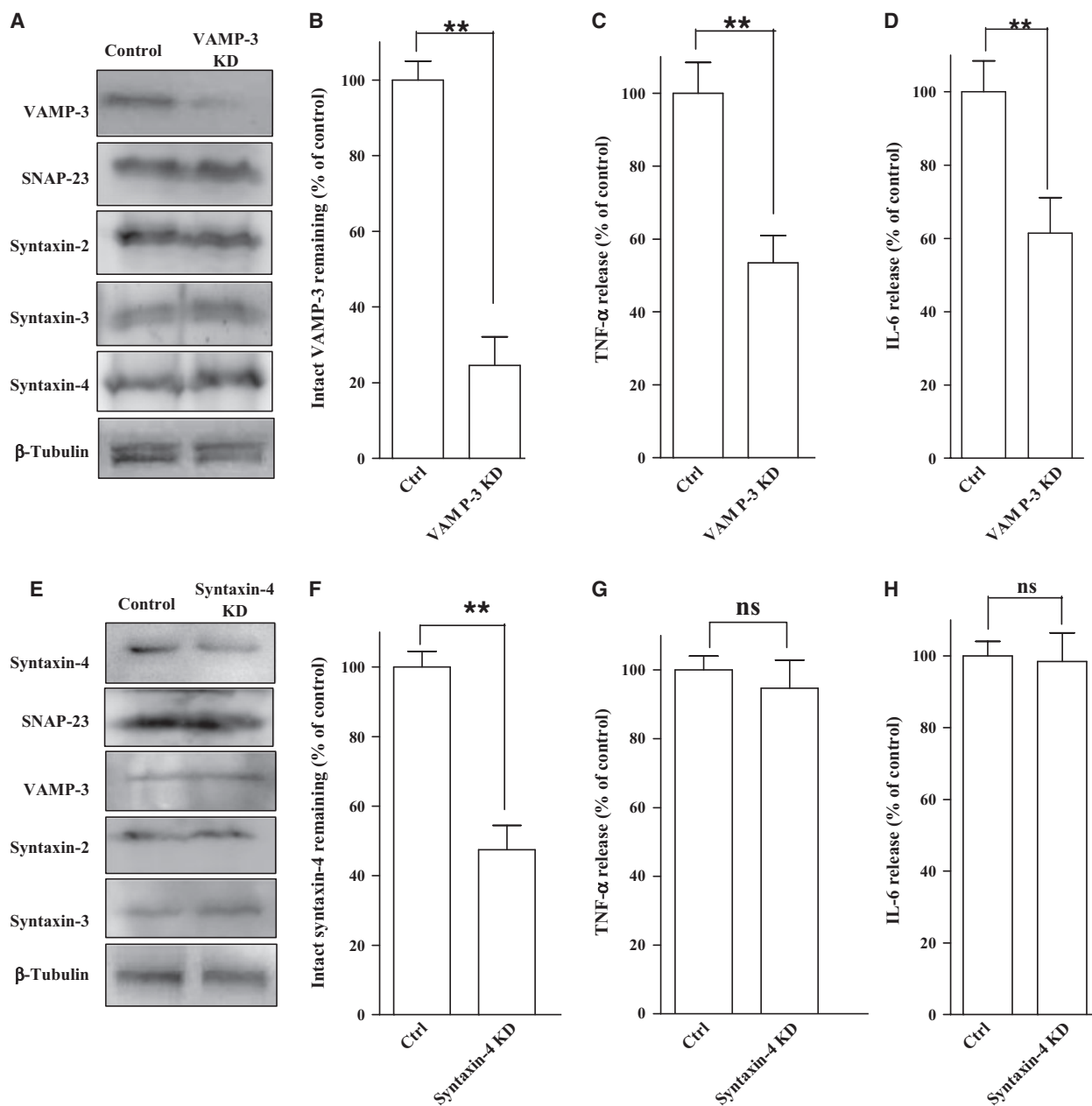
Fig. 4. Knockdown of VAMP-3, but not syntaxin-4, significantly decreased the IL-1β-stimulated release of IL-6 and TNFα from SW982 cells. (A) Immunoblotting reveals that VAMP-3 was decreased in the knockdown cells. (B) Densitometric scanning and calculation of the level of VAMP-3 relative to that in the control, using β-tubulin as a reference. (C,D) Cells were incubated for 20 h with IL-1β (100 ng·mL^{-1}) in complete medium before collecting the supernatant to quantify the amounts of released TNFα (C) and IL-6 (D). VAMP-3 knockdown caused significant reductions in their release compared with non-treated controls. (E,F) Western blot analysis (E) showed approximately 50% knockdown of syntaxin-4 (F), calculated as in (B). (G,H) Stimulation with complete medium containing IL-1β (100 ng·mL^{-1}) for 20 h did not inhibit the release of IL-6 (G) or TNFα (H) after knockdown of syntaxin-4. Values are means and SEM (n = 3) for each experiment; asterisks indicate statistically significant differences (**$P < 0.01$).

is presumably due to incomplete and less extensive knockdown than that of SNAP-23 and VAMP-3, and/ or any of the other isoforms present compensating for their function. In macrophages, multiple syntaxin

isoforms (4, 6 and 7) are implicated in TNFα release [37].

Knockdown of SNAP-23 significantly reduced the amount of SDS-resistant complexes formed that contain
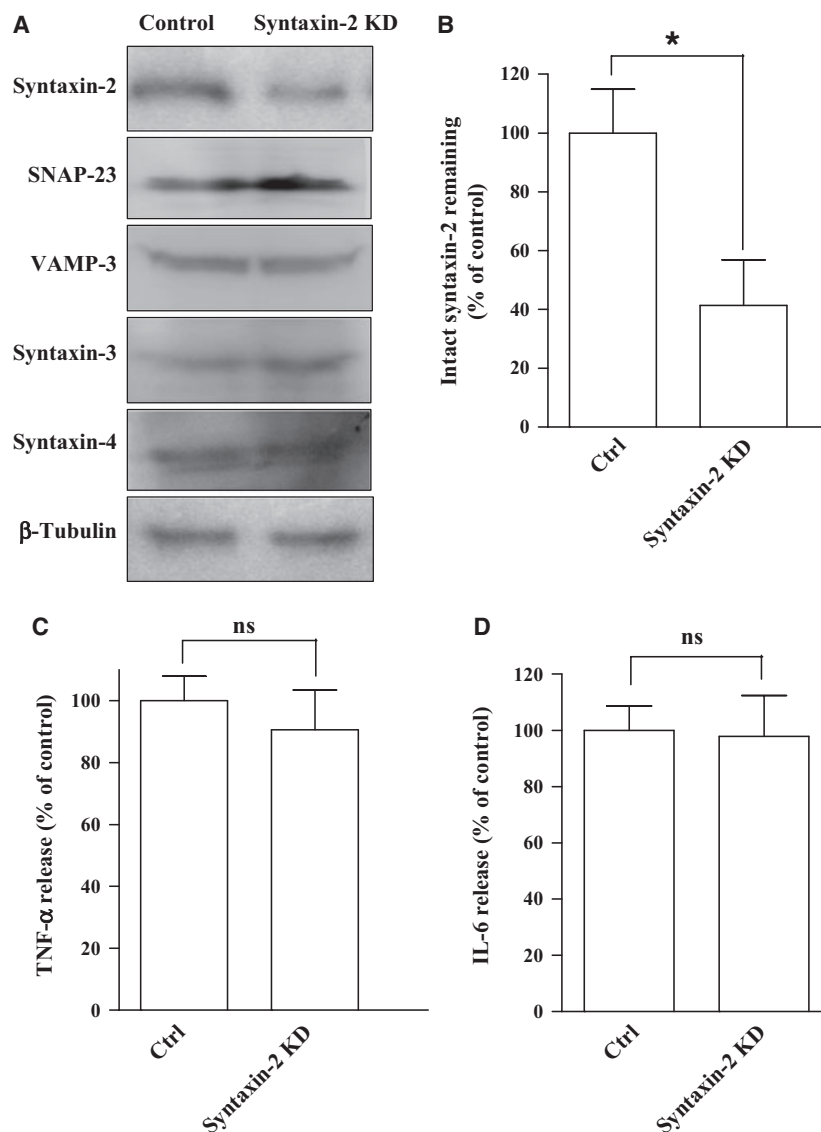
Fig. 5. Knockdown of syntaxin-2 failed to reduce the release of two cytokines from SW982 cells. (A) Immunoblots show a significantly reduced level of syntaxin-2 compared to the control, without alterations in other SNAREs. (B) Percentage knockdown of syntaxin-2 relative to the control was calculated using β-tubulin as an internal control. Knockdown of syntaxin-2 did not inhibit the evoked release of TNFα (C) and IL-6 (D). Values are means and SEM ($n = 3$) for each experiment; asterisks indicate statistically significant differences (*$P < 0.05$).

SNAP-23 and VAMP-3, but did not affect the surface content of IL-1R, although the filamentous-like distribution virtually disappeared. As such complexes are known to be essential for transport of TNFα vesicles and membrane fusion [38,39], their decrease appears to underlie the reduced cytokine exocytosis from SNAP-23 knockdown cells, suggesting that SNAP-23 and VAMP-3 are involved in fusion of vesicles with plasmalemma. However, a role in the trafficking of cytokine-containing vesicles in synoviocytes cannot be excluded, and warrants in-depth future studies.

It is well knows that Ca^{2+} binding to its sensor triggers exocytosis of vesicles by assembly of SNARE complexes [40]. External Ca^{2+} was found to be required for cytokine release, as incubation with IL-1β in the presence of extracellular Ca^{2+} enhanced this

release and did not affect survival of the SW982 cells. Consistent with the Ca^{2+} dependence of cytokine release, voltage-dependent Ca^{2+} channels, mainly L-type, occur in SW982 cells [41]. Also, secretory carrier membrane proteins have been implicated in the Ca^{2+} regulation of cytokine trafficking in immune cells [14]. Secretory carrier membrane proteins directly bind to the Ca^{2+} sensor in immune cells; thus, these proteins have potential roles in cooperation with the SNARE machinery in Ca^{2+}-regulated exocytosis of cytokines [14]. The observed ability of IL-1β to increase K^+-stimulated release of IL-6 approximately 3.5-fold over the basal level within 4 h, and its inhibition upon depletion of SNAP-23, reaffirms the requirement for extracellular Ca^{2+} in SNARE-mediated cytokine release from SW982 cells.
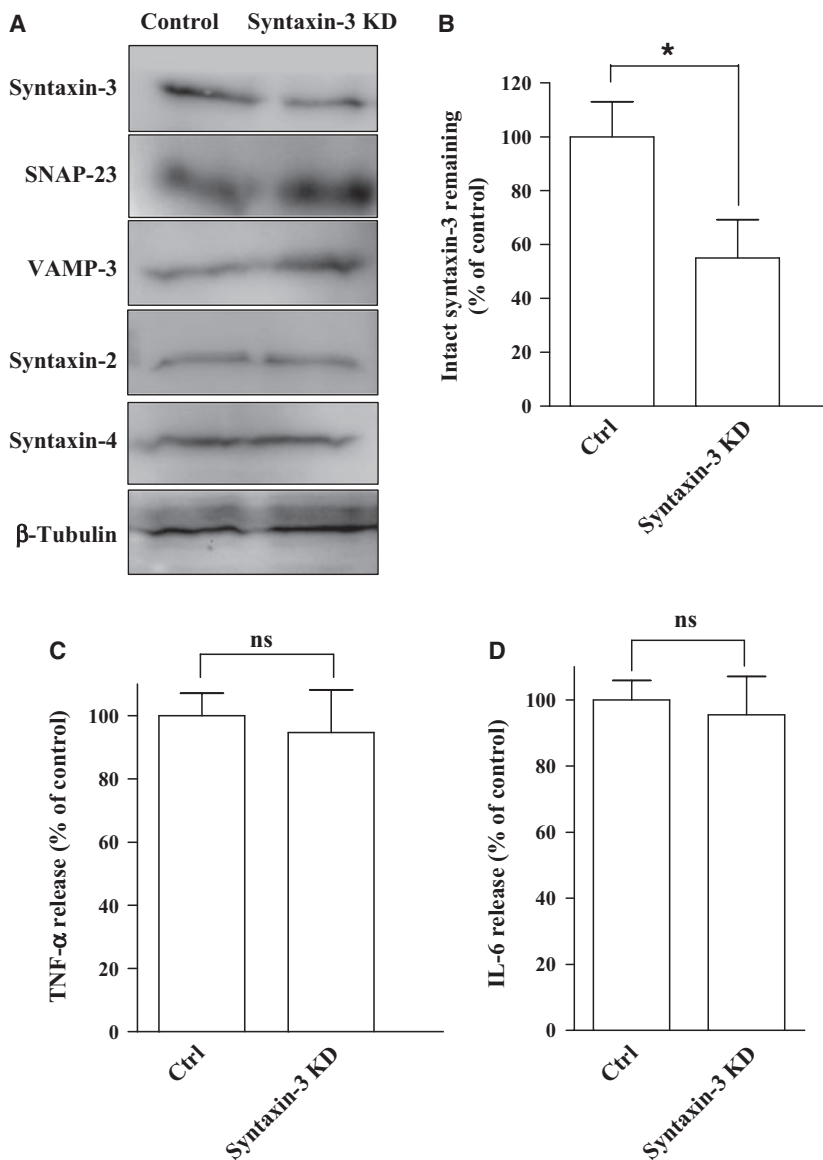
Fig. 6. No decrease in the release of cytokines was observed after knockdown of syntaxin-3 in SW982 cells. (A) Western blots demonstrating decreased expression of syntaxin-3 and unaffected levels of other SNAREs. (B) Percentage knockdown of syntaxin-3 compared to control was analysed, with β-tubulin serving as an internal control. (C,D) The release of TNFα (C) and IL-6 (D) stimulated by IL-1β (100 ng·mL^{-1}) was not inhibited after knockdown of syntaxin-3. Values are means and SEM (n = 3) for each experiment; asterisks indicate statistically significant differences (*P < 0.05).

The finding of increased peri-nuclear localization of SV2 protein after SNAP-23 knockdown, suggests participation of the former in transportation of cytokines from this locus, presumably *trans*-Golgi or endoplasmic reticulum regions. Unfortunately, suitable paired antibodies were not available for counterstaining. Although the role of SV2 in regulating the expression and trafficking of the Ca^{2+} sensor protein synaptotagmin has been well documented [29], nothing is known about the function of this transmembrane protein in non-neuronal cells except for its location on secretory vesicles as visualized by immunoelectron microscopy [42]. Nevertheless, the enhanced occurrence of SV2 in the peri-nuclear region in SNAP-23 knockdown cells implicates this

protein in package and/or delivery of cytokines to the cell surface.

Because of the importance of synovial cells in propagation of the inflammatory response in rheumatoid arthritis and osteoarthritis, our finding regarding the involvement of these SNAREs in the release of cytokines may assist in the design of novel and effective therapeutic agents. It is known that serotypes of BoNTs cleave SNAREs and subsequently inhibit the release of cell mediators [43]. Accordingly, intra-articular injection of BoNT/A or BoNT/B into patients or murine models of arthritis reduces the associated pain [44–47]. The latter probably results from blockade by BoNTs of the release of transmitters (e.g. calcitonin gene-related peptide, substance P,

Fig. 7. Knockdown of SNAP-23 in SW982 cells reduces the formation of SDS-resistant SNARE complexes. Control and SNAP-23 knockdown SW982 cells were solubilized in LDS buffer without boiling, and the proteins were separated on pre-cast 4–12% gels by SDS/PAGE. Gel sections containing the separated proteins were excised according to migration distances, and extracted by boiling in LDS sample buffer before re-electrophoresis and immunoblotting using antibodies specific for SNAP-23 and VAMP-3. (A) SNAP-23 formed complexes with VAMP-3 in control cells after IL-1β (100 ng·mL^{-1}) stimulation for 20 h. (B) Knockdown of SNAP-23 resulted in minimal formation of complexes with VAMP-3 under stimulation conditions. (C) VAMP-3 forms complexes with SNAP-23 or syntaxin-2 in stimulated control SW982 cells. Total lysate (50 μg input) and 50% of the eluted protein were subjected to SDS/PAGE. Only the lower halves of the gels are shown because excessive staining of the rabbit IgG overlapped the SNARE complexes on the top halves of the blots. Note that SNAP-23 associated with VAMP-3 was readily detected by western blotting, confirming the result in (A).
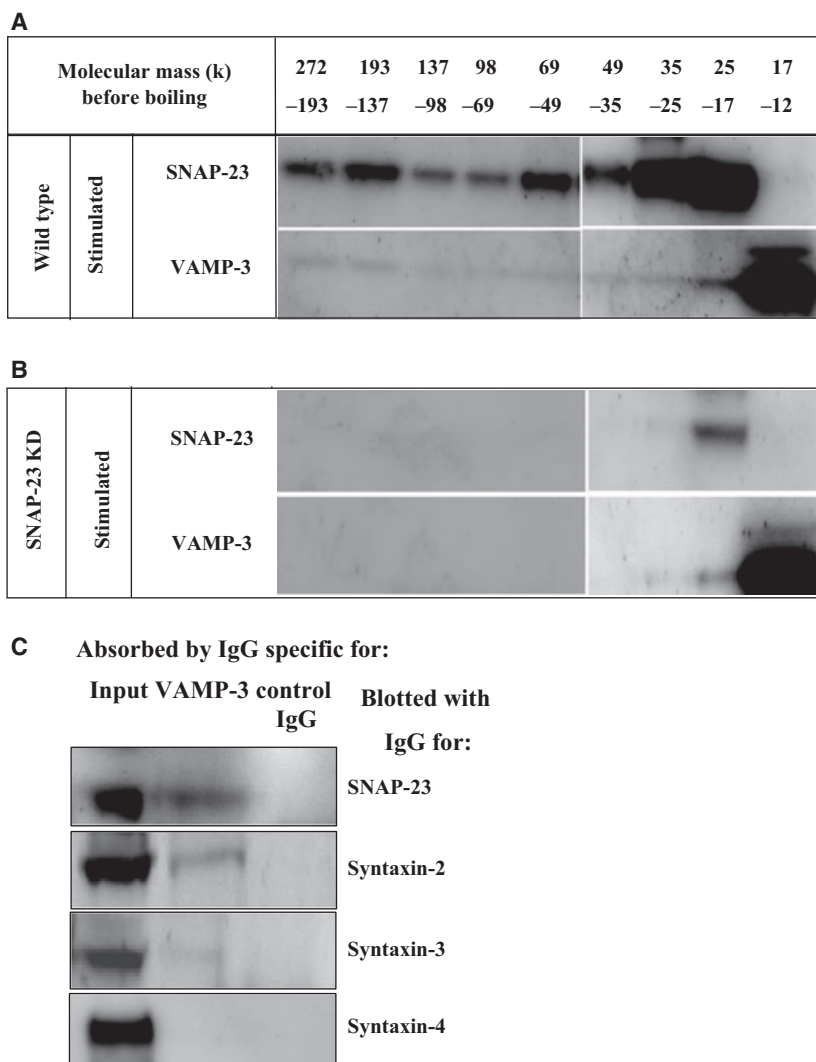
glutamate) from peripheral sensory fibres. Inhibition of the release of these mediators reduces their activation of non-neuronal cells and thus reduces cytokine release from the surrounding synoviocytes, macrophages and other inflammatory cells in the joints. Such indirect action is likely because the latter cells normally possess too low a density of BoNT acceptor for efficient toxin entry or lack the susceptible substrates. It is worth noting that SNAP-23 may be inactivated by a mutant of type E light chain in digitonin-permeabilized HeLa cells, with a subsequent reduction in the release of cytokines [48]. Although rat cultured synoviocytes were found to express SV2 isoforms (receptors for BoNT/A, /D, /E, /F and tetanus toxins) [30,49–53], their densities on the cell surface are much lower than in neurons, and thus these non-neuronal cells are only susceptible to high

concentrations of the BoNT BA chimera [54], generated by substituting the C-terminal half of the BoNT/A heavy chain into BoNT/B. When a relatively high concentration of the BoNT BA chimera is used, it delivers the type B protease via the BoNT/A acceptor into rat synoviocytes and cleaves VAMP-3 [54]. Future studies may attempt to specifically re-target the above-mentioned BoNT protease(s) into inflammatory cells by replacing the BoNT neuronal receptor binding domain with a cell type-unique ligand, a strategy that was successfully used in a previous study [55].

In conclusion, certain SNAREs and SV2 have been identified in SW982 cells; knockdown of SNAP-23 or VAMP-3 impaired the release of IL-6 and TNFα upon stimulation with IL-1β, implicating these SNAREs in exocytosis of cytokines.
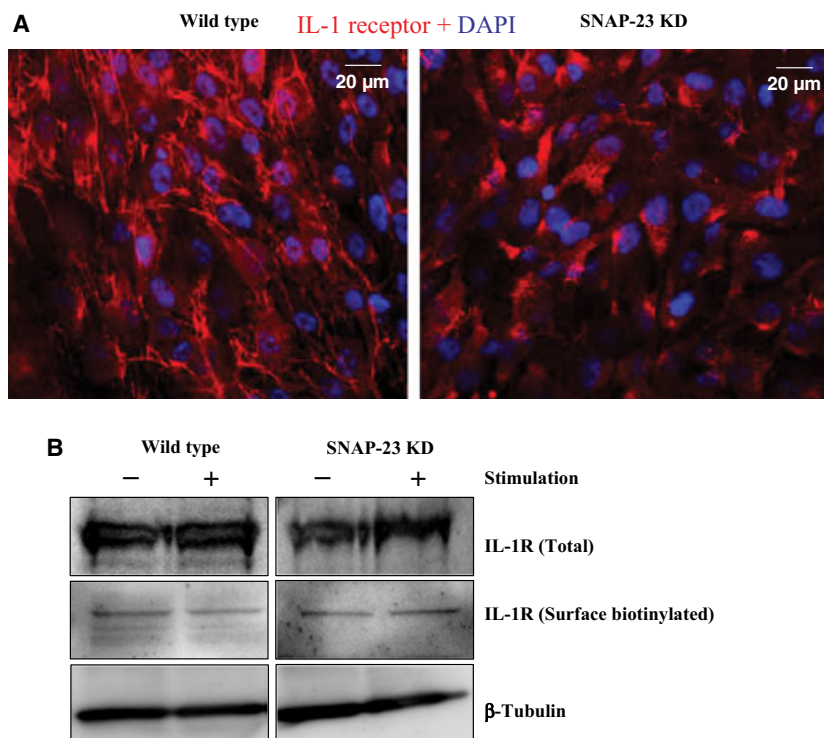
Fig. 8. Loss of filamentous distribution of IL-1R resulted from SNAP-23 knockdown in SW982 cells. (A) Wild-type SW982 cells and SNAP-23 knockdown cells were stimulated 20 h with IL-1β before being fixed, permeabilized, and labelled with IL-1R rabbit antibody at 4 °C for 16 h. Alexa Fluor 594-conjugated goat anti-rabbit was used as the fluorescent secondary antibody. Nuclei were stained using DAPI. The confocal images show that, compared to control SW982 cells, the distribution of IL-1R on the cell bodies and filaments was altered after SNAP-23 knockdown, showing decreased expression on the cell body surface and filaments and accumulation near nuclei. (B) IL-1β did not alter the cell surface content of IL-1R in wild-type and SNAP-23 knockdown SW982 cells. The top panel shows total IL-1R expression in whole-cell extracts. The middle panel shows western blots of the surface-expressed biotinylated IL-1R with (+) or without (−) IL-1β stimulation. β-tubulin acted as internal control for biotinylated samples (bottom panel). Knockdown of SNAP-23 in SW982 cells did not alter the level of surface IL-1R in the presence or absence of IL-1β.

Experimental procedures

Ethics statement

Maintenance, care and the experimentation on rodents complied with the European Communities (Amendment of Cruelty to Animals Act 1876) Regulations 2002 and 2005. All procedures were approved by the Research Ethics Committee of Dublin City University, and licensed by the Irish Ministry of Health and Children.

Antibodies and reagents

Rabbit affinity-purified polyclonal antibodies specific for IL-6 and rabbit polyclonal anti-IL-1R were purchased from Abcam (Cambridge, UK); cell culture reagents, targeted and non-targeted shRNA lentiviral particles, rabbit polyclonal antibodies against SNAP-25, a syntaxin-1 mouse monoclonal antibody, protein A–agarose, fetal bovine serum, penicillin-streptomycin (Pen-Strep) and shRNAs were purchased from Sigma-Aldrich (St Louis, MO, USA). Synaptic Systems

GmbH (Goettingen, Germany) supplied rabbit polyclonal antibodies specific for SNAP-23, VAMP-2,-3, -7 or -8, syntaxin isoforms 2, 3, 4, 5 or 6, and SV2A, B or C. Alexa Fluor 594-conjugated goat anti-rabbit (red fluorescence) and Alexa Fluor 488-conjugated donkey anti-mouse (green fluorescence) were purchased from Bio-Sciences (Dun Laoghaire, Ireland); horseradish peroxidise-conjugated donkey anti-rabbit and anti-mouse secondary antibodies were purchased from Jackson ImmunoResearch (West Grove, PA, USA). The ECL reagent was supplied by Merck/Millipore (Cork, Ireland), Vectashield was purchased from Vector Labs (Peterborough, UK), TrueBlot horseradish peroxidase-conjugated secondary antibody was purchased from eBioscience (Hatfield, UK), and Cell Surface Protein Biotinylation & Purification Kit was purchased from Pierce (Rockford, IL, USA).

Cell culture

A human synovial sarcoma cell line (SW982), obtained from the American Tissue Culture Collection (Manassas,

VA), was maintained in T-150 flasks (Corning, Tewksbury, MA, USA) in RPMI-1640 medium containing 2 mM L-glutamine, 10% fetal bovine serum and 1% Pen-Strep at 37 °C, 5% CO_2 [56]. The mouse macrophage cell line RAW264.7 was cultured in Dulbecco's modified Eagle's medium containing 10% fetal bovine serum and 1% Pen-Strep. Cerebelli were dissected from Sprague–Dawley rats on postnatal day 7, and rat cerebellar granule neurons were cultured as described previously [54].

shRNAs for knockdown of expression of human SNAP-23, VAMP-3, syntaxin isoforms 2, 3 or 4 in SW982 cells

Targeted and non-targeted (control) shRNA lentiviral particles, at a multiplicity of infection of 20 for each clone, were used to knockdown the expression of individual SNAREs in SW982 cells. After adding the requisite shRNA to the cells and culturing for 7–8 days, stable SNAP-23 knockdown cells were established by incubating with puromycin (5 μM) for 4–5 days before use in experiments. These cells were sub-cultured in the presence of puromycin to maintain knockdown of SNAP-23. Transient knockdown of VAMP-3, syntaxin isoforms 2, 3 or 4 was achieved by incubating SW982 cells with shRNA for 7–8 days, followed by culture in medium containing puromycin for 3–4 days, before evaluation of protein expression by western blotting. Knockdown of each protein, relative to an internal control (β-tubulin) was measured by densitometric scanning of the blots and analysed by ImageJ (http://rsb.info.nih.gov/ij). The value for the protein of interest relative to the internal control for shRNA-treated cells was subtracted from the value for control cells, and the resulting number was expressed relative to that for the control to give the percentage knockdown.

SDS/PAGE and western blotting

The protein samples were solubilized in LDS sample buffer, loaded onto 12% or 4–12% pre-cast Bis/Tris gels, and electrophoresis was performed at 180 V using MOPs running buffer (50 mM MOPs, 50 mM Tris, 1 mM EDTA and 0.1% SDS) until the pre-stained protein markers were well separated. After electrophoretic transfer to an Immobilon™ poly (vinylidene difluoride) membrane (Thermo Fisher Scientific Inc., Waltham, MA, USA), the proteins were detected using the appropriate antibodies in conjunction with ECL reagents, and images were recorded using a G-Box gel documentation system (Syngene, Cambridge, UK).

2D gel electrophoresis

An established protocol [57] was used to investigate whether SNAP-23, VAMP-3 and syntaxin-4 form SDS-resistant complexes in control, IL-1β-stimulated or SNAP-23 knockdown cells. SW982 cells were solubilized in LDS sample buffer without boiling, and proteins were separated on 4–12% gels; each resulting sample lane was cut into strips reflecting the various distances of migration, chopped into small pieces and boiled for 10 min. The extracted proteins were then separated in a second 4–12% gel, and the SNAREs that were released from complexes after boiling were detected by western blotting using specific antibodies.

Co-immunoprecipitation

SW982 cells were incubated for 20 h with IL-1β (100 ng·mL^{-1}) in complete medium (RPMI-1640, 2mM L-glutamine, 10% fetal bovine serum and 1% penicillin-streptomycin), before centrifugation for 5 min at 170 **g**; cell pellets were lysed in 20 mM HEPES, pH 7.4, containing 150 mM NaCl, 1 mM $MgCl_2$, 1 mM EGTA and 0.1% Triton X-100, supplemented with a cocktail of protease inhibitors, for 30 min followed by brief sonication. After centrifugation at 15 000 **g** for 10 min, the protein concentration of the supernatant was determined by Bradford's assay as approximately 1 mg·mL^{-1}. Protein extracts (300 μg in 300 μL) were incubated with VAMP-3-specific mouse antibodies (30 μg in 50 μL), pre-complexed with protein A–agarose for 1 h, before washing the unbound for five times (5min each) with ice-cold lysis buffer. Negative controls were performed using non-immune mouse IgG, pre-labelled protein A–agarose. Before immuno-precipitation, 50 μg of protein extracts in 20 μL of input were retained to analyse the efficiency of co-immunoprecipitation. The sealed agarose-bound samples were boiled for 10 min in 50 μL reducing LDS sample buffer, before subjecting 50% of the eluate to SDS/PAGE and western blotting, using rabbit polyclonal antibodies specific for SNAP-23, syntaxin isoforms 2, 3 or 4, and mouse TrueBlot horseradish peroxidase-conjugated secondary antibody.

Enzyme-linked immunosorbent assay

ELISA kits for IL-6 or TNFα were used according to protocols provided by Mabtech AB (Nacka Strand, Sweden). SW982 cells were stimulated for 20 h with IL-1β (100 ng·mL^{-1}) in complete medium (containing Ca^{2+}), or, in some cases, buffer containing 60 mM K^{+} (with adjustment of the NaCl concentration) and 2.5 mM Ca^{2+} with and without EGTA (3 mM) [57]. Cell viability was determined using methylthiazolyldiphenyl tetrazolium bromide, as described previously [58].

Cytochemical staining and analysis of microscopic images

Wild-type or knockdown SW982 cells cultured on collagen-coated cover slips (IBIDI, Martinsried, Germany) were stimulated with or without IL-1β (100 ng·mL^{-1}) for 20 h, washed three times for 5 min at room temperature with Dulbecco's phosphate buffer saline (lacking Mg^{2+} and Ca^{2+}) and then fixed for 20 min using 3.7% paraformaldehyde in the latter buffer at room temperature. After washing three times for 5 min at room temperature with NaCl/P$_i$, the cells were permeabilized using 0.2% Triton X-100 in NaCl/P$_i$ for 5 min before blocking with 1% bovine serum albumin in NaCl/P$_i$ for 1 h. Primary antibodies were applied in the same solution and left for 20 h at 4 °C; following extensive washing, Alexa Fluor-conjugated secondary antibodies were added for 1 h at room temperature. After rinsing with NaCl/P$_i$, the cover slips were mounted on slides using Vectashield medium containing DAPI for nuclei staining. Negative controls were performed using the same procedure without primary antibody but were incubated with secondary antibodies. Immunofluorescent images were obtained using a Zeiss LSM 710 confocal microscope (Zeiss, Jena, Germany) or an Olympus IX71 microscope (Olympus, Tokyo, Japan) equipped with a CCD camera [57].

Biotinylation of cell-surface proteins

Two T75 flasks of wild-type or SNAP-23 knockdown cells were grown to 90–95% confluence before treatment with or without IL-Iβ (100 ng·mL^{-1}) for 20 h. Cells were washed twice in the flasks using ice-cold NaCl/P$_i$, pH 8.0, before incubation with 0.5 mg·mL^{-1} EZ-Link NHS-SS-biotin in ice-cold NaCl/P$_i$ for 1 h at 4 °C. The biotinylation of cell-surface proteins was terminated by adding quenching solution (TBS; 25mM Tris, 0.15 M sodium chloride; pH7.2) and rinsing with Tris-buffered saline. The cells were then harvested by scraping cells and transferring them to the tube before centrifugation at 500 *g* for 3 min. Cell pellet were lysed in lysis buffer containing protease inhibitors; to improve solubilization, the cells were sonicated on ice and centrifuged at 10 000 *g* for 2 min at 4 °C. The biotinylated membrane proteins were adsorbed from the supernatant using immobilized NeutrAvidin gel slurry (Pierce, Rockford, IL, USA), which was washed twice in washing buffer (0.05 M sodium acetate, pH 5.0); proteins were eluted from the gel by heating at 95 °C for 5 min in SDS/PAGE sample buffer in the presence of 50 mM dithiothreitol and subjected to

western blotting using an anti-IL-1R antibody. IL-1R expression in whole-cell extracts (total) prior to incubation with agarose–NeutrAvidin was also determined by western blotting.

Statistical analysis and data presentation

Data were analysed and plotted using GraphPad Prism 4.0 (GraphPad, Software Inc., San Diego, CA, USA). Values presented are means ± SEM with sample sizes; *P* values were calculated using the non-paired, two-tailed Student's *t* test.

References

1 Kidd BL, Langford RM & Wodehouse T (2007) Arthritis and pain. Current approaches in the treatment of arthritic pain. *Arthritis Res Ther* **9**, 214.

2 Lotz M (2012) Osteoarthritis year 2011 in review: biology. *Osteoarthritis Cartilage* **20**, 192–196.

3 McInnes IB & Schett G (2011) The pathogenesis of rheumatoid arthritis. *N Engl J Med* **365**, 2205–2219.

4 Feldmann M (2001) Pathogenesis of arthritis: recent research progress. *Nat Immunol* **2**, 771–773.

5 Wallberg-Jonsson S, Ohman ML & Dahlqvist SR (1997) Cardiovascular morbidity and mortality in patients with seropositive rheumatoid arthritis in Northern Sweden. *J Rheumatol* **24**, 445–451.

6 Moskowitz RW, Kelly MA & Lewallen DG (2004) Understanding osteoarthritis of the knee – causes and effects. *Am J Orthop* **33**, 5–9.

7 Tak PP & Bresnihan B (2000) The pathogenesis and prevention of joint damage in rheumatoid arthritis: advances from synovial biopsy and tissue analysis. *Arthritis Rheum* **43**, 2619–2633.

8 Kinne RW, Stuhlmuller B & Burmester GR (2007) Cells of the synovium in rheumatoid arthritis. Macrophages. *Arthritis Res Ther* **9**, 224.

9 Bromley M & Woolley DE (1984) Chondroclasts and osteoclasts at subchondral sites of erosion in the rheumatoid joint. *Arthritis Rheum* **27**, 968–975.

10 Gravallese EM, Harada Y, Wang JT, Gorn AH, Thornhill TS & Goldring SR (1998) Identification of cell types responsible for bone resorption in rheumatoid

arthritis and juvenile rheumatoid arthritis. *Am J Pathol* **152**, 943–951.

11 Choy EH & Panayi GS (2001) Cytokine pathways and joint inflammation in rheumatoid arthritis. *N Engl J Med* **344**, 907–916.

12 McInnes IB & Schett G (2007) Cytokines in the pathogenesis of rheumatoid arthritis. *Nat Rev Immunol* **7**, 429–442.

13 von Banchet GS, Richter J, Huckel M, Rose C, Brauer R & Schaible HG (2007) Fibroblast-like synovial cells from normal and inflamed knee joints differently affect the expression of pain-related receptors in sensory neurones: a co-culture study. *Arthritis Res Ther* **9**, R6.

14 Han C, Chen T, Yang M, Li N, Liu H & Cao X (2009) Human SCAMP5, a novel secretory carrier membrane protein, facilitates calcium-triggered cytokine secretion by interaction with SNARE machinery. *J Immunol* **182**, 2986–2996.

15 Stow JL, Manderson AP & Murray RZ (2006) SNAREing immunity: the role of SNAREs in the immune system. *Nat Rev Immunol* **6**, 919–929.

16 Evidente VG & Adler CH (2010) An update on the neurologic applications of botulinum toxins. *Curr Neurol Neurosci Rep* **10**, 338–344.

17 Ranoux D, Attal N, Morain F & Bouhassira D (2008) Botulinum toxin type A induces direct analgesic effects in chronic neuropathic pain. *Ann Neurol* **64**, 274–283.

18 Meng J, Wang J, Lawrence G & Dolly JO (2007) Synaptobrevin I mediates exocytosis of CGRP from sensory neurons and inhibition by botulinum toxins reflects their anti-nociceptive potential. *J Cell Sci* **120**, 2864–2874.

19 Yeh FL, Zhu Y, Tepp WH, Johnson EA, Bertics PJ & Chapman ER (2011) Retargeted clostridial neurotoxins as novel agents for treating chronic diseases. *Biochemistry* **50**, 10419–10421.

20 Logan MR, Odemuyiwa SO & Moqbel R (2003) Understanding exocytosis in immune and inflammatory cells: the molecular basis of mediator secretion. *J Allergy Clin Immunol* **111**, 923–932.

21 Stow JL, Low PC, Offenhauser C & Sangermani D (2009) Cytokine secretion in macrophages and other cells: pathways and mediators. *Immunobiology* **214**, 601–612.

22 Huse M, Lillemeier BF, Kuhns MS, Chen DS & Davis MM (2006) T cells use two directionally distinct pathways for cytokine secretion. *Nat Immunol* **7**, 247–255.

23 Kay JG, Murray RZ, Pagan JK & Stow JL (2006) Cytokine secretion via cholesterol-rich lipid raft-associated SNAREs at the phagocytic cup. *J Biol Chem* **281**, 11949–11954.

24 Murray RZ, Kay JG, Sangermani DG & Stow JL (2005) A role for the phagosome in cytokine secretion. *Science* **310**, 1492–1495.

25 Oynebraten I, Barois N, Hagelsteen K, Johansen FE, Bakke O & Haraldsen G (2005) Characterization of a novel chemokine-containing storage granule in endothelial cells: evidence for preferential exocytosis mediated by protein kinase A and diacylglycerol. *J Immunol* **175**, 5358–5369.

26 Tsuji F, Oki K, Senda T, Horiuchi M & Mita S (1999) Effects of mitogen-activated protein kinase inhibitors or phosphodiesterase inhibitors on interleukin-1-induced cytokines production in synovium-derived cells. *Immunol Lett* **68**, 275–279.

27 Zwerina J, Redlich K, Schett G & Smolen JS (2005) Pathogenesis of rheumatoid arthritis: targeting cytokines. *Ann NY Acad Sci* **1051**, 716–729.

28 Schivell AE, Mochida S, Kensel-Hammes P, Custer KL & Bajjalieh SM (2005) SV2A and SV2C contain a unique synaptotagmin-binding site. *Mol Cell Neurosci* **29**, 56–64.

29 Chang WP & Sudhof TC (2009) SV2 renders primed synaptic vesicles competent for Ca^{2+}-induced exocytosis. *J Neurosci* **29**, 883–897.

30 Dong M, Yeh F, Tepp WH, Dean C, Johnson EA, Janz R & Chapman ER (2006) SV2 is the protein receptor for botulinum neurotoxin A. *Science* **312**, 592–596.

31 Hayashi T, McMahon H, Yamasaki S, Binz T, Hata Y, Sudhof TC & Niemann H (1994) Synaptic vesicle membrane fusion complex: action of clostridial neurotoxins on assembly. *EMBO J* **13**, 5051–5061.

32 Schaible HG, Schmelz M & Tegeder I (2006) Pathophysiology and treatment of pain in joint disease. *Adv Drug Deliv Rev* **58**, 323–342.

33 Houssiau FA (1995) Cytokines in rheumatoid arthritis. *Clin Rheumatol* **14** (Suppl. 2), 10–13.

34 McNearney TA, Ma Y, Chen Y, Taglialatela G, Yin H, Zhang WR & Westlund KN (2010) A peripheral neuroimmune link: glutamate agonists upregulate NMDA NR1 receptor mRNA and protein, vimentin, TNF-α, and RANTES in cultured human synoviocytes. *Am J Physiol* **298**, R584–R598.

35 Manderson AP, Kay JG, Hammond LA, Brown DL & Stow JL (2007) Subcompartments of the macrophage recycling endosome direct the differential secretion of IL-6 and TNFα. *J Cell Biol* **178**, 57–69.

36 Lacy P & Stow JL (2011) Cytokine release from innate immune cells: association with diverse membrane trafficking pathways. *Blood* **118**, 9–18.

37 Stanley AC & Lacy P (2010) Pathways for cytokine secretion. *Physiology* **25**, 218–229.

38 McMahon HT & Sudhof TC (1995) Synaptic core complex of synaptobrevin, syntaxin, and SNAP25 forms high affinity α-SNAP binding site. *J Biol Chem* **270**, 2213–2217.

39 Pagan JK, Wylie FG, Joseph S, Widberg C, Bryant NJ, James DE & Stow JL (2003) The t-SNARE syntaxin 4 is regulated during macrophage activation to function

in membrane traffic and cytokine secretion. *Curr Biol* **13**, 156–160.

40 Chen YA, Scales SJ, Patel SM, Doung YC & Scheller RH (1999) SNARE complex formation is triggered by Ca^{2+} and drives membrane fusion. *Cell* **97**, 165–174.

41 Kochukov MY, McNearney TA, Fu Y & Westlund KN (2006) Thermosensitive TRP ion channels mediate cytosolic calcium response in human synoviocytes. *Am J Physiol* **291**, C424–C432.

42 Feany MB, Yee AG, Delvy ML & Buckley KM (1993) The synaptic vesicle proteins SV2, synaptotagmin and synaptophysin are sorted to separate cellular compartments in CHO fibroblasts. *J Cell Biol* **123**, 575–584.

43 Dolly JO, Wang J, Zurawski TH & Meng J (2011) Novel therapeutics based on recombinant botulinum neurotoxins to normalize the release of transmitters and pain mediators. *FEBS J* **278**, 4454–4466.

44 Krug HE, Frizelle S, McGarraugh P & Mahowald ML (2009) Pain behavior measures to quantitate joint pain and response to neurotoxin treatment in murine models of arthritis. *Pain Med* **10**, 1218–1228.

45 Mahowald ML, Singh JA & Dykstra D (2006) Long term effects of intra-articular botulinum toxin A for refractory joint pain. *Neurotox Res* **9**, 179–188.

46 Singh JA, Mahowald ML, Kushnaryov A, Goelz E & Dykstra D (2009) Repeat injections of intra-articular botulinum toxin A for the treatment of chronic arthritis joint pain. *J Clin Rheumatol* **15**, 35–38.

47 Singh JA, Mahowald ML & Noorbaloochi S (2009) Intra-articular botulinum toxin A for refractory shoulder pain: a randomized, double-blinded, placebo-controlled trial. *Transl Res* **153**, 205–216.

48 Chen S & Barbieri JT (2009) Engineering botulinum neurotoxin to extend therapeutic intervention. *Proc Natl Acad Sci USA* **106**, 9180–9184.

49 Dong M, Liu H, Tepp WH, Johnson EA, Janz R & Chapman ER (2008) Glycosylated SV2A and SV2B mediate the entry of botulinum neurotoxin E into neurons. *Mol Biol Cell* **19**, 5226–5237.

50 Fu Z, Chen C, Barbieri JT, Kim JJ & Baldwin MR (2009) Glycosylated SV2 and gangliosides as dual

receptors for botulinum neurotoxin serotype F. *Biochemistry* **48**, 5631–5641.

51 Mahrhold S, Rummel A, Bigalke H, Davletov B & Binz T (2006) The synaptic vesicle protein 2C mediates the uptake of botulinum neurotoxin A into phrenic nerves. *FEBS Lett* **580**, 2011–2014.

52 Peng L, Tepp WH, Johnson EA & Dong M (2011) Botulinum neurotoxin D uses synaptic vesicle protein SV2 and gangliosides as receptors. *PLoS Pathog* **7**, e1002008.

53 Yeh FL, Dong M, Yao J, Tepp WH, Lin G, Johnson EA & Chapman ER (2010) SV2 mediates entry of tetanus neurotoxin into central neurons. *PLoS Pathog* **6**, e1001207.

54 Wang J, Zurawski TH, Bodeker MO, Meng J, Boddul S, Aoki KR & Dolly JO (2012) Longer-acting and highly potent chimaeric inhibitors of excessive exocytosis created with domains from botulinum neurotoxin A and B. *Biochem J* **444**, 59–67.

55 Somm E, Bonnet N, Martinez A, Marks PM, Cadd VA, Elliott M, Toulotte A, Ferrari SL, Rizzoli R, Huppi PS *et al.* (2012) A botulinum toxin-derived targeted secretion inhibitor downregulates the GH/IGF1 axis. *J Clin Invest* **122**, 3295–3306.

56 Yamazaki T, Yokoyama T, Akatsu H, Tukiyama T & Tokiwa T (2003) Phenotypic characterization of a human synovial sarcoma cell line, SW982, and its response to dexamethasone. *In Vitro Cell Dev Biol Anim* **39**, 337–339.

57 Meng J, Ovsepian SV, Wang J, Pickering M, Sasse A, Aoki KR, Lawrence GW & Dolly JO (2009) Activation of TRPV1 mediates calcitonin gene-related peptide release, which excites trigeminal sensory neurons and is attenuated by a retargeted botulinum toxin with anti-nociceptive potential. *J Neurosci* **29**, 4981–4992.

58 Stockert JC, Blazquez-Castro A, Canete M, Horobin RW & Villanueva A (2012) MTT assay for cell viability: intracellular localization of the formazan product is in lipid droplets. *Acta Histochem* **114**, 785–796.